TECHNISCHE UNIVERSITÄT MÜNCHEN

Lehrstuhl für Energiewirtschaft und Anwendungstechnik

Integration of Variable Renewable Energies in the European power system: a model-based analysis of transmission grid extensions and energy sector coupling

Katrin Schaber

Vollständiger Abdruck der von der Fakultät für Elektrotechnik und Informationstechnik der Technischen Universität München zur Erlangung des akademischen Grades eines

Doktor-Ingenieurs

genehmigten Dissertation.

Vorsitzender:	Univ.-Prof. Dr.-Ing. Rolf Witzmann
Prüfer der Dissertation:	1. Univ.-Prof. Dr.rer.nat Thomas Hamacher
	2. Univ.-Prof. Dr.-Ing. Reinhard Haas, Technische Universität Wien/Österreich

Die Dissertation wurde am 24.06.2013 bei der Technischen Universität München eingereicht und durch die Fakultät für Elektrotechnik und Informationstechnik am 17.12.2013 angenommen.

Max-Planck-Institut
für Plasmaphysik

Lehrstuhl für
Energiewirtschaft und Anwendungstechnik
Ordinarius Prof. Dr.-Ing. U. Wagner · Prof. Dr. rer. nat. Th. Hamacher (komm.)

Abstract

This thesis studies the effects of increasing shares of variable renewable energies (VREs), such as wind and solar energy, in the European power system and evaluates two VRE system integration measures, transmission grid extensions and energy sector coupling. Their benefits for the power system are quantified, but also their contribution to reduce the impacts of VREs on the electricity markets are analyzed. This dual approach adds a new perspective to the current debate on VRE system and market integration.

For the combined analysis, an energy system model, based on linear optimization of total costs, is employed. The model includes a high level of technical detail, high spatial and temporal resolution, while covering a wide geographic area and a large range of possible future VRE scenarios, thanks to a parametric approach. These features make the approach uniquely positioned to evaluate VRE integration measures.

The results show that a powerful overlay transmission grid, a supergrid, can facilitate the integration of VREs considerably. The achievable contribution of VREs to power supply can be increased from 60% to more than 85% with a European supergrid. Through smoothing, the grid reduces excess electricity and consequently the necessary VRE capacity. The resulting savings outweigh the grid's costs by a factor three approximately. Thanks to the parametric approach, ideal system design features in terms of VRE mix and share, supplementary power mix and crucial transmission corridors can be identified. At the same time, the smoothing effect of the supergrid impacts positively on the electricity prices. The merit order effect caused by projected VRE capacities is found to be reduced from 5 €/MWh without to 3 €/MWh with grid extension. This is to the advantage of most generators. Their revenues and market values increase as a consequence of higher and smoother prices and increased full load hours of dispatchable plants.

The analysis of the more local measure of energy sector coupling reveals a central role of the heat sector, which provides a large and economically attractive sink for temporary excess electricity from VREs. According to the results, the power-to-heat coupling displaces the usage of long term electricity storage or methanation. The identified optimal conversion paths from power to heat are complementary to the regional VRE supply. Again, the adaption of the power system to high VRE shares reduces their impact to the electricity prices. Compared to grid extensions, the coupling acts more directly on VREs. It sets a lower bound to electricity prices, as excess electricity regains a value in the coupled sectors. The market value of VREs increases as a consequence.

The findings suggest that both measures are highly beneficial for VRE system integration. Furthermore, the analysis of their interaction reveals that the simultaneous investment in both measures would not be contradictory: the local measure of energy sector coupling mitigates grid extensions initially, but with increasing VRE shares, transmission grid extensions are still desirable. The analysis from the market perspective demonstrates that the adaption of the power system to increasing shares of VREs boosts the value of VREs to the system, their market value. At the same time, the infrastructure measures also bear important benefits for other generators.

Zusammenfassung

In der vorliegenden Arbeit wird der Einfluss steigender Anteile von Wind- und Solarenergie auf das Stromversorgungssystem in Europa untersucht und zwei Maßnahmen für die Integration der fluktuierenden erneuerbaren Energien werden bewertet: der Ausbau des Europäischen Übertragungsnetzes und die Kopplung des Stromsektors an den Wärme- und Wasserstoffsektor. Die Vorteile dieser Maßnahmen für eine Stromversorgung mit hohen Anteilen an erneuerbaren Energien werden quantifiziert. Zusätzlich wird gezeigt, dass diese Infrastrukturmaßnahmen den Einfluss von Wind- und Solarenergie auf den Strommarkt abschwächen können. Diese duale Herangehensweise bietet eine neue Perspektive in der Debatte zur Integration erneuerbarer Energien.

Die Analyse wird mit einem Energiesystemmodell durchgeführt. In dem auf Kostenoptimierung basierenden Modell können kosteneffiziente Infrastrukturmaßnahmen identifiziert aber auch die Dynamik der Preisbildung am Strommarkt abgebildet werden. Das Modell zeichnet sich durch seine hohe zeitliche und räumliche Auflösung, den hohen Detailierungsgrad, sowie der Abdeckung eines großen Gebiets und der Berücksichtigung von vielen möglichen Szenarien in einem parametrischen Ansatz aus.

Die Ergebnisse zeigen, dass ein leistungsfähiges Europäischen Übertragungsnetz, ein sogenanntes "Supergrid", die Integration von fluktuierenden erneuerbaren Energien erheblich vereinfachen kann. Der mögliche Beitrag von Wind- und Solarenergie zur Stromversorgung kann durch ein Supergrid von 60% auf über 85% angehoben werden. Durch die Ausgleichseffekte kann ein höherer Anteil an Erneuerbaren Energien direkt genutzt werden, was die auftretenden Überschüsse und den notwendigen Ausbau an Erzeugungskapazitäten für Wind- und Solarenergie reduziert. Die hierdurch erzielten Einsparungen überschreiten die Kosten des Netzes in etwa um den Faktor drei. Durch den parametrischen Ansatz können zudem ideale Systemeigenschaften identifiziert werden, so wie der Beitrag von Wind- und Solarenergie, die Struktur des konventionellen Kraftwerksparks und die entscheidende Netzausbautrassen. Die Ausgleichseffekte des Netzausbaus mildern gleichzeitig den Einfluss der fluktuierenden erneuerbaren Energien auf die Strompreise. Während ohne Netzausbau, der berechnete, mittlere Strompreis aufgrund der prognostizierten Wind und Solarkapazitäten um 5 €/MWh sinkt, ist er mit Netzausbau nur um 3 €/MWh niedriger. Durch den höheren und auch weniger fluktuierenden Strompreis sowie den höheren Volllaststunden der konventionellen Kraftwerke, steigt der Marktwert und Umsatz für die Mehrheit der erneuerbaren *und* konventionellen Stromerzeuger.

Bei der Untersuchung der vermehrt lokal wirkenden Maßnahme der Sektorkopplung, stellt sich heraus, dass der Wärmesektor ein großes und wirtschaftlich sehr attraktives Potenzial zur Nutzung kurzzeitiger Stromüberschüsse bietet. Die Ergebnisse zeigen, dass durch die enge Kopplung des Strom- und Wärmesektors saisonale Stromspeicher und Methanisierung aus dem kostenoptimalen Maßnahmenportfolio verdrängt werden. Die idealen Kopplungstechnologien zwischen dem Strom- und Wärmesektor ergeben sich aus der regional vorherrschenden Mischung von Wind- und Solarenergie. Auch hier hat die Anpassung des Stromsystems an hohe Anteile fluktuierender erneuerbarer Erzeugung zur

Folge, dass deren Auswirkungen auf die Strompreise abgeschwächt werden. Die Effekte der Sektorkopplung wirken sich jedoch hauptsächlich positiv für Wind und Solarenergie aus. Durch die Sektorkopplung wird eine Untergrenze für den Strompreis eingeführt, da Stromüberschüsse in die gekoppelten Sektoren verkauft werden können. Der Marktwert von Wind- und Solarenergie steigt stark an.

Die Ergebnisse zeigen, dass beide Maßnahmen Vorteile für eine Stromversorgung mit hohen Anteilen an Erneuerbaren Energien mit sich bringen. Zusätzlich konnte dargelegt werden, dass gleichzeitige Investitionen in beide Maßnahmen nicht widersprüchlich wären. Durch die Einführung der Sektorkopplung kann zwar zunächst Übertragungsnetzausbau vermieden werden, mit steigenden Anteilen fluktuierender Erzeuger ist Übertragungsnetzausbau jedoch wieder notwendig um eine volkswirtschaftlich optimale Lösung zu erreichen. Die Analyse aus Marktperspektive lässt positive Auswirkungen der Infrastrukturmaßnahmen für die Marktintegration von erneuerbaren Energien erkennen. Umso besser das System an hohe Anteile Erneuerbarer Energien angepasst ist, umso höher ist ihr Wert für das System. Gleichzeitig profitieren auch andere Marktteilnehmer von den Infrastrukturmaßnahmen.

Contents

1. Introduction

To combat global warming and to address the fossil fuel scarcity, a shift to less carbon intensive resources in energy supply is necessary [73]. The power sector plays a central role in the decarbonization of the energy sector. Today, more than 40% of energy-related carbon emissions stem from the power sector [79]. Furthermore, the final energy carrier electricity is widely applicable and can thus contribute to the decarbonization of other sectors such as the residential, industry or transport sector. Finally, the power sector offers the possibility to efficiently use renewable energies and therewith provide carbon-free electricity from non-exhaustable resources. Already today, the majority of renewable energy deployment takes place in the power sector and the observed learning and growth rates suggest that the share of renewable energies in electricity supply will continue to rise steeply [74, 34].

Especially in Europe, where ambitious green house gas emission reduction targets have been legislated, renewable energies play a key role. Wind and solar energy are bound to be the most important sources, due to their large potential in Europe [e.g. 26, 134], the observed growth rates, but also the existing support schemes [78].

Wind and solar generators, however, are not just another type of power plant that is set to replace other means of generation. They differ from conventional, i.e., thermal dispatchable, generation in at least three respects: First, generation from wind and sun fluctuates: the temporal availability of wind and solar energy is driven by the meteorological conditions, such as the momentary wind speed or solar irradiation. They are therefore called Variable Renewable Energies (VREs) in the following. Second, wind and solar supply is not spread uniformly over Europe: regions with high meteorological potential for renewable generation are dispersed. Above all, they are not aligned with load centers, as the bulk of today's power generation is. Third, generation from wind and solar energy has no fuel costs. This can be challenging for electricity markets, where market prices are mostly driven by the marginal costs of generation, being the fuel costs of conventional power plants. The inclusion of fluctuating generation with low marginal costs can affect the prices significantly.

The integration of VREs in the power sector thus entails important challenges. On the technical system side, the temporal and regional variability of the resources may not be compatible with the current system operation and design. Also on the market side, the influence of fluctuating generation at low marginal costs challenges current electricity markets.

In the last five years, the installed wind capacity in Europe has doubled and solar photovoltaic capacity increased by a factor ten [57, 51]. The growing contribution

of VREs in power supply, promoted by national support policies and the goal of the European Union (EU) to strongly curb its greenhouse gas emissions emissions [40, 41], suggests that adaption measures may be needed in the power system in the years to come. On top of that, the political goal of coupling the European electricity markets also points to changes in the system. National power markets shall be linked more closely to facilitate international electricity trade [39], which implies additional cross-border flows [50].

The European Network of Transmission System Operators for Electricity (ENTSO-E) plans the addition and refurbishment of more than 50 000 km or 15% of the transmission lines until 2020 [50, 3]. This is a first step to comply with the increasing importance of power transmission in Europe driven by the two above mentioned trends.

This thesis analyses the effects of large shares of VREs on the European power system and evaluates two VRE system integration measures. Following the above described developments, first, the role of international transmission grid extensions for VRE integration is studied. Second, adapting electricity demand to the VRE supply via the coupling of the power sector to the heat and hydrogen sector is analyzed for the example of Germany as alternative VRE integration measure. Both measures are evaluated with respect to their contribution to the technical system integration and the market integration of VREs.

In the following two sections of the introduction, the VRE integration challenges are described in more detail, and the research questions of this thesis and its structure defined.

1.1. Challenges of renewable energy integration

The challenges of power generation from wind and solar energy are the temporal fluctuations of the resources, which are only partly predictable, their regional availability constraints and also the small unit size of the technologies potentially leading to a more decentralized system.

Today's electricity system, however, is based on centralized supply in proximity to load centers. The different power plant types are designed to follow the demand pattern, while power transmission over large distances and storage play only a minor role. This changes significantly in energy systems with high shares of VREs.

As mentioned above, the temporal availability of wind and solar resources fluctuates. It underlies seasonal and diurnal fluctuations but also short term fluctuations from hour to hour or from minute to minute. Figure 1.1 illustrates the resulting problem for the power system. The upper part shows the hourly electricity supply from VREs together with the load for selected months in a scenario of high VRE share (70%). The supply from wind and solar is highly variable: hours of oversupply but also hours of very low VRE supply occur. The remaining system has to be able to fill the so-called residual

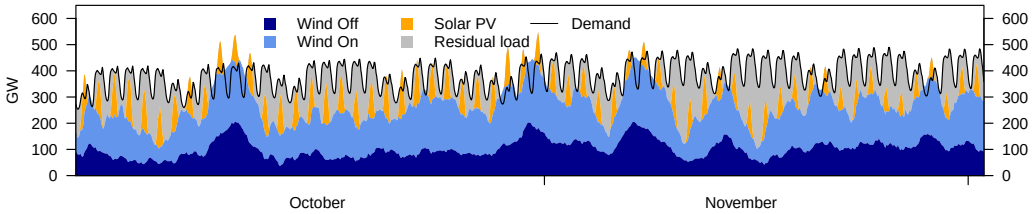

(a) Hourly electricity generation for selected months

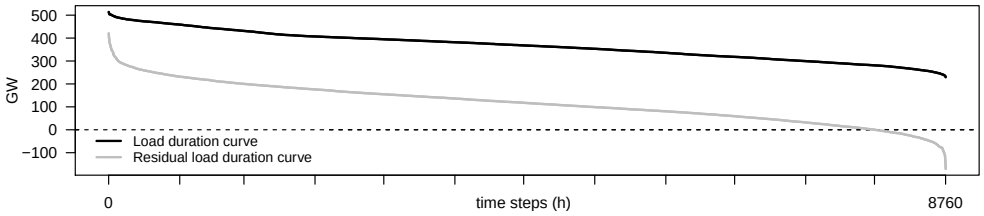

(b) Residual load duration curve for one year

Figure 1.1.: Illustration of the residual load and residual load duration curve in Europe with a high share of VREs (70%) (based on data from 2006 [64])

load, the electricity load minus the electricity provided by VREs. Conventional power plants, such as gas or coal power plants, have to supply the highly variable residual load, where fast ramps can pose difficulties. The lower part of the figure shows the sorted annual hourly load, also called the load duration curve together with the residual load duration curve, the sorted annual hourly residual load. The residual load duration curve is steeper than the load duration curve: the maximal load remains similar, but the total annual residual electricity demand is lower. The necessary supplementary dispatchable capacity remains similar, but it will be used at lower rates. Furthermore, overproduction occurs in several hours as can be read off the negative residual load.

The power system has to balance the VRE fluctuations and provide adequate infrastructure to satisfy the residual load.

Additionally, the residual load contains more elements of uncertainty than the load. For solar energy, the position of the sun, and therewith the hours of daylight, are predictable, but cloud cover, fog and snow cover of the photovoltaic (PV) modules adds a component to the availability of solar energy, which is difficult to predict. The diurnal and short term fluctuations of wind energy do not follow a regular patter and are also only partly predictable.

Figure 1.2 illustrates the second major problem of VREs: the geographic distribution of wind and solar resources in Europe is not well aligned with the load centers. The figure shows the average wind speed and global solar irradiation in Europe from 1980-2010, together with a satellite image of Europe at night from 2012. The regional distribution of light emissions is a good indicator for electricity demand.

High wind speeds and thus good wind park sites are located at the coasts: in and

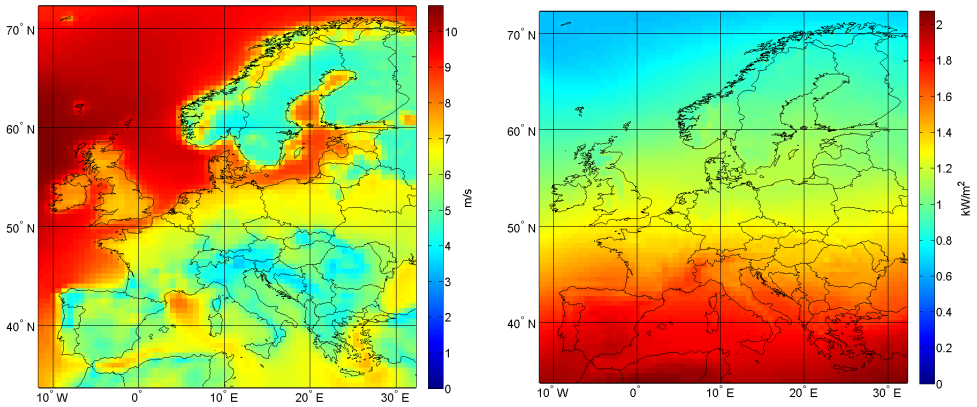

(a) Average wind speed at 80 m height

(b) Average global solar irradiation

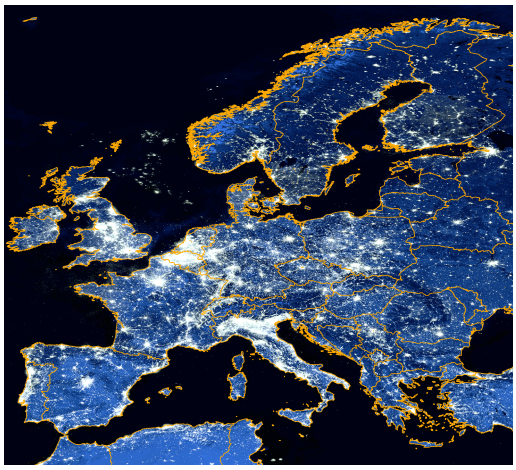

(c) View of the Earth at night, 2012

Figure 1.2.: Distribution of VRE resources and load centers in Europe [105, 100]. Average wind speed and solar irradiation data are from the years 1980-2010.

around the North Sea, at the shore of the Atlantic Ocean, etc. The annual solar irradiation increases from North to South. The usage of solar power is thus most advantageous in southern Europe. The load centers show a different distribution. They are located in Northern Italy, North-Western Germany, Northern England and in and around the capitals, such as Paris, Madrid and Amsterdam. Also Belgium has an important electricity demand, but as its highways are illuminated, the satellite image overrates the Belgian electricity demand.

To use VRE resources efficiently, the VRE generation sites should be located in areas with high potential. As a consequence, these remote sites need to be connected to the load centers or the load centers shifted to areas of high VRE supply.

Furthermore, VRE technologies, especially solar PV units are installed at low voltage

levels of the power grid. Historically, power flow was directed from large power plants at high voltage levels to consumers connected at the low voltage level. With increasing decentralized generation connected to the grid at low voltage levels, the direction of the power flow changes. This challenges the grid operation and can require adaption or extensions at the low voltage level, in the distribution grid.

1.1.1. VRE system integration challenge

The technical adaption of the power system design to efficiently integrate large shares of VRE generation is called VRE system integration in this thesis. System integration measures refer to all infrastructure measures, which facilitate system reliability and cost-effectiveness in the presence of high VRE shares. Overproduction should be avoided and the maximal residual load, i.e., necessary peak capacity of conventional power plants, reduced. Furthermore, the fast changes in residual load should be reduced or followed by the power system.

The four major infrastructure measures available for VRE system integration are [27]:

- Grid extensions to connect remote sites of high VRE potential and allow increased exchange between regions.
- Additional storage capacity to balance VRE supply and demand.
- More flexible demand, via demand side management shifting demand to periods with high VRE supply.
- More flexible power plants that can adjust to VRE supply quickly.

The measures can act on different timescales. On the short, operational timescale, the measures can increase the system's flexibility. More flexible power plants, storage and demand side management raise the system's ability to react to unforeseen load changes on short timescales of seconds to hours. On a longer timescale, relevant for investment decisions, all four measures can contribute to form an adequately designed energy system which efficiently accommodates large shares of VREs, while maintaining the system's reliability. The focus of this thesis lies on this adequacy of the power system design. Two system integration measures, transmission grid extensions and the flexibilization of the electricity demand via energy sector coupling are evaluated with respect to their contribution to reduce total system costs from a system planner perspective.

1.1.2. VRE market integration challenge

In addition to the temporal and geographic variability of wind and solar energy, their low level of variable costs influences the electricity market: VREs and other renewable energies such as hydro or geothermal power have negligible variable costs.

Bids on current European wholesale electricity markets are mainly based on the marginal costs of generation. In periods of scarcity, they can be increased by mark-ups. The supply curve in these so-called energy-only market is obtained by the sorted

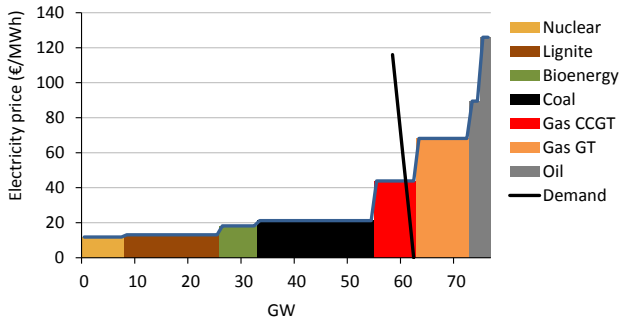

(a) Merit order without renewable energies

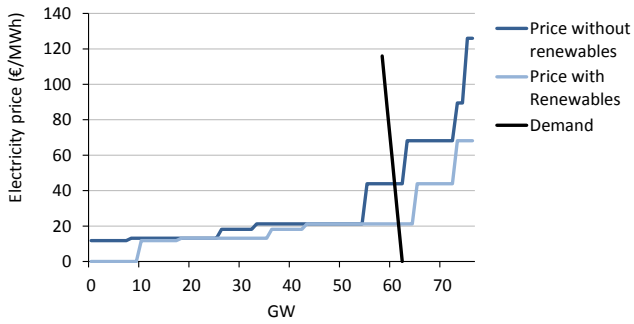

(b) Theoretical shift of the merit order curve with renewable energies

Figure 1.3.: Schematic merit order curves for the German electricity market

variable costs of available generation units. It is also called the merit order curve and shown in Figure 1.3a. Wind and solar energy technologies rank first in the merit order: they are the cheapest power supply in terms of variable costs. Due to this cost structure and additionally fixed by the regulator through priority feed-in, the supply curve is shifted to the right whenever renewable energies contribute to the satisfaction of demand. Consequently, the demand curve intersects the supply curve at lower prices and the price level declines due to renewable supply (see Figure 1.3b). This is called the "merit order effect" [135].

The momentary electricity price level is lowered whenever wind or solar energy is entering the market. This has considerable consequences for the electricity market and its participants. Volatile prices affect conventional generators and also VRE technologies, if they participate in the market.

The integration of VREs in the electricity market thus entails important challenges. Questions arise, which power system properties aggravate the price effects of large VRE shares and which can possibly reduce or mitigate them. Furthermore, the impacts on the profitability of different market participants has to be examined in detail. Especially, the question under which circumstances VREs can be competitive at the wholesale market

is pertinent. These questions define the VRE market integration challenge.

In this thesis, the market effects of VREs in Europe in terms of price and revenue changes are quantified. The marginal costs of electricity generation are used as indicators for electricity prices. This corresponds to assuming a perfectly competitive market excluding strategic mark-ups. The implications of the two analyzed infrastructure measures for VRE market integration are evaluated.

1.2. Objective and structure of this thesis

If high shares of VREs are to be integrated in the European power sector, large system changes are necessary. Yet, it is not at all clear, which changes of this rather complex system would be most advantageous. Thus, for a successful power system transformation, the analysis of different VRE system integration measures is necessary.

The objective of this thesis is to analyze how transmission grid extension and energy sector coupling can facilitate the integration of VREs in the European power system. The system advantages are examined with an energy system model based on cost-optimization. Subsequently, the market effects of the two VRE system integration measures are studied based on the marginal costs of electricity resulting from the optimization.

This overall objective is broken down in individual research questions defining the structure of this thesis, which is depicted in Figure 1.4. In Chapter 3 the system advantages of a powerful European overlay transmission grid are examined. Chapter 4 focuses on the market effects of this VRE integration measure. In Chapter 5 energy sector coupling is analyzed as an alternative VRE integration measure. Its system and market implications are studied.

An overarching requirement for the analysis is to dispose of a suitable analytical framework. Chapter 2 presents the applied methodology, an energy system model. First, the requirements to the model are specified and an overview on existing energy system models given. Then, the employed methodology, the URBS model generator, is introduced. Based on URBS, two energy systems are implemented, to analyze high VRE shares in Europe and to evaluate infrastructure measures for their integration. A benchmark of the modeling framework demonstrates its suitability for the defined objective.

The regional dispersion of VRE sources in Europe, but also by the political efforts to foster international transmission grid extensions motivates the focus on a powerful European overlay transmission grid. The distribution grid is not included in the analysis.

Chapter 3 studies the role of large transmission grid extension for VRE system integration in Europe. Concerning this measure, the first research question is: To what extend can a powerful European overlay transmission grid, a so-called supergrid, facilitate the integration of wind and solar electricity in Europe? To answer this question, the exact challenges of increasing VRE shares have to be quantified first. What is the effect of

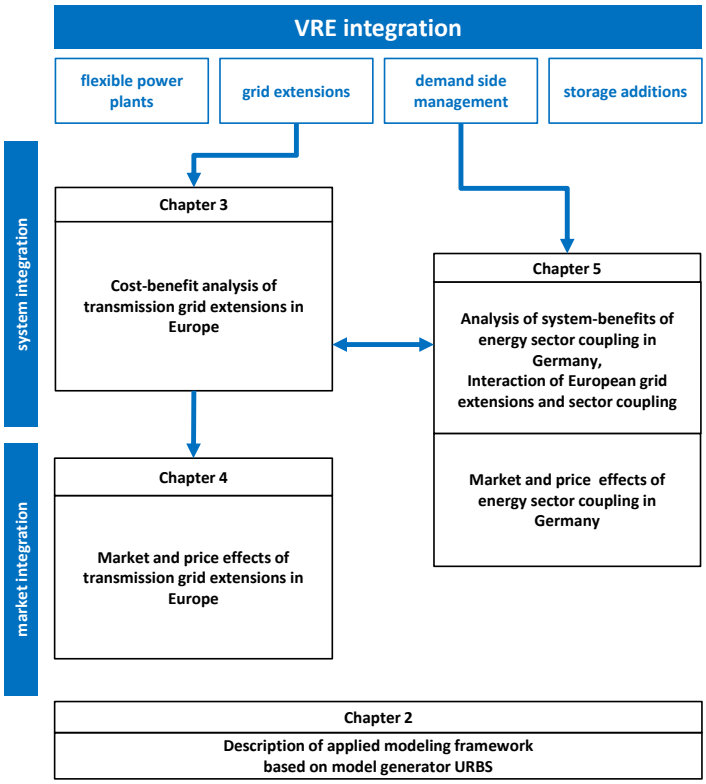

Figure 1.4.: Infrastructure measures for VRE system integration and structure of this thesis

different shares of VREs in the electricity generation? How does the mix between wind and solar energy influence the results? The effects of a supergrid are analyzed in a second step. What are the benefits of a supergrid for different VRE shares and mixes? Which VRE shares and mixes are achievable, which desirable? How do the costs of this measure compare to its benefits?

Chapter 3 contributes to the literature in providing a systematic and comprehensive cost-benefit analysis of transmission grid extensions in Europe exploring a large parameter space of different VRE shares and mixes. While previous studies have shown, that a powerful European overlay transmission grid, is advantageous for fully or highly renewable power supply in Europe [e.g. 26, 32, 134, 63], a comprehensive study of costs and benefits of this measure for different VRE shares and mixes has not yet been presented. Furthermore, the detailed modeling framework, yet covering a large parameter space, provides insights about robust design features of a future system with high VRE shares.

Having identified the benefits of transmission grid extensions for VRE system integration, the second research question arises: what are the effects of transmission grid extensions for the market integration of VREs in Europe?

Chapter 4 addresses this question. Again, first, today's market environment has to be studied and the market effects of VREs in this current environment and infrastructure quantified. Based on this, the impact of transmission grid extensions can be analyzed. How are the electricity prices influenced by VREs with and without transmission grid extensions? What are the effects of VRE for the different market participants with and without transmission grid? How do benefits or disadvantages of a grid extension differ between region or technologies?

Chapter 4 analyses the effects of VREs on the European electricity market together with the effects of transmission grid extension. The analysis of the regional electricity prices and the generators' revenues per technology reveals who benefits where from the transmission grid extensions. Several studies have analyzed the price effects of VREs and the principal implications for market participants [e.g. 135, 142]. The region- and technology-dependent effects, however, are resolved for the first time in Chapter 4, revealing important insights on potential pro- and opponents to transmission grid extensions. Furthermore, the combined analysis of the VRE system and market integration sheds light on a new aspect in the current discussion on VRE market integration.

The VRE system integration measure of a European supergrid implies the construction of large transmission corridors. However, the public acceptance and timely feasibility of this approach is questionable. Without transmission grid extensions, high VRE shares can lead to temporary regional excess electricity generation. The question arises, how to integrate this excess electricity, if no transmission grid extensions are realized.

Chapter 5 explores the possibility of adapting the electricity demand to the VRE supply as alternative system integration measure. The coupling of the power sector to the heat and hydrogen sector is analyzed for the example of Germany. Through this coupling the temporary excess electricity can be integrated – it can be used to supply heat or hydrogen demand – and the possibility for large storage is opened. To evaluate this integration option, the multitude of technical options for the energy sector coupling has to be untangled first. Is the coupling to the heat or the hydrogen sector more economic? Which technologies are economically most attractive and how do they interact? Having identified the economically most viable options, their effects for VRE integration can be analyzed: what are the benefits of the identified coupling configurations for VRE system integration? Second, what are the effects of the energy sector coupling for VRE market integration? How does this measure compare and interact with the European supergrid?

Chapter 5 adds to the existing literature in three respects. First, to the author's best knowledge, it provides the first regionally resolved analysis of energy sector coupling for Germany. Existing literature focuses mainly on Nordic countries or only on one other sector [e.g. 95, 141]. Second, the interaction of a European supergrid and the usage of excess electricity for other sectors has not yet been analyzed. Finally, in analogy to Chapter 4, the analysis of energy sector coupling from a market integration perspective contributes to the current debate.

Finally, overall conclusions are provided in Chapter 6. It summarizes the findings from the individual chapters.

2. The modeling framework

2.1. Modeling a highly renewable power system

To accommodate high shares of VREs in power supply systems, integration measures are necessary. These can involve important infrastructure investments, such as transmission grid extensions. To evaluate VRE system integration measures a mathematical representation, i.e., a model of the energy system is required. This chapter introduces the employed energy system model.

2.1.1. Choice of included model features

Modeling energy systems with a large share from renewable energies requires high spatial resolution to account for regionally differing potential, as well as high temporal resolution to capture the short term fluctuations, especially those of VREs. For the evaluation of the VRE system integration measures, the relevant technical and economic properties of these measures need to be included. To capture the challenges of stable power system operation for example, variations within seconds in one specific unit can be crucial. At the same time, due to long investment cycles in the energy sector, the long-term development of an energy system is of interest. To take into account the long-term development and path dependency of investments, for example in power grid or plants, time frames of several decades would need to be included in the analysis. The impact of green house gas emissions on our climate occurs on even larger timescales of at least 100 years. On top of that, unpredictability of VRE supply but also of the behavior of market participants can play an important role.

As the model size is limited by the available computational power, a choice of desired modeling depth and scope has to be made.

In this thesis, VRE integration measures are evaluated with respect to their contribution to an adequate, cost-efficient system design. The power system therefore needs to be modeled in sufficient detail to resolve the VRE integration challenges and the effects of different integration measures. In addition to that, the model should be able to identify, which investment decisions for new infrastructure are beneficial.

Figure 2.1 shows the most important features and properties, that an energy system model ideally should have for the analysis of VRE integration into the power sector (after Haller [63]). The features are classified with respect to their corresponding temporal and spatial resolution and range from a temporal resolution of seconds to decades and a spatial resolution of single utilities to the entire world. The higher the temporal resolution of the model, the stronger is commonly the focus on system operation and

its technical details. With increasing focus on the long-term development of energy systems, the operational details are neglected and macro-economic dynamics included instead. However, for infrastructure investment decisions, as much operational detail as possible should still be taken into account. The diagonal shape resulting from the classification shows that the temporal and spatial model resolution are related: the inclusion of certain features can only be realized with a certain temporal and spatial resolution.

In addition to the temporal and spatial scope, a third dimension can be added to distinguish between different modeling approaches. Strategic behavior or uncertainty in terms of prices or VRE forecasts can influence the decisions on system operation or investment in new utilities considerably. How this aspect is treated adds a third dimension to the classification of energy system models.

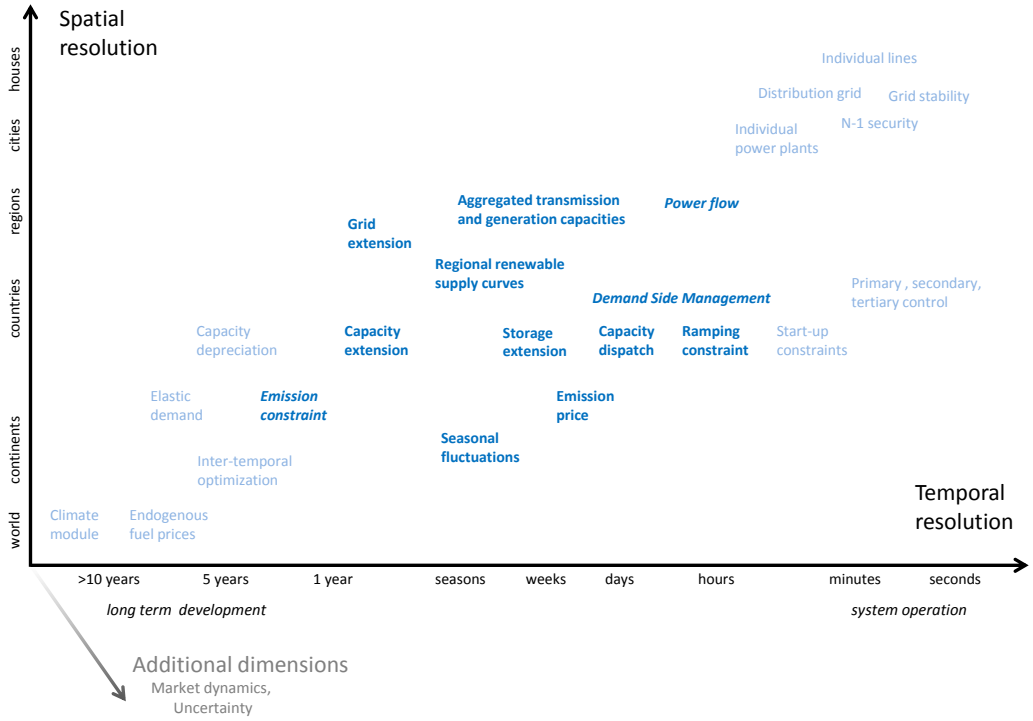

Figure 2.1.: Classification of model features for energy and power system models (after Haller [63]). Model features included in the model URBS-EU and URBS-D are in **bold**, ***italic*** features are optional.

Not all of these features are necessary to address the research questions defined in the introduction. According to the scope of the analysis, the evaluation of different VRE integration measures and their contribution to adequate energy system design, selected features are included in the modeling framework in this thesis. They are shown in bold in the figure.

Hourly temporal resolution and a scope of one typical year are chosen for the analysis of the power system design. This allows to capture the short term and seasonal variations in VRE supply, but excludes variations on timescales of seconds and minutes, highly relevant for the flexibility requirements or grid stability, but less so for the system design. Depending on the model setup, the inclusion of all 8760 hours of the year can exceed the available computing power. In this case, selected representative periods of the year are modeled only.

The technical details of the power system, such as hourly power plant and storage dispatch are included. Ideally, a high level of technical detail of power plant operation such as ramping, start-up constraints and balancing should be simulated, especially if the integration measure of more flexible power plants is to be analyzed. Here, the focus lies on transmission grid extensions and energy sector coupling. Therefore, a simplified representation of these restrictions via ramping constraints is chosen.

To account for regional differences in VRE supply and load, and to resolve the grid structure, high spatial resolution is essential. While the analysis of individual transmission lines would be desirable, the general effects of smoothing through transmission grid extensions can also be captured on an intermediate level of spatial resolution. This allows to keep the size of the model manageable. Therefore, aggregated transmission and generation capacities are taken into account.

In the same time, infrastructure extensions, such as investment in generation capacity, transmission lines or energy sector coupling technologies have to be included. The inclusion of infrastructure extensions provides insights to advantageous system design for VRE integration. Elastic demand and the effects of emissions from the power sector to the climate are excluded, as these points do not directly influence power system design. The path-dependency of investment decisions, i.e., the long-term effects of investments, are not included either, but the analysis is performed for one typical year only. By defining different scenarios, representing different steps in future, the development of the power system can be analyzed nonetheless.

Finally, perfect foresight and a central planner are assumed in the model: decisions are taken based on perfect information about the situation in all regions and time steps.

The models developed in this thesis are based on the energy system model generator URBS, which includes all the above listed features. URBS (Urban Research ToolBox Energy System) was introduced by Richter in 2004 [124] and has since steadily been enhanced through further research projects, including this thesis. More detail on the evolution, properties and application fields of the model generator is provided in Section 2.2.

URBS is based on the optimization of total system costs. The properties of the energy system are described via boundary conditions to the cost-minimization. URBS computes the capacity and storage dispatch as well as grid usage for the energy sector: it simulates the energy systems operation. At the same time, capacity expansion for a typical year can be optimized and therewith cost-optimal system design proposed.

The inclusion of the above listed model features results in a large number of variables,

for example the hourly power plant dispatch in different model regions and technologies. Due to the large size of the problem, a linear approach is taken, i.e., all system properties are described with linear equations. Linear programming is a powerful approach for large optimization problems and standard solver algorithms can be applied (see Annex B).

The URBS model generator is applied to the European and German power system in Chapter 3-4 and Chapter 5 respectively. In Chapter 5, the heat and hydrogen sector are included as well.

2.1.2. Positioning of the modeling framework

Before going into the details of the modeling methodology, its position relative to other energy system models is specified in this section.

In analogy to the classification of model features, energy system models can be categorized. Based on the temporal scope, three groups have been proposed by Pina et al. [119] and Haller [63]: models focusing on the long term development, models focusing on the short term, operational system behavior and those in between, the "hybrid" models. The later gain importance in the light of increasing shares of renewable energies. The nature of renewable energies make the inclusion of more operational detail necessary when analyzing investment decision and long term development. The URBS-models developed in this thesis contribute to the field of hybrid energy models.

Just as the URBS model generator, most of the energy system models are based on optimization. Total costs or welfare are optimized under a set of boundary conditions describing the properties of the energy system. Mostly, linear optimization problems are formulated, as linear programming allows for the inclusion of a large number of variables.

Figure 2.2 categorizes an exemplary selection of energy system models with respect to their temporal scope and spatial resolution.

To study the long term development of energy systems, an inter-temporal optimization has to be realized. Pursuing an inter-temporal approach means, that several years or decades are included in the optimization. The optimization can choose between possible system configurations for the entire modeled time period, for example for 50 years. As a consequence, investment decisions are taken for the entire period. The decision in one year depends on future and past investments. This allows to compute optimal pathways of decarbonization for example, but also to analyze the long term drivers of energy system development. The system boundaries of these models differ: in General Equilibrium Models (GEMs), demand and fuel prices are determined endogenously based on a macroeconomic equilibrium across all markets and sectors. Partial Equilibrium Models only include an equilibrium within one commodity, as it is the case for example in EFDA-TIMES [e.g. 104]. In GEMs, often an integrated approach including the environmental restrictions and response of the climate (climate module) is chosen. One of the first models of this kind is the DICE model by Nordhaus [108] and its regionally resolved version RICE [109]. Other prominent examples of such Integrated Assessment Models (IAMs), are ReMIND [90], WITCH [17] and POLES [128] (see Figure 2.2).

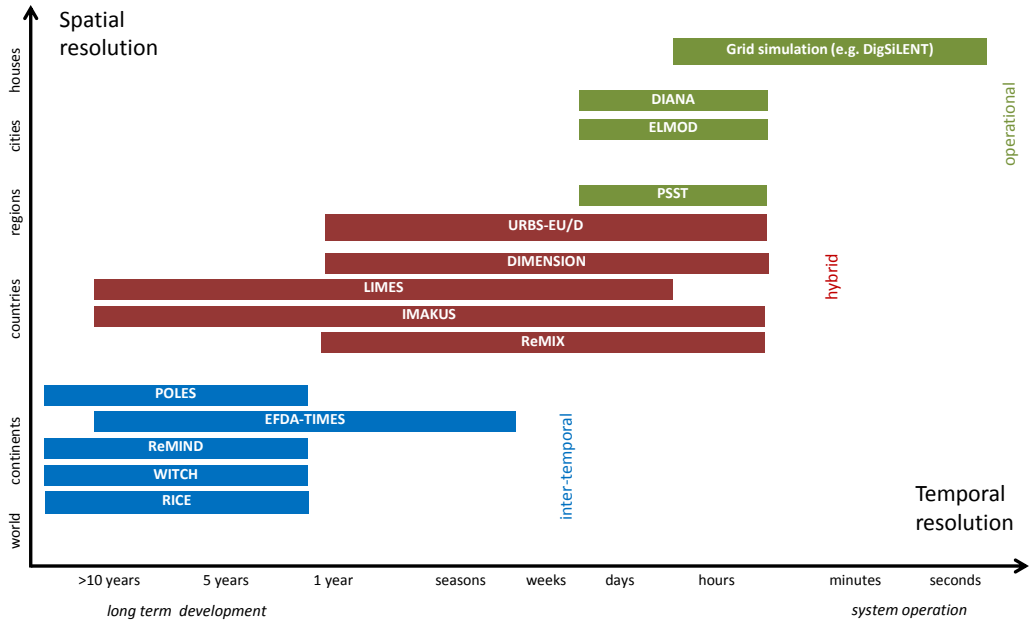

Figure 2.2.: Classification of selected energy system models

Operational models have higher temporal and spatial resolution. They have a large depth of technical detail and are technology explicit. A dynamic transmission grid simulation, for instance, has a temporal resolution of seconds and simulates transmission lines individually. Unit commitment problems, which take into account many of the technical restriction such as start-up or ramping constraint in the optimization of power plant dispatch, commonly have a resolution of 15 minutes to one hour. They often model every power plant individually. Operational models can be pure simulation, like the grid simulation, or also optimization problems. Mostly, the capacity dispatch, but not the infrastructure expansion is studied in pure operational models. Furthermore market mechanism or regulatory restriction can be captured in detail in these models. The DIANA model for example optimizes power plant dispatch and network usage, but also includes market-specific restrictions [94]. PSST is developed to study the integration of wind energy in Europe and combines a detailed unit-commitment and grid utilization optimization with a detailed market simulation, including also balancing markets [138]. The ELMOD model, in turn, has a stronger focus on the technical restrictions of the European transmission grid: it includes details on grid operation in a welfare optimization [93].

Hybrid models cover a large range of timescales, as can be seen in Figure 2.2. One step towards energy system planning is to include capacity expansion in operational models. Here, grid, storage and/or generation unit additions and dispatch are optimized simultaneously. This can be realized for one year, which is assumed to be representative,

like it is done in this thesis. The restriction to one representative year allows to include technical details and high spatial and temporal resolution. For the optimization of grid and storage infrastructure this high resolution is crucial. The more technical detail is included and the higher the resolution, the more technically realistic are the optimization results for infrastructure investment. However, this approach is not inter-temporal. Examples are DIMENSION [123], ReMIX [134] and the models implemented in this thesis URBS-EU [131, 132] and URBS-D [133] based on the URBS model generator.

To also account for long term dynamics of infrastructure investments, the renewable integration challenges are included in intertemporal models. Due to the large complexity and size of long term scope models, the degree of detail possible to include is limited. Current practice therefore includes, parametrization, i.e., simplified modeling of renewable integration challenges (LIMES [63]), coupling of operational and inter-temporal model [e.g. 148] and iterative approaches (IMAKUS [87]).

2.2. The URBS model generator

The Urban Research ToolBox Energy System was introduced in 2004 for the analysis of the urban energy system of Augsburg [124]. One part of the toolbox is an energy technology tool, where, based on linear optimization of overall system costs, the cost-optimal technology mix for an energy system is determined. This energy technology tool developed into the URBS energy system model generator, designed to analyze the effects of high shares of renewable resources in energy systems.

While initially developed for the analysis of urban energy systems, URBS was soon applied to power systems[a]. In 2005, Heitmann applied the linear optimization to the German power system for the analysis of grid extensions for wind energy integration [65]. One year later, Haase showed that the simplified simulation of power flow carried out in URBS is not in contradiction with the results from more detailed grid simulations [61]. A stochastic version of the URBS model was introduced in 2008 by Heitmann and Hamacher, where the cost-optimization is carried out under stochastic fuel prices or wind availability [66]. In 2011, Aboumahboub analyzed the global power system with URBS and performed a benchmark of the model's power plant dispatch against a detailed unit commitment model [1]. A URBS version, where power plant dispatch is simulated in more detail was developed by Huber et al. in 2013 [72] and the inclusion of electric vehicles introduced in by Wimmer 2012 [153].

In this thesis the URBS model generator is applied to the European power sector and the German power, heat and hydrogen sector. To shed light on the impact of simplified power transmission simulation, a more realistic approach, a load flow module, is introduced in the model generator. The results of both methodologies are compared. Furthermore, a benchmark against historic data on European power system operation is performed (Section 2.4). Following Heitmann [65], a routine to select representative

[a] Also in the field of urban energy systems the model generator was developed further [e.g. 67, 106]

periods of the modeled year is implemented, as the user may wish to simulate only selected periods, for example weeks, due to restrictions in computational power. (Subsection 2.2.4). Furthermore, a coupling to a time series analysis is introduced together with the development of a parametric approach. Finally, methodologies introduced for urban energy system analysis for decentralized generation and combined heat and power generation are applied to the German power system (Section 2.2.3 after [124]).

In the following the structure of the model generator is introduced and its mathematical formulation described. After that, the setup of the implemented models is laid out together with the input data. Finally, the power system model generated with URBS is benchmarked against a load flow simulation and historic data.

2.2.1. Model structure

The model generator URBS allows to compile energy system models designed for the analysis of high shares of renewable resources in the energy supply. At its core is a set of equations describing the energy system.

Figure 2.3 shows the structure of the model generator URBS. The model is based on linear optimization. Total system costs are minimized under a set of boundary conditions, which describe the behavior of the energy system. The system properties are characterized by the input parameters. As model results, cost-optimal capacity extension and dispatch of generation, transmission and storage units are computed. Furthermore, total costs, as well as overall emissions result from the model. The marginal costs of energy generation are used as indicators for energy prices. The model generator allows to realize high spatial and temporal resolution.

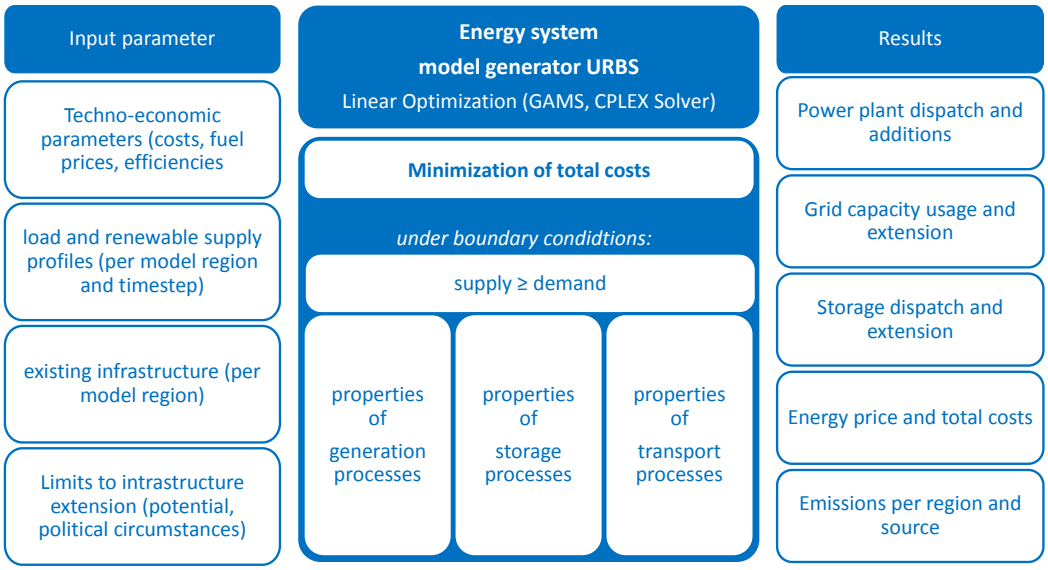

Figure 2.3.: Model structure

The driver of the model is the energy demand. A given demand for an energy commodity co has to be met in every time step t and model region x.

$$\text{supply}(co, x, t) \geq \text{demand}(co, x, t) \tag{2.1}$$

This equation ensures the energy balance and is the most important boundary condition to the cost optimization, as it drives the energy supply. To satisfy the demand, commodity production, storage and transport are realized, as well as capacity extension of these technologies, if necessary. In this thesis, the URBS model generator is mainly applied to the power sector, i.e., the electricity load has to be satisfied. However, URBS can also be applied to other commodities, such as heat or hydrogen like in Chapter 5. The above sketched equation is valid for any demand commodity. The energy balance needs to be respected in every model time step and region, reflecting the regionally and temporally resolved analysis of the energy system.

The other boundary equations describe the technical properties of the energy system. They can be classified in three groups. The first group includes the equations describing the generation processes, such as power plants, heat generation plants, etc. Energy storage is described in a second group of equations and commodity transport, for example, electricity transmission, in a third. All of these boundary conditions have to be respected for every time step and region and define the possibilities to supply the demand.

Other restrictions concerning several technologies can be included as well, such as emission constraints or minimal shares of renewable energy supply.

The model computes the cost-optimal solution to supply the demand, under these boundary conditions. The objective function z of the optimization is the total cost function. It consists of three parts. For capacity additions of generation, storage or transport units, the investment costs have to be taken into account. Fixed operation and maintenance costs occur for all, new and old capacities. The third part includes the variable costs, such as fuel costs, variable O&M costs and costs for emission allowances.

$$z = K^{inv} + K^{fix} + K^{var} \tag{2.2}$$

$$K^{inv} \propto \text{capacity additions} \tag{2.3}$$

$$K^{fix} \propto \text{all installed capacity} \tag{2.4}$$

$$K^{var} \propto \text{energy supplied} \tag{2.5}$$

The detailed mathematical realization of the model is described in Subsection 2.2.2.

This optimization is performed based on exogenous input parameters specifying the characteristics of the analyzed system. The total costs are computed based on the specific generation, storage and transport cost and hence the costs assumptions are crucial for cost optimization.

An other input is the load curve. For each region and time step the load level has to be provided to the model. Also, the temporal and regional availability of some resources, such as VREs, is taken into account via the input of respective time series.

Finally, the existing infrastructure and limits to its extensions are exogenous to the model. Generation infrastructure extension for example can be restricted by the technical potential for renewable deployment, but also by political circumstances, for example, for nuclear power plants in Germany. A detailed description of the databases and assumptions used for the model input is given in Section 2.3.

Depending on the mode of operation, the model can provide different results and insights. URBS can be used as simulation tool or for infrastructure planning. The capacity extension can be disabled setting the upper limits for capacity extensions to current or exogenously defined capacities. In this simulation mode, the model determines cost-optimal capacity dispatch to supply the demand. On demand, i.e., relaxing the upper bounds for capacity expansion, it also computes cost-optimal extensions of the power plant, storage and transport infrastructure and is thus used as system planning tool. Partly relaxation of the capacity extension bounds, allows for compromises between these two operation modes. For example, only grid extensions can be computed, based on the regional cost-optimal capacity dispatch of generation and storage units.

All three elements, model input, model equations and the model results exist for every model region or every connection between regions. The regional resolution can be chosen to the user's convenience. The input data has to be provided accordingly. Due to computing and data availability restrictions, aggregated regions are chosen in this thesis. Instead of including every single power grid node, power plant etc., the energy infrastructure is summed up to form an aggregated representative node, which stands for an entire model region. The total power plant and storage capacities in the region are aggregated. Also, the total available grid connections between two regions are summed up to form the connection between the representative nodes.

The temporal resolution of one hour allows the inclusion of dispatch dynamics in a system with high shares of VREs but excludes short term dynamics relevant for system stability, which are out of the scope of this analysis.

2.2.2. Model formulation

This section describes the mathematical implementation of the linear optimization. The three groups of boundary conditions are introduced consecutively, followed by the energy balance. Finally the objective function, the cost function, is defined. Capital letters denote variables – quantities determined by the model – and small letters denote input parameters and sets. The list of symbols is given for each group of equations respectively, a comprehensive list in alphabetical order can be found in Annex D.

Generation processes

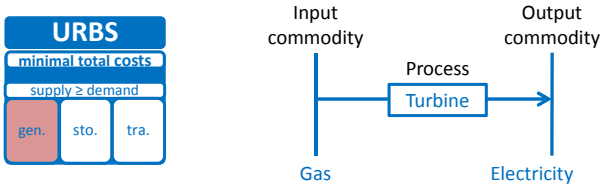

Figure 2.4.: Reference energy system for generation processes

$$E^{out}(\underbrace{p, co^{in}, co^{out}, x}_{i}, t) = \eta(\underbrace{p, co^{in}, co^{out}, x}_{i}) \cdot E^{in}(\underbrace{p, co^{out}, co^{in}, x}_{i}, t)$$

$$E_i^{out}(t) = \eta_i \cdot E_i^{in}(t) \qquad \forall i \in I \quad (2.6)$$

$$E_i^{out}(t) \leq af_i \cdot C_i \qquad \forall i \in I \quad (2.7)$$

$$E_i^{out}(t) = cf_i(t) \cdot af_i \cdot C_i \qquad \forall i \in I^{vre} \quad (2.8)$$

$$|E_i^{out}(t) - E_i^{out}(t-1)| \leq \tau_i \cdot C_i \qquad \forall i \in I \backslash I^{vre} \quad (2.9)$$

$$C_i = c_i^0 + C_i^N \qquad \forall i \in I \quad (2.10)$$

$$c_i^{min} \leq C_i \leq c_i^{max} \qquad \forall i \in I \quad (2.11)$$

The above equations control the generation processes. They are valid for all model regions, time steps, commodities and transformation processes ($\forall x \in X$, $\forall t \in T$, $\forall co^{in}$, $co^{out} \in Co$ and $\forall p \in P$), if not noted differently. The list of symbols is given in Table 2.1.

The energy generation E^{out} of an ouput commodity (co^{out}) is fueled by input commodities co^{in}. In Figure 2.4, the reference energy system of an exemplary transformation process is shown. In the reference energy system, commodities are shown as vertical lines and transformation process as horizontal lines [10]. In the example, electricity is generated from natural gas via a turbine, the transformation process p.

The transformation losses between the input E^{in} and the ouput E^{out} are taken into account with the efficiency of the process η (equation 2.6). To simplify the notation, the index i for every single transformation unit[b] is introduced.

The total capacity C of a unit limits its maximal possible generation. Reduced average unit availability due to planned and unplanned outages are included with an availability factor af (equation 2.7).

For VREs the meteorologic availability of the resources has to be taken into account additionally. Just as for wind and solar energy, the power generation from run-off river hydro power plants is also subject to the natural availability of the resource, the water inflow. Run-off river hydro power plants are therefore described as VREs in the model as well (see also Subsection 2.3.2). Based on solar irradiation, wind speed and hydrologic

[b] With representative nodes, the index i refers to one transformation technology type and region.

data, the capacity factor $cf(t)$ is computed. It gives the degree of capacity utilization for every time step, model region and VRE input commodity. The generation from VREs is bound to follow the capacity factor defined by the meteorological availability (equation 2.8).

Limited flexibility in the operation of the transformation processes is captured in equation 2.9, where the up- and down-ramping of the units is restricted. This is particularly important for thermal power plants. Thermal power plants have to respect start-up times and minimal down times, once they have been shut down. When running, the maximal possible ramping depends on the utilization rate. Furthermore, minimal output levels can restrict the plant operation. In detailed power plant dispatch models, such as unit commitment problems, these restrictions are taken into account individually. This often requires the introduction of integer variables for the power plant operation status and is therefore computationally expensive. To avoid this Mixed Integer Programming in URBS, these restrictions are simplified and summed up in the ramping constraint τ_i instead of including them individually. Aboumahboub showed, that thanks to this ramping restriction, the results from the purely linear URBS model converges with those of a unit commitment model: the deviation in terms of discarded wind energy can be reduced by 91% for the example presented in Aboumahboub [1, Ch. 2.4].

The last two equations (equation 2.10 and 2.11) introduce the existing generation units c_i^0 and lower and upper limits for capacity expansion.

Symbol		Explanation
Sets	Size	
$x \in X$		Model regions
$t \in T$		Modeled time steps
$co, co^{in}, co^{out} \in Co$		Commodities
$Co^{vre} \subset Co$		Variable renewable commodities
$p \in P$		Generation process type
$i \in I$	$\lvert X \times P \times Co \times Co \rvert$	Generation unit
$I^{vre} \subset I$	$\lvert X \times P \times Co \times Co^{vre} \rvert$	Generation unit with variable renewable input
Variables	Domain	
$E_i^{in}(t)$	$T \times I$	Energy consumption (input)
$E_i^{out}(t)$	$T \times I$	Energy production (output)
C_i	I	Generation unit capacity
Parameters	Domain	
af_i	I	availability factor
η_i	I	transformation efficiency
τ_i	I	power change factor
$c_i^{0,min,max}$	I	Installed, minimal and maximal capacity
$cf_i(t)$	$I^{vre} \times T$	Capacity factor for VREs

Table 2.1.: List of symbols for generation processes. All variables and parameters are positive

Storage

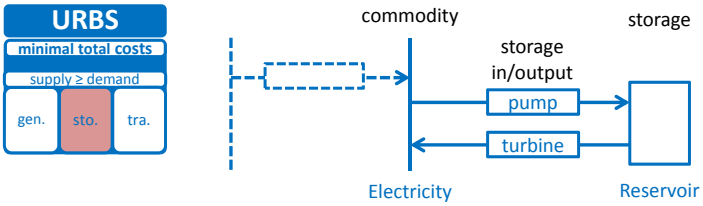

Figure 2.5.: Reference energy system for storage processes

$$V(\underbrace{st,co,x}_{j},t) = V(\underbrace{st,co,x}_{j},t-1) + ESt^{in}(\underbrace{st,co,x}_{j},t)\cdot\eta^{in}(\underbrace{st,co,x}_{j}) - ESt^{out}(\underbrace{st,co,x}_{j},t)/\eta^{out}(\underbrace{st,co,x}_{j})$$

$$V_j(t) = V_j(t-1) + ESt_j^{in}(t)\cdot\eta_j^{in} - ESt_j^{out}(t)/\eta_j^{out} \quad \forall t \notin \{t0, TF\} \tag{2.12}$$

$$V_j(t) \leq CSt_j \tag{2.13}$$

$$ESt_j^{in}(t) \leq CStin_j \tag{2.14}$$

$$ESt_j^{out}(t) \leq CStout_j \tag{2.15}$$

$$CSt_j = cSt_j^0 + CSt_j^N \tag{2.16}$$

$$cSt_j^{min} \leq CSt_j \leq cSt_j^{max} \tag{2.17}$$

$$CStin_j = cStin_j^0 + CStin_j^N \tag{2.18}$$

$$cStin_j^{min} \leq CStin_j \leq cStin_j^{max} \tag{2.19}$$

$$CStout_j = cStout_j^0 + CStout_j^N \tag{2.20}$$

$$cStout_j^{min} \leq CStout_j \leq cStout_j^{max} \tag{2.21}$$

Storage is described by the above equations, valid for all model regions, time steps, commodities and storage types ($\forall x \in X$, $\forall t \in T$, $\forall co \in Co$ and $\forall st \in St$), if not indicated differently. The list of symbols is given in Table 2.2.

For energy storage, the commodity is fed to the storage, stored in the reservoir and released later in time (see Figure 2.5). Equation 2.12 describes this process: storage input is denoted by ESt^{in} and discharge by ESt^{out}. The in- and output losses are taken into account via η^{in} and η^{out}. V tracks the stored energy across the time steps (equation 2.12). To simplify the notation, the index j for every storage unit or aggregated storage capacity per model region and type is introduced. Equation 2.12 is valid only if the previous time steps is included in the model, it is not thus not valid for the first modeled time step $t0$ for example.

To total storable energy is restricted by the storage size CSt_j in equation 2.13. Fur-

thermore, storage in- and ouput capacities need to be respected (equation 2.14 and 2.15). Equation 2.16 to 2.21 introduce the existing storage and lower and upper limits for in- and output capacity and storage size expansion.

Symbol		Explanation
Sets	Size	
$t0, tN$		First and last modeled time step
$st \in St$		storage type
$j \in J$	$\lvert X \times St \times Co \rvert$	storage unit
Variables	Domain	
$ESt_j^{in}(t), ESt_j^{out}(t)$	$J \times T$	Storage in- and output
$V_j(t)$	$J \times T$	Stored energy
$CStin_j$, $CStout_j$	J	Storage in- and output capacity
CSt_j	J	Storage size
Parameters	Domain	
$\eta_j^{in,out}$	J	In- and output efficiency
$cStin_j^{0,min,max}$	J	Installed, min. and max. storage input capacity
$cStout_j^{0,min,max}$	J	Installed, min. and max. storage output capacity
$cSt_j^{0,min,max}$	J	Installed, min. and max. storage size
$w(t)$	T	Weight of modeled time step

Table 2.2.: List of symbols for storage. All variables and parameters are positive

If only selected periods of the year are modeled, additional equations are necessary to ensure that the stored energy is accounted for correctly in the non-modeled periods. Figure 2.6 illustrates this problem: if the storage filling level at the beginning and end of a modeled period differ, this seasonally stored energy needs to be extrapolated to the next modeled period.

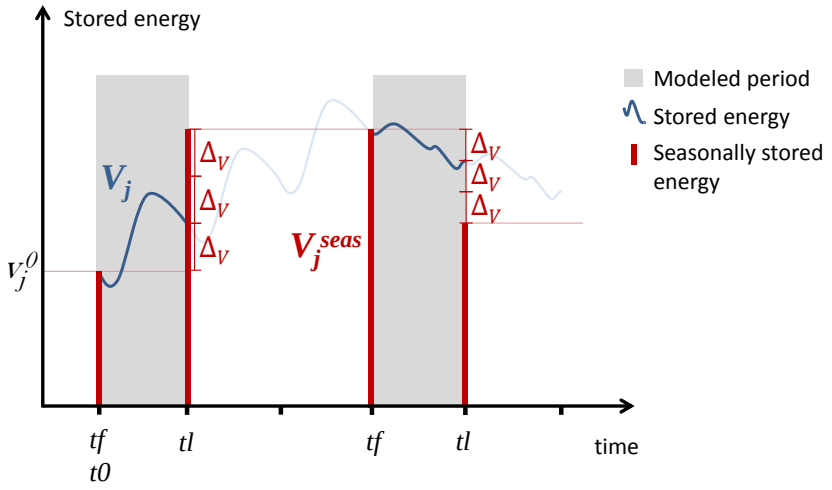

Figure 2.6.: Modeling seasonal storage

It is assumed that the modeled periods, stand for the non-modeled periods after it. If, for instance, every third week is modeled, this week stands for the two following weeks. Accordingly, a weight $w(t)$ of each modeled time step is introduced. It denotes for how many real time steps t^r the modeled time step t stands.

$$V_j^{seas}(tl_t) = V_j(tl_t) + (w(tl_t) - 1) \cdot \underbrace{(V_j(tl_t) - V_j^{seas}(tf_t))}_{\Delta_V(tl_t)} \quad \forall t \quad (2.22)$$

$$V_j^{seas}(tf_t) = V_j^{seas}(tl_{t-1}) \quad \forall t \quad (2.23)$$

$$V_j(tf) = V_j^{seas}(tf) + ESt_j^{in}(tf) \cdot \eta_j^{in} - ESt_j^{out}(tf)/\eta_j^{out} \quad \forall tf \neq t0 \quad (2.24)$$

$$V_j^{seas}(t0) = V_j(t0) \quad \forall t0 \quad (2.25)$$

$$V_j(t0) = v_j^0 \cdot CSt_j \quad \forall t0 \text{ (optional)} \quad (2.26)$$

$$V_j(t0) = V_j(tN) + (w(tN) - 1) \cdot (V_j(tl_{tN}) - V_j(tf_{tN})) \quad \forall t0, \forall tN \quad (2.27)$$

$$V_j^{seas}(te) \leq CSt_j \quad \forall te \in TE \quad (2.28)$$

$$V_j(t) \leq CSt_j + (w(t) - 1) \cdot (V_j(tl_t) - V_j(tf_t)) \quad \forall t \quad (2.29)$$

A counter V^{seas} for the seasonal storage is introduced. Equation 2.22 extrapolates the seasonal storage level across the non-modeled period. At the last time step of a modeled period tl_t, the counter for seasonal storage is set to the change in stored energy within the modeled period, Δ_V. This Δ_V is than also added for the non-modeled periods (see Figure 2.6).

Equation 2.23 carries over the seasonal storage to the next modeled period. At the first time step of the next modeled period tf_t, the amount of seasonally stored energy recorded in the counter V^{seas} is added to the stored energy V (equation 2.24). Normal usage of the storage unit, i.e., storage in- and output, can happen in the mean time in this first time step of the modeled period. For all other time steps, the normal storage equation (2.12) applies. For the notation of time steps see Table 2.3.

The initial level of seasonal storage is set to the stored energy in the first modeled time step $t0$ (equation 2.25). Optionally, the stored energy can be determined exogenously via v^0 (equation 2.26). To respect energy conservation, the stored energy at the final modeled time step tN needs to equal the initially stored energy. Again, the extrapolation of seasonally stored energy has to be included: the trend in seasonal storage after the end of the last modeled period needs to be taken into account as well. Equation 2.27 describes the stored energy for the last modeled time step tN.

Finally, the storage size has to be large enough to absorb also the seasonally stored energy (equation 2.28). As the variations of the stored energy within a modeled period are assumed to stand for the following periods, the storage size has to be sufficient to also accommodate these variations on top of the seasonally stored energy in non-modeled periods (equation 2.29). The third period depicted in Figure 2.6 shows such a case.

Symbol		Explanation
Sets	Size	
$t^r \in TR$		Real time steps
$t \in T, T \subset TR$		Modeled time steps
$tf \in TF, TF \subset T$		First time steps in modeled periods
$TF := \{t \vert (t_n - t_{n-1}) > (t^r_m - t^r_{m-1})\}$		
$tl \in TL, TL \subset T$		Last time steps in modeled periods
$TL := \{t \vert (t_{n+1} - t_n) > (t^r_m - t^r_{m-1})\}$		
$te \in TE, TE := TF \cup TL$		Edge time steps of modeled periods
tf_t, tl_t		First and last time steps for period of time step t
Variables	Domain	
$V^{seas}_j(te)$	$J \times TE$	Counter for seasonal storage
Parameters	Domain	
v^0_j	J	Storage filling level at $t0$

Table 2.3.: List of symbols for seasonal storage. All variables and parameters are positive

Transport

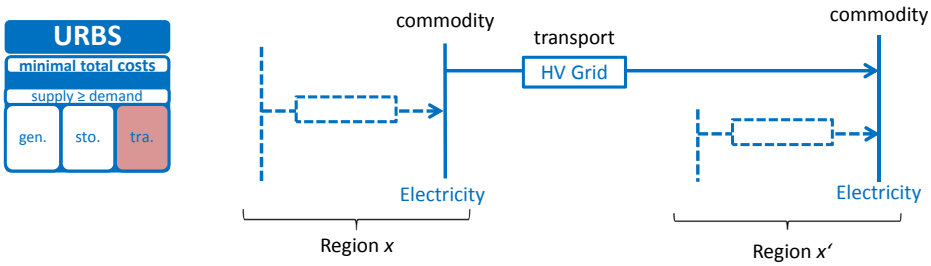

Figure 2.7.: Reference energy system for transport

$$F^{imp}(\underbrace{g, co, x, x'}_{k}, t) = (1 - \lambda(\underbrace{g, co, x, x'}_{k})) \cdot F^{exp}(\underbrace{g, co, x, x'}_{k}, t)$$

$$F^{imp}_k(t) = (1 - \lambda_k) \cdot F^{exp}_k(t) \tag{2.30}$$

$$F^{exp}_k(t) \leq CTr_k \tag{2.31}$$

$$CTr_k = cTr^0_k + CTr^N_k \tag{2.32}$$

$$cTr^{min}_k \leq CTr_k \leq cTr^{max}_k \tag{2.33}$$

Energy commodity transport is described by the above equations. They are valid for all time steps, commodities, grid types, and for all model regions and their neighbors ($\forall t \in T$, $\forall co \in Co$ and $\forall g \in G$, $\forall x, \in X$, $\forall x' \in \mathcal{N}(x)$). The list of symbols is given in Table 2.4.

As depicted in the in Figure 2.7, a commodity can be transported to another model region via a grid. The energy transport between regions is only possible if they are defined to be neighbors. Furthermore, transport losses are included. Equation 2.30 describes

this in a simplified notation, where k stands for an individual grid line or connection. Two positive variables are introduced: one for each direction. $F^{imp}(g, co, x, x', t) = F_k^{imp}$ stands for the import along a line k from the perspective of region x and F^{exp} for the export along this line. This approach allows to take into account the losses.

The capacity limit is applied to the export flow in equation 2.31. Equation 2.32 and 2.33 introduce the existing transport capacities and lower and upper limits for grid extensions.

Applying these equation to the commodity of electricity, a simplified simulation of electricity transmission between regions results. Kirchhoff's first law, the conservation of currents in each node of an electricity network, is respected in the model, while the second, the voltage law, is not included. Electricity transmission is thus modeled as a transport problem, neglecting effects of load flows. Subsection 2.4.1 compares this approach to a simplified load flow simulation.

Symbol		Explanation
Sets	Size	
$g \in G$		grid type
$k \in K$	$\lvert X \times \mathcal{N}(x) \times G \times Co \rvert$	grid line
Variables	Domain	Note: all variables are positive
$F_k^{imp}(t)$	$K \times T$	Import along grid line k
$F_k^{exp}(t)$	$K \times T$	Export along grid line k
Parameters	Domain	
λ_k	K	Losses along line k
$cTr_k^{0,min,max}$	K	Installed, minimal and maximal grid capacity

Table 2.4.: List of symbols for transport. All variables and parameters are positive

Energy balance

Having introduced all three possibilities to supply the energy demand in each region and time step, the energy balance can now be defined in detail.

$$\begin{aligned} d(co, x, t) \leq \sum_{p \in P} [\sum_{co^{in}} E^{out}(p, co^{in}, co, x, t) - \sum_{co^{out}} E^{in}(p, co^{out}, co, x, t)] \\ + \sum_{st \in St} [ESt^{out}(st, co, x, t) - ESt^{in}(st, co, x, t)] \\ + \sum_{\substack{x' \in \mathcal{N}(x) \\ g \in G}} [F^{imp}(g, co, x, x', t) - F^{exp}(g, co, x, x', t)] \qquad \forall co \in Co^{de} \end{aligned} \tag{2.34}$$

Equation 2.34 ensures, that the energy commodity demand d, for example the electricity load, is supplied in every model region x and every time step t. The supply can be met via local generation E^{out}, import F^{imp} or storage output ESt^{out}. Storage input ESt^{in}, export F^{exp} and other usage of the demanded commodity E^{in} have to be subtracted in the balance.

The commodity balance is valid only for demand commodities $co \in Co^{de}$ (see Table 2.5). In this thesis, the model is mainly applied to power systems, the most important demand commodity is therefore electricity. In Chapter 5, heat and hydrogen demand are included additionally. For stock commodities, such as coal or natural gas, but also for renewable resources, such as wind of solar, an infinite stock is assumed and thus no energy balance needs to be respected. Subsection 2.2.3 introduces secondary commodities for which a similar energy balance is valid.

Symbol		Explanation
Sets	Size	
$Co^{de} \subset Co$		Demand commodities
Parameters	Domain	
$d(co, x, t)$	$X \times T \times Co^{de}$	Demand for a commodity

Table 2.5.: List of symbols for the energy balance

Objective function

All above defined equations are boundary conditions to the cost-minimization carried out in URBS. The objective function of the optimization is the total cost function z. It gives the annual costs of energy supply for the modeled year.

$$z = K^{inv} + K^{fix} + K^{var} \tag{2.35}$$

$$K^{inv} = \sum_i \kappa_i^{inv} C_i^N + \sum_j (\kappa_j^{inv} CSt_j^N + \kappa_j^{inv,in} CStin_j^N + \kappa_j^{inv,out} CStout_j^N) + \frac{1}{2} \sum_k \kappa_k^{inv} CTr_k^N \tag{2.36}$$

$$K^{fix} = \sum_i \kappa_i^{fix} C_i + \sum_j (\kappa_j^{fix} CSt_j + \kappa_j^{fix,in} CStin_j + \kappa_j^{fix,out} CStout_j) + \frac{1}{2} \sum_k \kappa_k^{fix} CTr_k \tag{2.37}$$

$$K^{var} = \sum_t w(t) \cdot [\sum_i (\kappa_i^{fuel} + \kappa_i^{co2} + \kappa_i^{varO\&M}) E_i^{in}(t) + \sum_j (\kappa_j^{var} V_j(t) + \kappa_j^{var,in} EStin_j(t) + \kappa_j^{var,out} EStout_j(t)) + \sum_k \kappa_k^{var} F_k^{exp}(t)] \tag{2.38}$$

$$\kappa_i^{var} = \kappa_i^{fuel} + \kappa_i^{co2} + \kappa_i^{varO\&M} \tag{2.39}$$

The total costs consist of three parts. The first part, the investment costs K^{inv}, take into account the costs for capacity additions. Investments in energy infrastructure are commonly amortized over several years or decades, while the optimization is carried

out for one typical year only. Therefore, the annuity of the investment costs have to be used here. The annuity is the annual capital expenditure corresponding to the total investment. It is determined by the depreciation period and the interest rate. Its computation can be found in Annex C. The total investment costs are determined by the exogeneously defined specific investment costs (see Table 2.6) and the capacity additions for generation units, all three storage components and transport units repectively. As each grid connection between regions is included twice in the model – one for each direction – only half of the total capacities have to be included for the computation of the investment costs for transport.

The second part, the annual fixed costs K^{fix}, are the capacity dependent operation and maintenance costs. They arise for all, new and old capacity. Specific fixed costs per unit are defined exogenously.

The variable costs K^{var} occur for each generated, stored or transported unit. For generation units, the variable costs include the fuel costs, eventual costs for emission allowances and variable operation and maintenance costs. All renewable energy sources except bioenergy have no fuel costs. Variable costs for storage and transport are the variable operation and maintenance costs. If only selected periods of the year are modeled, these costs need to be weighted with $w(t)$ to give the total annual costs.

Symbol		Explanation
Variables		
$K^{inv}, K^{fix}, K^{var}$		Cost components
z		Total system costs
Parameters	Domain	
κ_i^{inv}	I	Annuity of investment costs for generation units
κ_i^{fix}	I	Fix O&M costs for generation units
κ_i^{var}	I	Variable costs for generation units
$\kappa_i^{fuel}, \kappa_i^{co2}, \kappa_i^{varO\&M}$	I	fuel, CO_2 and variable O&M costs for generation
$\kappa_j^{inv}, \kappa_j^{fix}$	J	Annuity of inv. and fix costs for storage
$\kappa_j^{inv,in/out}, \kappa_j^{fix,in/out}$	J	Annuity of inv. and fix costs for storage in- and output
κ_j^{var}	J	Variable storage in- and output costs
$\kappa_k^{var}, \kappa_k^{fix}, \kappa_k^{inv}$	K	Annuity of inv., fix and variable costs for transport

Table 2.6.: List of symbols for the total costs. All variables and parameters are positive

In addition to the total costs, the marginal costs of energy supply are an important result of the model, as they can be used as approximation for energy prices. These are obtained from the dual solution of the linear problem (see Annex B). The dual solution of a boundary equation gives the change in the objective function, if this restriction was relaxed by one unit. Thus, the dual solution of the energy balance equation (equation 2.34), gives the marginal costs of the energy supply. For electricity, assuming a fully competitive electricity market, these marginal costs are a good indicator of the wholesale electricity prices [16].

The model is formulated and optimized using the General Algebraic Modeling System (GAMS) software package and the CPLEX solver for linear optimization problems (see Annex B).

2.2.3. Additional model features

On top of the above described standard equations of the URBS model generator, additional features are introduced. The first is an approach to describe distributed generation without increasing the geographic resolution. Second, the concept of secondary commodities is presented together with additional boundary conditions. This allows to model more complex multi-commodity processes, such as combined heat and power generation (CHP) with URBS. Both of these feature are applied in the URBS-D model in Chapter 5.

Distributed generation

Through the aggregation of several generation units to one representative node, the requirements for decentralized or distributed generation units are neglected. While this approximation is justifiable for large centralized power or heat plants connected via a grid, distributed off-grid processes operate differently. The heat generation in a house for example, has to be proportional to the local heat demand. If all generation technologies are local generation units, the task to follow the hourly load within a model region can not be shared between peak and baseload technologies, like it is the case for power generation. Each local generation technology has to follow the hourly load, as it is not linked to the other generating units in the model region.

For the combined analysis of the power and heat sector in Chapter 5, an additional restriction for distributed generation is introduced following Richter [124] (valid $\forall x \in X, \forall t \in T, \forall co \in Co^{de}$, list of symbols in Table 2.8).

$$E^{out}(p, co^{in}, co, x, t) = \epsilon(p, co^{in}, co, x, t) \cdot \frac{d(co, x, t)}{\sum_{t'} d(co, x, t')} \quad \forall \{(p, co^{in}, co, x) \,|\, lg(p, co^{in}, co, x) = 1\} \tag{2.40}$$

The energy production of local, distributed generation units have to follow the local demand. Based on the assumption, that all small units (e.g. houses) within one model region have the same load profile, equation 2.40 is added to the model for local generation units. The generation profile E^{out} follows the normalized demand profile. Only the scaling factor ϵ, the total generation, is determined by the model, while the hourly dispatch is prescribed by the load profile.

Symbol		Explanation
Variables	Domain	
$\epsilon(p, co^{in}, coout, x)$	$P \times Co \times Co^{de} \times X$	Total local generation per unit
Parameters	Domain	
$lg(p, co^{in}, co^{out}, x)$	$P \times Co \times Co^{de} \times X$	Flag indicating local generation

Table 2.7.: List of symbols for distributed generation

Modeling multi-commodity flows and process chains

To model complex conversion processes, the inclusion of longer process chains in the model can be necessary. To represent a gas-fired combined heat and power (CHP) production for example, at least three different process steps are necessary: first, natural gas is burned in the gas turbine. One part of the generated energy is transformed to electricity, the other part is used to generate useful heat. The energy generated from burning the natural gas can be understood as an additional, intermediate commodity, as can be seen in Figure 2.8.

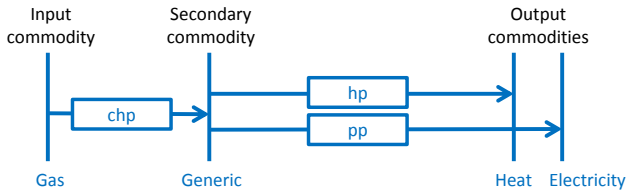

Figure 2.8.: Reference energy system for combined heat and power production. *chp* stands for the combined heat and power production, *hp* for heat production and *pp* for power production.

The secondary commodity introduced in the reference energy system creates the link between the three involved commodities: natural gas, heat and electricity. To respect energy conservation, an additional energy balance is introduced for the secondary commodities Co^{sec} in equation 2.41. This is in analogy to the energy balance for demand commodities in equation 2.34, except that demand for secondary commodities is zero.

$$\begin{aligned} 0 \leq & \sum_{p} [\sum_{co^{in}} E^{out}(p, co^{in}, co, x, t) - \sum_{co^{out}} E^{in}(p, co^{out}, co, x, t)] \\ & + \sum_{st} [ESt^{out}(st, co, x, t) - ESt^{in}(st, co, x, t)] \\ & + \sum_{g, x' \in \mathcal{N}(x)} [F^{imp}(g, co, x, x', t) - F^{exp}(g, co, x, x', t)] \quad \forall co \in Co^{sec} \end{aligned} \tag{2.41}$$

With the help of secondary commodities, process chains can be included in URBS models. In the above mentioned example, it allows to introduce two output commodities, while keeping the model structure concise.

For some processes, the share between different in- or output commodities needs to be restricted. In the example of CHP generation, the mix between heat and power production is set by the technical realization of the power plant. To include this process property, two additional equations are introduced. They allow to control the share of different in- and output commodities in the model ($\forall x \in X, \forall t \in T, \forall co \in Co$, list of symbols in Table 2.8).

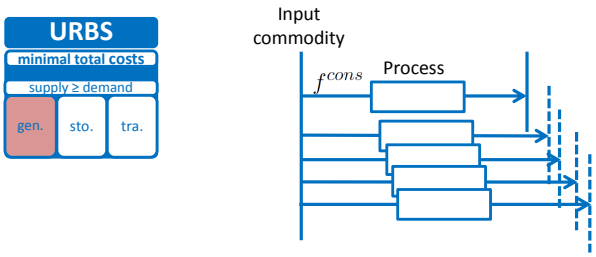

Figure 2.9.: Reference energy system for consumption share

$$Cons(x, co, t) = \sum_{p, co^{out}} E^{in}(p, co, co^{out}, x, t) + \sum_{st} ESt^{in}(st, co, x, t) + \sum_{g, x \in \mathcal{N}(x)} F^{exp}(g, co, x, x', t) + d(co, x, t) \quad (2.42)$$

$$E^{in}(p, co^{in}, co^{out}, x, t) = Cons(x, co^{in}, t) \cdot f^{cons}(p, co^{in}, co^{out}, x) \quad (2.43)$$

The above equations allow to define the share of one process in the consumption of a given input commodity. Equation 2.43 specifies which portion of a commodity co is consumed by one process, as shown in Figure 2.9. The total consumption of the commodity is defined in equation 2.42. In the example of the CHP plant, the consumption share is used to fix the power-to-heat ratio: only a certain, fixed share of the secondary commodity is consumed for heat supply, the other part is transformed to electrical power.

Similarly, the share of one generation process in all technologies producing a certain commodity can be defined ($\forall x \in X, \forall t \in T, \forall co \in Co$).

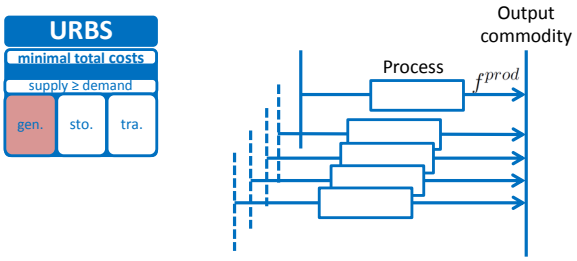

Figure 2.10.: Reference energy system for production share

$$Prod(x, co, t) = \sum_{p, co^{in}} E^{out}(p, co^{in}, co, x, t) + \sum_{st} ESt^{out}(st, co, x, t) + \sum_{g, x \in \mathcal{N}(x)} F^{imp}(g, co, x, x', t) \quad (2.44)$$

$$E^{out}(p, co^{in}, co^{out}, x, t) = Prod(x, co^{out}, t) \cdot f^{prod}(p, co^{in}, co^{out}, x) \quad (2.45)$$

The share of one process in the production of a given commodity co can be defined with equation 2.45. As shown in Figure 2.10, the relative contribution of one commodity flow within the total production of that commodity is defined. The total production $Prod$ is defined as the sum over all inputs to the output commodity co (equation 2.44). The fixed production share can be relevant for a fixed share of co-fireing for example.

Symbol		Explanation
Sets		
$Co^{sec} \subset Co$		Secondary commodities
Variables	Domain	
$Prod(x, co, t)$	$X \times T \times Co$	Total commodity production and import
$Cons(x, co, t)$	$X \times T \times Co$	Total commodity consumption and export
Parameters	Domain	
$f^{prod}(p, co^{in}, co^{out}, x)$	$X \times P \times Co \times Co$	Share of one generation unit in total commodity production per region
$f^{cons}(p, co^{in}, co^{out}, x)$	$X \times P \times Co \times Co$	Share of one generation unit in total commodity consumption per region

Table 2.8.: List of symbols for multi-commodity flows. All variables and parameters are positive.

Both additional model features can be illustrated with the example of distributed CHP generation.

As illustrated in Figure 2.11, heat and power are produced from the input commodity, natural gas, via a secondary commodity. The share of heat and power respectively is defined with consumption shares of the processes. Additionally, a peak load boiler is introduced with the help of another secondary commodity. The combined operation of the CHP plant and the peak load boiler need to supply the local demand profile. The local generation constraint is thus applied to the last process in the chain, which generates heat to supply the local demand.

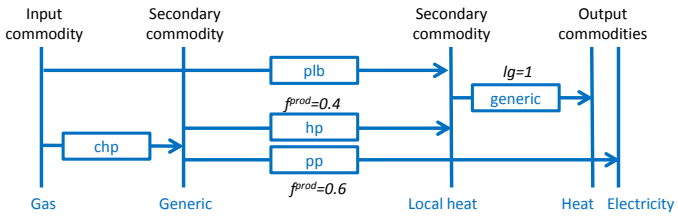

Figure 2.11.: Reference energy system for distributed combined heat and power production. *chp* stands for the combined heat and power production, *hp* for heat production, *pp* for power production and *plb* for the peak load boiler.

2.2.4. Model setup

The size of above described model increases considerably with the number of modeled time steps and regions as shown in Figure 2.12. Choosing the model regions and time steps, a compromise between high resolution and a manageable size of the optimization problem has to be found.

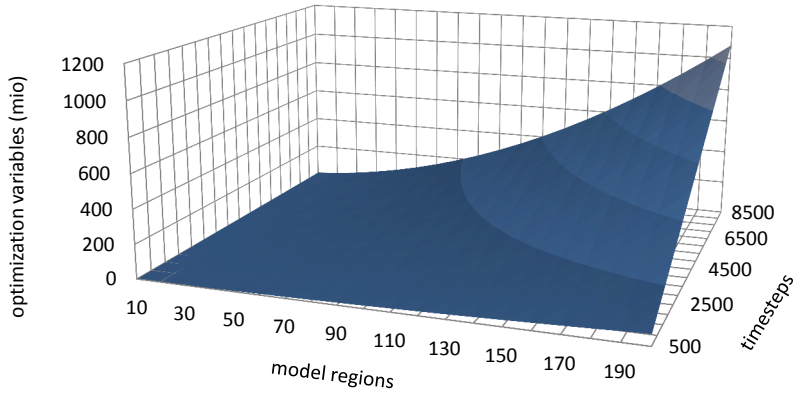

Figure 2.12.: Size of the optimization problem in dependence of regions and time steps. In this example, full interconnection between regions, 3 supply commodities, 10 generation processes, 1 storage and 1 grid technology are assumed.

Selection of representative time steps

In the temporal domain, hourly resolution is chosen. The model is applied to one typical year. However, modeling every hour of the year would result in large model size (see Figure 2.12). In a lot of time steps, very similar problems will be solved, for example a windy afternoon in winter, an afternoon in autumn without wind or solar supply, or a sunny summer day. Therefore, instead of modeling an entire year, representative periods of the year, for example, weeks or days, are modeled to reduce the model size.

Those representative periods are chosen according to the following criteria in order to closely reflect the properties of the entire year.

- The average residual load in the selected time steps should be close to the average annual residual load.
- The selected time steps should include extreme values of residual load.
- The seasonal cycle, daily cycle and ideally also weekly cycle of the year should be reflected in the representative time steps.

These criteria translate into an optimization problem, which allows to determine representative time steps.

$$\text{Objective function: } min[\overline{\Delta_{t^r}} - \overline{\Delta_t}] \tag{2.46}$$

where Δ_t is the residual load:

$$\Delta_t = \sum_x (d(co, x, t) - \sum_{p, co^{in} \in Co^{vre}} E(p, co, co^{in}, x, t))$$

Boundary conditions: include period with minimal residual load
include period with maximal residual load
select contiguous periods
distribute representative periods equally over the year

The optimization is solved via exhaustive search. First the periods with minimal and maximal residual load are identified. The remaining periods are then chosen such that the deviation of the average residual load of the selected time steps and the annual average is minimal. The solution of this optimization problem provides representative periods of the year, which can than be analyzed in the URBS model. As shown in Heitmann, a careful selection of the representative periods allows to achieve better results: modeling few, carefully selected periods allows to achieve similar results to a case where longer periods of the year are included in the model [65].

In this thesis, six weeks (1008 time steps) are chosen with the above described methodology. One time steps thus stand for about eight hours of the year. The modeled time steps are weighted accordingly. The weighting is uniform. Depending on the share and mix of VREs in the analyzed scenarios, the representative weeks are different.

Symbol	Explanation
Sets	
t^r	Real time steps, e.g. [1,...,8760]
Variables	
t	Selected time steps, length: $DP \cdot NP$
Parameters	
Δ_{t^r},Δ_t	Residual load

Table 2.9.: List of symbols for choice of time steps

The optimization can be applied to any commodity, i.e., the representative times steps can be chosen with respect to any residual load. In this thesis, the representative time steps are chosen with respect to the residual load for electricity.

Model regions

The areas of interest, Europe or Germany, are divided in regions modeled as representative nodes. The model regions are defined in accordance to the transmission grid topology and the control areas of Transmission System Operators (TSOs). The individual

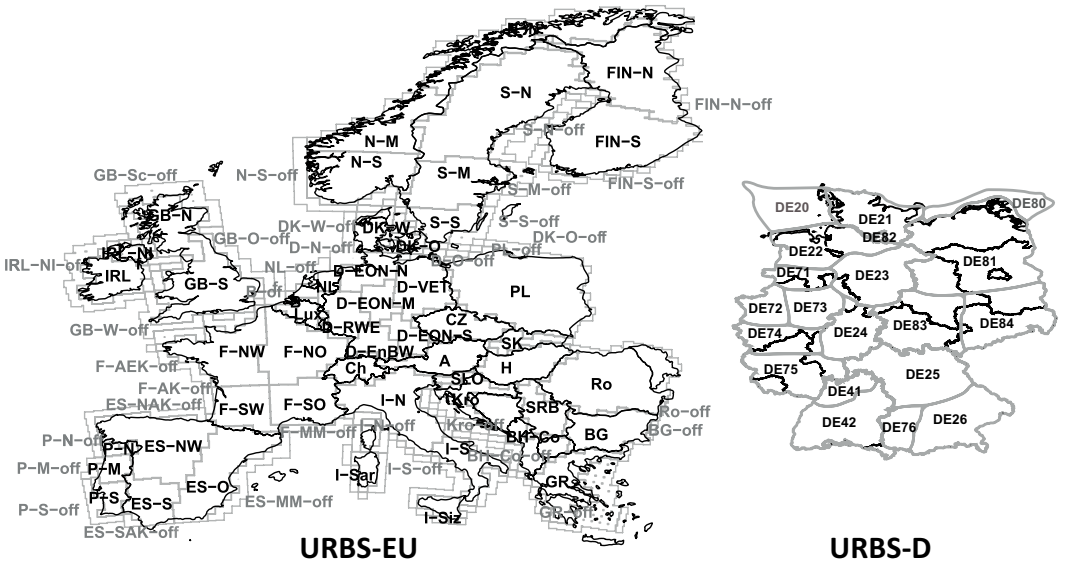

Figure 2.13.: Model regions for Europe and Germany

generation and storage units, as well as transmission lines are aggregated to representative nodes in each model region. Storage and power plant capacities are summed up for each model region. The technological properties such as efficiencies, ramping, etc. are determined based on average technology standards. Transmission grid capacity is aggregated based on the natural power of each individual line (see Subsection 2.3.4).

For the application of the model to Europe (URBS-EU, Chapter 3 and 4), 50 onshore and 33 offshore regions are assumed based on Heide et al. [64]. They approximately reflect the TSO regions in Europe (Figure 2.13). For the analysis of Germany in Chapter 5, the TSO control areas are sub-divided to 18 on- and 2 offshore regions, following the German Energy Agency dena [30]. These regions reflect comparatively well connected areas.

2.3. Model data

The input parameters to the model describe the current power system as well as the characteristics and specific costs of the technologies. The URBS model generator is applied to the European power sector (Chapter 3 and Chapter 4) and expanded to the German heat and hydrogen sector in Chapter 5. This section describes the input parameters to the model for both applications. Additional data necessary for the analysis in Chapter 5 is presented there. First, the general costs assumptions are given, followed by the the meteorologic and load data and the power system infrastructure data.

2.3.1. Assumptions on costs and technical parameters

The assumptions for the specific investment, fixed and variable costs for conventional power plants and the transmission grid are shown in Table 2.10. The assumptions are based on literature [75, 101, 122] and a detailed study of different transmission technologies and projects (Subsection 2.3.5).

Technology	Inv. Costs €/kW$_{el}$	Fix O&M Costs €/kW$_{el}$	Fuel Costs €/MWh$_{th}$	Var. O&M Costs €/MWh$_{el}$	CO_2 intensity t/MWh$_{th}$	Var. Costs + CO_2 Costs €/MWh$_{el}$
Bioenergy	2500	50	5	4	-	18
Coal	1400	35	8	4	300	21 + 22
Gas GT[a]	400	18	25	1	200	68 + 16
Gas CCGT[b]	650	18	25	1	200	44 + 10
Geothermal	2800	80	0	4	-	4
Lignite	2300	40	4	4	400	13 + 28
Oil GT	800	18	44	2	310	126 + 27
Oil CCGT	900	18	44	1	310	89 + 18
Nuclear	3000	65	3	2	-	12
Hydro run of river	1400	20	0	5	-	5
Hydro storage	900	20	-	-	-	-
Hydro reservoir[c]	6.5	-	-	-	-	-
HV lines[d]	400	1	-	-	-	-
HV cable[d]	1300	1	-	-	-	-

Table 2.10.: Specific investment, fixed operation & maintenance and total variable costs for all regions (κ). The fuel costs are given in €/MWh$_{th}$, while the total variable costs take into account the transformation losses (see Table 2.12). Carbon certificate costs per MWh$_{el}$ are computed based on a carbon price of 30 €/t.

[a] Gas Turbine, [b] Combined Cycle Gas Turbine, [c] €/kWh, [d] €/MWkm

For the computation of the annuity of investment, a weighted average cost of capital (WACC) of 7% is assumed, depreciation periods are given in Table C.1 (see also Annex C). The costs for carbon allowances are computed based on the carbon intensity of the respective fuels.

Technology	*High* Inv. Costs (€/kW$_{el}$)	*Medium* Inv. Costs (€/kW$_{el}$)	*Low* Inv. Costs (€/kW$_{el}$)
Wind Onshore	1600	1000	800
Wind Offshore	3400	2000	1000
Solar Photovoltaic (PV)	2000	1100	600

Table 2.11.: Cost scenarios for VRE technologies. Fix costs are assumed at 2% of the investment costs, variable costs are zero.

The costs for VRE technologies have reduced considerably in the last years and are projected to do so in the future [51, 57]. Therefore, different costs scenarios for the VRE technologies are used throughout this thesis (Table 2.11), where the *High* costs scenario roughly corresponds to current costs and the *Medium* and *Low* investment costs cases are two projections for their future development.

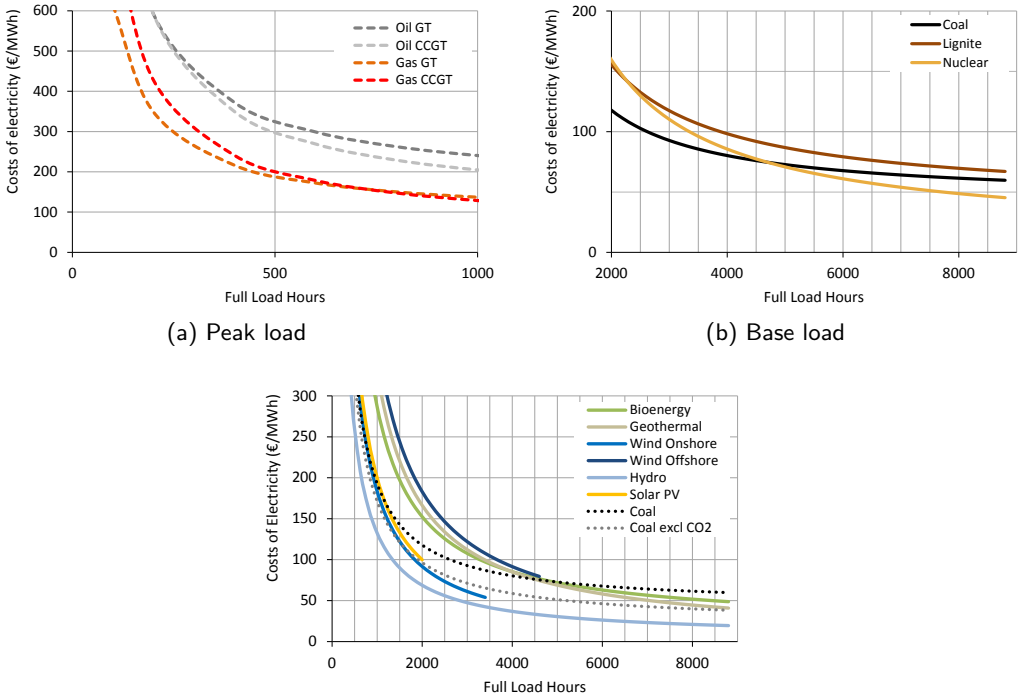

(a) Peak load

(b) Base load

(c) Renewable energies (High Costs)

Figure 2.14.: Cost of electricity for renewable energy, peak and baseload technologies. The costs include the costs for emission allowances at a carbon price of 30 €/t.

Figure 2.14 shows the specific costs of electricity (CoE) as a function of the Full Load Hours (FLHs) with a carbon price of 30 €/t. The corresponding total annual costs per kW/a curves are shown in so-called screening curves in Figure 2.15. Screening curves are defined by the fixed capital and O&M costs at the intercept and the variable costs as slope. From these screening curves, or the CoE, the role of the different power plants can be identified. At low utilization rates, Gas GT or Gas CCGT power plants are the cheapest option. These are peak load technologies. High FLHs are advantageous for technologies with high investment and fixed costs, but low variable and fuel costs. This is the case for base load technologies such as nuclear or coal power. Renewable energies have very low or zero variable costs, but high investment costs. To be competitive with conventional power plants, high utilization rates or reduced investment costs are neces-

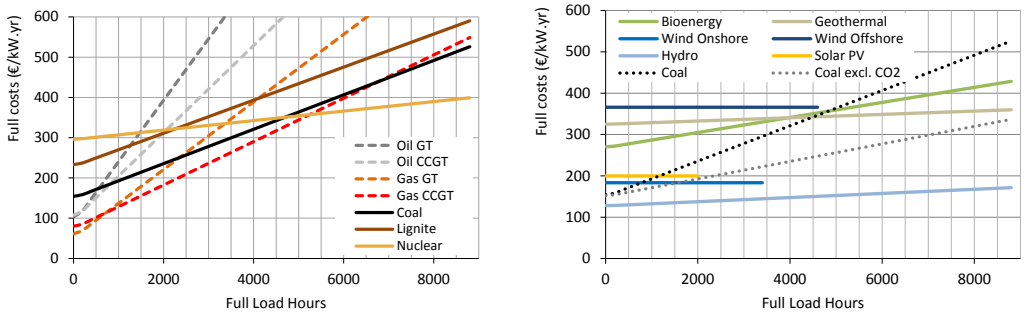

(a) Fossil fuels

(b) Renewable energies (High Costs)

Figure 2.15.: Full costs for renewable energy and conventional technologies. The costs include the costs for emission allowances at a carbon price of 30 €/t.

sary. In Figure 2.14c and Figure 2.15b, the high cost scenario is shown. In this scenario, Onshore wind is competitive with coal from 750 FLHs on and solar PV from 1100 FLHs, if there is a carbon price of 30 €/t. Without carbon price, wind is competitive at FLHs of 1500 and solar PV at unrealisticly high FLHs of 2000.

Technology	η %	λ %/1000km	af %	τ %/h
Bioenergy	38%	-	40%	25%
Coal	46%	-	80%	22%
Gas GT	38%	-	100%	100%
Gas CCGT	60%	-	90%	22%
Geothermal	100%	-	100%	25%
Lignite	43%	-	80%	14%
Oil GT	35%	-	100%	100%
Oil CCGT	50%	-	90%	22%
Nuclear	33%	-	80%	8%
Hydro run of river	75%	-	100%	100%
Wind Onshore	100%	-	100%	100%
Wind Offshore	100%	-	100%	100%
Solar PV	100%	-	100%	100%
Hydro storage	85%	-	100%	100%
HV lines	-	4%	100%	100%
HV cable	-	4%	100%	100%

Table 2.12.: Technical parameters: efficiencies, transmission losses, availability factors and ramping constraints

Table 2.12 lists the technical parameters, such as conversion and storage efficiencies η_i, transmission losses λ_i, restricted availability af_i and ramping constraints τ_i. The ramping constraints include the technical ramping restrictions for each individual power

plant, but also the inertia of the aggregated generation capacity per generation technology in each model region. Some power plants might be shut off and have to respect minimal time of non-use or cold start restrictions. This inertia outweighs the effect of increased ramping flexibility in a larger power plant fleet and the aggregated ramps are slower than the individual ones, as the benchmark of an URBS model to a detailed plant-specific unit commitment model by Aboumahboub shows [1]. The results from the unit commitment model can only by reproduced with URBS, if slower ramp rates are assumed.

2.3.2. Meteorological and load data

To determine the weather-dependent availability of wind and solar energy supply, highly resolved weather data provided by Heide et al. [64] is used. They derived the hourly capacity factors for wind and solar energy based on an eight years dataset (2000-2007) of highly resolved (50 km) reanalysis data [105]. The aggregation of capacity factors from the 50 km cells to the European model regions is based on a wind and solar capacity distribution across the 50 km cells determined in accordance to planned projects, national policies and actual potential [15]. Most recent wind turbine generators and solar PV are assumed. Figure 2.16 shows the FLHs per model region in Europe.

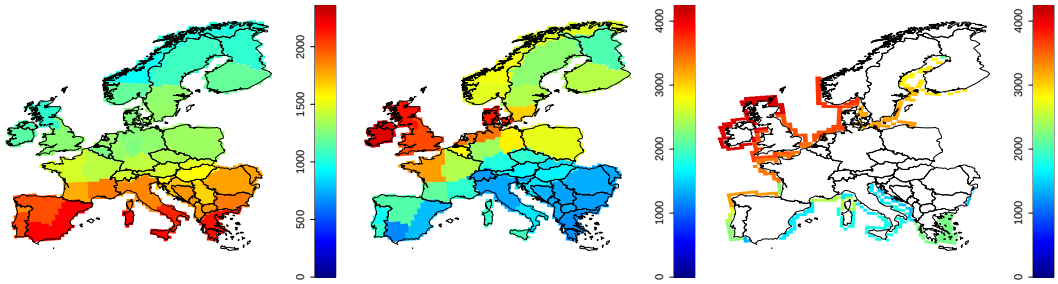

(a) Solar Photovoltaics (b) Wind Onshore (c) Wind Offshore

Figure 2.16.: Full load hours based on meteorological data [15]

Seasonal variations in run-of-river hydro power availability is taken into account through monthly values of hydro power production. The monthly values are determined based on an hydrological model (WATER-GAP, [26]) and shown in Figure 2.17. For regions with little hydro power capacity (Czech Republic, Germany, Denmark, France, Great Britain, Poland and Slovakia) a constant output of the run-of-river plants over the whole year is assumed. This predefined supply of hydro thus is a VRE source as well.

Hydro power plants disposing of a reservoir are more flexible. Therefore a certain share (10% - 15%) of the hydro power plant capacity is assumed to be flexible and freely dispatchable. This share is chosen in accordance to the character of the hydro power plants for each model region: regions with more reservoir power plants have a

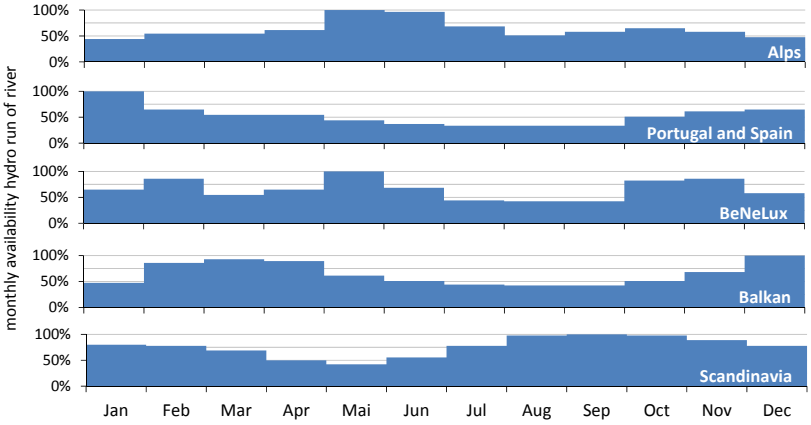

Figure 2.17.: Monthly hydro power availability [26]. Alps include Austria, Switzerland and Italy; BeNeLux includes Belgium, the Netherlands and Luxembourg; Balkan includes Albania, Bosnia, Bulgaria, Greece, Croatia, Romania, Slovenia and Hungary; Scandinavia includes Finland, Norway and Sweden.

larger share of flexible hydro power capacity.

The hourly load curve for the years 2000 - 2007 stems from the ENTSO-E [46] and is scaled to total consumption data given by the International Energy Agency (IEA) [77].

2.3.3. Power plants

To determine the installed power plant and pumped hydro storage capacity per model region, a geo-referenced power plant database is established. The database combines the UDI power plant database [120] and a second data base including geographic location, energy production and emissions of each power plant [152]. Coupling these two datasets on power plant level provides a powerful and exhaustive geo-referenced database for Europe. For modeling purposes, the power plant types are aggregated by fuel and conversion technology. The aggregated capacity per region and type is shown in Figure 2.18. The pumped hydro storage in- and output capacities are included in the database. The storage size is estimated based on the German average reservoir size of 6.5 hours [88].

The UDI database includes the age of the power plants and thus future power plant fleet per region can be extrapolated with technology specific lifetimes (see Table E.1). The capacity depreciation of the existing European power plant capacity due to retirements is shown in Figure 2.19.

2.3.4. Transmission grid capacities

In the European and the German model setup, electricity transmission is modeled on an aggregated level based on the representative nodes. This section explains the principal

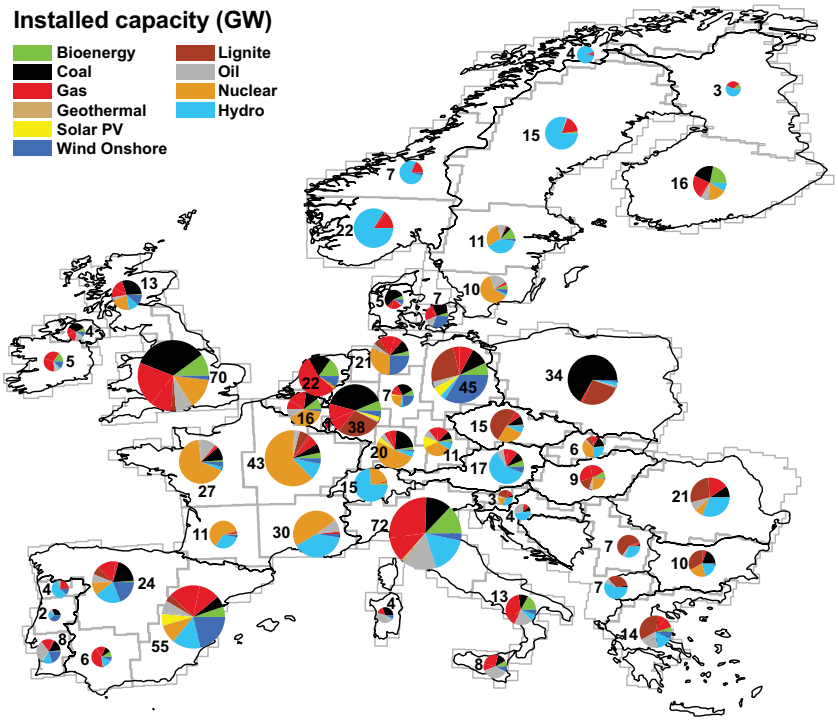

Figure 2.18.: Installed power plant capacity per model region (the German nuclear moratorium is not included in this database)

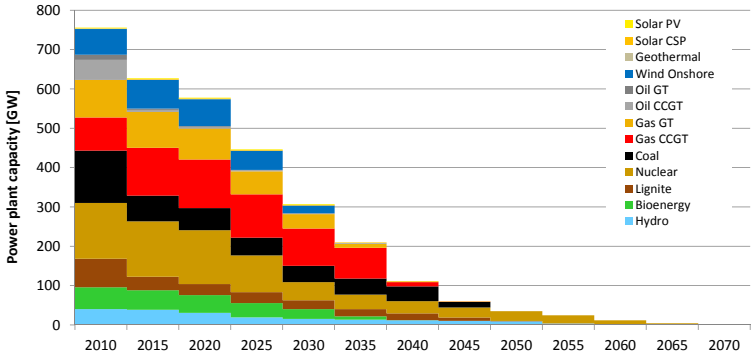

Figure 2.19.: Capacity depreciation in Europe

properties of electricity transmission including the concept of natural power, which is used for the aggregation of existing transmission grid capacities.

Principal properties of AC electricity transmission

High voltage electricity transmission in Europe is mainly realized via alternating current (AC) systems. The synchronous ENTSO-E grid is a three phase AC system running at

the grid frequency of 50 Hz. Its voltage levels are 220 and 380 kV. For stable system operation, voltage and frequency levels must be kept within certain thresholds.

In an AC system, voltage and current follow a sinusoidal function with ω being the system's frequency and $\varphi_{U/I}$ the respective phase (for a detailed description see [84]):

$$I(t) = I_0 \sin(\omega t + \varphi_I) \tag{2.47}$$

$$U(t) = U_0 \sin(\omega t + \varphi_U) \tag{2.48}$$

In the complex plane voltage and current are oscillating vectors (see Figure 2.20a). Their relative position is described by their relative phase $\varphi = \varphi_U - \varphi_I$ resulting from the impedance of the system $\mathbf{Z} \epsilon \mathbb{C}$ ($\mathbf{U} = \mathbf{Z} \cdot \mathbf{I}$). Ohmic systems cause no phase-shift between voltage and current ($\varphi = 0$), inductive systems a delay of the current ($\varphi > 0$, counting counterclockwise) and capacitive systems a delay of the voltage ($\varphi < 0$).

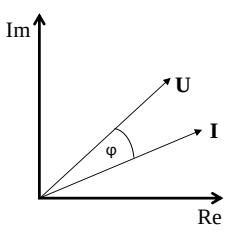

(a) Voltage and current in the complex plane for an inductive system

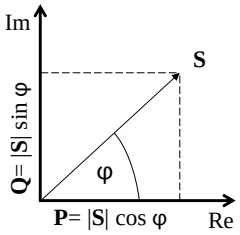

(b) Apparent power in the complex plane

Figure 2.20.: Voltage, current and apparent power in the complex plane

The momentary complex power resulting from $\mathbf{U}(t)$ and $\mathbf{I}(t)$, is composed by its real and complex part. The real part can be computed based on above definitions[c] and the complex part deduced accordingly based on Euler's formula ($e^{i\varphi} = \cos\varphi + i \sin\varphi$).

$$\mathbf{p}(t) = \mathrm{Re}\{\mathbf{p}(t)\} + i\,\mathrm{Im}\{\mathbf{p}(t)\} \tag{2.49}$$

$$\mathrm{Re}\{\mathbf{p}(t)\} = I(t) \cdot U(t) = \frac{1}{2} U_0 I_0 \left[\cos(\varphi_U - \varphi_I) - \cos(2\omega t + \varphi_U + \varphi_I)\right] \tag{2.50}$$

$$\mathrm{Im}\{\mathbf{p}(t)\} = \frac{1}{2} U_0 I_0\, i \left[\sin(\varphi_U - \varphi_I) - i \sin(2\omega t + \varphi_U + \varphi_I)\right] \tag{2.51}$$

$$\Rightarrow \mathbf{p}(t) = \frac{1}{2} U_0 I_0 \left[e^{i(\varphi_U - \varphi_I)} - e^{i(2\omega t + \varphi_U + \varphi_I)}\right] \tag{2.52}$$

Introducing the complex effective voltage and current, the complex power can be

[c] applying $\sin a \sin b = \frac{1}{2}\left[\cos(a-b) - \cos(a+b)\right]$

decomposed in its constant, effective part and an oscillating term.

$$\hat{\mathbf{U}} = \frac{U_0}{\sqrt{2}} e^{i\,\varphi_U} = \hat{U} e^{i\,\varphi_U} \tag{2.53}$$

$$\hat{\mathbf{I}} = \frac{I_0}{\sqrt{2}} e^{i\,\varphi_I} = \hat{I} e^{i\,\varphi_I} \tag{2.54}$$

$$\mathbf{p}(t) = \hat{\mathbf{U}}\hat{\mathbf{I}}^* - \hat{\mathbf{U}}\hat{\mathbf{I}}\, e^{i2\omega t} \tag{2.55}$$

The effective complex power is called apparent power $\mathbf{S}$. It consists of a real part, the active power P and a complex part, the reactive power Q. As equation 2.57 and 2.58 show, the phase shift φ determines the absolute value of active and reactive power. The active power is maximal, if φ is zero (see Figure 2.20b).

$$\mathbf{S} = \hat{\mathbf{U}}\hat{\mathbf{I}}^* = \hat{U}\hat{I} e^{i(\varphi_U - \varphi_I)} = P + iQ \tag{2.56}$$

$$P = \hat{U}\hat{I}\cos\varphi \tag{2.57}$$

$$Q = \hat{U}\hat{I}\sin\varphi \tag{2.58}$$

The relative phase φ between two nodes is determined by their relative impedances. Here, not only the generator's and consumer's impedance, but also the impedance of the line itself has to be taken into account. Along the transmission line, ohmic losses occur, but also capacitive and inductive losses take place. The resulting total impedance of the line $\mathbf{Z_0}$ is called characteristic impedance. Differences between the characteristic impedance and the consumer's impedance lead to a difference in reactive power, which needs to be balanced along the transmission line. The transmission of reactive power however causes voltage drops and can therefore not be realized over long distances [e.g. 85]. It furthermore reduces the transmitted active power (see Figure 2.20b). To transmit the maximum of active power from a to b, no reactive power should be transmitted.

This can be achieved by imposing the characteristic impedance at end of the line, i.e., compensating the effect of the transmission line itself to the power transmission. This corresponds to transmitting the so-called natural power,

$$P_{nat} = \frac{U_a^2}{Z_0}\,, \tag{2.59}$$

where U_a is the voltage level at the exporting node. The transmission of natural power underlies ohmic losses only and no balancing of reactive power is necessary. Table 2.13 gives the natural power and thermal transmission limits for typical HVAC transmission systems.

As the natural power lies well below the thermal transmission limits, transmission lines are not always operated on their natural power. To balance the mismatch in reactive power, compensation measures are taken, through the addition of capacitive or inductive elements.

Voltage level	line type	thermal limit [MW]	natural power [MW]
220 kV	2 x Al/St 265/35	246	175
380 kV	4 x Al/St 240/40	1700	600

Table 2.13.: Natural power and thermal transmission limits of typical 220 and 380 kV AC transmission overhead lines [85]

Transmission capacities assumed in the model

In the model, it is assumed that all electricity transmission is carried out at the level of natural power. As the comparison to the thermal transmission limits shows (Table 2.13), this is a very conservative assumption, but it ensures, that stable system operation is possible, as no voltage drops occur or no balancing of reactive power is necessary.

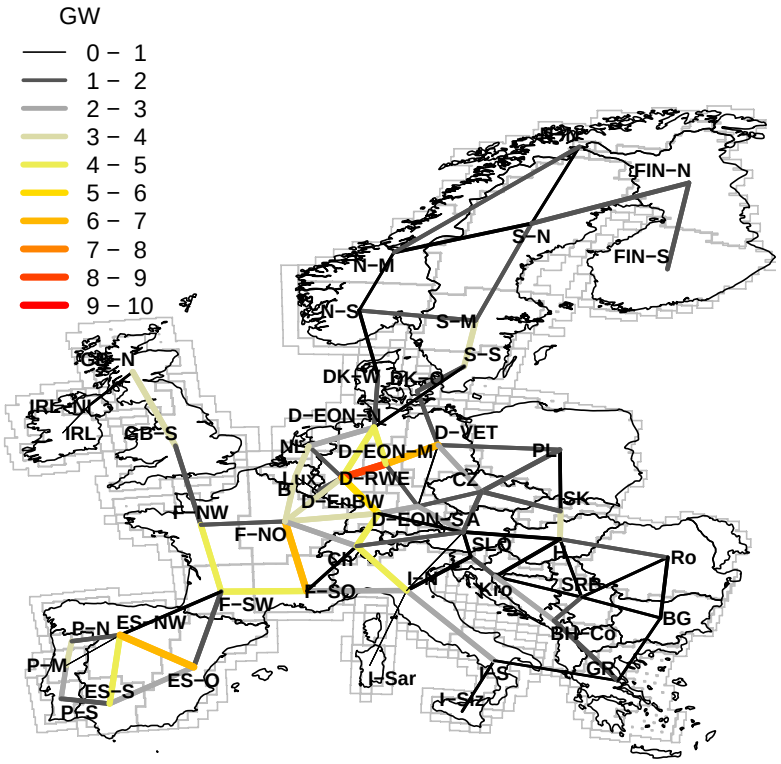

Figure 2.21.: Transmission capacities between model regions (based on the natural power)

To determine to total available transmission capacity between two model regions, the existing 220 and 380 kV lines are aggregated based on their natural power shown in Table 2.13. For international connections, the Net Transfer Capacities (NTCs) published

by the ENTSO-E are respected [48]. The NTCs are determined based on detailed load flow simulations and reflect the ability of the respective national transmission networks to import or export electricity. They are not necessarily the physical limit of the interconnection. This is a second assumption ensuring stable system operation, given the simplified simulation of electricity transmission.

Today's HV transmission network is obtained from freely available data on the European high voltage (HV) electricity grid (220kV and 380kV) [46]. A Geographic Information System is applied to intersect the individual transmission lines and cables provided in the ENTSO-E map with the model regions in order to determine the total transmission capacity between two representative nodes, based on the natural power. The obtained existing transmission capacities between model regions are shown in Figure 2.21.

2.3.5. Transmission technologies and costs

The different technological options for transmission grid extensions and their costs are presented in this section. This provides a sound basis for the costs assumptions introduced above in Table 2.10.

For overhead transmission, HVAC lines are used almost exclusively today. This technology has the benefit of more than 60 years of experience. However, direct current transmission (DC) has the advantage of higher current densities as the effective voltage is higher and the skin-effect does not occur. As a consequence, the losses per conductor area are lower and less space is required for the transmission of a given capacity.

Figure 2.22 compares the relative losses between the technologies [136]. For HVDC technologies, conversion losses occur, but the length-dependent losses are smaller than for HVAC overhead transmission. For connections larger than about 250 km this advantage leads to a higher overall efficiency of HVDC systems compared to HVAC overhead transmission.

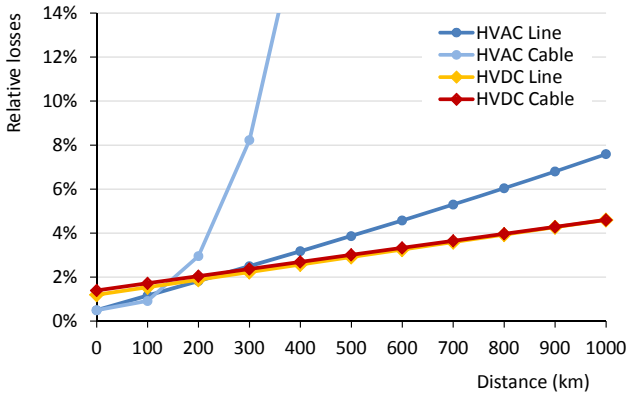

Figure 2.22.: Estimation of relative losses per technology (after Siala [136])

The required space for transmission lines can be described by their row of way (ROW). For overhead lines the ROW is the pylon width plus a safety strip which takes into account the swaying of the lines. It is shown for different HVAC and DC transmission system in Figure 2.23 together with the number of pylons or cable systems necessary to transmit 10 GW.

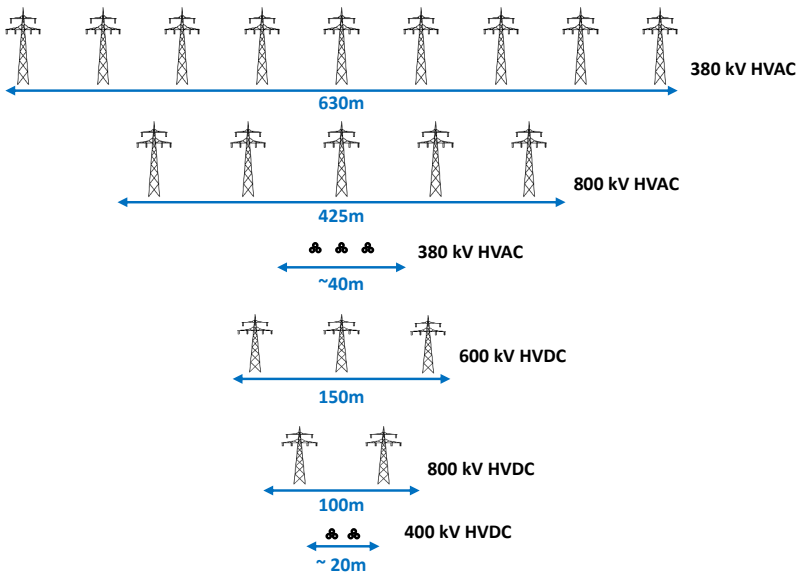

Figure 2.23.: Right of way for and required number of pylons to transmit 10 GW [136, 99]

For offshore connections power transmission has be realized in cables, but also for onshore connections, cable-based transmission is discussed to address public concerns. Again, alternating or direct current systems are available.

In HVAC cable systems, the three phases lie very close to each other and the capacitive coupling between them induces charging flows and causes losses which are rising steeply with length, as depicted in Figure 2.22. Compensation facilities are necessary every 20 - 30 km to balance the reactive power. HVAC cables are therefore not suitable for offshore connections. HVDC cables are the only possibility for off-shore transmission. There construction is very space-efficient (see Figure 2.23), but large costs due to their more complex construction occur.

Figure 2.24 shows the result of a literature survey by Siala on the specific costs per technology for a transmission length of 100 km [136] . The costs of transmission systems vary considerably not only across technologies, but also from project to project. The differences are mainly driven by the geography and soil characteristics. Whether a line is built across mountains or a flat open space, for example, has an important influence on the costs. While for DC systems, an important share of the costs is due to the converter stations at the beginning and end of the line, the length dependent costs per MW and

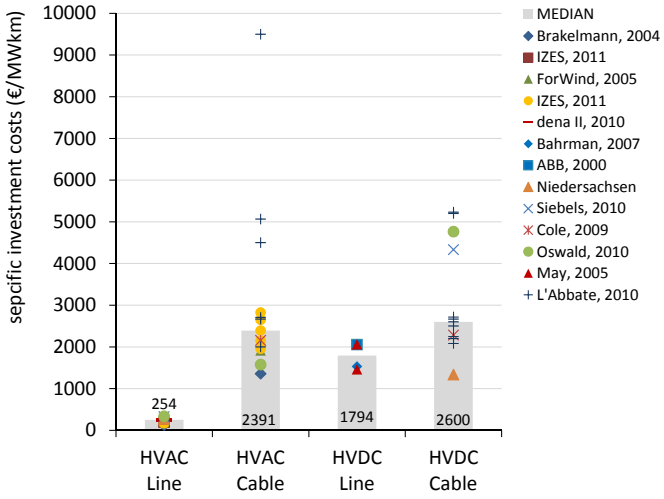

Figure 2.24.: Comparison of specific investment cost of the transmission technologies for a transmission length of 100 km [136]. The costs are given per MW of thermal transmission limit P_{therm}. Primary references are [127, 9, 19, 30, 116, 91, 89, 99, 107, 117, 137].

km are lower for DC systems as they have a smaller ROW and require less material for conductors, pylons, etc. At 600 km, the costs for the overhead systems amount to 235 and 360 €/MWkm for AC and DC respectively. They are thus a lot closer than the costs for 100 km of 245 and 1794 €/MWkm for AC and DC.

In the model, HVDC cables are assumed for all offshore connections. Based on the literature review, specific investment costs of 2500€/MWkm are assumed, accounting for a slight reduction of the investment costs in the future.

The different technological options for overhead lines are not taken into account in the model, as the transmission lines are not modeled individually, but aggregated to transmission corridors. The inclusion of different technologies would require a more detailed modeling approach, than the one chosen here. Consequently, a generic overhead transmission technology is assumed, with specific investment costs of 400 € per km and MW (natural power). In the model, the power transmission is limited by the natural power P_{nat}, while the costs from literature are provided in € per MW thermal limit. The above mentioned 235 €/MWkm for HVAC lines translate to 540 € per km and MW natural power for a transmission length of 600 km. For HVDC system, the costs remain the same: 360 €/MWkm. The cost assumption in the model this lies between the HVAC and HVDC technology, for a typical length of transmission in Europe.

For both technologies, losses of 4% per 1000 km are assumed.

2.4. Model benchmark

2.4.1. Simulation of electricity transmission

As described above, when applying the URBS model equations to the power system, a simplified simulation of electricity transmission between regions is carried out. Electricity transmission is modeled as a transport problem, neglecting the nature of AC load flows.

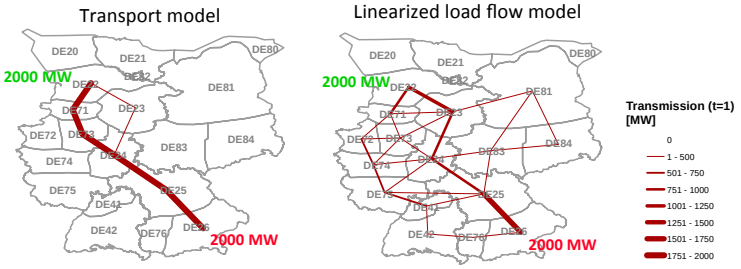

Figure 2.25.: Comparison of power flow with transport and linearized load flow model for a simple example of lossless transmission from North to South

Figure 2.25 illustrates the fundamental shortcoming of the transport model for a simple example of lossless power transmission of 2000 MW in Germany from north to south. The left side shows the maximal power flow resulting from the transport model, used in this thesis, the right side the results from a simplified load flow simulation. While with the transport model, the shortest distance is used almost exclusively (the second branch used is due to capacity limitations on the parallel line), all lines are used in the load flow method, according to their reactance.

In this section, the robustness of the transport model is analyzed by comparing, the results from URBS to a load flow simulation for a realistic scenario of power transmission in Germany.

The simplified load flow simulation applied for the comparison is a linearization of the AC load flow problem, which was developed to include the nature of AC load flow in larger models designed for system planning [e.g. 62, 25]. The simplified load flow simulation is derived from the comprehensive mathematical description of power flow in an AC network. For simplification, it is assumed, that the reactive power is compensated. Furthermore, for the active power ohmic losses are neglected, the voltage is held constant, and the small-angle approximation taken. A linear equation for a power flow between node a and b results. A detailed derivation can be found in Anderson [7].

$$P_{ab} = \frac{U_a U_b}{X_{ab}} \cdot \sin(\varphi_a - \varphi_b) \approx \frac{U_0^2}{X_{ab}} \cdot (\varphi_a - \varphi_b) \tag{2.60}$$

φ_a is the phase angle in node a, U_a the nodal and U_0 the network voltage and X_{ab} the reactance of the grid connection between a and b. This linearized load flow simulation reveals that, in an AC grid, the phase difference between two nodes drives the power flow

between these nodes. This is because a phase difference leads to a momentary voltage difference, which than drives current and therewith power flow along the transmission line.

As the structure of the equation resembles to a direct current flow ($P_{ab} = \frac{1}{R_{ab}^2}(U_a - U_b)$), this approach to simulate AC load flow is often confusingly called DC-model.

To carry out the comparison, the linearized load flow (LLF) simulation is implemented in URBS based on the above. The equations are valid $\forall x \in X, x' \in \mathcal{N}(X)$ and only for the energy transport processes set to be simulated with the load flow ($\forall k \in K^{LLF}$, see Table 2.14).

$$F_k(t) = \frac{u_0^2}{\mathsf{x}_k} \cdot \Phi_k \qquad k \in K^{LLF} \quad (2.61)$$

$$\text{with} \quad \Phi_k = \Phi(\underbrace{g, co, x', x}_{k}, t) := \Phi(g, co, x, t) - \Phi(g, co, x', t)$$

$$\varphi_k^{min} \leq \Phi_k \leq \varphi_k^{max} \qquad \forall k \in K^{LLF} \quad (2.62)$$

$$F_k(t) = F_k^{exp}(t) - F_k^{imp}(t) \qquad \forall k \in K^{LLF} \quad (2.63)$$

Equation 2.61 is the translation of the linearized load flow (equation 2.60) to URBS notation. F_k is the power flow along line k and it is driven by the phase difference between the connected nodes. To ensure stable network operation, the difference in phase angles can be restricted via equation 2.62. The power flow F_k is a real number and can also take negative values. It represents the net flow along the line k. To account for transmission losses, the direction-dependent, positive flow is determined in equation 2.63. These im- and export variables are fed back to the main URBS equations.

Symbol		Explanation
Sets		
$K^{LLF} \subset K$		transport processes to be simulated with LLF
Variables	Domain	
$\Phi(g, co, x, t)$	$G \times Co \times X \times T$	Phase angle at node x ($\in \mathbb{R}_0^+$)
Φ_k	K^{LLF}	Phase angle difference along line k ($\in \mathbb{R}$)
F_k	K^{LLF}	Power flow along line k ($\in \mathbb{R}$)
Parameters	Domain	
u_k	K^{LLF}	Voltage level
x_k	K^{LLF}	reactance
$\varphi_k^{min,max}$	K^{LLF}	Min. and max. phase angle difference along line k

Table 2.14.: List of symbols for linearized load flow simulation. All parameters are positive

Even if these equations allow for a more realistic simulation of power flow, they cannot be included in scenarios, where grid extensions are optimized, as this leads to a non-linear problem. The phase angle adjusts as a function of the nodal power balance. It is

a free variable in the optimization. At the same time, the reactance x_{ab} is a function of the grid line properties and most importantly the capacity of the connections, subject to optimization in capacity-extension scenarios as well. The simultaneous inclusion of the linearized load flow simulation and grid extension in a model therefore results in a non-linear optimization due to equation 2.61.

The simplified example introduced above makes the principal differences of the two LLF and the transport model evident. The application of the two methods to a more realistic scenario, however, shows less difference. Applying the two methods for the simulation of current German power supply (2010), the differences are a lot smaller. Six representative weeks are modeled. In the presented example, current infrastructure – power plants, storage and transmission grid – are assumed. As binding capacity limit for power transmission, the thermal limit is assumed for the linearized load flow simulation, while for the transport model, the natural power is assumed as transmission capacity (see Table 2.13). As discussed above, this conservative assumption ensures stable operation of the grid, while excluding the simulation of reactive power flows from the model.

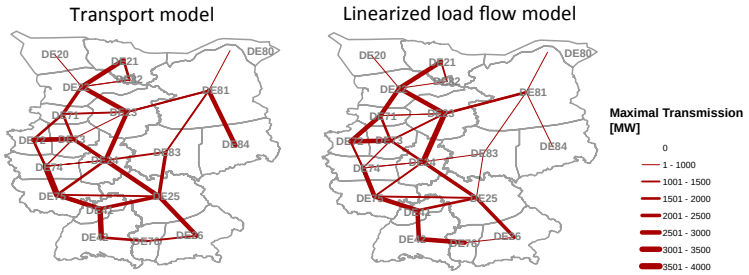

Figure 2.26.: Comparison of transport and linearized load flow simulation for current power supply in Germany (2010)

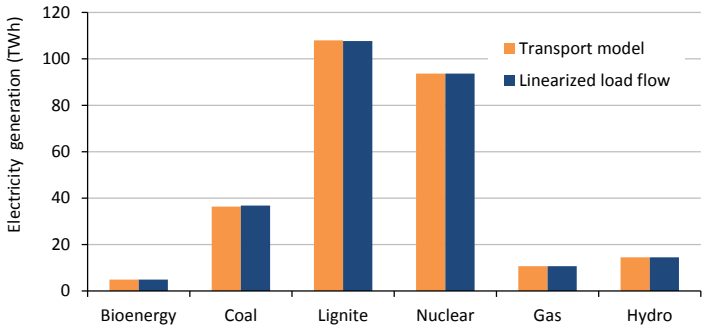

Figure 2.27.: Comparison of electricity mix with transport and linearized load flow simulation for current power supply in Germany (2010)

Figure 2.26 demonstrates that the resulting pattern of maximal power flow is very similar for both methods. Yet, in total, the maximal transmission in the transport model is 20% lower than in the linearized load flow model. This is partly due to the security margin introduced by assuming power flow at natural power in the transport model. However, also on connections where the upper transmission limit is not binding, the relative difference never exceeds the difference between thermal transmission limit and the natural power. This indicates that the introduced security margin may be sufficient. A comparison of the transport model to a full AC simulation of power flow, shows that the errors of the simplified transport approach are reduced, if conservative assumptions on capacity per line are taken [5].

The electricity mix for the dispatchable power plants resulting from the two methodologies is presented in Figure 2.27. The power plant dispatch is hardly influenced by the simulation method for the power flow in the presented example.

2.4.2. Benchmark with today's system

To validate the model's ability to reproduce a real power system, the European electricity system of 2008 is simulated with URBS-EU. In a Benchmark scenario, current infrastructure is included in the model and only the capacity dispatch is optimized. Capacity extensions for grid, power plants or storage are excluded. All cost assumptions are as described above, except that a carbon certificate price of 15 €/t is assumed. The comparison of the results with statistical data of 2008 shows, that the model reproduces the real behavior of the system in adequate accuracy.

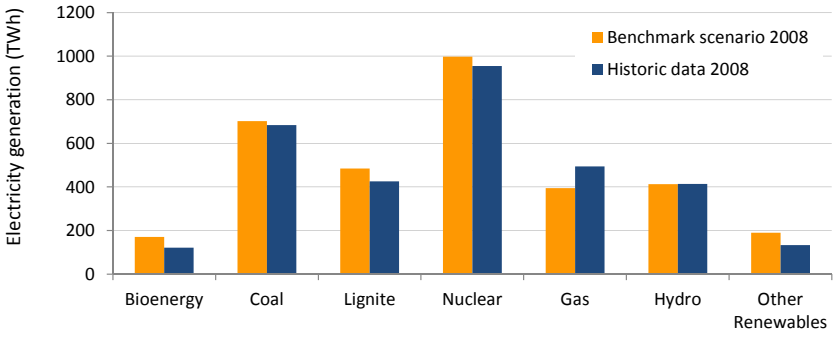

Figure 2.28.: Comparison of modeled electricity production in Europe to historical data [76].

Figure 2.28 compares the total European electricity generation by fuel resulting from the model to historical data [76]. The model results show a good fit of the produced power for the base load plants (coal, lignite, nuclear and hydro). The model slightly underestimates the power production of peak load power plants (gas). This is due to the deterministic nature of the optimization model. Unforeseen outages of power plants and forecast errors are not included in the model, while peak load power plants are often

used exactly to counterbalance these events.

Wholesale electricity prices are deduced from the marginal costs of electricity generation and are consistent with historical average wholesale prices (see Figure 2.29). The model furthermore reproduces extreme values of the electricity price and the computed price shows 70% correlation with real day ahead market prices for Germany [44].

Modeled cross-border electricity exchange is similar to historical data as shown Figure 2.30. One reason for remaining deviations might be a non cost-optimal cross-border scheduling in reality.

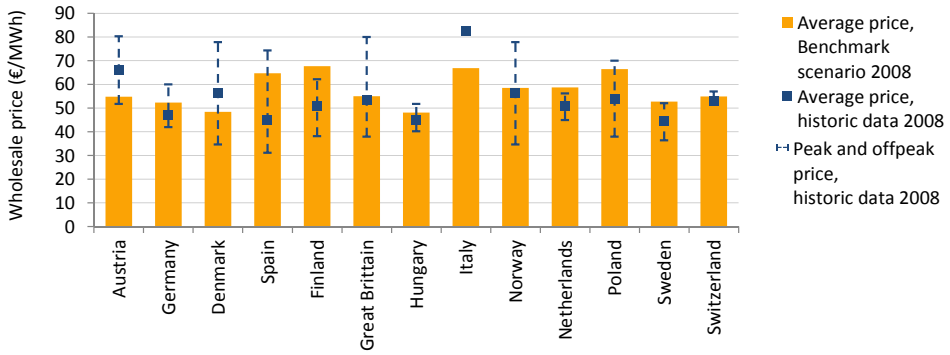

Figure 2.29.: Comparison of the average electricity prices in Europe [18, 103, 35, 44, 110] with the modeled average marginal costs of electricity generation

2.5. Discussion of the modeling framework

The model generator URBS contributes to the field of hybrid models. It unites the optimization and simulation of future power systems.

The model includes the relevant properties of power plant dispatch, storage, HV transmission and VREs. Furthermore, the comparatively high temporal and regional resolution chosen in the model setup allows for a detailed analysis of VREs and their integration in the power system.

In addition to the simulation of system dispatch, cost-optimal system design can be determined based on the minimization of total system costs. In the optimization all interactions between the modeled technologies and resources are taken into. This leads to coherent recommendations for future system design and VRE system integration measures.

Finally, the cost-optimization also provides the marginal costs of electricity generation. They are a good indicator for electricity prices and provide the basis for the analysis of the market integration challenge of VREs.

The benchmark of the European power system model URBS-EU shows that the model provides a realistic simulation of the actual power system. Furthermore, it was demonstrated that the simplified simulation of electricity transmission with the transport model

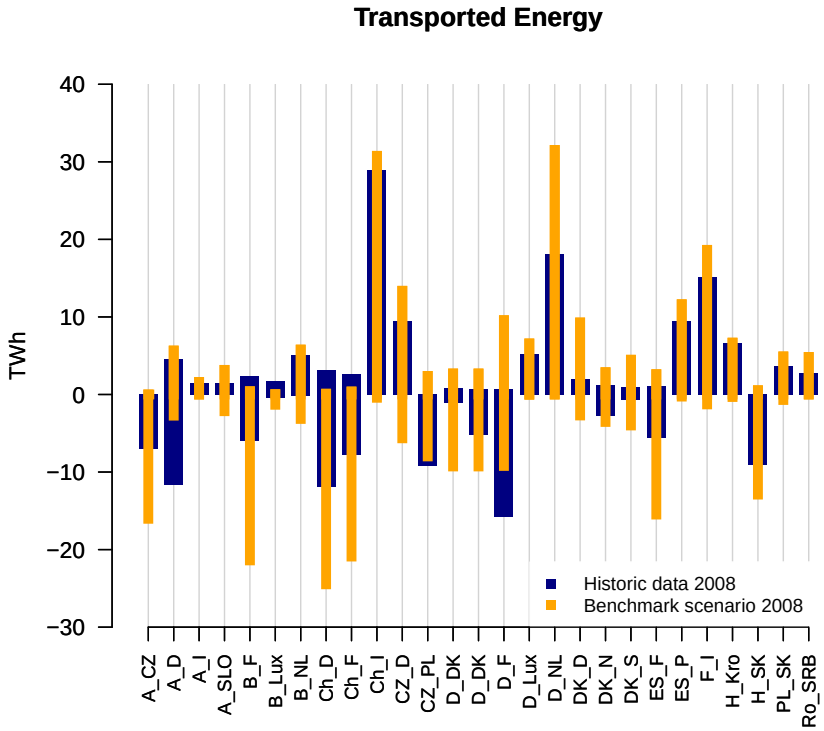

Figure 2.30.: Cross-border electricity exchange: model results and historical data [46]

leads to tolerable deviations of the transmission corridor usage and power plant dispatch compared to a load flow simulation.

The careful selection of representative periods allows to reduce the error introduced by including only representative periods in the optimization instead of several years compared to a random or equidistant choice of representative periods.

Yet, several simplifications were made in the development of the modeling framework. The model excludes technical details concerning the dispatch of power plants such as start-up times, load-dependent efficiencies, etc. Through the inclusion of ramp rates, which account for the combined effect of ramping and start-up restrictions of conventional power plants, one part of the inflexibility of the system is included. However, due to the approximations taken, the flexibility of the system is most likely overestimated.

Power flow is modeled as transport problem neglecting the nature of physical AC load flow as well as grid stability requirements. While the introduced errors in transmission grid usage are tolerable, this simplification possibly leads to an underestimation of necessary grid extensions. This shortcoming is counteracted by the conservative assumption of using transmission lines only at their natural power in the model and with this assuming perfectly balanced reactive power.

By aggregating all infrastructure within the model regions to representative nodes, it

is assumed that no grid bottlenecks within each region and especially in the distribution grid occur, although important challenges and potentially costs can arise at low voltage levels in the context of VRE integration [31].

The model assumes perfect foresight and a central planner taking cost-optimal decisions. This model setup allows to identify advantageous future system design, but excludes uncertainties. Especially for electricity wholesale prices, these can play an important role. This deterministic setup, equivalent to the assumption of a perfectly transparent market, in turn allows to clearly identify the drivers for changes in electricity prices. Furthermore, the benchmark with historic data for Europe showed, that the simplified representation of the electricity price is still quite close to the historic prices.

Finally, the model analysis is carried out for typical years, providing a snapshot of possible futures. Path-dependency of the future system development is not included in the model.

The simplifications introduce shortcomings of the model which have to kept in mind when defining the scenario setup and when interpreting the results. At the same time, it is only thanks to the carefully selected simplifications that a large hybrid energy system model can be set up. The model allows to analyze a large area in high temporal and geographical resolution, and is thus well suited for the analysis of VRE integration challenges and measures in Europe and Germany.

3. Systematic advantages of a powerful European transmission grid

3.1. Transmission grid extensions as VRE integration measure

This chapter studies the system implications of wind and solar PV power and investigates a way to partly overcome these: transmission grid extensions. The VRE integration challenge is analyzed as a function of the penetration and mix of wind and solar energy. In a second step, the role of transmission grid extensions as a measure to address the temporal fluctuations and the geographical dispersion of VREs is examined in the same parameter space.

The effect of different VRE penetration levels and mixes between wind and solar power on fundamental power system properties, such as overproduction and required supplementary dispatchable capacity, is quantified. This is done for different levels of interconnection between model regions. This approach allows to quantify the benefits of transmission grid extensions for VRE system integration. URBS-EU is applied to quantify the size and costs of a powerful overlay transmission grid, a so-called supergrid, for VRE integration. Finally, robust design features of a power system with high VRE penetration are presented: the results reveal crucial grid connections in Europe and provide insights on the role and suitability of different dispatchable power plant technologies.

The systematic analysis of the VRE integration challenge and the effects of a supergrid has several advantages. First, it provides insights on how the VRE system integration challenge changes with VRE share and mix. Second, the sampling of a large parameter space allows for the identification of design features that are beneficial for a large range of possible future power systems. Lastly, the estimates of the costs of a large transmission grid extensions for VRE integration derived from the parametric analysis are very robust.

The applied methodology consists of a time series analysis coupled to the power system model URBS-EU (see Section 2.2). It is described in Section 3.2 after a literature review in Subsection 3.1.1. The results are presented in Section 3.3: the technical feasibility and economic suitability of different VRE supply configurations with and without transmission grid extensions are analyzed in Subsection 3.3.1. Subsection 3.3.2 shows examples for other regions. The costs and structure of the European high voltage transmission grid, which is cost-optimal for the integration of VREs, are quantified in Subsection 3.3.3. The suitability of different supplementary, dispatchable technologies is studied in Subsection 3.3.4. An illustration of the results is provided in a case study

in Subsection 3.3.5. Finally, Section 3.4 summarizes and discussed the results of this chapter.

3.1.1. Related work

Already in the early 1970s, grid extensions have been identified as a necessary condition to achieve large shares of renewables: Buckminster Fuller proposes a global link to harvest energy resources most efficiently [21] . On the European level, first detailed studies on the feasibility and principal advantages of a supergrid have been presented by Biberacher [12], Czisch [26] and the German Aerospace Center (DLR) [32]. In the light of actual growth of wind and solar energy and the institutional and political barriers to grid extensions, analyses of the actual and near future situation have been carried out recently. In the TradeWind study, overall grid extensions for wind energy until 2030 are quantified [138]. Grid strengthening can furthermore reduce the impacts of VRE on the electricity market and their participants, as shown by the author [131] (Chapter 4). On a longer time horizon, McKinsey and PricewaterHouseCoopers (PWC) present possible roadmaps towards a carbon free power supply in 2050 in Europe [101, 122]. The first roadmap presents a technically and economically feasible pathway to a zero-emitting European power sector in 2050, which includes nuclear power, carbon capture and storage, and renewable energies. The second proposes a 100% renewable scenario for Europe under the prerequisiste of a European "SuperSmartGrid", a combination of a supergrid and increase of information exchange between grid nodes.

In addition to these detailed techno-economic studies mostly based on advanced power system modeling, important information can be drawn from statistical analyses of the supply time series. Giebel and a study by Greenpeace quantify the statistical smoothing of wind volatility through increased interconnection between generating regions [55, 59]. In Grotz [60] and Heide et al. [64] the seasonal fluctuations of wind and solar availability in Europe are understood as an opportunity rather than a challenge: The optimal combination of wind energy, mainly available in winter, and solar energy, mainly available in summer, allows to minimize the need for inter-seasonal storage or supplementary dispatchable capacity. While analyses based on energy models mostly are limited to a relatively small number of scenarios, time series analyses cover a larger range of the possible system configurations.

In the analysis in this chapter, the advantages of the two approaches are combined. Based on a time series analysis covering a large parameter space and including several years of meteorological data, the VRE system integration challenges are quantified as well as the benefits of large transmission grid extensions. With the model URBS-EU, which includes the relevant technical details of the power system, the cost-optimal transmission grid extensions for VRE integration and other system design features are determined.

3.2. Methodology for conducting the parametric study

To analyze the effects of VREs on a power system and the role of a powerful transmission grid in Europe, a wide parameter space of possible system configurations for different VRE penetration levels and mixtures is explored. For each system configuration, necessary transmission grid extensions are determined with the URBS-EU model and their effects on VRE integration evaluated.

Before applying the model, the underlying demand, wind and solar supply time series are studied. This allows to include several years of meteorological data, which would exceed the practicable size of the model setup. The results of the time series analysis are fed to the model. This combination of a highly resolved eight-year meteorological time series with a detailed power system model leads to a robust methodology.

3.2.1. Definition of the parameter space and the time series analysis

For the systematic analysis of VRE system integration, a two dimensional parameter space is defined by the total share of VREs in the satisfaction of load α and the share of wind energy in total energy from VREs β.

$$\alpha = \frac{\sum_t \min(E_w(t) + E_s(t), d(t))}{\sum_t d(t)} \tag{3.1}$$

$$\beta = \frac{\sum_t E_w(t)}{\sum_t [E_w(t) + E_s(t)]} \tag{3.2}$$

where $E_w(t) = \sum_x E^{out}(w, Elec, x, t)$ is the total power generation from wind in region x at time t and $E_s(t) = \sum_x E^{out}(s, Elec, x, t)$ the power generation from solar photovoltaics. $d_t = \sum_x d(Elec, x, t)$ is the electricity demand. The VRE share α excludes renewable generation that exceeds the demand. α is the share of demand covered by VREs.

Traditionally, power supply systems are built to follow the load and this determines the structure of the power system. However, in highly renewable scenarios the residual load, which has to be satisfied by the power supply system, is mostly determined by the share and type of the VREs. The two parameters α and β are thus central in the comparison of systems.

The total power generation from wind and solar energy are computed based on the capacity factor $cf(x,t)$ of the respective technology and the installed capacities $C(x)$ per region (see equation 2.8). The model regions are as defined in Chapter 2 (Figure 2.13). If several regions are aggregated, a spatial distribution of wind and solar capacities has to be assumed. Here, the wind and solar capacities are assumed to be distributed in accordance to their technical potential, as derived by Scholz [134]. The contribution of wind offshore capacity to the total European wind capacity is assumed to be 50%. Figure 3.1 shows the technical potential normalized to the respective regions' surface.

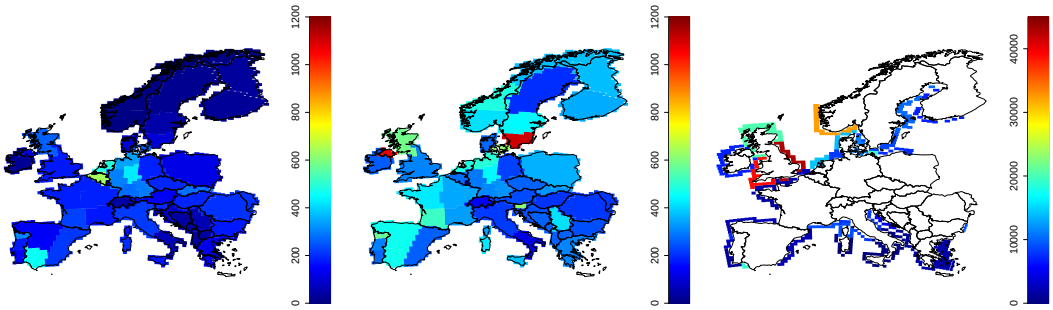

(a) Solar Photovoltaics (b) Wind Onshore (c) Wind Offshore

Figure 3.1.: Technical potential of wind and solar electricity generation in $MWh/m^2.yr$ [134]

The technical potential gives the total energy possible to harvest per region in one year. On top of the restrictions from concurrent land use, such as sea, urban or protected area included in the geographic potential, it includes also the technical conversion losses.

As Table 3.1 shows, the cummulative technical potential for VRE supply in Europe is largely sufficient to supply electricity demand on an annual basis, i.e., if momentary wind and solar supply would match the load. The table also indicates, that the estimations of renewable potential vary considerably. In this study, the technical potential determined by the DLR is assumed [134].

Annual electricity generation TWh/a	Solar PV buildings	Solar PV open area	Wind Onshore	Wind Offshore	Total	% of EU demand
DLR Europe [134]	679	137	1 869	11 078	13 748	435%
Literature Review [13]	2 201	1 933	1 147	2 923	8 203	260%
Geographic potential [143, 20]	15 842		15 818	2 338	33 998	1 070%
DLR MENA[a] [134]	152 936	125 730	27 284	2 992	308 942	9 745%

Table 3.1.: Technical and geographic potential for wind and solar electricity generation in Europe and MENA: estimates from different sources. The last column compares the potential to the power generation in Europe of 3170 TWh (2008) [77]

[a] Middle East and North America: Algeria, Morocco, Egypt, Tunisia, Turkey, Libya, Syria, Lebanon, Israel, Jordan and Western Sahara

Based on the load, wind, and solar time series, the fundamental properties of the power system are computed. These are the necessary VRE and supplementary dispatchable capacities, C_{vre} and C_s, the amount of overproduction Δ^-, and the distance between supply and demand time curve, i.e., the absolute value of the residual load $|\Delta|$. If the "mismatch parameter" $|\Delta|$ was zero, there would be no VRE integration challenge. $\Delta(t)$ is the residual load.

$$C_{vre}(\alpha,\beta) = \sum_i C_i(\alpha,\beta) \qquad \forall i \in vre = \{w,s\} \quad (3.3)$$

$$\Delta(t,\alpha,\beta) = d(t) - E_{vre}(t,\alpha,\beta) \quad (3.4)$$

$$C_s(\alpha,\beta) = \max_t \left(d(t) - E_{vre}(t,\alpha,\beta)\right) = \max_t \Delta(t,\alpha,\beta) \quad (3.5)$$

$$\Delta^-(\alpha,\beta) = \sum_t \max_t (E_{vre}(t,\alpha,\beta) - d(t), 0) \quad (3.6)$$

$$|\Delta|(\alpha,\beta) = \sum_t |d_t - E_{vre}(t,\alpha,\beta)| \quad (3.7)$$

The total VRE capacity necessary to achieve a given VRE share α is obtained with a while-loop: the VRE capacity is increased until the total VRE generation is large enough to achieve the desired VRE share α. The other parameters are computed based on the obtained VRE capacity $C_{vre}(\alpha,\beta)$, the VRE generation $E_{vre}(t,\alpha,\beta) = \sum_i C_i(\alpha,\beta) \cdot cf_i(t)$ and the resulting residual load. The VRE mix β is obtained by choosing the right ratio between wind and solar capacities.

This time series analysis can be applied to different regions or at different regional resolution in computing the above described variables for different subsets of model regions X. It can be applied to individual model regions, a selected country or to Europe in total.

When applying it to larger regions, for example to Europe, different levels of grid extensions can be simulated. If all regional VRE generation profiles are aggregated (based on the assumed regional distribution of capacities), perfect interconnection within Europe is assumed. By building the weighted average of the capacity factor all smoothing effects between regions are included. To simulate a system with no connection between model regions, the system properties are computed for each model region individually and are only aggregated afterwards. The system parameters are then summed up according to the resulting overall, European VRE share. For the VRE mix, it is assumed, that the mix between wind and solar is achieved on the European level, i.e., the distribution of wind and solar capacities across Europe remains the same in the non connected case and in the connected case. Intermediate levels of connection can be achieved by building average VRE generation profiles for a selection of model regions. To simulate perfect interconnection within each country for example, system properties are first computed based on the average national VRE generation profiles. These are then aggregated to a European total in analogy to the no-connection case.

3.2.2. Capacity credit and capacity factor

High temporal fluctuations and low correlation of VREs leads to overproduction and the necessity of supplementary capacity. These properties of VREs limit their contribution to power system supply and adequacy. Commonly, two further parameters are used to describe the properties of VREs. Their average availability, the *capacity factor*, and their contribution to reliable capacity, their *capacity credit*.

As excess energy has to be discarded, the capacity factor is reduced with increasing VRE share α. The capacity credit indicates the reliability of the renewable generation technology. It is the dependable share of the VRE capacity, being the amount of other generation capacity that can be removed from the system without reduction of the security of supply. Both of these parameters can be computed based on the above defined system properties.

$$\begin{aligned} CC(\alpha,\beta) &= \frac{max_t(d(t)) - max_t(d(t) - E_{vre}(t,\alpha,\beta))}{C_{vre}(\alpha,\beta)} \\ &= \frac{C_s(0,0) - C_s(\alpha,\beta)}{C_{vre}(\alpha,\beta)} \end{aligned} \tag{3.8}$$

$$\begin{aligned} CF(\alpha,\beta) &= \frac{\sum_t(E_{vre}(t,\alpha,\beta)) - \sum_t max(E_{vre}(t,\alpha,\beta) - d(t), 0)}{C_{vre}(\alpha,\beta)} \\ &= \frac{\sum_t(E_{vre}(t,\alpha,\beta)) - \Delta^-(\alpha,\beta)}{C_{vre}(\alpha,\beta)} \end{aligned} \tag{3.9}$$

The computation of the capacity credit proposed here excludes the probabilistic properties of this parameters and is only based on the time series of VRE supply and load.

3.2.3. URBS-EU model setup and scenario definition

The above designed time series analysis is coupled to the URBS-EU model via the wind and solar capacities necessary to reach a certain VRE share. VRE capacities are determined by the requirements to achieve certain shares α and β based on the eight years time series. The resulting VRE capacities $C_{vre}(x,\alpha,\beta)$ serve as input to URBS-EU, which is applied to analyze the behavior of the European power supply system for each α and β. The residual power system is subject to the cost-optimization implemented in the model. Transmission grid extension and dispatch of conventional power plants and storage are optimized. For the grid extensions it is distinguished between cables for offshore connections and HV overhead lines for onshore connections.

All grid extensions resulting from the model are on top of the existing ENTSO-E grid, which is included in the model. For the conventional power plants, two different scenarios are studied (Table 3.2). In the *Grid Only* scenario grid extensions are planned in response to the total – VRE and conventional – generation infrastructure. For the conventional power plants it is assumed, that today's existing dispatchable capacities remain unchanged (for specifications on input data see Section 2.3). In the *Grid and Power Plants* scenario, the grid and the supplementary power plant fleet are optimized simultaneously for given VRE configurations from green field. All dispatchable power plant capacities and grid extensions are determined by the optimization. Depending on the planning and regulatory policy in each country, VRE capacities influence only grid infrastructure planning or also capacity additions of dispatchable power plants. The effects of VREs on investment decisions will depend on their contribution to total generation. The two scenarios examine the possible range of consequences of different planning policies.

As the focus lies on the role of transmission grid extensions, storage capacities are assumed to remain at today's level. The effects of demand side management as VRE system integration measure are treated in Chapter 5.

Scenario	Grid extension	Conventional power plants
Grid Only	optimized	current power plant fleet
Grid and Power Plants	optimized	optimized

Table 3.2.: Scenario definition

The assumed costs and technical parameters are the benchmarked values (Section 2.3, Table 2.10).

Electricity demand is assumed to remain at today's level. While population and economic growth raise electricity demand, efficiency measures counteract [101]. To account for these diametrical trends and to ensure comparability, current hourly load profiles and current total electricity demand are used (see Subsection 2.3.2).

For the optimization, six representative weeks from meteorological data of 2007 are used. Sensitivity analyses demonstrate that grid extensions and supplementary electricity mix do not change significantly if longer time series or another meteorological year are employed.

3.3. Results: advantages and costs of a European supergrid

3.3.1. Benefits of grid extension for VRE system integration

The fundamental system properties for a case with optimal grid extensions and one without are computed with the time series analysis described above. In the first case, unrestricted electricity transport across the entirety of Europe is assumed (*Optimal Grid*), in the second case, each model region acts independently (*No Grid*). This allows to assess the effect of increased interconnection for the VRE system integration.

Figure 3.2 shows the overproduction for increasing VRE-share α and for different contributions of wind energy β. With optimal grid (Figure 3.2a), the overproduction is below 10% for VRE shares up to 40% and then rises steeply with α. The detaching point, however, occurs a lot earlier with large solar shares: on the European scale, wind energy provides smoother supply than solar, as the solar cycle only differs by a few hours within Europe and the smoothing is less pronounced. Without grid extensions (Figure 3.2b), larger overproduction occurs. Especially for high wind shares, the detaching point of overproduction shifts to lower VRE shares if no grid extensions are assumed.

To gain an overall impression of the system behavior in dependence on VRE share and mix, the results are presented in contour plots. The penetration level of VREs α and the share of wind β span the parameter surface, where α is plotted on the abscissa and β on the ordinate. The color coding in the spanned surface shows the value of the system properties.

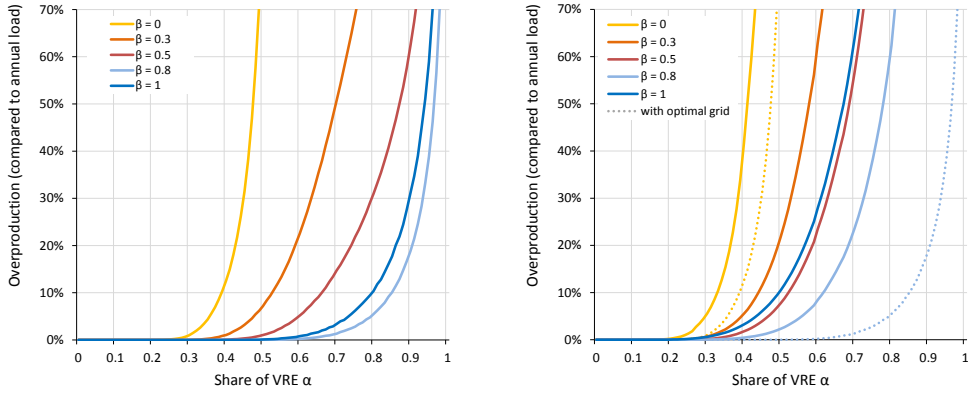

(a) *Optimal Grid* (b) *No Grid*

Figure 3.2.: Overproduction with and without perfect interconnection between model regions

Figure 3.3 shows the overproduction for each α-β combination, the necessary VRE capacity as well as the required supplementary capacity, the overproduction and the mismatch between supply and demand $|\Delta|$. The capacities are shown in units of peak load ($max_t\, d(t)$), overproduction and mismatch in units of total load ($\sum_t d(t)$). In the left column, an optimal grid within Europe is assumed, in the right column, no interconnection is assumed.

Some combinations of α and β are infeasible within the assumed capacity limits for VRE technologies. For these points on the surface, no variable value exists and the surface remains white. Large VRE shares with high solar contribution are infeasible. With grid extensions, the maximal possible VRE share amounts to about α=50%, if only solar PV is used ($\beta = 0$, left column of Figure 3.3). As the sun only shines during day time and no storage extensions are assumed, it can be easily understood, that 100% satisfaction of demand is impossible with solar energy only. Without grid extensions larger areas of the parameter space remain empty and thus infeasible (right column of Figure 3.3).

The first row of Figure 3.3 shows the overproduction. As discussed above, the overproduction's dependence on α is similar to an exponential function: it is very flat in proximity to the origin, but from a certain VRE share on, it rises steeply. The detaching point varies with the share of wind energy: more wind energy leads to less overproduction. Also, higher levels of interconnection entail lower excess production for identical VRE shares.

The second row of Figure 3.3 shows that VRE capacity rises steeply with increasing α in the parameter space. It increases with the discarded energy: for very high VRE shares, an additional MW of wind or solar power contributes only little to satisfy the load, as large shares of the produced electricity has to be discarded. The realization of a

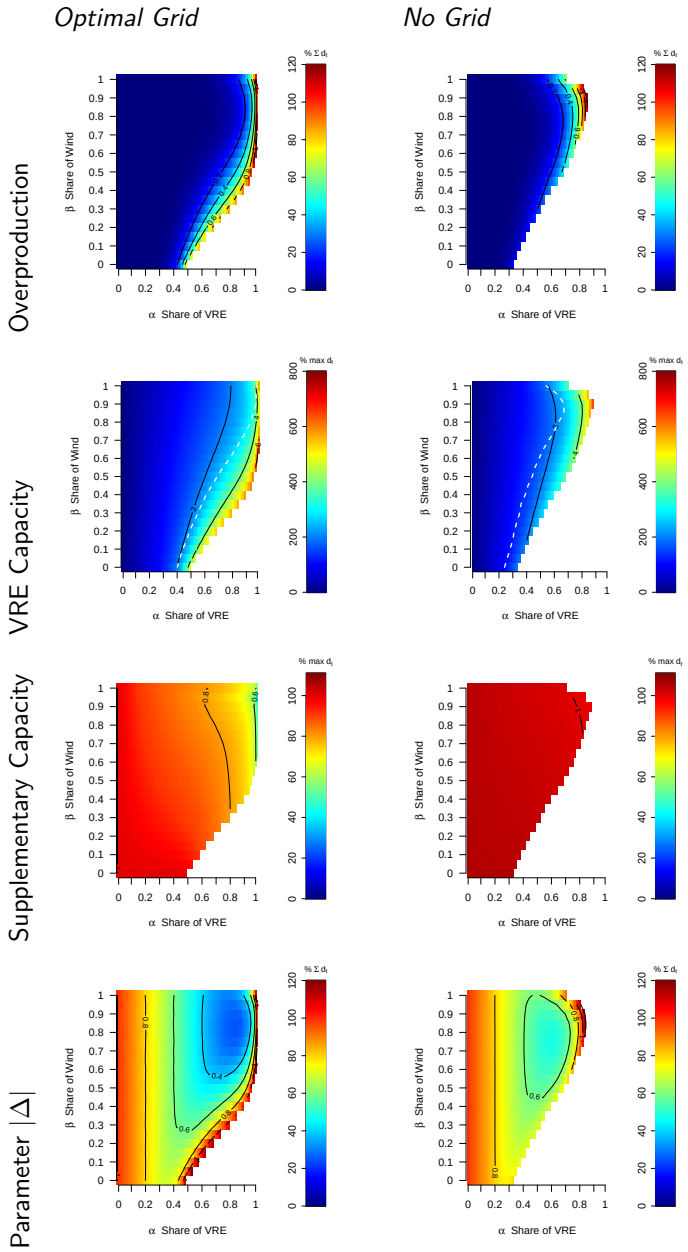

Figure 3.3.: Fundamental properties of VRE power systems in Europe with optimal grid and without grid. The first row indicates the overproduction, the second the necessary VRE capacities for each α and β. The third and fourth row show the supplementary capacity and the mismatch parameter. In the results shown here, the capacity of each VRE technology is limited to five times the peak load. The dashed line in the second row indicates the maximal possible VRE shares with a lower VRE capacity limits of two times the peak load per VRE technology.

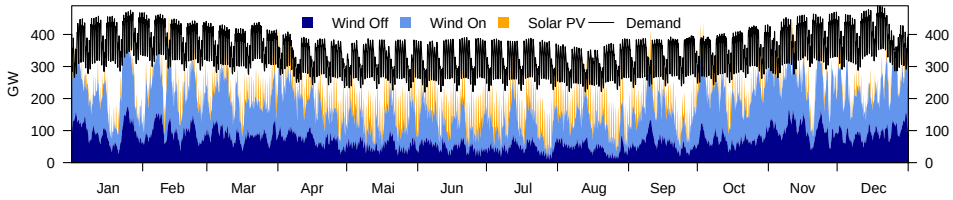

(a) Hourly electricity generation (α=60%, β=85%)

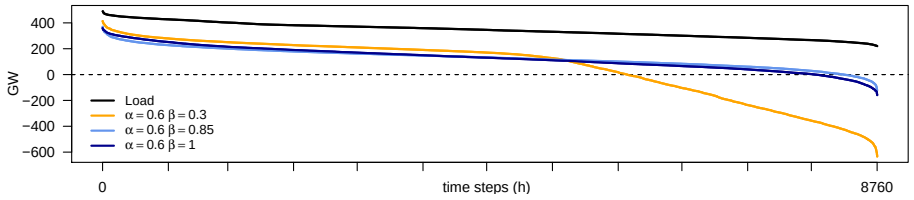

(b) Residual load duration curve for different wind shares β

Figure 3.4.: Hourly electricity generation and residual load duration curve for α= 60% and *Optimal Grid*. The figure is based on the meteorological data from 2001.

configuration at the rim of the colored area in the parameter space translates into a VRE capacity of 8 times the peak load. In the results shown here, the capacity of each VRE technology – solar PV, wind onshore and wind offshore is limited to 5 times the peak load. The theoretical maximal VRE capacity in the analysis thus amounts to 15 times the peak load. If larger overcapacity was allowed for, higher shares of VRE were possible, if lower overcapacity is allowed, lower VRE shares can be achieved. The dashed line shows the maximal shares with a limit of 2 times the peak load per technology. This corresponds to the technical potential of wind and solar generation according to the German Aerospace Center (DLR) [134]. With grid extensions, more than 85% VRE share can be achieved within the limits of the technical potential. Without grid extensions the maximum share is reduced to about 60%.

To ensure reliable electricity supply, sufficient supplementary capacity is necessary. The third row of Figure 3.3 shows that all VRE configurations need considerable supplementary capacity. This is due to the fluctuating availability of VREs and the resulting low reliability of these energy sources. With an optimal grid, necessary supplementary capacity can be reduced to less than 60% of the peak load. Without grid the necessary supplementary capacity remains close to 100% of the peak load in the entire parameter space. For both cases, the maximum of the European load serves as reference. As the peak load does not happen at the same time all over Europe, the sum of local peak loads exceeds the European peak load. This is why the supplementary capacity requirements can reach values larger than 100%. The supplementary capacity is determined by the time series analysis, which does not include transport losses, ramp up or availability restrictions. The presented capacity requirements should thus be understood as lower limits, which increase if all technical details and security margins are taken into account.

The current power generation capacity in Europe, for instance, amounts to about 1.4 times the peak load [46]. As the analysis is based on the eight-years time series, the estimation of this lower limit is, however, quite robust.

The last row of Figure 3.3 shows the mismatch $|\Delta|$ (equation 3.7). If one considers storage as an integration option for VRE, minimal mismatch would be desirable, as this translates into minimal distance between load and supply and thus a minimal amount of energy to be stored and released in total. With an optimal grid, a VRE share of 83% and a wind contribution of 85% result in minimal $|\Delta|$, and therewith minimal adaption needs of the residual power system. The lower interconnection case favors higher shares of solar energy; here the mismatch is minimal at α=60%, β=75%. Wind energy is highly variable, while solar energy supply is less stochastic and closer to the load pattern in the temporal and spatial domain. Solar capacity is furthermore more evenly distributed than wind (see Figure 3.1). Therefore, wind energy profits more from interconnection, while solar energy has a systematic advantage in low-connection cases. Yet, the absolute mismatch is lower with an ideal grid. The grid smoothens the wind supply and the resulting total European wind generation pattern is closer to demand than the solar pattern.

However, even with optimal grid extensions in Europe, the supply pattern by VREs remains challenging (see Figure 3.4). It is highly fluctuating, and the residual load curve is steep, especially for high contributions from solar PV.

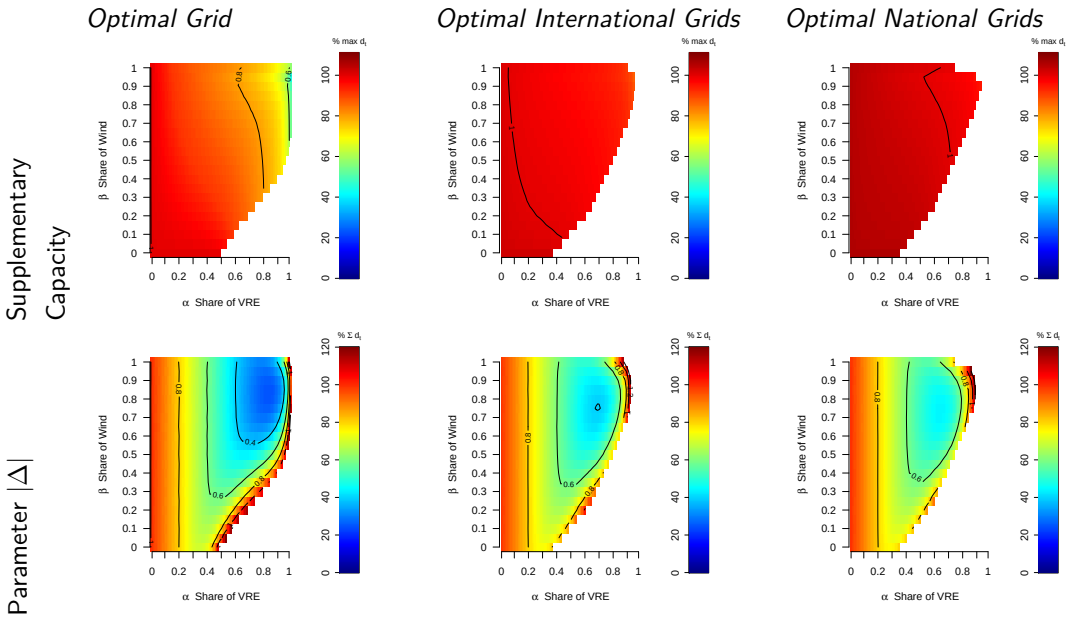

Figure 3.5.: Supplementary capacity and mismatch parameter for VRE power systems in Europe with intermediate levels of interconnection. The capacity of each VRE technology is limited to five times the peak load. The *Optimal Grid* case is shown for comparison in the first column.

Having analyzed the two extreme cases of ideal connection and entirely independent regions, intermediate grid levels are studied in the next step. Figure 3.5 shows the supplementary capacity and mismatch $|\Delta|$ for intermediate levels of interconnection. These intermediate grid levels are simulated by aggregating the VRE supply profiles for different subsets of the European model regions. In the *Optimal National Grids* scenario it assumed that an optimal grid exists within each country. In *Optimal International Grids* larger European regions are aggregated[a]. The results indicate that the intermediate levels of interconnection lead to a reduction of the mismatch. The necessary supplementary capacity is however not reduced substantially. That means that the effective smoothing contributing to system reliability of supply can only be realized on a pan-European level.

Based on the VRE and supplementary capacities, the average CoE in Europe can be determined. Assuming 40% capacity margin as of today, and coal and gas turbine power plants as supplementary technologies, the CoE range between 70 and 92 €/MWh with grid extension and between 72 and 145 €/MWh without grid extensions (*High Costs*). The costs vary considerably with VRE share and mix, but also with the assumed wind and solar investment costs and therefore the *High* and *Low* cost scenarios for VRE technologies are analysed (see Table 2.11).

€/MWh	*High Costs*	*Low Costs*
	Optimal Grid	
α=10%, β=50%	70	64
α=50%, β=70%	82	55
α=60%, β=80%	84	52
α=80%, β=90%	92	49
	No Grid	
α=10%, β=50%	72	66
α=50%, β=70%	88	60
α=60%, β=80%	94	60
α=80%, β=90%	145	74

Table 3.3.: Average European Costs of Electricity (CoE) per MWh load for different VRE configuration and different levels of interconnection. Two cost scenarios for VREs are studied (see Table 2.11).

For high α, large VRE over-capacities are necessary and therefore the CoE, computed with respect to electricity demand, exceed the CoE of the VRE technologies themselves. Higher costs in the non-connected case are caused by larger supplementary and VRE capacity needs. As can be seen in Table 3.3, the non-connected case is always more costly than the connected case. Compared to current CoE of conventional technologies,

[a]The regions are: Balkan south (Slovenia, Croatia, Greece and FYROM), Balkan North (Romania, Hungary, Serbia and Bulgaria), Eastern Europe (Poland, Czech Republic, Slovakia), BeNeLux, Central Western Europe (Germany, France, Denmark), Alpine Region (Austria, Switzerland, Italy), UK (GB and Ireland), Iberia (Portugal and Spain) and Scandinavia (Sweden, Norway and Finland).

such as 43 €/MWh for coal power plants and 84 €/MWh for gas turbines (see Table 2.10), high VRE scenarios (α=80%) might not be economically viable. Assuming a cost reduction for the VRE technologies, the CoE only amount to 74 €/MWh without grid and 49 €/MWh with grid at the same share of 80% and thus come a lot closer to today's electricity prices.

If, in addition to an increase in α, the wind share β is increased, the CoE can decrease, as solar PV is more expensive than wind turbines. The CoE exclude costs for grid extension, treated separately in Subsection 3.3.3.

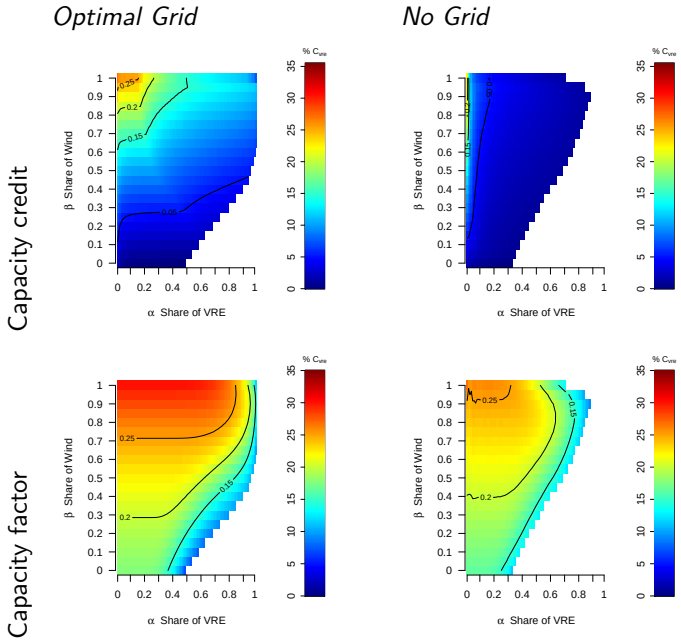

Figure 3.6.: Capacity credit and capacity factor of VREs in Europe with and without grid extension

Figure 3.6 shows the capacity factor and the capacity credit. Both, the capacity credit and capacity factor decrease with increasing VRE share and increasing contribution from solar PV, reflecting the above discussed findings for supplementary capacity and overproduction. Furthermore, optimal interconnection can raise the level of capacity credit and average capacity factor considerably.

The comparison of adaption needs of the power system and costs for highly renewable supply with and without grid extension shows that increased interconnection bears important benefits for VRE integration. Grid extension reduces VRE and supplementary capacity needs and with it the costs. Furthermore, smaller mismatch between supply and demand plus lower overproduction occur.

3.3.2. Analysis of grid extension on other geographical scales

The above analysis focuses on Europe. Similar effect of optimal interconnection can be observed on other geographical scales. In this section the time series analysis is expanded to Middle East and North Africa and applied at the German and the global level.

EUMENA

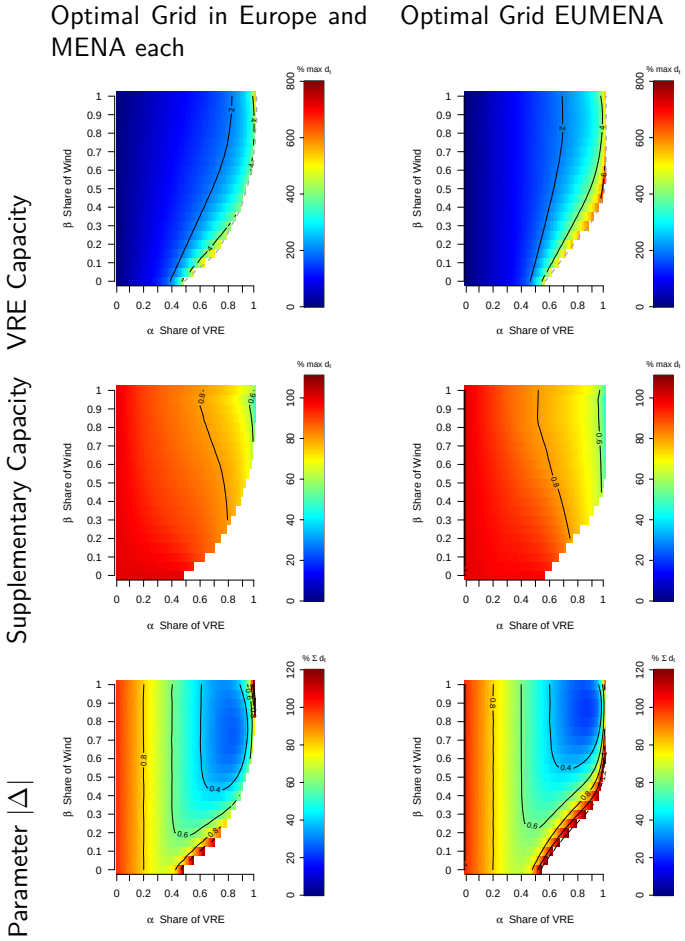

Figure 3.7.: Capacities and mismatch parameter for the EUMENA region with and without connection between Europe and MENA. The dashed line indicates the technical potential of wind and solar energy in EUMENA.

Connecting the Middle East and North Africa (MENA) to Europe bears important benefits [26, 32, 71]. One reason for this is the large technical potential for solar and wind generation in the MENA region, as can be seen in Table 3.1. Furthermore, connecting wind generation sites across larger areas including different weather systems can be advantageous, as important smoothing may occur [147].

The results from the time series analysis confirm this. Figure 3.7 shows the necessary VRE and supplementary capacity for Europe and the MENA region (EUMENA) with and without linkage of the two regions, together with the mismatch parameter. With a connection between Europe and the MENA region, the VRE capacity's increase with α is slower and supplementary capacity is reduced earlier. The minimal mismatch can be reduced from 26% to 21% thanks to the smoothing. Another important advantage is the large technical potential for VRE generation available in the MENA region. As the dotted line in the figure indicates, the total technical potential in EUMENA is sufficient to accomodate five times the peak load per technology and therewith achieve very high shares of VREs.

Germany

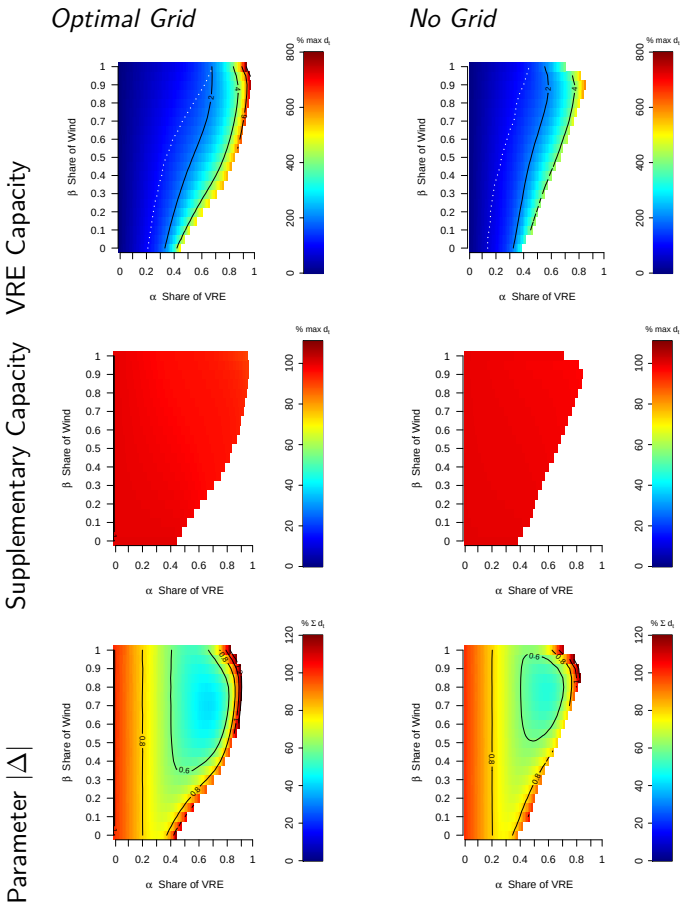

Figure 3.8.: Capacities and mismatch parameter for Germany with optimal grid and without grid. The dashed line indicates the maximal possible VRE shares with a capacity limit of one times the peak load per technology.

Singling out of one European country allows to evaluate, whether a smaller, German, supergrid could already have important benefits.

Figure 3.8 shows the VRE and supplementary capacities and the mismatch parameter for the example of Germany. The results indicate that the positive effects of interconnections are the reduced mismatch and VRE capacity. The supplementary capacity is not reduced substantially through German transmission grid extensions. Furthermore, the possible maximal share is low compared to the European value, but it is larger with an optimal grid. The potential for VRE generation in Germany is sufficient to install about 1 times the peak load per technology [134].

World

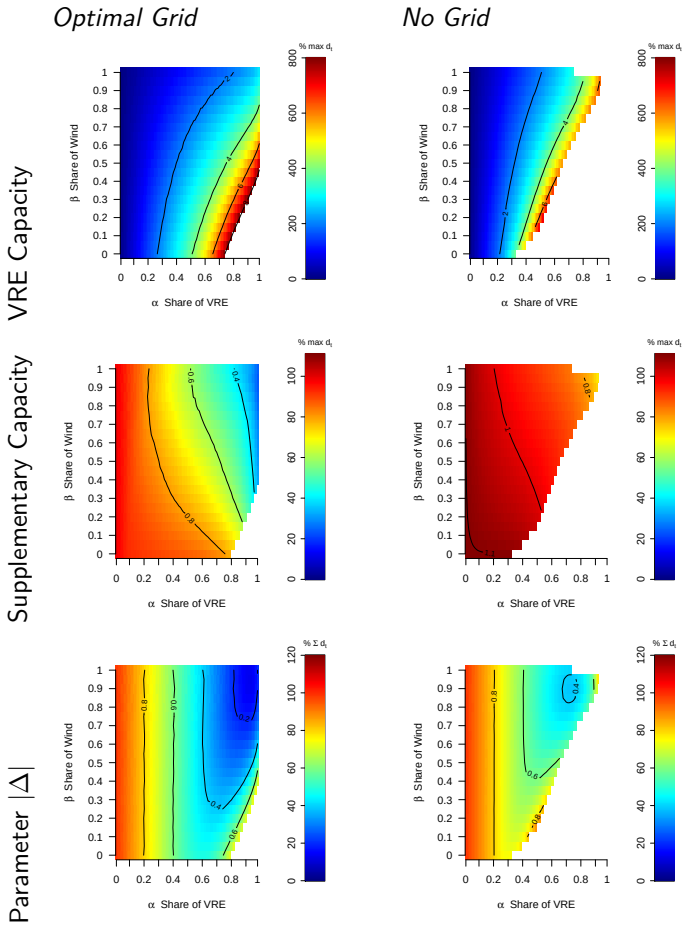

Figure 3.9.: Capacities and mismatch for a global VRE power system with optimal grid and without grid. The capacity of each VRE technology is limited to five times the peak load.

On the global scale, a hypothetical supergrid spanning all continents has important advantages, as the findings presented in Figure 3.9 show. The necessary supplementary capacity would be reduced to less than 30% of peakload, 60% of the European value. This is in line with the estimate of necessary supplementary capacity based on power system models in Aboumahboub et al. [2]. Through a global supergrid, the minimal mismatch is at 15%.

Furthermore, the number of infeasible $\alpha - \beta$ combinations is a lot smaller, than in the European case, due to the time-shift: solar energy can be used at different times and is therefore smoothed out (see also Biberacher [12]). However, as the total capacity per technology is still assumed to be limited to 5 times peak load, the contribution of solar power is limited by this assumption. Increasing this limit to 20 times the peak load, a small area of infeasible combination remains. This reflects the inhomogeneous distribution of continents on the globe. If the continents where distributed evenly, the average global solar power PV generation would be constant.

The global meteorological data is taken from the World Wind Atlas [130] and Bishop et al. [14]. It is described in detail in Aboumahboub et al. [2]. The spatial distribution of the wind and solar capacity across the world is assumed to be proportional to the FLHs.

3.3.3. Grid costs and structure

The foregoing section showed, that some VRE system integration challenges can be reduced through a powerful overlay transmission grid across Europe. A European supergrid reduces the necessary VRE and supplementary capacity and consequently the cost of electricity. The costs and dimensions of this grid are specified in this section.

Figure 3.10 shows the total HV transmission grid capacity and its costs resulting from the optimization model URBS-EU.

The capacity of the grid is measured in GWkm and thus contains its length and capacity. With increasing VRE share, the total transmission grid capacity increases to about a triple of the capacity of today's existing grid. For medium VRE shares of 30% to 50%, large transmission grid extensions result from the optimization, while a saturation effect occurs a very high shares. At these high shares, the regional energy production already is high enough and the advantage of electricity transmission is lower. In the results shown in Figure 3.10 it is assumed that todays power plant fleet remains (*Grid Only* scenario). Each country has sufficient dispatchable capacities available. In cases with very high VRE shares it is more cost-effective to use these national supplementary capacities in the few hours of regional VRE shortage instead of investing in transmission grid extension for electricity import.

The second observation is that grid capacity rises with β: the linkage between regions is less preferable for solar than for wind energy. This is due to the long correlation length of solar supply in Europe concerning intra-diurnal variations [60]: it is night at about the same time all over Europe. Also, as pointed out earlier, solar supply is geographically more evenly dispersed in Europe and temporally closer to the load.

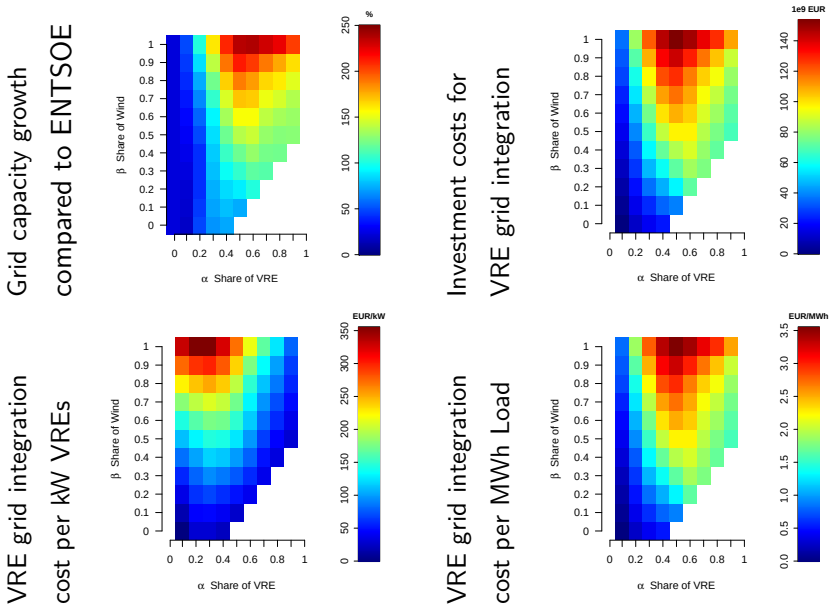

Figure 3.10.: Grid extensions and costs for the *Grid Only* scenario. Grid extensions are the increase in grid capacity and length (MWkm) with respect to the current ENTSO-E grid. Costs are the additional costs due to VRE deployment. They are deduced from incremental grid extensions between the reference case where $\alpha = \beta = 0$ and configurations with VRE contribution ($\alpha > 0$).

The total investment costs for grid extensions to integrate VREs reach 150 billion € at their maximum (upper right Figure 3.10). Compared to the projected 100 billion € investment in transmission grid extensions due to demand increase and refurbishment necessary until 2035 by the International Energy Agency (IEA) [77], this means adding more than the double of the "normally required" investment in transmission grid extensions. Note, that the VRE grid integration costs are deduced from incremental grid extension, which occurs on top of the reference case where $\alpha = \beta = 0$. In the reference case, transmission grid extensions result from the cost optimization, reflecting a non-cost-optimal structure of the grid today. These grid extensions are thus not due to VRE capacity additions and are subtracted to obtain the investment costs for VRE integration.

The grid costs per VRE capacity are shown in the lower left graph of Figure 3.10. At their maximum, they slightly exceed 350 €/kW, but generally range between 50 and 250 €/kW. The relative costs peak at medium VRE shares of $\alpha = 30\%$, which is due to the maximal total grid extensions at medium VRE shares and the large VRE capacities for higher values of α.

The comparison of the cost to the VRE capacity shows, that despite the impressive absolute transmission grid costs, relative to the investment costs for VRE capacities, the total investment costs for a supergrid in Europe are low. They stay below 10% for the

High Costs case presented in Table 2.11. Assuming *Low Costs* for VRE capacities, grid integration costs stay below 25%, even in extreme scenarios with α=20% and β=100%.

The specific VRE grid integration costs resulting form the analysis are in accordance with other studies. The European Wind Energy Association (EWEA) provides an overview of different studies, where the specific transmission grid costs range between 10 and 370 €/kW for scenarios of intermediate VRE share [54]. The RoadMap 2050 study by McKinsey find the transmission grid costs to amount 83 €/kW for a scenario corresponding to $\alpha \approx 40\%$ and $\beta = 30\%$ [101]. The IEA estimates the investment costs for additional interconnection to be about 110 €/kW for a scenario which corresponds to $\alpha = 40\%$ and $\beta = 80\%$ [77].

Sharing the annuity of the investment costs for VRE grid integration between the consumers, additional CoE arise. They are shown in the lower right graph of Figure 3.10 and reach 3.5 € per MWh load at their maximum.

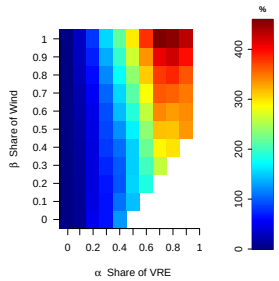

Figure 3.11.: Grid extensions with cost-optimal supplementary capacity (*Grid and Power Plants* scenario).

For the computation of VRE grid integration costs, it was assumed, that each country disposes of the necessary supplementary capacity. In the *Grid and Power Plants* scenario, where transmission grid extensions and supplementary capacities are optimized simultaneously reflecting a holistic system planning and neglecting national concerns about security of supply, the amount of cost-optimal transmission grid extensions increases.

Figure 3.11 shows the total grid extensions for a case with cost-optimal supplementary capacity distribution. Here, grid extensions and supplementary capacities are optimized simultaneously in the model. This results in a cost-optimal distribution of supplementary capacities across Europe, which is largely driven by the grid geometry and VRE capacities. It is more attractive to build more grid and reduce the costs for the supplementary energy and capacity, than to provide supplementary energy locally. Therefore, larger grid extensions result. From a system design perspective, this scenario would be very beneficial, but would require a European consensus on important aspects of energy policy.

The geographical structure of the transmission grid, which facilitates the VRE integration, is presented in Figure 3.12. It depicts the minimal grid extensions in the *Grid Only* scenario for any wind share between 60% and 100% for α=30% and α=60%. This "must have" grid shows the interconnections, which are cost optimal in a large range

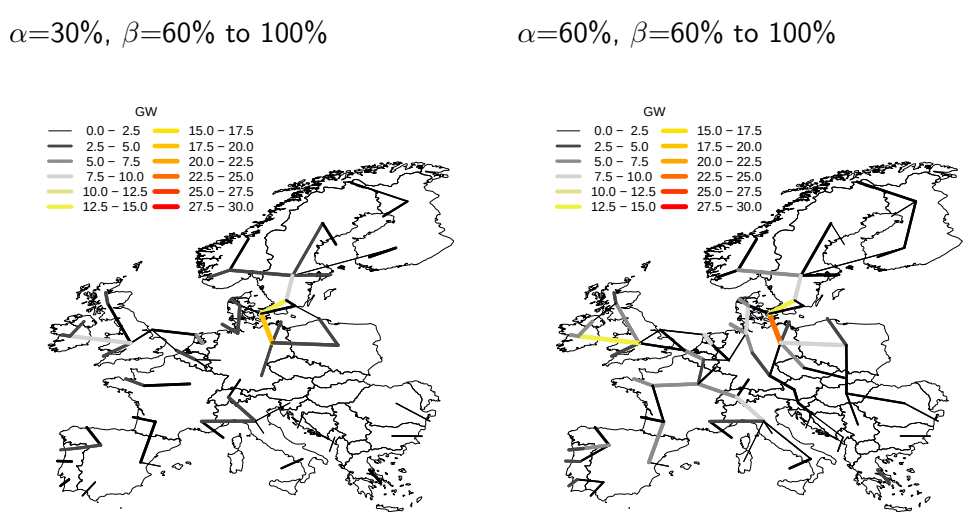

Figure 3.12.: "Must have" grid. Minimal transmission grid extensions on top of existing ENTSO-E grid for varying wind share between 60% and 100% for the *Grid Only* scenario.

of scenarios. The structure of the grid is determined by the relative distribution of VRE capacities and load centers.

Strong north-south connections from north-western Europe to the load centers further south are prominent features. These power tramsission "highways" across Germany and France traversing the BeNeLux states and also across Poland export the wind energy generated in and around the North and Eastern Sea southwards. Furthermore, an offshore grid in the North Sea as well as the connection of Spain and France across the Pyrenees, are crucial. With increasing VRE share, north-south connections in central Europe and the connection of Italy over the Alps to the rest of Europe as well as connections to South-Eastern Europe gain importance.

3.3.4. Mix of supplementary supply and emissions reduction

The major transmission grid extensions presented in the previous section facilitate the integration of VREs to the power system considerably, but do not solve all problems. The residual load is still highly fluctuating and the dispatchable power plants have to balance these fluctuations (see Figure 3.4). In the URBS-EU model, power plant dispatch is optimized as well. The suitability of different supplementary technologies for each VRE configuration can therefore be inferred from the results.

Figure 3.13 shows the contribution of different power plant types to the satisfaction of residual load and the resulting emission reductions. The supplementary energy mix strongly depends on the installed capacity of thermal power plants. The left column

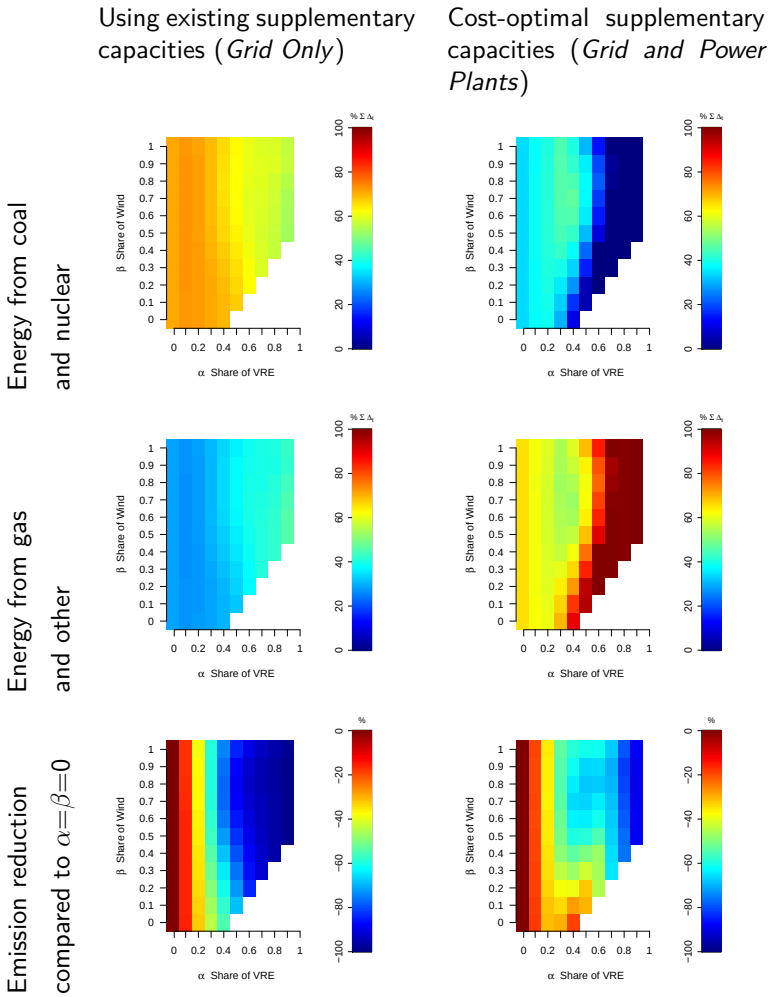

Figure 3.13.: Energy by dispatchable power plants and emission reduction. The supplementary energy is shown as share of total residual demand, being total energy to be supplied by supplementary power plants. "Other" refers to bioenergy, hydro and oil power plants.

of Figure 3.13 shows the supplementary energy mix for the *Grid Only* scenario, where today's capacity mix is assumed. The right column shows the supplementary energy mix for a cost-optimal capacity mix for each VRE configuration (*Grid and Power Plants* scenario).

The findings show that with increasing VRE share, more flexible dispatchable technologies are necessary. Coal and nuclear, today's rather inflexible mid- and baseload power plants, become unsuitable with increasing VRE shares. In turn, more flexible technologies, such as gas, hydro and biomass power plants, are needed. The extent of this fuel switch however depends on the speed of VRE capacity build up and, of course,

the relative fuel costs.

The *Grid Only* scenario reflects the effects of VRE supply in the short term. If Europe realized one of the VRE scenarios instantaneously, today's dispatchable capacities would still be on line and the left column would be valid. In this scenario, coal and nuclear are still cost-effective as supplementary energy up to VRE shares of 80%, as only their variable costs are taken into account. Due to the ramping contraints included in the model (Table 2.12), the usage of these rather inflexible technologies becomes less advantageous with increasing VRE higher shares. If start-up costs were included in the model, this threshold would occur at lower VRE shares.

The *Grid and Power Plants* scenario shows the long term impacts of VRE supply to investments in new power plants. If the build up of VRE capacity takes longer than the lifetime of the existing power plants, this scenario is more realistic. The results show, that from a VRE share of 40%-50% on baseload power plants such as coal and nuclear are no longer part of the cost-optimal mix. The reduction of FLHs for coal and nuclear power plants through VRE penetration renders new investments in these capital-intensive technologies uneconomic.

As both scenarios contain cost-optimal grid extensions, the thresholds for technology suitability have to be understood as upper limits. Especially for regions with high VRE shares inflexible dispatchable technologies face economic difficulties at lower overall α if fewer transmission grid extensions are realized (see also Chapter 4).

The last row of Figure 3.13 shows the emission reduction for both scenarios compared to the reference case, where no VRE generation is assumed. The results show, that with high VRE shares, emission reductions of more than 85% are possible. Already at VRE shares of 50% these large reductions can be achieved in the *Grid Only* scenario, where existing nuclear but also hydro and bioenergy plants provide low carbon supplementary energy. In the *Grid and Power Plants* scenario, mainly coal and gas power plants supply the supplementary energy, leading to slower emission reduction.

3.3.5. Case study: 60% VRE penetration in 2050

A large range of VRE scenarios was presented and their respective impacts on the power system. To provide guidance to the reader, an exemplary VRE scenario is studied based on the above findings and a possible roadmap how to reach this scenario from today's situation is sketched.

The exemplary scenario is based on the following assumptions. Until 2050, strong emission reductions have to be achieved by the European power sector [40] (see Chapter 1). Wind and solar energy will play an important role in the electricity supply in 2050 and satisfy 60% of electricity load.

Based on the results, advantageous design features of a power system with 60% VRE penetration can be determined.

Figure 3.3 provides a good overview on the integration challenges of 60% VRE penetration and the role of grid extensions. With minimal mismatch $|\Delta|$, lowest adaption needs of the power system occur, as supply is closest to demand. As can be read from

	Optimal Grid	*No Grid*
Ideal mix to achieve minimal $\|\Delta\|$ at α=60%	β=85%	β=75%
Parameter values at the identified point		
Mismatch $\|\Delta\|$	40% of total demand	48% of total demand
Overproduction	<1% of total demand	8% of total demand
supplementary capacity	81% of peak load	102% of peak load
CoE (high VRE costs)	84 €/MWh	97 €/MWh
CoE (low VRE costs)	52 €/MWh	60 €/MWh
Grid integration costs	3 €/MWh	-

Table 3.4.: Power system properties with VRE penetration of 60%.

the last row of Figure 3.3, minimal mismatch $|\Delta|$ for a VRE share of 60% translates to wind share of 85% with and to 75% without grid extension (see Table 3.4). The systematic advantage of solar energy for low connection cases due its good fit to the diurnal load pattern re-emerges, but the absolute mismatch is lower with transmission grid extensions, thanks to the resulting smoothing of the wind supply.

Table 3.4 lists the different advantages of transmission grid extensions for a 60% case. The necessary supplementary capacity is reduced by 20%, or around 100 GW. Overproduction decreases from 8% to 1% corresponding to about 250 TW. Finally, the CoE, driven by total – dispatchable and VRE – capacity can be lowered by about 10 €/MWh, while the costs for the grid only amount to 3 €/MWh. Thus, the transmission grid extensions, coming at total investment costs of 120 billion €, are cost-effective.

Until 2050, large parts of today's power plants will be shut down (see Figure 2.19) and an adapted supplementary capacity mix is possible. Following the analysis in Figure 3.13, only flexible power plants, mainly gas, will be suitable for a VRE penetration of 60%. As Figure 3.4 shows, even with transmission grid extensions, the highly fluctuating residual load requires flexible supplementary power plants. The achieved emission reduction through the VRE capacity is roughly 60% (Figure 3.13) in the case with grid extension. Deploying carbon free dispatchable power plants such as bioenergy, geothermal or hydro power would allow to reduce the emission further.

An advantageous system with 60% VRE should thus have a high share of wind energy, ideally 85% and a powerful transmission grid to integrate wind and solar energy. It should also provide supplementary energy from flexible power plants, such as biogas, hydro or gas power plants.

Today's VRE penetration in Europe amounts to 5% with a contribution of wind of 86% [77]. The necessary steps in terms of system design to reach 60% VRE penetration with more than 60% wind in 2050 can be identified from our results. First, the necessary wind and solar capacity has to be built. A total of about 775 GW wind and solar capacity has to be installed in 2050, of which about 35% are wind on- and offshore each and 30% solar PV capacity. Compared to todays 176 GW of installed wind (106 GW) and solar (70 GW) capacity about 16 GW/year would have to be added [57, 51]. In the

last three years, 10 GW of new wind and 18 GW of new solar PV capacities have been installed on average. Thus, the general VRE build up speeds are sufficient to reach 60% VRE share in 2050, however a shift away from fast solar PV growth towards more investment in wind turbines, especially offshore wind parks would be required. Second, important transmission grid extensions should be built to integrate these large capacities. The necessary grid capacity extensions amount to about the triple of the existing grid and planning should therefore start as soon as possible. The "must-have grid" shown in Figure 3.12 can provide valuable guidance for the infrastructure planning. Finally, new dispatchable capacities should be chosen in accordance to the increasing flexibility requirement. In total about 400 GW dispatchable supplementary capacity are required at least. Including a capacity margin of 20%, 480 GW would be required. Although in total sufficient dispatchable power plant would be available today, in the long term, not all of these technologies are advantageous. The cost-optimal dispatchable fleet should be provided by flexible power plants, such as gas, bioenergy, hydro and geothermal power plant. Their capacity would have to be doubled until 2050 compared to their current cummulative capacity of 270 GW [120].

3.4. Discussion and conclusion

This chapter studies the system integration of VREs in Europe and the role of transmission grid extensions as a measure to facilitate the VRE integration. A time series analysis and the model URBS-EU are applied to analyze each possible VRE configuration on the defined parameter space, spanned by the VRE penetration α and share of wind energy in VRE supply β. This parametric study allows to identify advantageous system design features for each level of VRE penetration, insights of high relevance for the conception of renewable energy policies and long term targets.

Generally, major system integration challenges occur with increasing VRE penetration: large VRE and supplementary capacity is required and important overproduction and mismatch between supply and demand occur. Grid extensions alleviate these challenges, as they smoothen the temporal fluctuations and remedy the geographical dispersion of VRE. Through the smoothing, overproduction can be reduced and less VRE capacity is necessary with a European supergrid. A second consequence of the smoothing is the reduction of required supplementary capacity from more than 100% to less than 60% of peak demand. Overproduction and the mismatch are also reduced considerably. Grid integration costs remain below 25% of the VRE investment costs for all possible VRE scenario. From the results the most important corridors for new transmission lines can be identified. Finally, the results show the need of increasingly more flexible power plants with rising VRE penetration.

Based on eight-year meteorological time series of wind and solar availability, it is proven on a theoretical basis that, with a European supergrid, a VRE share of more than 85% is possible in Europe. This is not only true when looking at the technical energy potential of the VRE technologies on average over the year, but also when considering their time-

and region-dependent generation pattern. Without grid extensions, the maximal share lies at 60% only. The maximal VRE share can be increased even further to more than 90%, if the MENA region is included in a highly renewable power system. The results show, that the interconnection of Europe and the MENA region allows to tap important wind and solar potential in this area and to achieve important smoothing effects through the connection of MENA to Europe.

The high VRE shares, however, come at the cost of large wind and solar capacities, excelling the peak load by up to 8 times for the European case. Due to the restricted availability of VREs with annual utilization rates of 30% or lower (i.e., FLHs of 2600 or lower), a VRE powered system always needs larger total capacity, than a system with dispatchable power plants. On top of that, large supplementary capacities are needed to ensure reliable power supply. These large capacities lead to high CoE of up to 145 €/MWh in the most extreme cases (*High Costs* case, without grid extensions). With grid extensions, the necessary supplementary and VRE capacities can be reduced and with it the costs of generating electricity to 92 €/MWh. Assuming a reduction of the VRE costs to the *Low Cost* case on top of that, the average European CoE amount to 49 €/MWh. This is cost competitive compared to a gas turbine, which has CoE of 85 €/MWh, at a carbon price of 30€/t.

The interconnection of different European regions, where the VRE generation differs, leads to a smoother power generation from VREs. The results show, that the necessary supplementary capacity can be decreased to less than 60% of peak demand through grid extensions, while the capacity credit of VREs increases from below 5% to more than 10% for VRE configurations with important contribution from wind energy.

Finally, with an overlay transmission grid, the overproduction and the mismatch between supply and demand are lowered. This entails less adaption need for the remaining power system, being dispatchable power plants and storage.

Having identified the advantages of a powerful overlay grid for the system integration of VREs in Europe, the costs of such a supergrid are of high relevance. The costs of a supergrid for VRE integration are computed for all possible VRE scenarios. They stay below 3.5 € per MWh load across all VRE scenarios. This is in the range of the transmission grid tariffs paid today (6.7 €/MWh in Germany for example [49]). Grid extensions generally increase with VRE share, but for very high shares, saturation effects occur. Solar energy needs less grid extension. This is due to the long correlation length of the solar availability pattern: it is night at about the same time all over Europe and therefore solar energy profits less from transmission grid extension, than wind energy.

Generally, the additional grid capacities to be build are large. For the scenario investigated in the 60% case study, about the triple of today's grid capacity would be necessary. This is in contrast to current infrastructure planning. The ten year plan of the ENTSO-E foresees grid extensions in Europe in the order of 15% only [50]. Furthermore, the acceptance and building process for new transmission lines can take several years. Thus, early planning and commitment of the responsible parties is crucial to realize the VRE integration measure of transmission grid extensions in Europe. The "must-have" grid,

resulting from the analysis, can provide guidance for infrastructure planning: it identifies transmission grid corridors, where grid extensions are beneficial in a large range of possible VRE configurations. Those are strong north-south connections from Northern Scandinavia and Denmark to the load centers in Germany and France traversing the BeNeLux states and an offshore grid in the North Sea. Better connection of Spain and France and the connection of Italy over the Alps to the rest of Europe are crucial as well.

Thanks to the sampling of a large parameter space, further advantageous system design features can be identified, in particular, an ideal share and mix of VREs. Firstly, solar PV cannot provide power at night and thus VRE shares above 40% can not be realized with solar energy only. To reach higher VRE shares, an important contribution of wind energy – 40% or more – is necessary. With optimal interconnection, a VRE share of 83% and a wind share of 85% lead to a minimal mismatch. Without grid extension, the minimal mismatch is achieved with a VRE share of 60% and wind share of 75%. Wind energy can – especially in combination with grid extensions – provide a "fairly smooth" supply. For large α ($>$40%) this results in lower overproduction and mismatch but also supplementary capacity requirements are reduced. Without grid extensions, wind supply is less smooth, while the diurnal pattern of solar energy fits rather well to the diurnal load pattern. This is why, without grid extensions, a larger share of solar energy is favorable.

Even with a powerful grid, the fluctuations in the residual load remain very high. The findings show that another important design feature of future power systems are flexible dispatchable power plants. For investment in new power plants, the contribution of VREs to the future power supply has to be taken into account. The results show that for coal and especially for nuclear power plants a limit in suitability occurs: at VRE shares above 40%, these power plants are no longer part of the cost-optimal mix. More flexible technologies and those having lower investment costs, such as gas power plants, are adequate.

The results of the parametric study can provide a helpful overview for the design of renewable energy policies. A case study for VRE penetration of 60% in 2050 illustrates that the results can guide decisions about how to design a power system that is well adapted to the desired VRE share. Also for this case study, transmission grid extensions are cost-effective and reduce the required supplementary power by 100 GW and annual overproduction by 7% of the total demand.

The analysis in this chapter quantifies the VRE system integration challenge for every possible VRE share and mix. It provides detailed information about the implications of different VRE configurations, vital for investment decisions, the conception of policies and decisions on VRE system integration measures. The analysis of transmission grid extensions shows that a powerful overlay transmission grid reduces the adaption need of the remaining power system considerably, while its costs remain below 25% of the VRE investment costs for all scenarios.

4. Market effects of VREs and transmission grid extensions

4.1. Change of perspective: who benefits from grid extensions?

Transmission grid extensions are a very cost-effective VRE system integration measure, as the results in Chapter 3 show. Overproduction and necessary VRE and supplementary capacity can be reduced substantially. For a cost-optimal system design investment in VRE and in transmission grid capacity should be taken simultaneously. While the analysis up to now was based on a central planner perspective, this chapter takes a market perspective. It focuses on the implications of VREs for the electricity market and the impacts of transmission grid extensions on the market integration of VREs.

The integration of highly fluctuating supply in the electricity wholesale price is challenging. Regional oversupply and low marginal prices of VRE technologies can lead to momentary price reductions. The power supply curve, the merit order, is shifted, whenever VREs contribute to the power supply, leading to a less stable and potentially lower average price seen by all generators. This is called the merit order effect (see Subsection 1.1.2).

Furthermore, due to the low capacity credit of VREs, large supplementary capacity has to stay on line, even if large shares of VRE are realized – assuming little storage capacity. As the capacity factor, i.e., the average energy supplied per VRE capacity, is larger than their dependable share of capacity, their capacity credit, the FLHs of the dispatchable power plants are reduced with increasing VRE penetration. In addition to lowered wholesale prices, this reduction of FLHs, also called "compression effect" [111], poses additional problems to the profitability of conventional generators.

As shown in Chapter 3, grid extensions can help to connect regions with high VRE potential to the load centers and to smoothen the power supply by VREs. The capacity credit of VREs can be increased and the residual load smoothened a little.

This chapter quantifies the effects of VREs to the wholesale electricity prices and analyses the VRE market integration challenge, including the effects of reduced FLHs for conventional power plants. Furthermore, it is evaluated whether the systematic benefits of transmission grid extensions for VRE integration are also reflected in the electricity market.

For the analysis, the year 2020 is chosen. For this medium term scenario year, political targets have been announced. The European Union seeks to provide 34% of the electricity by renewable energies in 2020 [38] and the member countries have published the pursued goals in terms of installed capacity per renewable technology for 2020 [11]. Major contributions will come from wind and solar energy due to their large potential, attractive feed-in tariffs in many countries and expected cost reductions [34, 77].

The URBS-EU model is applied to analyze the role of transmission grid extensions for the market integration of the projected wind and solar capacities for 2020 in Europe. The regional economic effects of VREs on electricity markets and their participants are quantified in dependence of different transmission grid extension levels. The electricity prices are derived from the marginal costs of electricity resulting from the optimization. In doing so, a fully competitive and transparent market is assumed, where no strategic mark-ups occur. The potential of grid extension to reduce the effects of VREs to the electricity market is studied and economic benefits for utility owners, but also potential additional barriers to grid extensions are identified.

The chapter proceeds as follows: An overview of related work is given in Subsection 4.1.1. Section 4.2 briefly describes the current regulatory and market framework. The methodology and scenario definition for the quantitative analysis are described in Section 4.3, results are given in Section 4.4. Finally, the findings are discussed in Section 4.5.

4.1.1. Literature review

The integration of power generation from VREs to the current electricity market spurred numerous research efforts.

Sensfuss et al. show in an econometric analysis that in 2006 the German average wholesale electricity price was lowered by about 8 €/MWh due to the integration of renewable energies [135]. They first introduced the term "merit order effect". As Hirth points out, VRE may also achieve higher prices than a baseload technology plant with constant power production [68]. This so-called "correlation effect" is opposite to the merit order effect and happens, if the VRE generation is positively correlated with demand – for example solar PV – and not price-setting, i.e., not exceeding the demand. An increasing VRE share may lead to an attenuation of the effect as Ketterer shows for the German example [83]. The merit order curve is less steep for lower residual demand and thus the effect of VREs is less pronounced.

If the merit order effect occurs and the average electricity price is reduced due to renewable electricity supply, redistribution of economic welfare results: consumer surplus increases and producer surplus is reduced, as Saenz de Miera et al. show [129]. But as MacCormack et al. prove with a probabilistic power generation model, the total costs of the power supply rises with increasing wind contribution opposite to the reduced electricity price [97]. With this, the possibility of cost recovery for renewable energies on the electricity market is called into question. Hirth and Ueckerdt show that a carbon tax would allow to realize a market, where all technologies cover their full costs, while

feed-in tariffs or politically motivated renewable capacity extension lead to a reduction in overall welfare [69] .

Not only the average level of electricity price changes with VRE, but also its dynamics. Based on the example of Texas, Woo at al. show that higher wind energy supply leads to lower average electricity prices, but also to higher price volatility [154]. This volatility is sensitive to the level of wind speed, the behavior of different market participants, as Green and Vasilakos show [58], and the distribution of market power, as proven in a theoretical framework by Twomey and Neuhoff [142].

Measures to alleviate the effects of VREs to the electricity price are investigated by Jacobsen and Zvingilaite for Denmark focusing on storage, demand side management and real time pricing [80]. Leuthold et al. demonstrate on an aggregate European level that the reduction of electricity prices due to wind integration can be diminished with grid extensions [92]. They find, that European grid extensions lead to an overall welfare gain.

In this chapter, the influence of the planned VRE capacities for 2020 on the electricity prices are quantified together with the effects of transmission grid extensions. In a first step, the cost-optimal grid extensions for Europe in 2020 to integrate VREs are determined. Second, the role of the grid for electricity markets and their participants are investigated.

The studies mentioned above showed the effects of VREs to the electricity prices. Here these effects are resolved in more detail: thanks to the technical and regional detail included in the model URBS-EU, the implications of lowered electricity prices can be analyzed for each model region and technology. The changes in electricity prices, technology-specific market values and the generator revenues due to VREs are determined. Furthermore, the inclusion of transmission grid extensions in the analysis leads to new insights. First, it allows to quantify the effects of the VRE system integration measures for VRE market integration and, second, it can be identified who would benefit where from transmission grid extensions for VRE integration.

4.2. Current regulatory framework

In the last decades, the electricity markets have undergone an important transformation from state-owned utilities to liberalized electricity markets. Current market operation and the most relevant regulations are described in this section. In the analysis in this chapter, a perfectly liberalized system with nodal prices and a fully coupled European electricity market, based on these nodal prices, are assumed. The background information provided in this section allows to identify the benefits and shortcomings of these assumptions.

4.2.1. From state to market: liberalization and unbundling

Since the 1990s the electricity and gas supply structures in the EU have been transformed gradually from state-owned monopolies to competitive markets, targeting a fully

Country[a]	Liberalization[b]	Market name	Market zones	Unbundling	Market coupling
Central West Europe (CWE)					
Austria[c]	2001	EXAA, EEX	1	legal	-
Belgium	1999	BELPEX	1	ownership	CWE
France	2000	EPEX	1	legal	CWE
Germany	1998	EPEX	1	ownership (50%), legal	CWE
Netherlands	1998	APX	1	ownership	CWE
British Isles and Ireland					
Great Britain	1989	APX	1	functional, ownership (33%)	-
Ireland	1999	SEMO	1	functional	-
Nordic markets (NP)					
Denmark	2000	Nord Pool	2	ownership	NP
Finland	1995	Nord Pool	1	ownership	NP
Norway[d]	1990	Nord Pool	5	public TSO	NP
Sweden	2002	Nord Pool	4	ownership	NP
Estonia[e]	2004	Nord Pool	1	ownership	NP
Latvia[e]	2004	Nord Pool	1	legal	-
Lithuania[e]	2004	Nord Pool	1	ownership	-
Central and Eastern Europe (CEE)					
Czech Rep.	2004	OTE	1	ownership	CEE
Slovakia	2004	OTE	1	ownership	CEE
Hungary	2004	OTE	1	NA	-
Poland	2004	TGE	1	ownership	-
Romania	2007	OPCOM	1	ownership	-
Slovenia	2004	BSP	1	ownership	-
Croatia[f]	2005	HROTE	1	public TSO	-
South East Europe					
Greece	since 1999	DESMIE	1	legal	-
Bosnia	2008	(CEZ)	1	functional	-
Bulgaria	2007	(CEZ)	1	functional	-
Iberian pensinsula					
Portugal	1991	OMEL	1	ownership (33%)	-
Spain	1994	OMEL	1	ownership	-
Other					
Italy	1999	IPEX	3	ownership (10%)	-
Switzerland[d]	2007	Swissix,EEX	1	functional	-
Luxembourg	2000		1	legal	-

Table 4.1.: Overview of European electricity markets and unbundling strategies for the transmission system, status 2012 ([42, 121, 43], own research)

[a] Cyprus and Malta are not included; [b] national legislation. Note: 1996: first EU directive, 2003: second EU directive, 2009: third EU directive; [c] Austria is not part of the CWE market coupling zone, but a de-facto coupling to Germany exists, as EXAA and EPEX market participants can trade on both platforms. [d] not in EU but in model; [e] not in model but in EU; [f] in model, set to become member of the EU in 2013

liberalized pan-European electricity market. Electricity is no longer provided by the state owned company, but by competing private companies.

After first experiences with the liberalization of the Britain electricity market in the late 1980s, the EU adopted the first liberalization directive in 1996 aiming to gradually open the electricity markets to private companies [36]. Further legislation prescribes the legal separation of electricity transmission and generation (second directive [37], 2003). This can be realized by clear "ownership unbundling", where the generation and the transmission and distribution grid are split in two companies, by "functional unbundling", where the operation and control of the transmission system is handled by Independent System Operators (ISOs) or by "legal unbundling", where an Independent Transmission Operator (ITO) autonomously manages the transmission system (third directive [39], 2009). The translation of the third directive in national law was foreseen for 2011, but is delayed in a number of member countries [42]. Table 4.1 gives an overview over the liberalization of electricity markets in European countries.

The directives establish common rules of all European countries. This is motivated by the priority objective of the European Union to couple all national markets to form a common internal European electricity market with nodal prices. By 2014 all member states should be fully integrated in an internal European electricity market [113]. As indicated in Table 4.1 already today larger areas with coupled markets exist.

4.2.2. Wholesale electricity market and grid regulation

Market

Figure 4.1 illustrates the principal structure of the electricity market in Europe. Electricity is traded on the wholesale electricity market and through bilateral Over The Counter contracts (OTCs). The share of electricity traded on wholesale markets, increased from about 30% to more than 40% from 2005 to 2011 [42]. OTCs thus still account for the majority of the market volume, but the wholesale prices are indicative for these contracts. The wholesale markets are energy-only markets, where the prices are largely determined by the marginal costs of generation. In hours of scarcity, increased prices, so-called scaricity mark-ups, can occur [126]. Generators, supplier but also large consumer can submit bids to the spot market.

On the physical level, the TSOs and Distribution System Operator (DSOs) deliver the electricity.

To ensure security of supply, regulation foresees that the physical balancing in the market area is checked in advance. The TSO is responsible for the physical balancing and stable operation of the grid. He coordinates the demand prognoses and dispatch schedules. Accordingly he requires or allocates redispatch and balancing energy.

Balancing power is held available to ensure stable operation of the system and prevent system failure. There are three stages: primary, secondary and tertiary control, acting on staggered time horizons frames from a few seconds to an hour.

In normal, fault-less operation, changes in the planned regional power plants, so-called redispatch, occur. As can be seen in Table 4.1, commonly, there is one market per

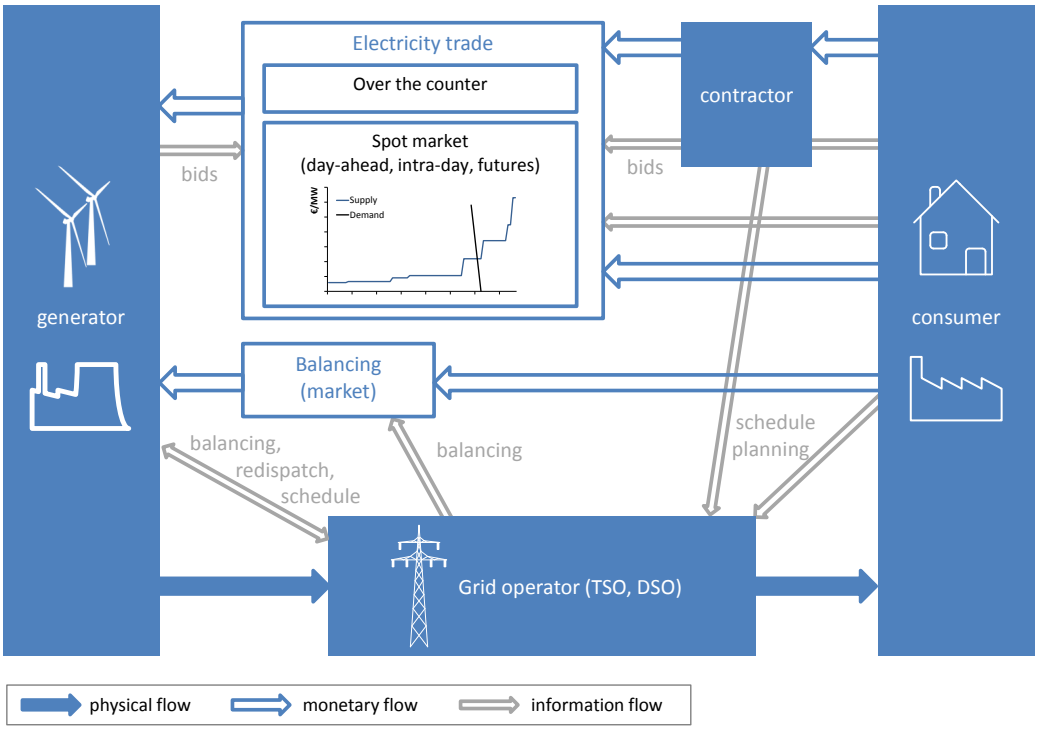

Figure 4.1.: Highly simplified wholesale electricity market: agents, institutions and monetary, physical and information flows

country. Scandinavia and Italy are an exception. In countries with one price, energy is traded regardless of internal transmission constraints. After market clearing, generators and consumers submit their preferred power plant and grid dispatch to the TSO. If congestion would occur with the scheduled dispatch, the system operator has to change the regional balances: he redispatches the system. The operator will, for example, pay a generator in the north to reduce production and a generator in the south to increase its production, if the north-south grid connection is insufficient to realize the planned dispatch. Both power plants, the northern and southern one, receive a compensation of their additional costs due to the changed schedule. These additional costs caused by the redispatch are passed to the consumers through the TSO.

International electricity exchange in the ENTSO-E

Transmission capacity between countries in the EU is allocated in two steps. Based on detailed load flow simulations the Net Transfer Capacities (NTCs) between countries are determined. The NTCs are direction-dependent and reflect the ability of the respective national transmission networks to import or export electricity, but are not necessarily the physical limit of the interconnection. These NTCs are auctioned between the neighboring countries. In short term contracts, the capacity already allocated by earlier auctions

(Already Allocated Capacity, AAC) has to be taken into account and only the Available Transfer Capacity (ATC = NTC- AAC) can be traded [47].

The EU aims to couple all electricity markets in Europe to form a common internal market. The market coupling is already realized in the CWE, CEE and the NordPool region (see Table 4.1). Here, the allocation of the cross-border trade (limited by the ATCs) is determined by the market coupling: market participants can trade directly between the market areas. This allows to achieve price convergence between the coupled regions and more efficient, market-based allocation of the cross-border transmission capacities [43].

National grid regulation

The independently operating transmission and distribution system operators cover their costs through grid tariffs. Generator and consumers linked to the grid pay the tariffs defined by the regulatory body, for example the German *Bundesnetzagentur*. To avoid discrimination, grid tariffs are homogeneous within the control area of one TSO.

The grid tariffs commonly also include system services, such as the costs of the redispach and the acquisition of balancing energy mentioned above.

The development of the market and grid regulatory framework reflects the political decision to gradually build a common European electricity market. The liberalization of electricity markets, the unbundling of grid and generation units and finally the market coupling are first steps to a fully liberalized European power market. At the same time, with increasing VRE generation in the power system, the challenge of their integration to the system, technically and market-wise, increases.

In this chapter, the model URBS-EU is deployed as a simplified representation of the European electricity market. By optimizing the total European system costs, a fully coupled, common European market is assumed. This reflects the political target. Furthermore, marginal costs are taken as indicator of electricity prices, excluding strategic mark-ups. In doing so, a transparent market is modeled, meaning a market, where technical limitations are reflected directly in the electricity price. This allows to identify the benefits of VRE system integration measures to the electricity prices directly. The influence of strategic behavior of different market participants is not taken into account (see also Section 2.1). Finally, nodal prices are assumed. While some countries already introduced nodal prices, it remains unclear, whether this approach will be adapted by all countries. Therefore, a sensitivity analysis towards this assumption is performed.

4.3. Model setup and scenario development

4.3.1. URBS-EU model setup

URBS-EU is applied to study the effects of increasing shares of wind and solar energy in Europe in 2020 for the electricity market and the role of transmission grid extensions.

The optimization of the power system in the model determines the HV transmission grid extensions, dispatchable power plant additions on top of the remaining fleet in 2020 and the exogenously defined VRE capacities, as well as the dispatch of all power plants, the transmission grid and existing storage capacities. Electricity prices are inferred from their marginal costs resulting from the optimization.

The optimization is performed for six representative weeks of each year of available meteorologic data (2000-2007, see Subsection 2.3.2). Each scenario is thus computed for 48 weeks (6×8) in total. Typical weeks have been selected based on the method introduced in Subsection 2.2.4. The results are presented as aggregation over the eight years, where energy-related variables are averaged over the eight years and for capacities, the maximal values are shown.

The power system infrastructure is based on the databases introduced in Section 2.3. For conventional power plants, the remaining fleet in 2020 is determined based on average technology-specific lifetimes of the power plants (Table E.1). The necessary power plant additions to replace the retired power plants ($C_i^N \quad \forall\, i \in \{\in I \backslash I^{vre}\}$) are determined by the cost-optimization for each scenario. For some technologies, such as nuclear power and other renewable power (hydro, bio- and geoenergy), political and geographical limits are taken into account.

VRE capacity additions for 2020 are exogenous to the model and drawn from the National Renewable Energy Action Plan (NREAP) of the European member states [11]. Regional distributions within countries are based on previous studies, political commitments and planned projects [15, 138, 52]. They are shown in Figure 4.2.

The total planned wind capacity of 218 GW is similar to previous studies assumptions: for wind on- and offshore power a total European capacity of 180 GW in 2020 was assumed by the EWEA [52], 128-238 GW by the Offshore Grid study [114] and 280 GW by the Global Wind Energy Council (GWEC) [56]. For solar PV, 92 GW are projected for 2020. The NREAP lies between the projection of 45 GW Solar PV capacity in 2020 by the IEA [77] and the projection of the European Photovoltaic Industry Association (EPIA) of 124 GW in 2017 [51]. The installed capacity per region are listed in the Appendix (Table E.2 and E.3).

The existing ENTSO-E grid is used as a starting point. URBS-EU is applied to compute cost-optimal transmission grid extensions between model regions on top of the existing HV transmission grid. In the scenarios, different levels of grid extensions are studied. Addition of storage capacity, is not included in this analysis focusing on grid extensions only. Current storage capacities are assumed for 2020, reflecting the limited geographic potential for additional pumped hydro storage capacity in Europe.

The cost assumptions are as specified and validated in Subsection 2.3.1, Table 2.10.

To analyze the market effects, the marginal costs of electricity are used as approximation for the electricity price [112]. As the model is deterministic, perfect foresight exists. The prices resulting from the URBS-EU model are thus the theoretical prices of a perfectly competitive and transparent market. However, they correspond well to real

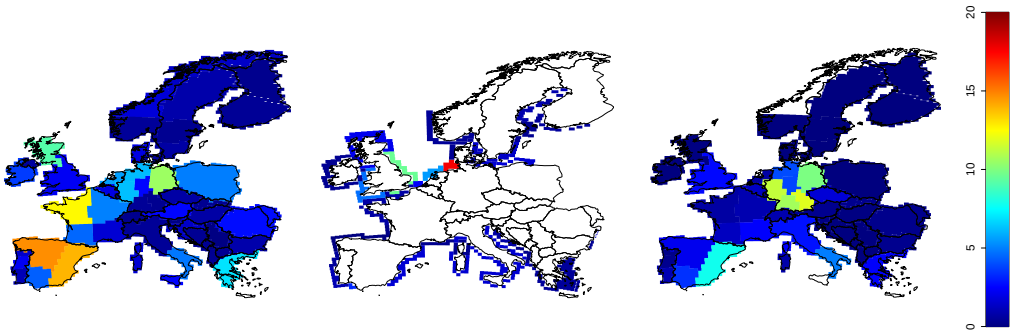

(a) Wind Onshore (152 GW) (b) Wind Offshore (66 GW) (c) Solar Photovoltaics (92 GW)

Figure 4.2.: Capacities of Variable Renewable Energies for 2020 in GW (according to NREAP [11]). Total European capacity per technology is indicated in brackets.

day-ahead market prices (see Section 2.4).

The prices resulting in the scenarios, do not necessarily reflect the total costs. In a perfect market, the prices would be sufficient to cover total costs of generation. In the modeling framework, this corresponds to a green-field optimization where generation, storage and grid capacities and their dispatch are solely determined by the cost-optimization. In this study, existing capacities and VRE capacity additions according to the political targets are included in the scenarios and therefore an imperfect market is modeled. For these power plants, the marginal costs reflect only the variable operation costs and therefore are not necessarily sufficient to cover the total costs.

Nodal prices are assumed, but a sensitivity analysis concerning this assumption is performed. In order to do so, actual market regions are implemented in URBS-EU by decreasing the regional resolution of the model. Simulating the power plant dispatch on this lower regional resolution yields the marginal costs of electricity per market region. Under the assumption that the NTCs are allocated cost-effectively, these results reflect the market prices in the current European market zones.

4.3.2. Scenario definition

Four scenarios are defined for the analysis. Their characteristics are listed in Table 4.2. The *Base* scenario serves as comparison for the VRE scenarios. It mimics the power supply system by 2020 without the projected VRE capacity additions. For the VRE scenarios three levels of grid extensions are analyzed: today's network (*No New Grid*) and two cases of cost-optimal grid extensions: in the *New Lines* scenario new overhead lines and offshore cables are allowed, in the *New Cables* scenarios only cable extensions on- and offshore are possible. Cables are about six times more expensive than overhead lines (see Table 2.10). The second case therefore results in less grid extensions. The *New Cables* scenario thus allows to identify the most important grid extension and

Input parameter	*Base*	*No New Grid*	*New Lines*	*New Cables*
VRE capacities	current capacities	projected capacities for 2020 [11]		
Dispatchable capacities	projected capacities for 2020 (retirements are taken into account), current hydro storage and run-of-river capacities [120]			
Limits for capacity additions	capacity addition for nuclear, geothermal and bioenergy are limited to maximum between 2020 extrapolations and current capacities, infinite for natural gas, coal, lignite and oil			
HV transmission grid	current ENTSO-E grid	current ENTSO-E grid and direct connections of offshore wind to shore	overhead line extensions between neighbors possible. Sea-cables allowed on selected connections	cable extensions between neighbors possible. Sea-cables allowed on selected connections

Table 4.2.: Definition of scenarios

furthermore represents a possible technical response to public resistance towards new overhead transmission lines.

The analysis of the VRE market integration and the effects of transmission grid extensions is carried out in three steps. In a first step cost-optimal HV transmission grid extensions for Europe in 2020 are determined. Second, the impacts of the planned VRE capacities to the existing power plants with and without grid extensions are analyzed. Finally, the effects of VREs in the electricity prices and the market participants are studied, again taking into account the effects of grid extensions.

4.4. Results: influence of VREs and grid extensions on prices and revenues

4.4.1. The cost-optimal grid

The cost-optimal grid extensions for the announced VRE capacities in 2020 in the *New Lines* and *New Cables* scenario are depicted in Figure 4.3. Large transmission capacities result from the optimization model. The total the grid capacity increases by about 120% in the *New Lines* scenario and by almost 50% in the *New Cables* scenario on top of the existing ENTSO-E grid capacity and length (in GWkm). This is plausible from an economic point of view, since new lines are relatively cheap compared to the additional use of fossil fuel (see Table 2.10, see also Chapter 3). Overhead lines are less expensive than cables and therefore, less grid extensions result in the *New Cables* scenario.

Germany, France and BeNeLux act as transit countries. In north-western France, northern Germany and Great-Britain substantial grid extensions are cost-effective in both scenarios to integrate the large wind capacities in these areas. Large new grid

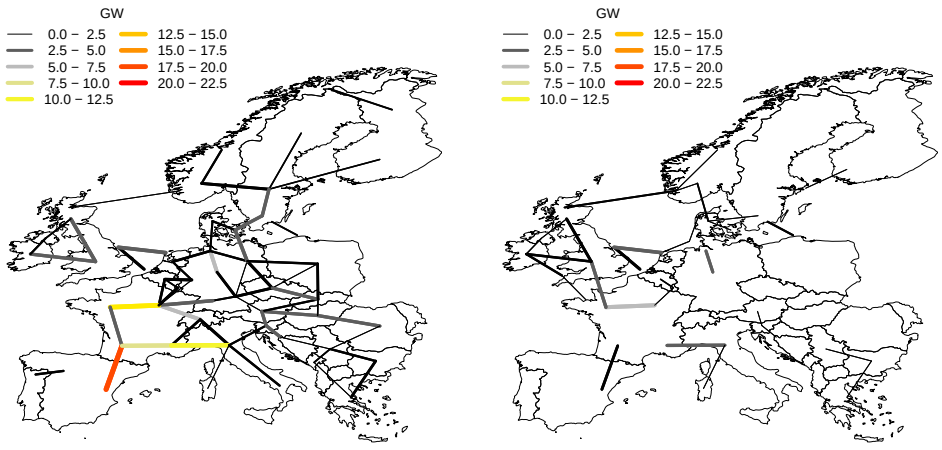

(a) *New Lines* (b) *New Cables*

Figure 4.3.: Cost optimal grid extensions for the announces VRE capacities in 2020. They exclude the imposed connection of offshore wind parks to the shore.

capacities result for the Spanish-French connection, where a only small connection exists today, but only little additions on the Iberian peninsula occur. Italy, having a rather weak electricity grid today, profits from a cost-effective enforcement of its connection to France and imports low-priced nuclear power from France. Offshore grid extensions are mainly located in the Northern and Baltic Sea, in proximity to important on- and offshore wind capacities. In the *New Lines* scenario the majority of grid extensions are onshore as overhead lines are cheaper than cables, while in the *New Cables* scenario larger shares of the grid extensions are offshore cables. Identical costs for on- and offshore cables are assumed. In BeNeLux for instance, offshore grid extensions are shorter and thus more cost-effective than onshore cable extensions in the *New Cables* scenario. If overhead lines can be built, the bulk power transmission takes place onshore.

In consistency with other studies, the results indicate that an offshore grid in the Northern sea is cost-effective. On- and offshore grid extensions for wind integration proposed in the TradeWind study [138] and by Kerner [82] show the same corridors as the ones identified in this study. A study by the EWEA focuses on European offshore wind parks and proposes a powerful interconnected offshore network in the Northern and Baltic Sea [53]. The proposed capacities for 2020 and 2030 by the EWEA are in line with the results.

Furthermore, the findings are consistent with the results presented in Chapter 3. The wind and solar production in the 2020 scenarios corresponds to a VRE share just above $\alpha = 20\%$ and a wind share of $\beta \approx 80\%$. Based on these shares, the total grid capacity can be compared between the two analyses.

In the parametric analysis, a grid capacity increase is about 80% for α=20% in the

Grid Only scenario and more than 120% in the in the *Grid and Power Plants* scenario. In the analysis in this chapter, part of the supplementary capacities are optimzed and therefore the resulting grid increase lies between these two scenarios. Furthermore, many of the connections identified in the "must-have grid" in Figure 3.12 are cost-optimal in the 2020 scenario as well, such as the North-sea connections, north-south connections in central Europe, mainly Germany, the stronger linking of Italy to central Europe and the connection across the Pyrenees.

4.4.2. Power plants

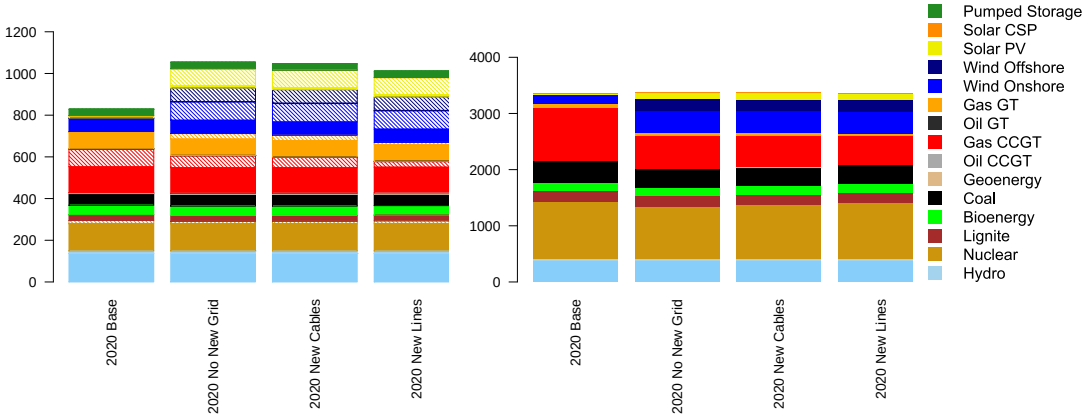

(a) Capacities (b) Total Energy Production

Figure 4.4.: Power plant capacities and energy production in 2020 for all scenarios. Shaded areas represent capacity additions.

Figure 4.4 presents the model results for power plant capacities and energy generation in Europe.

To the 690 GW of the power plants that will still be on line in 2020, the optimization model adds about 105 GW new dispatchable capacity in the *Base* scenario to replace retired power plants and those shut down for political reasons, such as the phase-out of nuclear power in Germany. Capacity additions are represented by shaded areas in Figure 4.4a. The additional 234 GW new VRE capacity lead to a slight reduction of conventional capacity additions in the *No New Grid* scenario, where 95 GW non-VRE capacity is added. This corresponds to a capacity credit of the VRE technologies of 4%. With grid extension less new thermal capacity is needed: about 52 GW is added in the *New Lines* and about 85 GW in the *New Cables* scenario. The capacity credit increases to 22% and 8% respectively. In all scenarios, nuclear and gas power plants are the only technologies, where new capacities are added. Compared with the European peak load of 619 GW, the conventional installations are, however, still able to supply peak load.

Again, the capacity credit determined is in line with the findings from the time series analysis in Chapter 3. As shown in Figure 3.6, the capacity credit of a system with α=20%, β=80% is 17% with and 4% without grid. As pointed out in Chapter 3, the time series analysis only provides an estimate of the necessary supplementary capacity and therewith the capacity credit. It does not take into account the existing power plant fleet and technical constraints such as ramping constraints, leading to higher supplementary capacity in the non-connected case. As a consequence, a slightly lower capacity credit results from the time series analysis.

Figure 4.4b shows the model's outputs regarding the energy mix. Since the VREs' share in total electricity production increases from 5% to 21% through the VRE capacity additions, the conventional power plants' output is significantly reduced, while conventional capacity remains close to current capacity. The averaged FLHs over all thermal generation types (Coal, Lignite, Gas, Oil, Nuclear and Bio- and Geoenergy) decrease by 9% in *No New Grid* case. With grid extensions (*New Lines*) the total average reduction of FLHs for thermal generation types amounts 5% and baseload power, mainly nuclear, replaces peaking technologies such as gas GTs and CCGTs, as can be seen in Figure 4.4a and b.

The reduction in power plant usage is most severe in regions with high VRE deployment and will create severe pressure for the conventional power plant operators. In regions with high VRE capacity, the FLHs of base load power plants such as nuclear and coal generation units decline sharply, if no grid extensions are realized, because they have to adapt to VRE supply (see Figure 4.5). With an extended, cost optimal grid, more traditional usage of the power plants is possible: baseload power is used more continuously, while the mid and peak load power plants also in the neighboring regions help to balance the VRE fluctuations. These technologies in turn supply less energy in total.

One of the most affected regions by new VRE capacities is North-Western Germany. For 2020, 18 GW offshore wind, 6 GW onshore wind and 4 GW solar PV capacity are projected for this model region (see Figure 4.2). Many important effects of the VRE integration for the power plants can be studied in detail from Figure 4.6, where the computed energy mix and the resulting energy prices for the North-Western German region *D-EON-N* are shown for one of the eight modeled meteorological years (2003).

In the *Base* scenario, the base load is covered by nuclear and coal power plants. Natural gas power plants and also electricity import from neighboring regions provide the mid and peak load. The region exports electricity. This can be read off from the difference between the yellow line and the orange line. The first shows the electricity demand within the region, the later depicts the net regional demand, where im- and export and storage charging are included. In the *Base* scenario, the current onshore wind capacity of 5.3 GW is installed.

In the scenarios *No New Grid* and *New Lines*, large amounts of additional wind energy from the North Sea are imported into north-western Germany, illustrated by the gray areas in Figure 4.6b and c. This results in drastic changes in the power plant dispatch, if

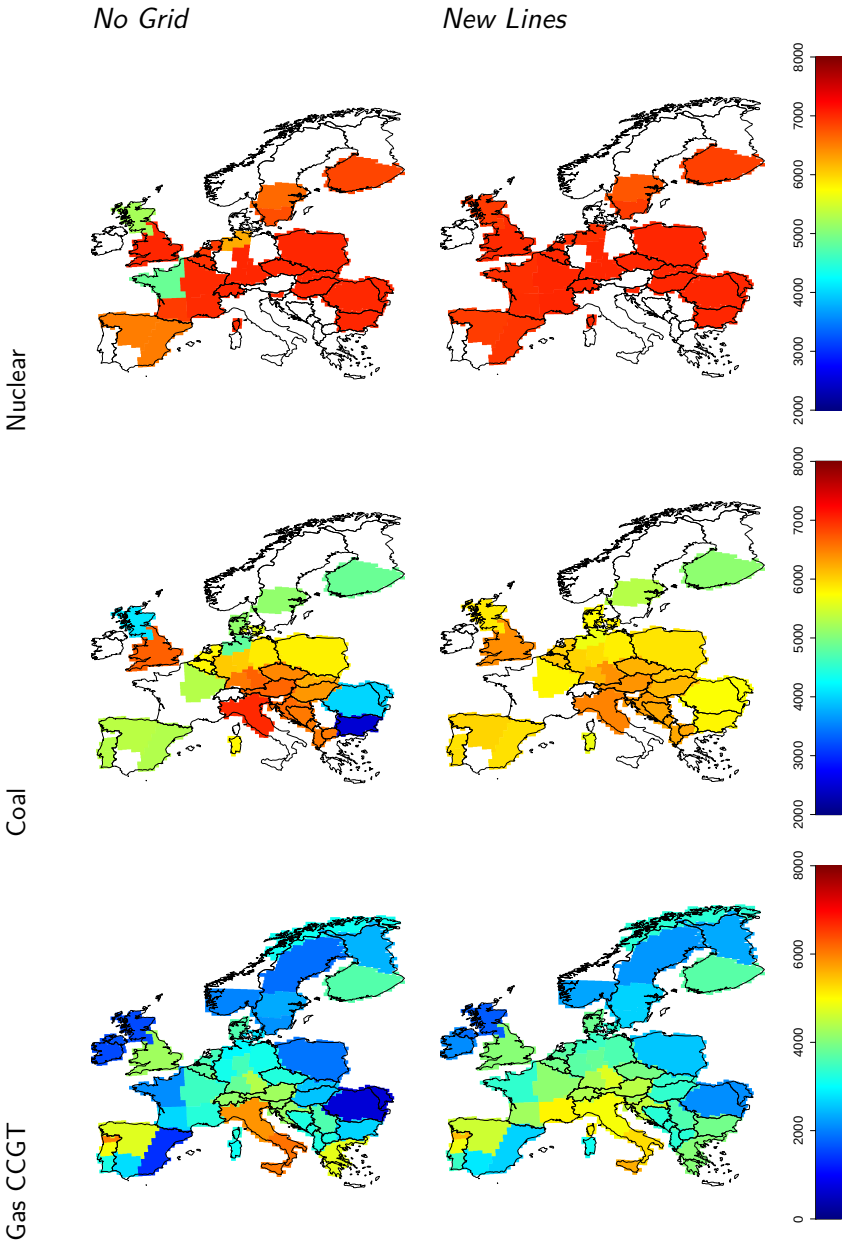

Figure 4.5.: Full Load Hours of nuclear, coal and gas power plants for the *No New Grid* and *New Lines* scenario

no grid extensions are carried out (*No New Grid*). In windy hours, wind energy replaces power from peak, middle and also base load power plants. Even nuclear power has to shut down several times. Allowing grid extensions (*New Lines*), the base load power plants can be used in a more traditional way. The burden of balancing the fluctuating wind energy is then shared between all peak and mid load power plants in the linked neighboring regions. Also the capacity additions alter slightly across scenarios: in the *Base* case slightly more new Gas CCGT capacity (1.3 GW) is installed.

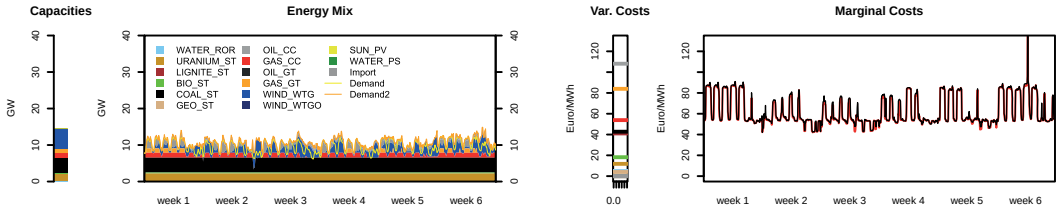

(a) *Base*

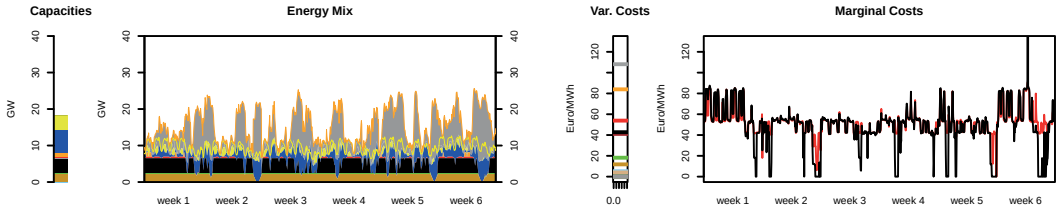

(b) *No New Grid*

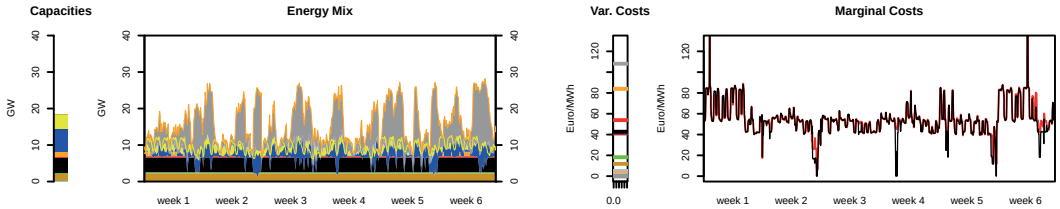

(c) *New Lines*

Figure 4.6.: Energy mix in north western Germany (*D-EON-N*) and electricity price for selected weeks in 2020 (the results for meteorological data from 2003 are shown here). The yellow line shows electricity demand, the orange one the net regional demand including im- and export and storage charging. The black lines shows the marginal costs for nodal price and the red line the corresponding hypothetical national price.

4.4.3. Electricity prices

The influence of VREs on power plant dispatch leads to significant changes in electricity prices, as can be seen for north western Germany in Figure 4.6. Due to their vanishing variable costs VREs enter at the first position in the merit order of power plants. When-

ever wind and solar energy contribute to the supply, the price is lowered (merit order effect). In cases where the VRE supply exceeds the demand, the electricity price drops to zero in the model setup.

Today's European electricity markets, except the Nordic zone and Italy, do not have nodal pricing (see Section 4.2), while in this analysis nodal prices for each model region are assumed. Changing the model setup to reflect the actual market zones results in slightly different electricity prices. In Figure 4.6, the prices assuming actual market areas are shown in red. Due to the large, national market areas, internal congestion of national transmission systems is not taken into account and the price drops are less pronounced. Especially with large VRE shares and without grid extensions (*No New Grid*), the differences between are significant. In the *Base* and the *New Lines* scenarios, the regional differences are less pronounced, as can also be seen from average annual prices shown in Figure 4.7, showing the weighted average electricity price per MWh for the four scenarios.

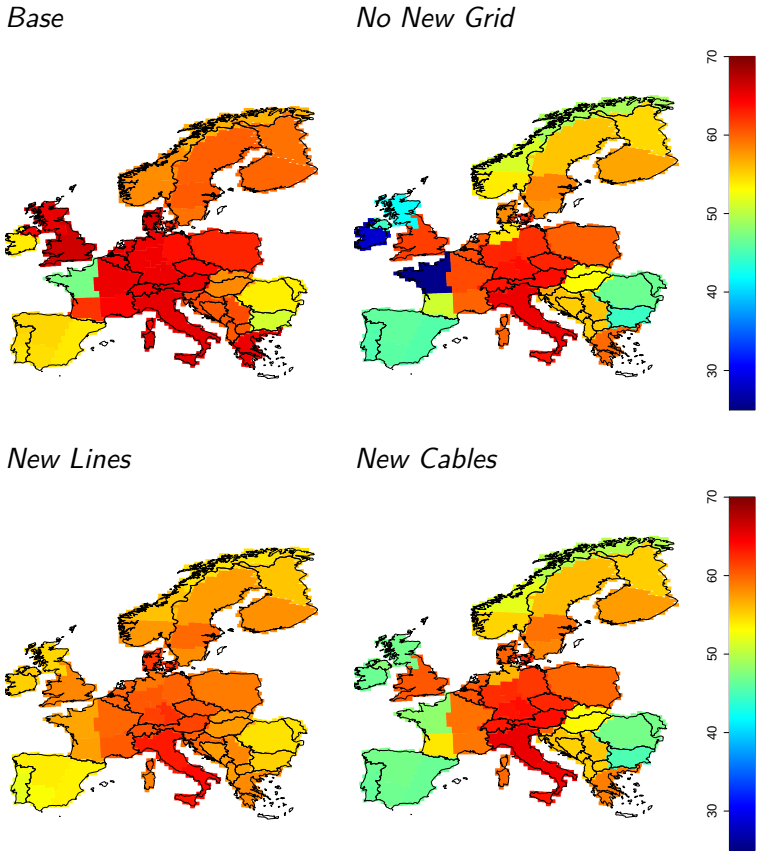

Figure 4.7.: Electricity price (€/MWh$_{el}$, weighted average over all modeled time steps)

The weighted average of the nodal electricity prices in Europe is 62 €/MWh in the *Base* scenario. In the *No New Grid* it drops to 57 €/MWh, 8% lower than the basecase.

With grid extensions the average price recovers to 59 €/MWh and 58 €/MWh with new lines or cables respectively. As can be seen from the maps in Figure 4.7, regions with high VRE capacity are most affected by the reductions in electricity price. In northwestern Germany, the average price drops from 65 €/MWh to 54 €/MWh with 2020 VRE capacity additions and no grid extensions and increases to 59 €/MWh in the *New Lines* scenario (see also Figure 4.6). The overall increase in electricity price occurs, because the merit order effect is reduced through transmission grid extension. The VRE supply is smoothened across Europe and the fluctuations in conventional power plant dispatch can be reduced.

The standard deviation of electricity prices across regions increases with increasing VRE capacity. In the *Base* case the standard deviation of elecricity prices across the European regions amounts 5 €/MWh. It increases to 9 €/MWh due to increased VRE capacity and can be lowered with grid extensions to 3 and 6 €/MWh respectively. Grid extensions lead to a homogenization of the electricity prices.

Furthermore, the dynamics of the prices changes. While in the current system and in the *Base* case, the electricity price is mainly determined by the load (see Figure 4.6), the average correlation between load and prices drops to around 26% in the 2020 VRE scenarios from 75% today. In turn, generation from wind turbines plays an increasingly important role for electricity prices. In regions with high VRE capacity strong anticorrelation between wind generation and electricity prices emerge, as shown in Table 4.3. Solar power generation is generally smaller and furthermore correlated to the diurnal pattern of the load. It can therefore achieve prices above the average thanks to this "correlation effect" (Section 4.1 [68]). Therefore, the effect of solar PV to the electricity price is not as pronounced. Transmission grid extensions can reduce the anticorrelation between price and wind supply by up to 50% in affected regions (see Table 4.3). However, in the case of North Western Germany, the anitcorrelation increases with grid extensions, as the build up of a north sea grid leads to larger imports of wind energy in the region.

Correlation price and wind	Spain NW	Scotland	Germany NW
No Grid	-63%	-51%	-12%
New Cables	-61%	-37%	-13%
New Lines	-30%	-28%	-17%
Wind capacity (GW)	18	11	23

Table 4.3.: Correlation between electricity price and generation from wind energy in selected regions. The last row lists the total on- and offshore wind capacity in the regions.

In summary, grid extensions raise the average European electricity price and homogenize it across the European countries. Furthermore, prices are less volatile and more predictability, as the anti-correlation between wind and price decreases and the burden of fluctuating renewable supply can be shared between regions.

4.4.4. Implications for the electricity market and its participants

The effect of VREs to the electricity price have important implications for all market participants. The above section shows that transmission grid extensions for VRE integration reduce the price drop and variability. The implications of this effect for the general functioning of the electricity market as well as the generators are analyzed in the following.

Comparison of costs of electricity to average prices

As pointed out above, VREs reduce the average electricity price in Europe through the merit order effect. Grid extensions raise the average level, to the disadvantages of the consumers of electricity. Additionally, the grid costs are paid by the consumer through tariffs.

However, the total costs are not covered by the electricity price. As pre-installed capacities are assumed, an imperfect market is modeled. The fixed costs for existing and predefined plants are not reflected in the marginal costs. The marginal costs, i.e., the electricity prices, mainly contain the variable costs only and therefore, the total electricity prices are lower than the overall system costs. The uncovered part of the costs needs to be paid by other means, for example by subsidies or other public charges for system services etc. These charges raise the end-user price again.

Figure 4.8 shows the average nodal electricity price and the average cost of electricity. The costs of electricity shown here include the total costs of the existing and newly added units. The total costs cannot be recovered in the imperfect market. However, grid extensions allow to reduce the system costs and with it the costs of electricity. Due to the smoothing effect, the electricity prices increase. The paid prices comes closer to the actual costs: the VRE integration measure counterbalances the increasing gap between the costs and electricity prices driven by growing VRE contribution. In the *Base* scenario the gap between price and CoE amounts to 4 €/MWh, it is increased to 9 €/MWh due VRE capacities but can be reduced again to 6 €/MWh in the *New Lines scenario*.

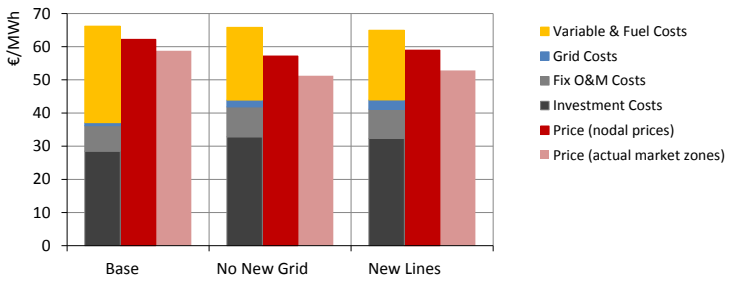

Figure 4.8.: Average electricity prices and total costs of electricity per scenario with nodal prices. For VREs the *Medium Cost* scenario is assumed.

If current market areas are assumed, lower electricity prices result. Congestion within the market area is not taken into account in the market and thus, the electricity prices are lower, as cheaper power plants are dispatched. The fictive wind and solar supply is thus also smoothed within the market area. Yet, the areas are not large enough to cause the same smoothing effect as in the European case and therefore the average prices are lowered. As a consequence the gap between average price and cost increases.

The redispatch costs, the additional costs arising from the internal congestion not captured in the current market areas, are commonly passed on to the consumer.

Generators

The benefits of higher electricity prices through transmission grid extensions for generators differs by technologies.

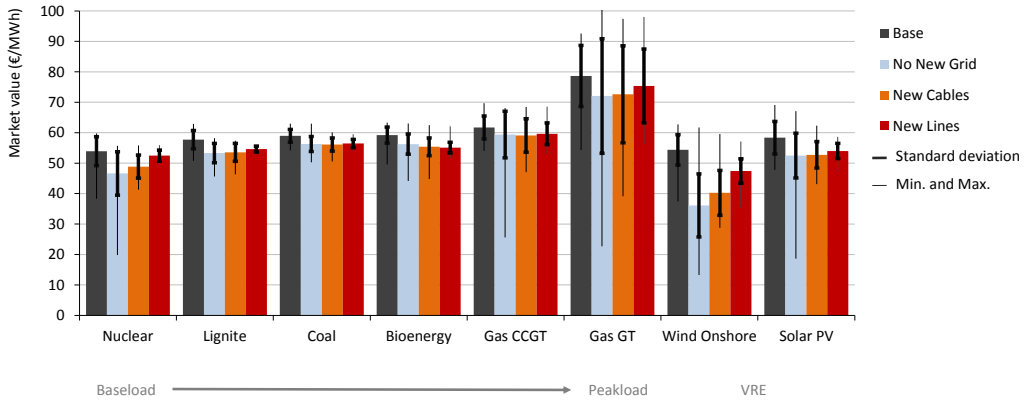

Figure 4.9.: Average market values per generation technology for the four scenarios. Standard deviation and minimal and maximal values across the model regions are indicated with the black lines.

The average price which each generation technology achieves at the electricity market is shown in Figure 4.9 for the four scenarios. The findings show that this so-called market value decreases for all technologies with increasing VRE share. With increasing interconnection, it is raised again. Without grid extensions, the standard deviation of market value increases due to the inhomogeneous distribution of VREs. With grid extensions, the variation of market values across regions is reduced due to the smoothing of VRE supply and the electricity prices. The change in market value across the scenarios is most pronounced for nuclear power plants, gas turbines, wind turbines and solar PV. The reduction of zero-price events during the VRE supply is the main advantage of the grid for VRE technologies. The nuclear baseload technology is most affected due to its high FLHs: it records the changes in average price very well. The reduction in market value of gas-based peakload technologies (GTs) is due to the fact, that oil power plants online in 2020 are setting the price in a few time steps. Whenever the oil power plant is used, the gas turbine will see a higher price. This happens in very few hours only, but

as the FLHs of gas turbines are rather low, they are very sensitive to this effect. For mid load power plants a slight decrease in market value with VREs in general can be observed.

In addition to the lower prices, FLHs of dispatchable power plants are reduced with increasing VRE share, as discussed above. The change in revenue is therefore more pronounced than the change in average market value. Figure 4.10 shows the average annual revenue per installed MW for each generation technology. The results reveal that all technologies are affected and achieve lower revenues due to VREs. Without transmission grid extensions for the new VRE capacity (*No New Grid*), the standard deviation of the revenue across regions increases due to the inhomogeneous distribution of VRE capacities in 2020. The profitability of conventional power plants will be strongly influenced by the amount of VRE capacity close by.

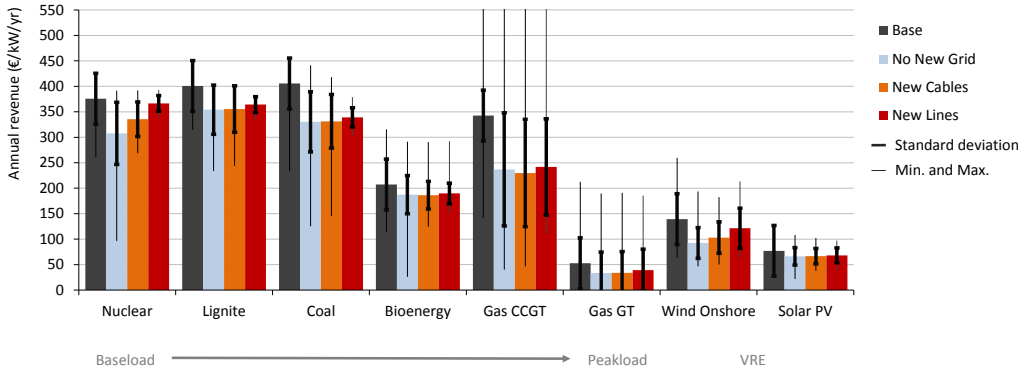

Figure 4.10.: Revenues per generation technology for the four scenarios. Standard deviation and minimal and maximal values across the model regions are indicated with the black lines.

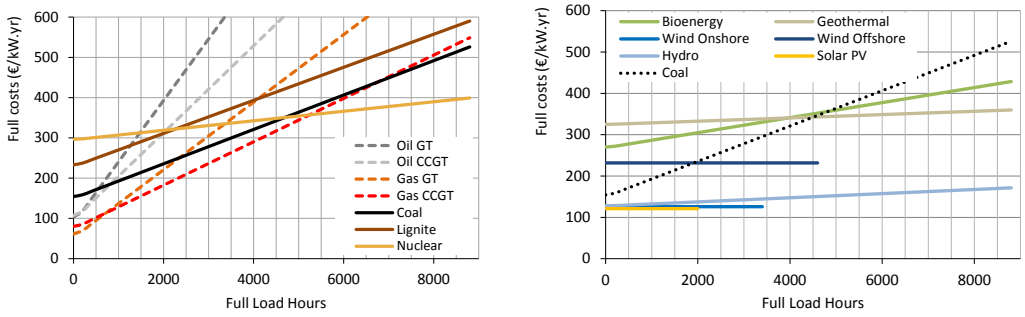

(a) Fossil fuels (b) Renewable energies (Medium Costs)

Figure 4.11.: Annual full costs of electricity for renewable energy, peak and baseload technologies. Costs for emission allowances of 30 €/t_{CO2} are included.

More uniform prices in time and space and smaller regional differences in FLHs thanks to network improvement align the revenues. The standard deviation of the revenues across the regions is reduced significantly. VREs are affected very positively by grid extensions since fewer low price situations occur. As large VRE generation mainly causes the low prices, these technologies can hardly earn important revenue in the current market structure. Grid extensions smoothen the electricity price. As a result, less low price events occur and the revenues for VREs increase. Baseload power plants such as nuclear, also benefit substantially from grid extensions. The average revenues reach current levels if cost-optimal overhead transmission extensions are realized. For mid and peak-load power plants, the economic situation remains difficult even with large grid extensions, due to important FLH reductions.

Comparing the average revenues to the screening curves in Figure 4.11, it becomes clear, that not every technology can recover its costs with the market prices achievable on an energy-only market including high shares of VREs. However, the regional prices and FLHs play an important role (see also Figure 4.12). Figure 4.10 only shows the average of the revenues per technology. New power plants may be used more frequently, due to higher efficiency and resulting lower variable costs. They may thus achieve higher revenues. However, for some peaking technologies, the benefit is small or vanishing and additional incomes are necessary, for example from balancing markets, system services etc. Stagnant investment in new power plants reflects the difficulties at the market which are already present today [29].

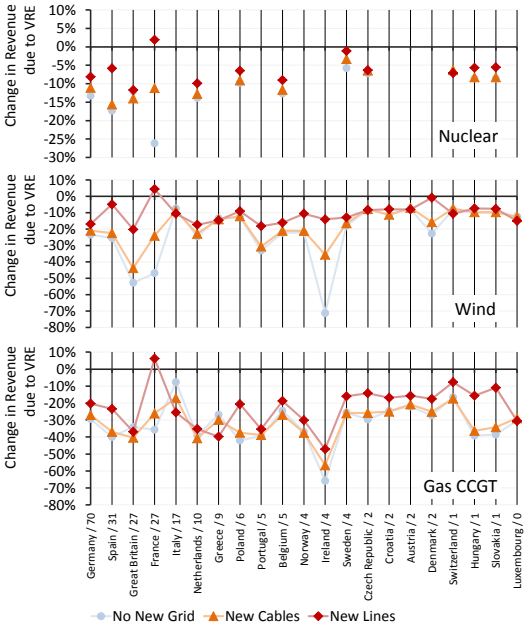

Figure 4.12.: Relative change in revenue with VRE additions compared to *Base*. The countries are plotted in decreasing order of VRE capacity additions. After the country names VRE additions until 2020 are indicated in GW.

Figure 4.12 shows the change in revenue due to VRE additions by country. Regions with largest additions are most affected, as for example Germany, Spain, France and Great Britain, where the revenues for nuclear power are reduced by up to 25%. Looking in more detail, in north-western France and in Scotland, the revenue for nuclear is reduced by more than 50% from the *Base* to the *No New Grid* scenario. VREs are, as pointed out before, most affected if they participate in the electricity market directly. For Gas CCGT power plants, a mid and peak load technology, transmission grid extensions show only little effect and the revenue remains low. In importing regions, such as Italy, grid extensions can lead to an additional decrease of revenues.

Assuming current market zones instead of nodal prices, the results in terms of market value and revenue are very similar. The results of this sensitivity analysis are shown in Annex F. Although the average electricity price is lower, international transmission grid extensions still raises the electricity price and as a consequence, most generators benefit from them in term of increased market value and revenue. The beneficial effect of transmission grid extensions for VRE market integration is thus independent of the size of the market zone. With nodal price and current market zones European transmission grid extensions lead to increase in revenues for all technologies on a European average.

4.5. Discussion and conclusion

In this chapter, URBS-EU is applied to quantify the effects of VREs on the European electricity prices in 2020 and how transmission grid extensions influence these effects. The results show that the announced VRE capacity additions for 2020 have significant impact on electricity markets and their participants. Average wholesale electricity prices decrease, their variance in time and space increases, and they are dynamically correlated with VRE supply rather than power demand. Transmission grid extension can help to reduce the market effects of VREs and thus facilitate the their market integration. It allows to raise the average electricity prices and therewith revenues of generator.

Two levels of grid extensions are investigated. In a first stage overhead grid extensions between all neighboring regions are optimized. The cost-optimal grid additions amount to 120% on top of the current grid capacity. In a second scenario, taking into account public acceptance and political challenges, only cable additions are allowed, and a 50% increase in grid capacity results. Furthermore, a sensitivity analysis towards the assumption of nodal prices is carried out.

Through the merit order effect, VREs lower the average simulated electricity prices by 8% or 5 €/MWh in 2020. The effect is especially pronounced in regions with large VRE capacities (see also Aigner et al. [6]). For example in North-Western Germany the average price is reduced by 17% or 9 €/MWh. Furthermore, the variability of prices increases considerably. Its standard deviation increases from 5 to 9 €/MWh due to the planned VRE capacities. The fluctuations in price are no longer correlated to the load, but to the VRE supply. These effects introduce additional uncertainties for the market

participants.

The merit order effect directly impacts on the market value of wind and solar energy. Whenever they contribute to the supply, they lower their own prices. This leads to a decrease in market value of 34% for wind onshore and 10% for solar PV in 2020 compared to the Base scenario. However, not only VRE technologies are affected. The decrease in market value for conventional generators ranges from 5% for Gas CGGTs to 14% for nuclear power plants.

The second impact of VREs to the conventional generators is the reduction of FLHs. Due to the limited capacity credit of wind and solar power. Conventional capacity is hardly reduced compared to current level, while the share of VRE in total electricity generation increases from 5% to 21%. This results in a reduction of FLHs for all conventional generation technologies. Without grid extensions, very high FLH reductions occur in proximity to important VRE capacities. Utility owners will face drastic FLH reduction and higher wearout of their turbines due to increased ramping if wind or solar capacity is built close by.

Due to these two effects, conventional power plants will face serious economic challenges. In regions with large VRE capacities, the reduction in revenues for conventional base, mid and peak load power plants can reach 60%. The average revenue for baseload technologies is reduced by more than 15%, for mid- and peakload by about 30%, according to the model results. As the real power plant dispatch is less flexible than the model assumes, these results most likely underestimate the impacts of VREs on conventional generators. VRE capacities in 2020 thus create major inequalities in Europe, if no grid capacity additions are carried out simultaneously.

With grid extensions, the average utilization of baseload technologies is raised again and less ramping of baseload technologies is necessary. The balancing of VRE supply is shared between more flexible power plants in the interconnected regions. The more continuous dispatch of conventional power plants leads to a recovery of the electricity prices. The results show that, thanks to the transmission grid extensions, the merit order effect is reduced to 3 €/MWh in the *New Lines* scenario.

At the same time, higher FLHs can be achieved by conventional generators. Therefore, both levels of simulated grid extensions increase the revenues of all generators. The effect is especially pronounced for baseload and VRE technologies. Revenues close to pre-VRE levels can however only be attained with a substantial grid growth of 120%. For mid- and peakload power plants, average revenues remain low. If VRE technologies participate in the market, they are most affected by the low prices due to the anti-correlation of electricity prices and VRE generation. The possibility to reduce this anticorrelation through increased interconnection creates a large incentive for grid extensions, as they raise the revenue for VRE technologies. As a result, grid extensions are economically very advantageous for baseload and VRE utility owners. The sensitivity analysis towards the assumption on nodal pricing shows, that these results also hold, if current market zones are assumed.

However, regions with low VRE capacity experience lower electricity prices and poten-

tially lower revenues through transmission grid extension. Mid and peak load generators in importing regions face the problem of increased ramping, lower FLHs and lower electricity prices. This can cause political barriers to increased international electricity market coupling. While today, existing infrastructure and fuel costs mainly determines international trade flows, in 2020, different trade flows, highly determined by the weather and also the installed VRE capacities, will occur in 2020. The importing region will still have to provide sufficient capacity to ensure security of supply, which in turn has lower utilization and revenue, because the neighboring country installs large VRE capacity and exports parts of its electricity generation. Increased coordination of the dispatch of interlinked regions and also of the balancing regulations are necessary to reduce the disadvantages for the importing region.

The results in this chapter show that announced VRE capacities for 2020 will cause increased investment uncertainty due to variable prices and create important inequalities among power plant owners in Europe. Close to VRE generation, lower utilization of disptachable power plants and reduced electricity prices lead to reduced revenues. Through grid extensions, the market integration of VREs can be facilitated. Transmission grid extensions increase the flexibility of the system. The model results show that this is also reflected in the electricity market. Average price levels increase and with it the possibility to recover the costs of electricity generation on the market. Furthermore the prices become more stable and less driven by the stochastic VRE supply.

For generators this translates into a re-increase of revenues. The higher flexibility of the system allows to achieve higher market values for all technologies, but especially the value of VREs to the system increases considerably, if VRE system integration measures are taken. For importing regions and mid to peak load technologies, however, disadvantages can occur through grid extensions. For successful planning of transmission grid extensions for VREs in Europe, the benefits and potential difficulties for market participants should be taken into account.

5. Energy sector coupling as alternative VRE integration measure

5.1. Inclusion of other energy sectors for VRE integration

An increasing share of electricity from wind and solar PV leads to significant temporary electricity surpluses if no VRE integration measures are taken. The case study in Chapter 3 showed, that with 60% directly usable VRE share, more than 250 TWh of excess electricity would occur every year, if no transmission grid extensions are realized (Subsection 3.3.5). This corresponds to about 8% of current annual consumption in Europe.

In this chapter, the coupling of the power to the heat and hydrogen sector is studied as an alternative VRE system integration measure. Through this energy sector coupling, analyzed for the example of Germany, the surplus energy potential may be used in an economic manner in the heat and hydrogen sector. Furthermore, through the coupling of the power to the hydrogen sector, an option for long-term energy storage is included. Finally, other than the above discussed transmission grid extensions, this integration measure acts locally and can be implemented on a modular basis. It may thus face less political, public or administrative barriers than transmission grid extensions.

The commonly proposed four major VRE system integration measures focus on the power sector. Major transmission grid extension smoothen VRE supply, as discussed in Chapter 3. Electrical storage allows to shift demand from hours of high VRE supply to periods of undersupply [e.g. 87, 64], VRE balancing could be facilitated by more flexible conventional power plants [e.g. 151] and electrical demand side management could counteract both periods of over- and undersupply [e.g. 149].

In contrast to these approaches focused on the power sector only, here, demand side management is expanded to other sectors. This bears two advantages: the heat and the hydrogen sectors can help to integrate fluctuating electricity generation from VREs. Second, the usage of carbon-free electricity generated from renewable energies can contribute to the decarbonization of the other energy sectors.

Today, the heat sector accounts for 56% of the total final energy consumption and 46% of direct energy-related CO_2 emissions [4]. It is thus a promising energy sector to be included in the coupling. The usage of excess electricity from VREs could help to decarbonize the heat sector. Furthermore, the export of excess electricity for heating is comparatively easy and can be based on well known technologies: electric heaters and heatpumps.

The replacement of fossil fuels in the transport sector is less straightforward, because the high costs of electric vehicles compared to traditional combustion engines hamper strong coupling of the power to the transport sector [33].

The hydrogen sector is included because it allows to increase the power system's flexibility as it offers the possibility for long term storage and for additional energy transport via methanation. Kuhn identifies hydrogen storage as the economically and technically most viable option for seasonal storage [87]. Furthermore, hydrogen can be transformed to natural gas via methanation. Bulk energy transport could be then realized with the produced natural gas via the existing natural gas-grid instead of building new electric power transmission lines [141].

A part from hydrogen storage and existing pumped storage units, no further options for electricity storage are included in the analysis. The potential for pumped hydro storage is limited as well as the potential of compressed air storage. Batteries currently come at very high costs. Even if they may become cost-effective in some cases if used as alternative to distribution grid extensions [140], batteries are unlikely to prevail compared to other storage options for large scale storage at the transmission level. Thus, only hydrogen storage offers the possibility to store large amounts of energy for longer timescales thanks to its high energy density.

The model generator URBS, introduced in Chapter 2, is applied to the German power, heat, hydrogen and natural gas sector. Different technical options to realize the energy sector coupling are analyzed jointly and several plausible conversion and storage technologies taken into account. For each commodity individual demands, that have to be covered, are also modeled. In this way, the energy conversion from the power to the hydrogen sector can, for example, either be used as a first step in an electric storage cycle or for directly covering the hydrogen demand. Moreover, the implemented model, URBS-D, is highly resolved within Germany and includes today's and possible future electric HV transmission grid capacities.

These ingredients make the approach well positioned to understand the economic value of energy sector coupling for VRE integration in detail, with all its complex interrelations between the different conversion technologies, storage options, the HV grid as well as location-dependent factors.

This allows to answer the major underlying question: which benefits bears energy sector coupling for the system and market integration of VREs? This question is addressed in several steps. First, the overall system effects of energy sector coupling are analyzed and the coupling strength between the sectors quantified. As a multitude of technological options is included, the sector-wise analysis of cost-optimal technology mixes can be carried out. It reveals the relative roles of the coupling technologies. In analogy to Chapter 4, the effects of the energy sector coupling for the electricity market are studied in a second step. Finally, the VRE system integration measure of energy sector coupling is compared to the option of building a European supergrid and their interaction is estimated applying the European power system model URBS-EU.

The detailed analysis is restricted to the German example, as the smaller geographical scope allows to include higher technological detail while keeping size of the optimization problem manageable. At the same time, Germany serves as good case study, since it has one of the most ambitious targets concerning the reduction of greenhouse gas emissions and shares of renewable energy in primary energy consumption [22]. Two scenario years are studied, 2020 and 2050.

This chapter proceeds as follows. After a literature review in Subsection 5.1.1, the model setup and scenario definition as well as assumptions and input data for the German heat and hydrogen sector are presented in Section 5.2. The results are presented in Section 5.3 in the three above mentioned steps. Subsection 5.3.1 provides insights to the system effects of energy sector coupling. Subsection 5.3.2 reveals the different roles of the coupling technologies. In Subsection 5.3.3 the effects of energy sector coupling for the VRE market integration is analyzed. The system integration effects of energy sector coupling are than opposed to the option of building a European supergrid in Section 5.4, where first the integration effects are compared and second their interaction on a European level is estimated. Finally, the results are discussed in Section 5.5.

5.1.1. Literature review

A number of previous studies, have investigated the possibility of VRE integration through energy sector coupling. The large majority of them are focusing on northern European countries, where large wind energy capacities are already installed or planned and the awareness of interaction between different energy sectors is likely to be high due to a high share of power generation from CHP plants, closely coupling the heat and the power sector.

Mathiesen and Lund [98] provide an overview of the literature on energy sector coupling. It has been shown for several northern European countries that through the inclusion of the heat sector the integration of wind energy can be facilitated [e.g. 102, 95, 96]. The hydrogen sector has been examined in Lund and Mathiesen [96] and Karlsson and Meibom [81], with a focus on its electrical storage capabilities and its role for the transport sector. Kuhn's analysis of electricity storage options for Germany reveals that hydrogen storage is the most promising option for long term storage [87]: While the potential for pumped hydro storage and compressed air storage is limited, hydrogen storage offers the possibility to store large amounts of energy for longer times thanks to its high energy density. Sterner studies the so-called power-to-gas option, where hydrogen is used to generate natural gas via methanation, opening the possibility for large-scale energy transports via the existing natural gas-grid [141].

In this chapter, energy sector coupling is analyzed for Germany using the energy system model URBS-D. Economically most viable option between the above mentioned technical solutions for the energy sector coupling are identified and their interaction evaluated.

5.2. Model setup and data

5.2.1. URBS-D model setup

The URBS model generator is applied for the analysis. The geographical scope, the expansion to other sectors and the inclusion of more technical details distinguishes the approach in this chapter from the model of the European power sector URBS-EU employed in the foregoing chapters. The new model is called URBS-D. The included energy sectors and conversion technologies are shown in Figure 5.1.

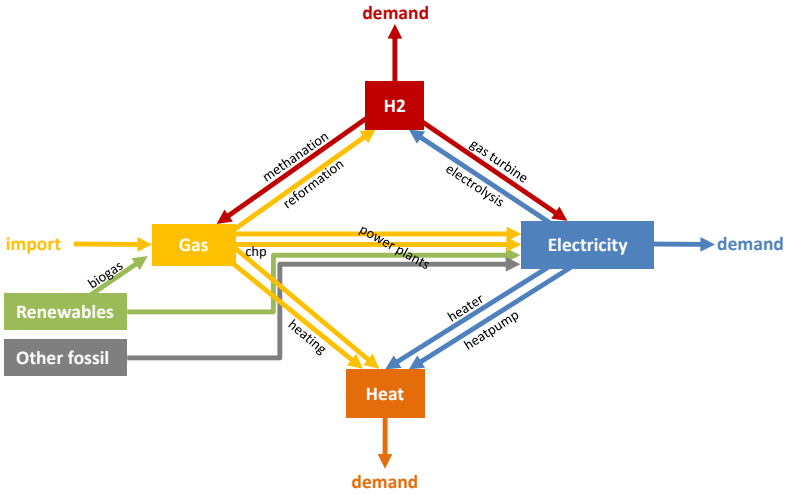

Figure 5.1.: Energy sector coupling in URBS-D: commodities and technologies

In each model region, electricity can be generated from renewable resources, natural gas or other fossil resources. Natural gas can be replaced by biogas. Renewable energies can be divided in dispatchable renewable resources, such as bioenergy and some hydro power plants, and VREs, making up for a large share of electricity generation in the future scenarios. The heat sector is not modeled in full technological depth, but with a reference technologies, natural gas heating, but CHP is included as well. Via electric heaters and heatpumps, the power sector can export energy to the heat sector and replace these reference technologies. Hydrogen is supplied by reformation of natural gas and oil-refinery by-products in Germany [139]. It is assumed, that only the gas reformation is replaceable by electrolysis, which couples the power sector to the hydrogen sector. Furthermore, hydrogen can be used to produce natural gas via methanation. Alternatively, hydrogen can also be retransformed into electric power via gas turbines, forming a long term storage option for electricity. Energy storage is possible in all sectors, however, the hydrogen sector has the largest storage size, due to the high energy density of the hydrogen gas. In the power sector, only the existing pumped storage and hydrogen storage are included, as the potential of other long term electricity storage options is limited. Energy transport is possible via HV power transmission or via the natural gas-grid.

As in URBS-EU, the model URBS-D includes transformation, storage and transport losses for all technologies, as well as ramping constraints for baseload power plants, such as coal and nuclear power plants (see Table 2.12).

To model the technical characteristics of decentralized generation and CHP plants, the additional model features introduced in Section 2.2.3 are used. Heating technologies for example are commonly installed for each house and the heat generation of the distributed units has to match the load profile of the respective house. These distributed generation technologies are forced to follow the local load profile via the additional restriction introduced in equation 2.40.

In CHP generation, several commodities are involved: the fuel is transformed to heat and electricity. To model those multi-commodity flows, secondary commodities are introduced (see equation 2.41). The technical realization of the co-generation defines the mix between heat and electricity. In the model, this mix is defined via production shares as introduced in equation 2.45.

As in the foregoing chapters, the optimization is performed for six representative weeks. The weeks are selected based on the routine presented in Subsection 2.2.4.

The model regions are defined following the dena [30] (see Figure 2.13). They reflect comparatively well connected areas. In this chapter it is assumed that international energy transport (power or natural gas) is impossible.

5.2.2. Scenario definition

Scenario Name	grid extensions	heat coupling	hydrogen coupling	gas price [€/MWh]	electrolysis costs [€/kW]	storage size (elec.) [predefined size]	storage size (heat) [hrs. of mean demand]	storage size (H2)
Base (New Grid, Coupling)	✓	✓	✓	25	500	1	1	unlimited
No New Grid, No Coupling	-	-	-	25	500	1	1	unlimited
New Grid, No Coupling	✓	-	-	25	-	1	1	unlimited
No New Grid, Coupling	-	✓	✓	25	500	1	1	unlimited
New Grid, No Heat Coupling	✓	-	✓	25	500	1	1	unlimited
gas price sensitivity	✓	✓	✓	50, 75	500	1	1	unlimited
electrolysis sensitivity	✓	✓	✓	25	200, 1000	1	1	unlimited
Methanation (2050)	-	-	✓	75	500	1	1	unlimited

Table 5.1.: Parameter settings for the scenarios for 2020 and 2050

To investigate the interaction of the different options for energy sector coupling, all storage and conversion technologies introduced in Figure 5.1 are implemented in the model. To determine the effects of different contributions from VREs in Germany, two

scenario years are included, 2020 and 2050. For each scenario year, a *Base* scenario is defined. In these *Base* scenarios, the optimization choses the economically most viable mix between the offered technologies (Table 5.1).

In a second step, the integration measures are studied individually and parameter variations are carried out to study the sensitivity of the relative roles of the technologies and energy sectors.

In additional to the data presented in Section 2.3, the properties of the heat and hydrogen generation and coupling technologies, as well as the energy demand per sector need to be specified. They are described in the following sections.

5.2.3. Cost assumptions

For conventional power plants the benchmarked costs are assumed (Table 2.10). For renewable generation technologies the three cost scenarios for VRE technologies are used (Table 2.11). The *High* costs scenario applies for 2010, the *Medium* for 2020 and the *Low* investment costs scenario for 2050.

Technology	Inv. Costs	Fix O&M Costs	Fuel Costs	Var O&M Costs	Var Costs + CO_2 Costs
Combined heat and power	€/kW$_{el}$	€/kW$_{el}$	€/MWh$_{th}$	€/MWh$_{el}$	
Bioenergy CHP	1000	50	5	4	18
Gas CHP	400	8	25	1	$11^a + 4^b$
Gas/Bio peak load boiler	330	3	endogenous	0	endog.
Heat sector	€/kW$_{heat}$	€/kW$_{heat}$	€/MWh$_{input}$	€/MWh$_{heat}$	
Gas heating	300	3	25	1	29 + 10
Electric heater	100	2	endogenous	1	endog.
Electric heatpump	2000	40	endogenous	1	endog.
Hydrogen sector (H2 prod.)	€/kW$_{H2}$	€/kW$_{H2}$	€/MWh$_{input}$	€/MWh$_{H2}$	
Gas reformation	500	50	25	1	32 + 11
Electrolysis	676	10	endogenous	1	endog.
Hydrogen sector (H2 as fuel)	€/kW$_{gas/el}$	€/kW$_{gas/el}$	€/MWh$_{H2}$	€/MWh$_{gas/el}$	
Methanation	1100	22	$(50)^c$	20	$(85)^c$
Hydrogen fueled GT	380	10	$(50)^c$	1	$(126)^c$

Table 5.2.: Investment, fixed operation & maintenance, fuel and variable costs per process. The total variable costs take into account the transformation losses. Carbon certificate costs are computed based on a carbon price of 30 €/t.

[a] Only 40% of the variable costs are allocated to the variable costs of electricity, as the remaining 60% of the energy is transformed to heat.; [b] Assuming natural gas from fossil ressources. Costs for emission allowances do not occur if the natural gas is generated from methanation.; [c] Fuel costs of hydrogen generated by gas reformation. Changes if electrolysis is used.

Table 5.2 shows the assumed costs for CHP processes and the heat and hydrogen

sector. The costs of CHP units vary considerably with unit size [8]. An average CHP size of 750 kW_{el} is assumed. This leads to specific investment costs of 400 €/kW_{el}.

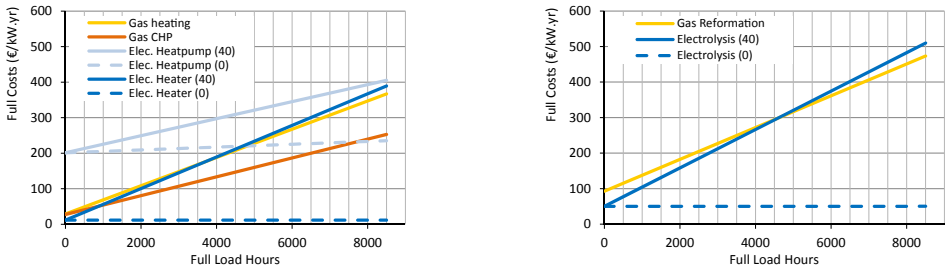

(a) Heat (b) Hydrogen

Figure 5.2.: Full annual costs of heat and hydrogen generation assuming different electricity prices (40 and 0 €/MWh). For CHP the costs are shared between heat and power production.

The resulting full annual costs of heat and hydrogen generation for selected processes are shown in Figure 5.2. The inclusion of different exemplary electricity prices for the heatpump, the electric heater and the electrolysis illustrates that the competitiveness of the coupling technologies depends on the electricity price.

Technology	η %	f^{prod} %	lg
Combined heat and power			
Bioenergy CHP	90%	40% Elec., 60% Heat	0
Gas CHP	90%	40% Elec., 60% Heat	0
Gas/Bio peak load boiler	90%	-	1
Heat sector			
Gas heating	90%	-	0
Electric heater	90%	-	0
Electric heatpump	200%	-	0
Hydrogen sector (H2 production)			
Gas reformation	80%	-	0
Electrolysis	74%	-	0
Hydrogen sector (H2 as fuel)			
Methanation	77%	-	0
Hydrogen fueled GT	39%	-	0

Table 5.3.: Technical parameters per process.

The technical parameters for CHP, heat and hydrogen processes are shown in Table 5.3. The share between heat and electricity generation from CHP power plants is defined via the production share f^{prod}. The peak load boilers are considered as distributed generation ($lg = 1$) and therewith the combined unit of CHP with peak load

boiler is modeled as a head-led process: it follows the regional heat demand. For gas heating the local generation constraint does not apply. It is assumed that it can be replaced on an hourly basis by electric heating (heater or heatpump). This means that within one house the two systems can be installed in parallel.

5.2.4. Meteorological data

As in the previous chapters, the availability of wind and solar power is deduced from meteorological data on wind speed and global irradiation.

The meteorological data is extracted from high resolution reanalysis data for Germany [86]. Based on wind speed and global irradiation from 2007, capacity factor time series for wind and solar PV power are computed for every HV-grid-node in Germany. For the analysis in this chapter, the values are aggregated for each model region assuming a capacity distribution within each model region as projected for 2050 by a report prepared for the German Ministry of Environment [86]. The resulting FLHs per model region are shown in Figure 5.3.

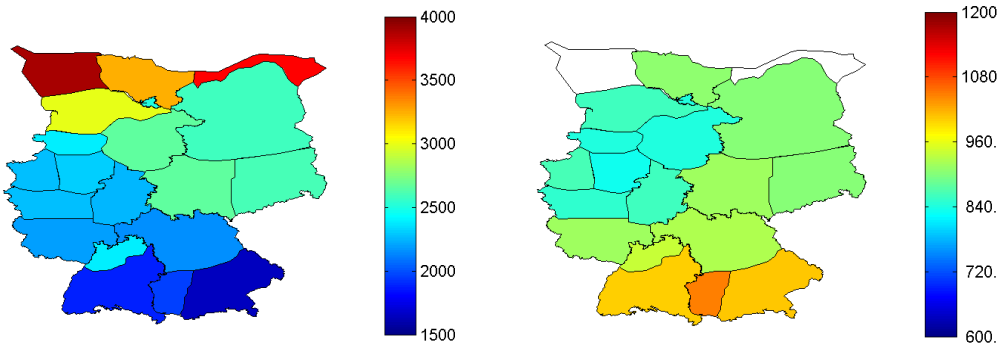

(a) Wind energy (b) Solar energy

Figure 5.3.: Full load hours

5.2.5. Final energy demand per energy sector

The total final energy demand and the hourly load profiles per energy sector are deduced based on different assumptions, as indicated in Table 5.4.

Electricity demand

Electricity demand is obtained based on the vertical grid load published by the ENTSO-E for Germany [46]. To disaggregate this data per model region, the regional population and economic activity are used [86]. For households, the Electricity demand is determined based on the Standard Load Profiles (SLPs) per sector. Different SLPs for weekdays, Saturdays and Sundays are used. The regional distribution of demand from

Demand	Annual demand	regional and temporal profile
Electricity	560 TWh	load profile as published by the ENTSO-E, regional distribution based on GDP and population
Hydrogen	60 TWh	constant load profile, regional distribution based on GDP
Heat	1410 TWh	load profile based on ambient temperature and day profiles, regional distribution based on ambient temperature, GDP and population

Table 5.4.: Assumptions for demand per energy sector for both scenario years (2020 and 2050)

the service sector and industry is determined based on regional GDP. This approach allows to take the regional difference in sectoral mix into account. The total electricity demand of 560 TWh corresponds to the annual demand in 2011 [76].

Hydrogen demand

Hydrogen demand amounts to 60 TWh in Germany as shown in Table 5.5 [139]. Half of it is supplied with refinery by-products, which is hard to replace by other processes and it is assumed that only natural gas reformation can be replaced, i.e., 30 TWh. The 2% of supply by electrolysis are negleceted.

German hydrogen sector	
Hydrogen demand in Germany	
bn m^3/a	20
TWh/a	60
Share in primary energy demand	1.5%
Compared to electricity demand	10.7%
Hydrogen supply in Germany	
Gas reformation	49%
Refinery by-products	49%
Electrolysis	2%

Table 5.5.: Hydrogen demand and supply in Germany [139]

Heat demand

Heat demand emerges from space heating (780 TWh), warm water (110 TWh) and process heat demand (530 TWh) [4]. As Figure 5.4 indicates, the shares of different types vary between the economic sectors.

Due to restrictions in temperature or humidity levels, not all heat types can be replaced by the analyzed coupling technologies. For the industry sector it is assumed that only low temperature process heat, space heating, and warm water heat demand is

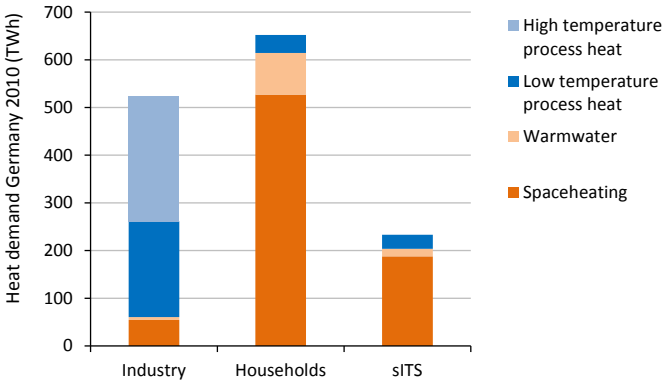

Figure 5.4.: Final energy use of heat in Germany, 2010 [4]

replaceable. The share of low-temperature process heat is derived from end-use energy balances following Hofer [70]. Based on a study by the German Association for CHP (BKWK) [24], it is assumed that process heat below 500^o C is replaceable with CHP or electricity based heat generation processes. In the residential and and the service sector all heat demand is replaceable.

The hourly profiles of the three heat demand types are different. In this study, warm water and process heat demand are assumed to be constant throughout the year. Space heating demand is determined based on heating degree days and daily load profiles in three steps.

1. Based on the ambient temperature, the average daily heat demand per model region is computed. Ambient temperature (T_a) per model region is extracted from the MERRA reanalysis database [125].

$$Q_{day}(x) = \begin{cases} \sum_{t \in day}(T_r - T_a(t,x)) & \forall T_a(t,x) \leq T_0 \\ 0 & \forall T_a(t,x) > T_0 \end{cases} \tag{5.1}$$

with $T_r = 20^o\,C$ Room temperature

$T_0 = 15^o\,C$ Threshold temperature

The resulting average daily temperature figures ($\sum_{day} Q_{day}$) for 2000-2011 in Germany are shown in Figure 5.5. For consistency with the wind and solar data, temperature data from 2007 is used for the computation of the heat demand profiles.

2. Second, hourly daily profiles p_t^s per economic sector s are applied to the average daily heat demand [23] . The normalized annual heating demand profile $\hat{q}_t^s(x)$ is obtained by multiplication of the daily heat demand (Q_{day}) and the day profiles. For the industry sector, demand is independent from ambient temperature and

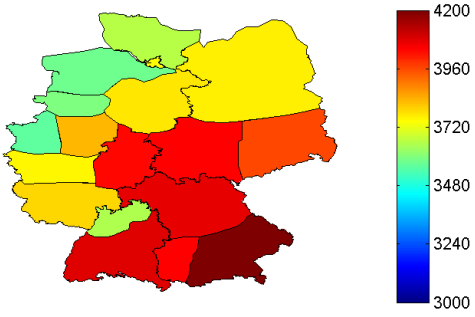

Figure 5.5.: Average daily temperature figure in Germany, based on temperature data of the years 2000 to 2010

assumed to be constant.

$$\hat{q}_t^s(x) = \frac{Q_{day(t)}(x) \cdot p_t^s}{\sum_t (Q_{day(t)}(x) \cdot p_t^s)} \qquad \forall s \in \{\text{Residential, Services}\} \tag{5.2}$$

3. Third, the constant warm-water and process heat demand are added to the normalized profiles according to their respective shares per region and sector. Through multiplication of this normalized profile with the total demand per region, the final hourly heat demand results.

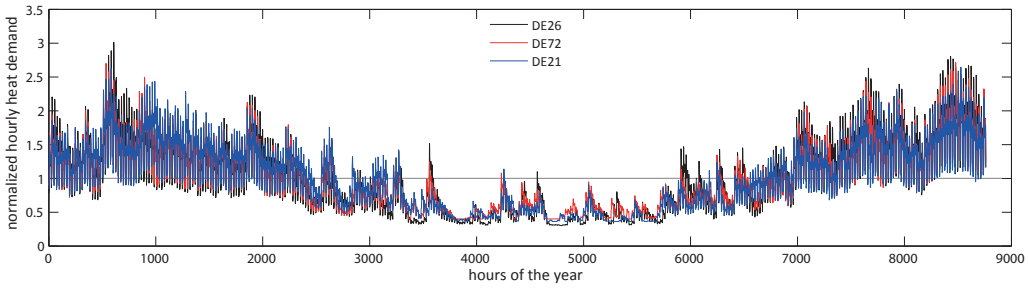

Figure 5.6.: Heat demand in selected regions in Germany. The heat demand is normalized to the respective annual average.

Figure 5.6 shows the resulting heat demand profiles for selected regions in the model. The seasonal variation driven by outside temperatures is similar in all selected regions. Germany is small enough to experience similar weather conditions all over the country. In summer, a constant base remains. The level differs, as the regions have different shares of industrial heat demand.

This heat demand profile determines the dispatch of the local generation units (see Subsection 5.2.1): the heat-led processes follow the computed heat demand. In average, the heat demand profile corresponds to 3038 FLHs.

5.2.6. Energy infrastructure: generation, coupling technologies and grid

For each energy sector, existing infrastructure is included in the scenarios. The assumptions for the energy infrastructure are summarized in Table 5.6.

Infrastructure	2020	2050
Capacity		
Electricity		
Conventional	set by scenario	optimized (Gas CCGT and GT)
Nuclear	4 GW	not available
Coal	24 GW	not available
Lignite	13 GW	not available
Oil	1 GW	not available
Gas GT	23 GW	optimized
Gas CCGT	20 GW	optimized
Renewables	set by scenario	set by scenario
Solar PV	60 GW	129 GW
Wind Onshore	42 GW	75 GW
Wind Offshore	16 GW	43 GW
Hydro	5 GW	4 GW
Bioenergy[a]	18 GW	11 GW
Heat		
CHP plants	bioenergy & distributed CHP set	bioenergy & distributed CHP set, gas CHP additions optimized
gas heating	60% of today, rest optimized	optimized
Hydrogen		
gas reformation	80% of today, rest optimized	50% of today, rest optimized
Storage size		
Electricity	current (67 GWh)	set to 80 GWh
Heat	1h of average demand	1h of average demand
Hydrogen	unlimited	unlimited
Grid size		
Natural gas	unlimited	unlimited
Electricity	current HV transmission grid (ENTSO-E + dena I), extension optimized	current HV transmission grid (ENTSO-E + dena I), extension optimized

Table 5.6.: Assumptions for infrastructure per energy sector in 2020 and 2050

[a] All bioenergy power plants are run as CHP plants. For 2020 it includes gas and waste CHP. For 2050, parts of the biogas is fed to the natural gas grid to provide more flexibility.

Power plants

For existing conventional power plants in Germany, the geo-referenced database introduced in Subsection 2.3.3 was refined based on the TUM-IfE power plant database [87]

and the UBA Database [145]. Currently installed power plants are shown in Figure 5.7a. In the 2020 scenarios, conventional power plants are predefined by a scenario developed by the VDE [151]. The projection includes planned capacity additions and units under construction. The distribution of capacities across model regions is assumed to be proportional to today's conventional power generation capacities. For 2050, the conventional power plant fleet is optimized, with the constraint that only Gas CCGTs or Gas GTs can be built.

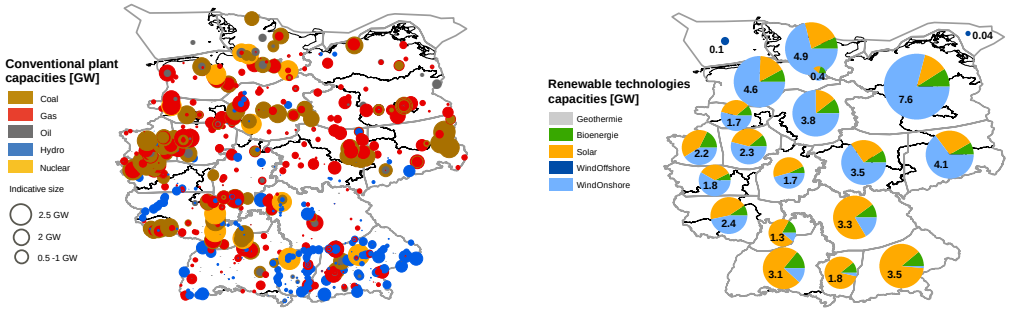

(a) Conventional power plants in Germany (based on [120])

(b) Total installed capacity of renewable energy technologies per model region (2011)

Figure 5.7.: Total installed capacity of conventional and renewable energy technologies per model region

For renewable energy capacities an additional database published by the German TSOs is used [144], as their capacities increase rapidly in Germany. Figure 5.7b shows the resulting total installed bioenergy, geothermal, hydro, solar and wind capacity per region (as of 31.08.2011). For 2020 and 2050 important VRE capacity additions are assumed, following the report prepared for the German Ministry of Environment [86]. These scenarios reflect the announced political targets. For 2020, the regional distribution of renewable capacities is assumed to be proportional to today's renewable power generation capacities. For 2050, the regional capacities are projections based on current installations, growth rates and the technical potential [86].

Heat and hydrogen sector

In the hydrogen sector, only the natural gas reformation is modeled and a lifetime of 50 years is assumed. Current capacity is deduced from the hydrogen demand to be covered in each region. The capacities per technology are listed in Table E.7 in the Appendix.

For the heat sector natural gas heating is assumed as reference technology. Its capacity in 2020 and 2050 is deduced assuming an average lifetime of 30 years. In addition to that, heat-led CHP plants are included in the model.

Combined heat and power generation

The assumptions for CHP generation taken for 2020 lead to a contribution of 20% to the power supply from heat- and power-led CHP plants. This is a conservative interpretation of the political target to reach 25% share in 2020 [22]. Only the heat-led CHP plants are simulated explicitly. Heat-led CHP processes include gas, waste and bioenergy fueled plants. In the 2020 scenarios, they are summarized to the *Bioenergy* process, which is classified as local generation and thus follows the heat demand (see Table 5.3). It contributes 10% of total electricity generation. On top of that, 22% of coal and 11% of lignite plants are CHP units, making up for another 10% of electricity supply. However, as these plants are power led, i.e., their dispatch is determined in the power sector and as they contribute only about 10% of heat supply, the heat production of these plants is not included in the model.

In 2050, gas CHP plants are added by the optimization. The CHP coefficient of gas CHP plants is assumed to be 0.6. Bioenergy CHP plants are included in the 2050 scenario as well (Table 5.6). The total biogas availability for CHP-plants and direct biogas use is determined based on the total Biogas potential in Germany [86].

Storage and HV transmission grid data

Energy storage is possible in all energy sectors. However, in the heat and the electricity sector it is rather limited. For the heat sector a storage capacity sufficient to store average demand for one hour is assumed. For electricity storage, existing pumped hydro units are included. Only in the hydrogen sector, long term storage is possible (see also [87]). Due to the high energy density of hydrogen, the hydrogen storage size is assumed to be unlimited. Through the coupling of the power to the hydrogen sector, it becomes also available for long term electricity storage.

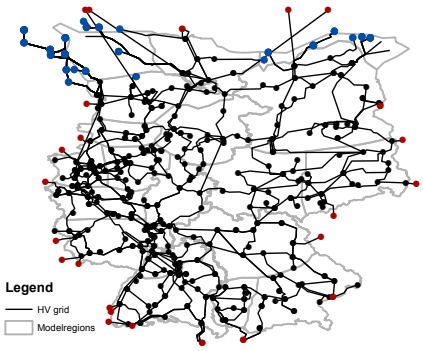

Figure 5.8.: HV-transmission grid in Germany

The HV power transmission grid is deduced from a database on the German 220 and 380 kV transmission grid [150]. It is furthermore assumed, that the grid extensions identified in the dena I study [28] are realized and that all power poles carry the maximum

possible number of systems, i.e., are fully used. For the natural gas grid, the transport capacities between regions are determined by the optimization.

5.3. Results: energy sector coupling as VRE integration measure

The optimization results show that energy sector coupling facilitates the integration of VREs into the German power sector. The description of the result starts with an overview of the systematic advantages of the energy sector coupling. Second, the individual coupling technologies and their interrelations are explored in more detail. Third, the implications of the energy sector coupling for the power market are analyzed.

5.3.1. System effects of energy sector coupling in Germany

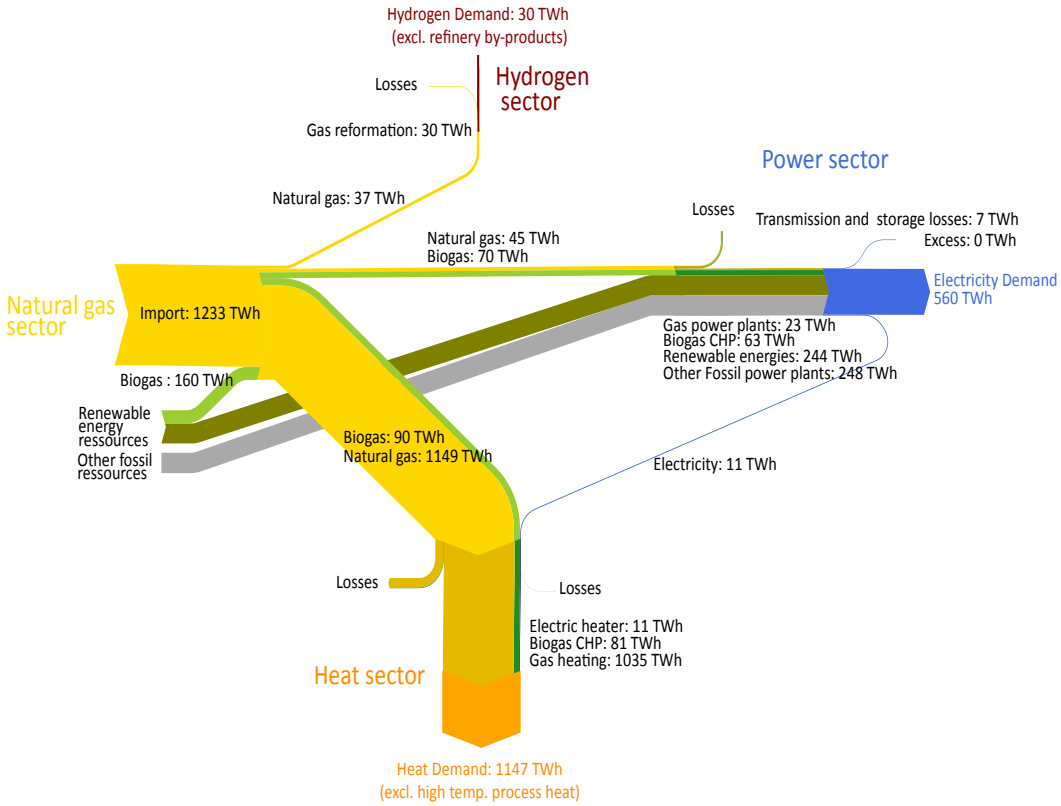

Figure 5.9.: Sankey diagram of the energy flows in the *Base 2020* scenario. Power plant conversion losses of other fossil resources are not shown.

Figure 5.9 and Figure 5.10 provide an overview of the resulting energy flows between the modeled energy sectors.

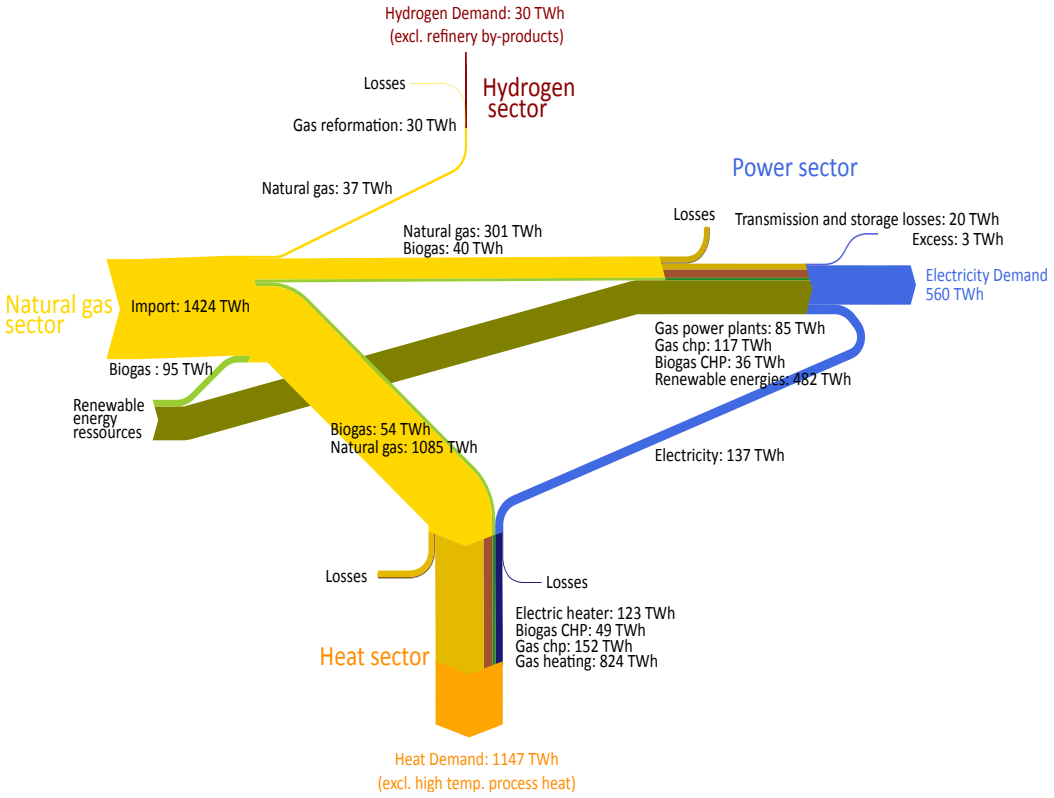

Figure 5.10.: Sankey diagram of the energy flows in the *Base 2050* scenario

The most prominent effect in the model is the strong coupling between the power and the heat sector. It increases with increasing VRE contribution, i.e., from the *Base 2020* to the *Base 2050* scenario. Natural gas is substituted with electricity. In most cases, this electricity stems from VREs, which cannot be integrated in the power sector: in hours of high VRE supply, temporary electricity oversupply is used to power electric heaters. The heat sector acts as sink for the oversupply due to VREs. In 2020, an export of 11 TWh electricity to the heat sector results. In 2050, the coupling between power and heat increases to 137 TWh of heat generated by electric heaters and also CHP is used for more efficient use of natural gas.

The options to use hydrogen as long term electricity storage or to produce gas from hydrogen via methanation are not used in the *Base* scenario for both years. The electricity oversupply is used to satisfy the heat demand and is thus no longer available to be exported to the hydrogen sector.

Figure 5.11 shows this effect in more detail. In the uncoupled case, important electricity oversupply results from the model for both scenario years. National HV transmission grid extensions already reduce the overproduction considerably. In the 2020 scenarios, national grid extensions and energy sector coupling both achieve to almost entirely elim-

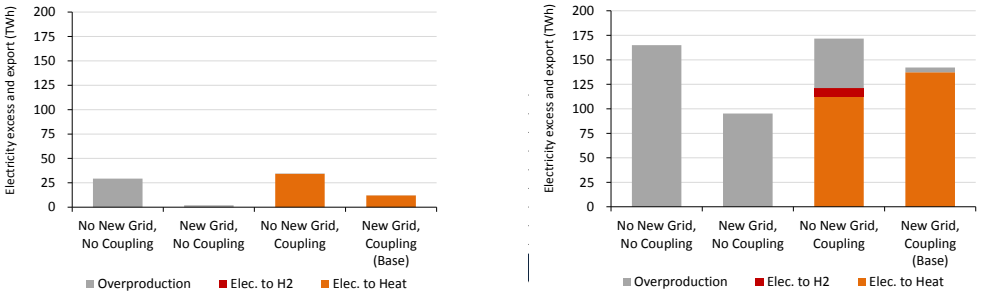

(a) 2020 (b) 2050

Figure 5.11.: Effects of energy sector coupling to overproduction and cross-sector balance

inate the overproduction. In the 2050 scenarios, this can only be realized with energy sector coupling and HV transmission grid extensions.

It is furthermore interesting to note, that in the *No New Grid, Coupling* scenario in 2050, electrolysis is part of a cost-optimal system. The large electricity oversupply can not be absorbed by the regional heat sectors alone and in regions with high VRE capacities, export of electricity to the hydrogen sector occurs simultaneously. With grid extensions (*New Grid, Coupling (Base)* scenario), the regional electricity oversupply can be transported to other regions and is used to supply the heat demand in other regions. In this case, and in the 2020 scenarios, the coupling of the electricity sector to the hydrogen sector is uneconomic. This is due to the lower investment costs of the coupling technology for the case of the heat sector: an electric heater costs only 90 €/kW$_{el}$, while the investment costs for electrolysis amount to 500 €/kW$_{el}$. Yet, the possible savings per MWh are similar, as the replaced fuel (natural gas) is the same in the two cases.

The third conclusion which can be drawn from the figure, is that the role of the transmission grid changes. While in 2020, energy sector coupling decreases with transmission grid extensions, in 2050, the energy sector coupling increases with grid extensions. With intermediate VRE shares (2020), energy sector coupling can help to mitigate grid extensions for the integration of VREs. With high VRE shares, transmission grid extensions are used for stronger energy sector coupling: the amount of heat generated from electricity increases with increasing power transmission capacities. The local electricity oversupply is too high to be absorbed by the local heat sector and thus transmission grid extensions are necessary to export local electricity oversupply to other regions' heat sector. This point will be elaborated in more detail in Subsection 5.4.2, where the effects on a European level are estimated.

In addition to the reduction of oversupply, the energy sector coupling has another advantage: if electricity from VREs replaces natural gas, total emissions can be reduced. The results show, that the electricity sector and the carbon free excess electricity act

as drivers for emission reductions in other sector. As figure Figure 5.12 indicates, the emission reduction in the *Base 2020* amount to 40% (compared to 1990 levels) and to more than 60% in the *Base 2050* scenario. In 2020, the coal power plants are partly used to power the electric heaters. This effect is compensated by reducing the discarded excess electricity from VREs. In 2050, the change in total emission reduction from the *No New Grid, No Coupling* case to the *Base* scenario amounts to 4 percentage points. This additional emission mitigation occurs mainly in the heat sector. It is driven by the excess electricity from VREs.

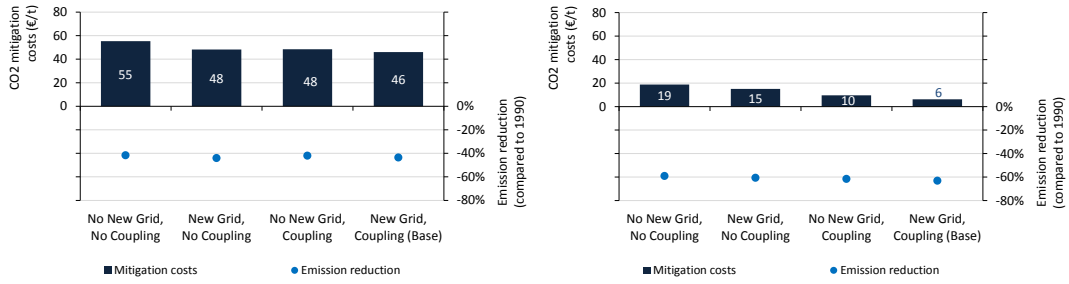

(a) 2020 (b) 2050

Figure 5.12.: Effects of energy sector coupling to emission reduction and CO_2 mitigation costs

The emission reduction is computed based on an estimate of 1990 CO_2 emissions. The 1990 emissions of the modeled sectors are estimated by backcasting the model results for the *Base 2010* scenario following the real emission reductions in Germany from 1990 to 2010. Emissions from CHP are split to the heat and power sector in accordance to the CHP coefficient. The 2010 model results are in accordance with statistic data: the United Nations Climate Change Secretariat (UNFCCC) reports 949 mio. tons of CO_2 for the analyzed energy sectors [146]: 302 mio. tons from the power sector and 647 mio. tons from the remaining energy sector excluding. The model results are only 3% lower (923 mio. tons).

While the level of achieved emission reduction compared to 1990 only changes very little due to the energy sector coupling, the CO_2 mitigation costs are reduced considerably, as Figure 5.12 shows. In the *Base 2020* scenario, the mitigation costs are reduced by more than 16% compared to the *No New Grid, No Coupling* scenario, thanks to national grid extensions and the coupling. In 2050, a reduction of more than 65% is achieved. The mitigation costs are computed compared to the *Base 2010* scenario. The overall costs reduction result mainly from reduced fuel costs, but also from the assumed cost reduction for VRE.

5.3.2. Relative roles of the coupling technologies

Heat sector

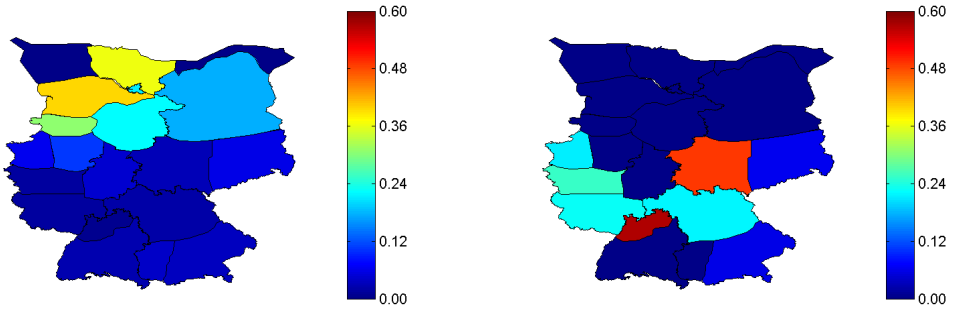

(a) Heat from Electricity (*Base 2050*) (b) Heat from Gas CHP (*Base 2050*)

Figure 5.13.: Share of heat supply from electricity and gas CHP power plants per region in 2050

In the *Base 2050* case, 10% of the heat demand is covered by electric heating technologies. Another 10% are supplied by natural gas CHP plants. These two technologies lead to a strong coupling between the power and the heat sector in the *Base 2050* scenario. In the *Base 2020* scenario the coupling is less strong.

The results from the regionally resolved model show, that these two heating technologies are used for different purposes. While the electric heater is used in the north, gas CHP plants are used in the south (see Figure 5.13). The highly fluctuating wind energy leads to highly fluctuating electricity excess with rather high peaks. Due to its low investment costs, the electric heater is well suited to absorb such fluctuations. The electric heatpump is not used in the *Base 2050* scenario, as its investment costs are comparatively high. In the south, power generation from solar PV is predominant. As identified by Richter for the city of Augsburg [124], the power generation from heat-led CHP combines well with the residual load. This is reconfirmed on a German level by the results shown in Figure 5.13. Electricity generation from heat-led CHP power plant is anti-correlated to the power supply from solar PV in Germany: it is high in winter and low in summer, when a large share of electricity is covered by solar power. In response to the projected regional distribution of wind and solar capacities, this leads to a regional distribution of different heating technologies.

A sensitivity analysis towards the assumed gas price (see Table 5.1) reveals further important properties of the technologies. As Figure 5.14 shows, higher gas prices lead to stronger replacement of natural gas in the model results. In the 2020 scenarios, where a total of 44 GW of coal, lignite and nuclear power plants are still on line, these cheap baseload power plants are used to feed electric heaters and heatpumps to reduce gas-consumption for very high gas price scenarios. Due to their high efficiency, electric

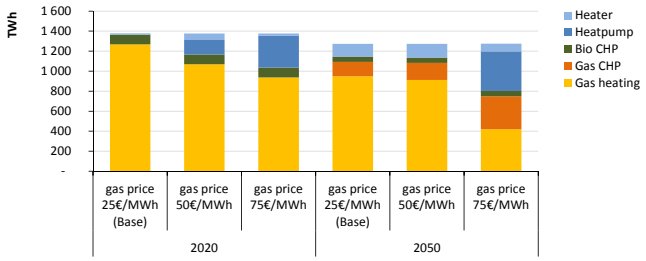

(a) Heat generation

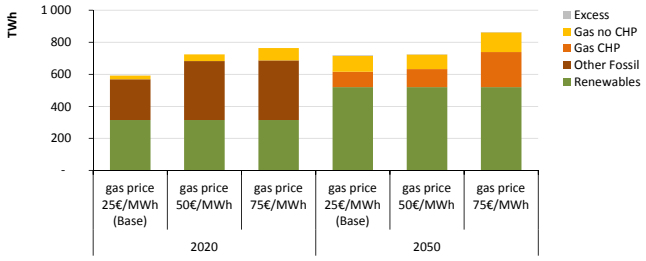

(b) Electricity generation

Figure 5.14.: Sensitivity of heat and electricity generation to the assumed gas price

heatpumps are an attractive technology if high gas prices are assumed. The same effect occurs in the 2050 scenarios. Furthermore, due to their high efficiencies, the usage of CHP plants increases with the gas price. For very high gas prices of 75 €/MWh, CHP plants are used to generate electricity efficiently, which is then in turn used to supply heat demand with heatpumps.

Hydrogen sector

Because of its smaller absolute size and the high costs of the coupling technologies in comparison with the heat sector, the hydrogen sector plays a smaller role in the energy sector coupling.

In the 2020 scenarios, only little excess electricity occurs and all of it is exported to the heat sector, even if electrolysis costs of 200 €/kW$_{el}$ are assumed (see Figure 5.15). This competitive situation becomes more evident for the 2050 scenarios. Without the coupling to the heat sector (*New Grid, No Heat Coupling*), about 45 TWh hydrogen is produced by 15 GW of electrolysis capacity. The market potential of the electrolysis is reduced to zero through the coupling of the heat sector to the electricity sector (*Base 2050* scenario). With high gas prices or without grid extensions, the coupling to the hydrogen sector is cost-optimal in regions with high VRE shares and 3-4 GW of electrolysis capacity results from the model. If the costs of electrolysis remain at today's level

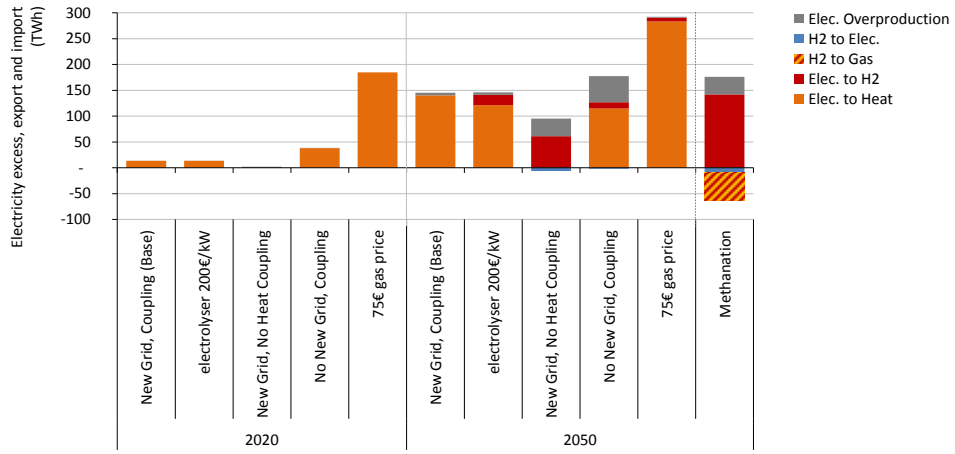

Figure 5.15.: Electricity excess and flows to and from other sectors: sensitivity of hydrogen coupling to heat coupling. All values are shown in electrical energy (TWh_{el}), except the hydrogen used for methanation, which is shown in terms of the lower heating value of hydrogen (TWh_{H2}).

of 1000 €/kW_{el}, it is not used in the model in both scenario years.

In the *Base* scenarios, long term hydrogen storage is not used for seasonal electricity storage. However, in the 2050 scenario, where no heat coupling is possible (*New Grid, No Heat Coupling*), hydrogen is used as seasonal storage. The total hydrogen storage capacity necessary to realize this scenario amounts to 18 TWh. This is in accordance with other studies. Based on an intertemporal optimization Kuhn [87] determines the storage additions for Germany until 2050. He finds, that about 11 TWh of hydrogen storage need to be added until 2050, assuming perfect interconnection within Germany. Due to the regional resolution in this analysis, the resulting storage size is higher than the one found in Kuhn [87].

If transmission grid extensions in Germany are not allowed, but the coupling to the heat sector is (*No New Grid, Coupling* scenario), the hydrogen storage is used as well, but a lot less. Hydrogen storage is only used in regions with very large VRE supply and where the heat sector is not large enough to absorb the electricity oversupply.

The power-to-gas option is also not used in the Base scenarios. The overall costs of power-to-gas, including electrolysis and methanation are very high and therefore it is only used in the model if a high gas price, no transmission grid extensions and an exclusive coupling of the power sector to the hydrogen sector are assumed. In this so-called *Methanation* scenario, about 140 TWh or 20% of power production are transformed to hydrogen, of which about 50% is then transformed to gas (see Figure 5.15). The other half of the produced hydrogen is used directly (25%) and retransformed to electricity after seasonal storage (25%). The natural gas generated from hydrogen allows to export the excess electricity to other regions. The electricity which cannot be used in the

respective regions is transported via the gas grid. The total annual transport is shown in Figure 5.16. It amounts to 10% of the regional gas demand at its maximum. The existing gas grid infrastructure may thus be sufficient to realize the additional gas energy transport.

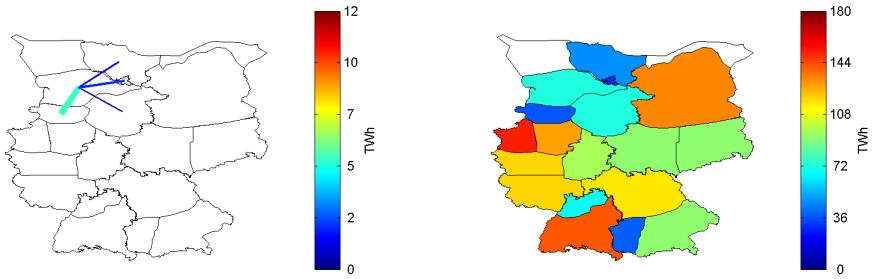

(a) Annual gas transport (b) Annual gas consumption

Figure 5.16.: Annual gas transport and gas demand in the *Methanation* scenario

Power sector

Figure 5.17a shows the total installed power plant capacity per technology and the supplementary power mix for selected scenarios. The VRE share increases from about 15% today to 66%[a] in 2050, while the capacity of dispatchable power plants remains close to the peak load in all cases, as the model setup does not allow to reduce peak demand level. Despite more flexible demand through the coupling, the dispatchable power plants thus face lower FLHs with increasing VRE penetration.

This effects of the energy sector coupling to the dispatchable power plants is shown in more detail in Figure 5.17b. In the 2020 scenarios, only little change in power plant dispatch occurs due to the coupling. With coupling and no grid extensions, the total supplementary power generation increases slightly. This is because conventional power plants use the energy sector coupling to export their electricity to the heat sector and therewith restore their level of FLHs. National transmission grid extensions counterbalance this effect: more VRE generation can be integrated in the power sector directly and thus less conventional power generation is required in total. In the 2050 scenarios, the same effect occurs. The contribution of Gas CHP plants increases with coupling and decreases again with national grid extensions. Through the coupling, the residual load can be flattened close to regions with high VRE penetrations, so-called VRE hotspots, and thus CHP generation can fit in the residual load. With grid extensions, less conventional power generation is needed.

[a]While the assumed capacity of wind and solar power for the 2050 scenarios is sufficient to supply 100% of the electricty demand in average, temporary oversupply leads to a lower contribution of VREs to the satisfaction of demand

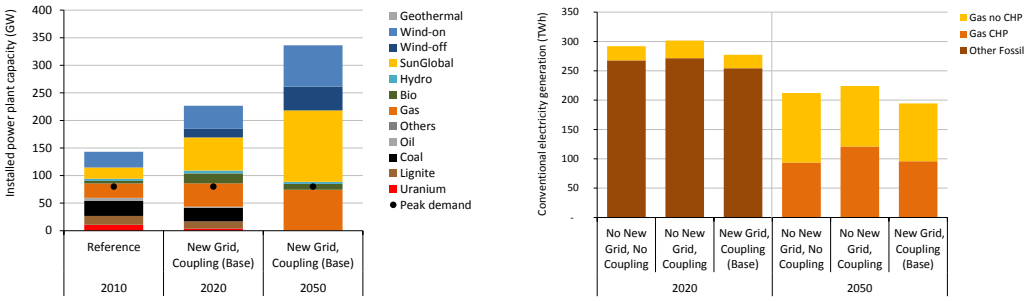

(a) The power plant capacity for the *Base* 2020 and 2050 scenarios

(b) Conventional generation with and without energy sector coupling

Figure 5.17.: Power plant capacity and conventional power generation with energy sector coupling

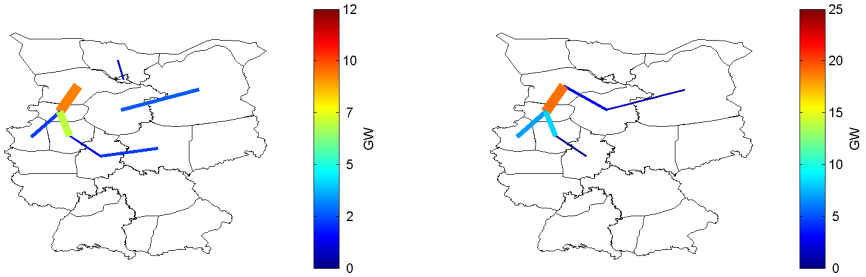

(a) 2020

(b) 2050

Figure 5.18.: Transmission grid additions in the *Base* scenarios

Grid extensions within Germany are built to export electricity from regions with high VRE supply to other regions. The smoothing effect of increased interconnection between these VRE hotspots is rather limited on this geographical scale, as was also shown in Chapter 3 in the time series analysis for Germany (see Figure 3.8). From the optimization, the most prominent grid extensions resulting from the optimization are connections from North-Western Germany, where large wind capacities are assumed, to load centers in South-Western and central Germany (Figure 5.18). Furthermore, increased east-west connections are cost-optimal, to integrate wind generation from North-East Germany. These connections are also used to increase the coupling of the power to the heat sector as soon as the regional sinks become insufficient.

5.3.3. Market effects of energy sector coupling in Germany

Through the merit order effect, an increasing VRE contribution can lead to a decrease in momentary but also in average electricity price, as shown in Chapter 4. Like transmission grid extensions, energy sector coupling increases the flexibility of the power system and

this is reflected in the electricity market. The results show that energy sector coupling reduces the low-price events and increases the market value and revenues of the power generation technologies, especially of VRE technologies.

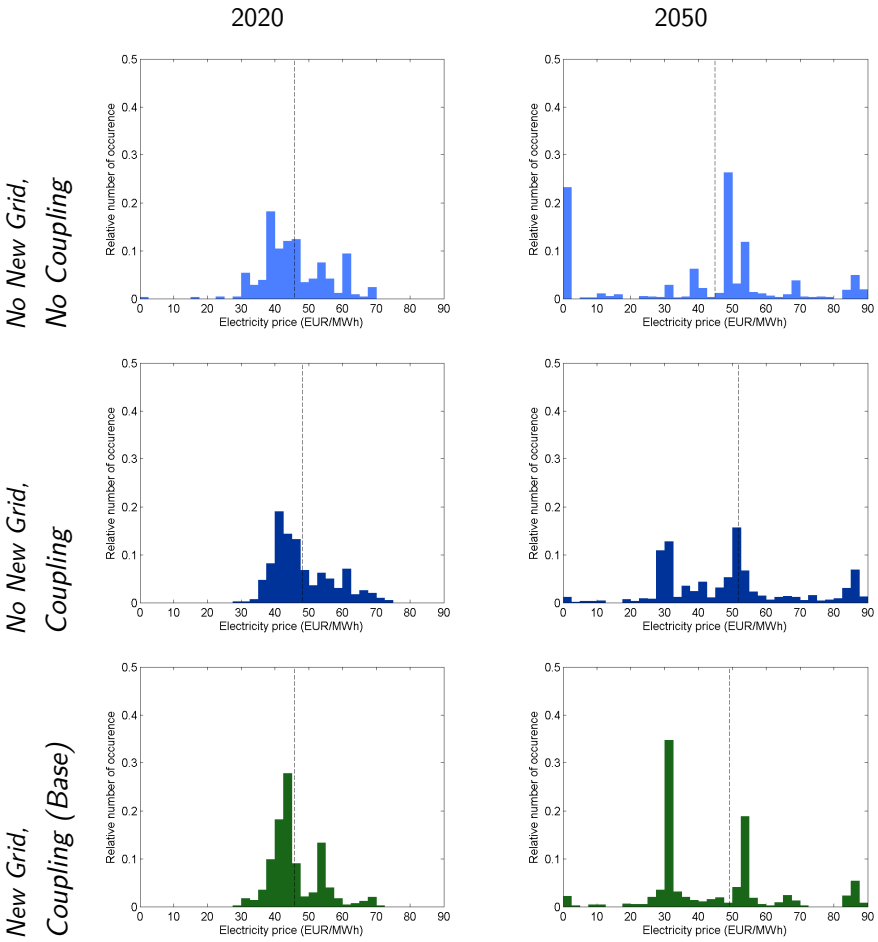

Figure 5.19.: Histogram of the average German electricity price. The dashed lines indicates the annual average.

Figure 5.19 shows the effects of energy sector coupling to the electricity prices, derived from the marginal costs of electricity resulting from the optimization. It presents the histograms of the prices with and without sector coupling and with and without national transmission grid extensions. The combined effect of both measures, energy sector coupling and grid extension, leads to a 4 €/MWh increase of the average electricity price in the 2020 scenario and to a 7 €/MWh increase in the 2050 scenario. The periods of low electricity prices are reduced through energy sector coupling, as the prices are lower bounded by the costs of the replaced fuel in the coupled energy sector. In the *Base* scenarios, this is natural gas used for space heating. The total fuel costs including

emission allowances amount to 31 €/MWh. In the *Base 2050* scenario, shown in the bottom right figure, this price level occurs in about 35% of the simulated hours due to the strong power to heat coupling.

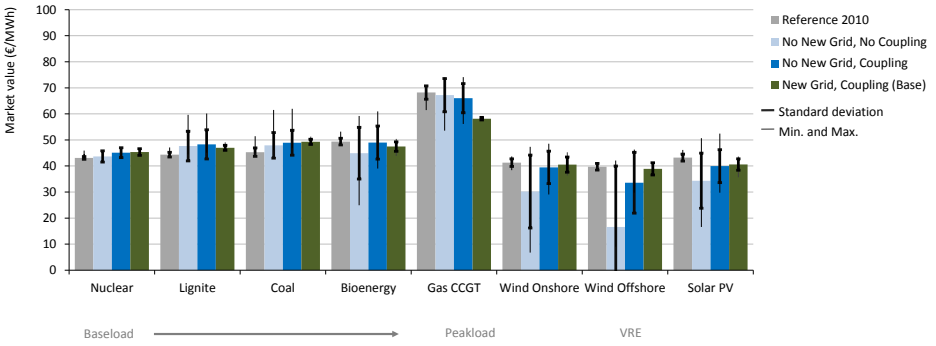

(a) 2020

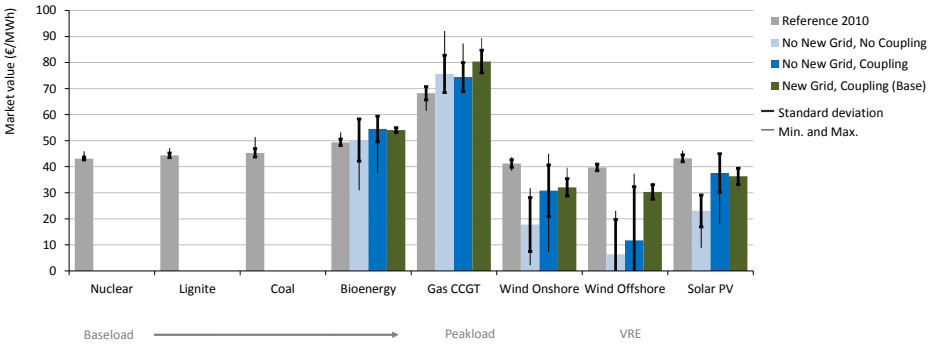

(b) 2050

Figure 5.20.: Market value per technology and the influence of energy sector coupling and transmission grid extensions in Germany. Standard deviation and minimal and maximal values across the model regions are indicated with the black lines.

Thanks to the reduction of low price events, the market values of the generating technologies increase through energy sector coupling. The market value is defined as the average price that a generator achieves at the electricity market (see Subsection 4.4.4). Figure 5.20 shows the market value per technology in Germany for different scenarios.

For the 2020 scenarios, similar conclusions as in Chapter 4 can be drawn from the results: baseload power plants profit from a smoothened residual load, be it through grid extensions or additional demand through energy sector coupling. Similarly, electricity from VREs has a higher value if the excess electricity is exported to other sectors. The market value of wind energy recovers to the 2010 level, while the increase of the market value of solar PV is less pronounced. This reflects the difference in cost-optimal coupling

technology between regions with high wind and regions with high solar capacity. Excess electricity from wind turbines is consumed by electric heating technologies directly, while in regions with large solar PV generation less excess generation is exported to the heat sector. For lignite and gas CCGT plants, a decrease in market value from the *No New Grid, Coupling* to the *New Grid, Coupling* scenario is observed. With cost-optimal German transmission grid extensions, increased import of electricity from VREs into western Germany results from the model. Lignite and gas power plants, mainly located in western Germany, can be identified as units, which are discriminated by the grid extensions.

For the 2050 scenarios, the market values for the dispatchable power plant types are higher. Gas power plants mainly set the electricity prices and thus the average electricity price is higher. With energy sector coupling and grid extensions the market values generally increase. If no VRE integration measure is taken, the market value of VRE technologies in turn is very low. With energy sector coupling, the regional excess electricity is exported to the heat sector and thus the prices become lower bounded and the market values rise, but neither for wind nor solar PV they recover to 2010 levels. National transmission grid extensions lead to a further increase of the market value of offshore wind. This technology benefits most from stronger connection of northern Germany to the rest of the country.

The annual revenues per technology and scenario are shown in Figure 5.21. They reveal the same effects as the market values: VREs and baseload power plants profit most from the integration measures in the 2020 and 2050 scenarios. For lignite and gas CCGTs, the above described disadvantageous position reappears: their revenues decrease with transmission grid extensions. Nuclear power plants benefit from the energy sector coupling, as they can be run more smoothly thanks to the coupling or even contribute to it.

Just as in Chapter 4, it is found, that the technical system integration measures of energy sector coupling, reduces the market effects of VREs. The higher flexibility in the system is also reflected in the market: VREs are easier to integrate an thus have a higher value for the system, a higher market value.

Although the overall effect of energy sector coupling to the electricity market is similar to the one of transmission grid extensions, several differences can be identified. The absolute German market values are lower than the European average presented in Figure 4.9. This is due to the different power plant fleets in Germany compared to the European average, including larger VRE capacities in Germany, but also to the assumption, that international trade is impossible in the analysis in this chapter. Finally, in the 2020 scenario setup in this chapter, conventional power plant capacity is imposed, while in Chapter 4, it is partly optimized. The level of the revenues, in turn, is comparable between the two analyses.

Despite these differences in absolute values, the relative effect of the VRE integration measures can be compared based on the change in market value. The increase in market

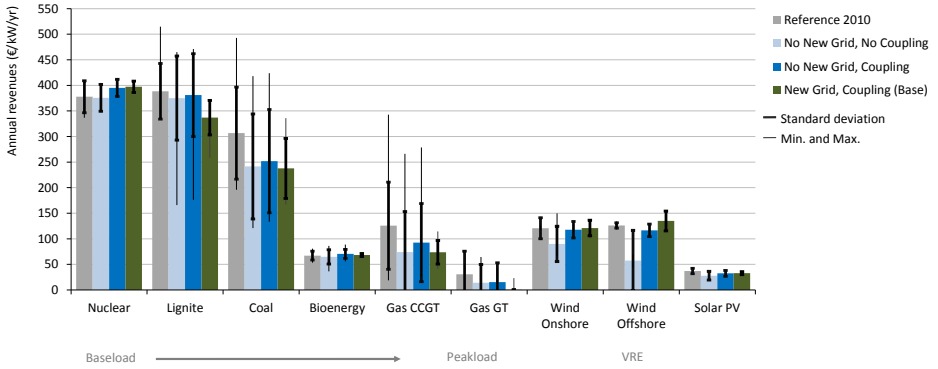

(a) 2020

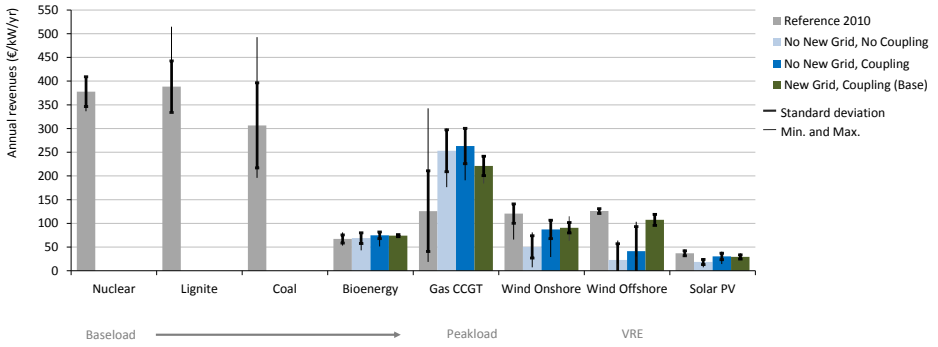

(b) 2050

Figure 5.21.: Annual revenues per technology and the influence of energy sector coupling and transmission grid extensions in Germany. Standard deviation and minimal and maximal values across the model regions are indicated with the black lines.

value between the *No New Grid, No Coupling* and the *No New Grid, Coupling* scenario of this chapter quantify the effect of energy sector coupling. The effect of a supergrid is measured by the relative increase of market value between the *No New Grid* and the *New Lines* scenario of Chapter 4. For wind onshore, the market value increases by about 30% due to coupling. A European supergrid raises the wind market value by 30% in European average as well, but in Germany by less than 10%. With a European supergrid, the import of wind power from other countries impacts on the market value of German wind power. For solar PV, the market value is increased by 16% due to the coupling, while with a European supergrid it only increases by 3% in Europe and in Germany. As discussed in the foregoing chapters, large transmission grid extensions are less beneficial for solar PV than for wind energy. For nuclear power plants, the average European market value is increased by 13% through the supergrid. In Germany, only a small share of European nuclear capacity is installed in the 2020 scenario and the

market values increase only by 2%. With energy sector coupling, the German market value of nuclear power plants is raised by 3%, comparable to the effect of a supergrid for German nuclear power plants. Also, all other conventional generators benefit from a European supergrid on a European average: their market values increase with grid extensions. This is not the case with energy sector coupling, which reduces the market value of natural gas according to the results. Energy sector coupling mostly affects VRE technologies directly, while the European supergrid influences the all power generation technologies.

5.4. Energy sector coupling versus European supergrid

The model results show that the heat sector can provide a very effective sink for temporary excess electricity. The power-to-heat option allows to smoothen the electricity demand and to reduce regional excess electricity. These two effects can also be achieved with a European supergrid. In this chapter, the VRE system integration achievable with the two measures of energy sector coupling and a European supergrid are compared. Furthermore their interaction is studied.

5.4.1. Comparison of the system integration benefits of both measures

To compare the two VRE system integration measures, the power system properties defined in Chapter 3 are used as metric. Overproduction and the mismatch parameter $|\Delta|$ with respect to the new, flexible demand are computed for cases with and without energy sector coupling, in order to asses the role of the coupling for VRE integration. Based on the VRE share and mix, the results from the different VRE system integration measures can be compared. The *Base 2020* scenario corresponds to α=39%, β=75% and *Base 2050* α=66%, β=75%. For the computation of α and β, perfect interconnection within Germany is assumed. Figure 5.22 shows the overproduction and mismatch $|\Delta|$ for the different scenarios. The blue bars show the mismatch and overproduction of the respective European scenario.

Both measures, energy sector coupling and a European overlay grid achieve almost complete elimination of excess electricity. The European supergrid eliminates excess through smoothing of VRE supply. With energy sector coupling, the heat and also the hydrogen sector act as sinks for the excess electricity. Through the additional demand, the total electricity demand adjusts to the VRE supply and the mismatch is reduced. With 38% VRE share (2020), the mismatch is reduced from 70% in the uncoupled, no-grid case by grid extensions within Germany and energy sector coupling to 62%. A European overlay grid achieves the same mismatch. In 2050 (66% VRE share), the reduction through grid-extensions and coupling is generally more pronounced. This is because higher VRE capacities are assumed for 2050 and thus larger excess electricity occurs initially. Also for the 2050 scenarios, both measures are comparable.

In contrast to the European supergrid, the energy sector coupling does not allow to reduce the necessary supplementary capacity. In the scenario definition in this analysis

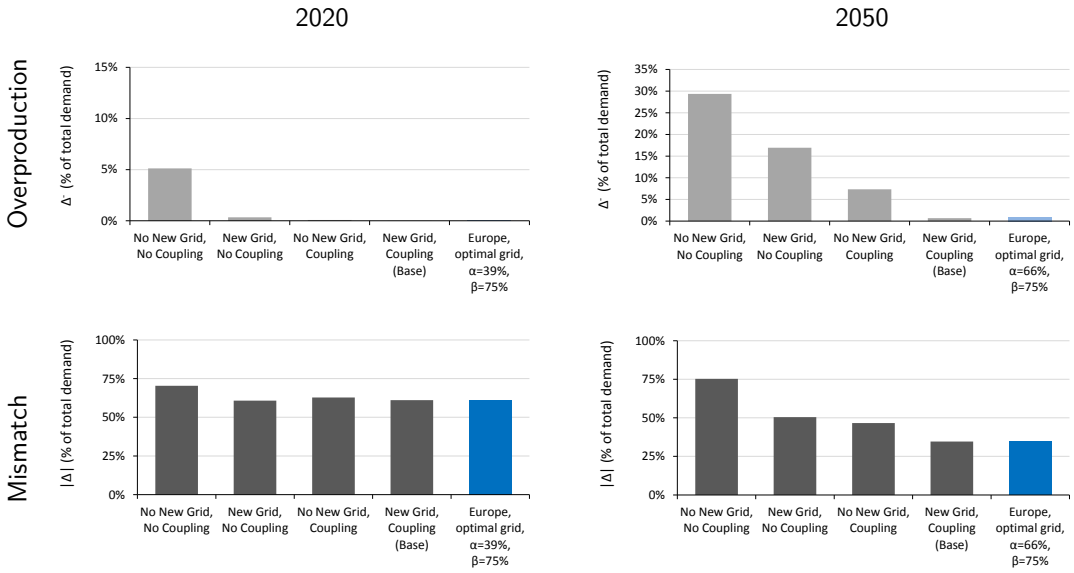

Figure 5.22.: Fundamental properties of the German power systems with different VRE integration measures

excess electricity can be exported to other sectors and thus electricity demand increased in hours of high VRE supply, while the reduction of demand in hours of low VRE supply is only possible via the usage of storage. In the optimization results, storage plays a minor role only and supplementary capacity is thus not reduced.

5.4.2. Interaction of a European supergrid and energy sector coupling

While up to now, both measures have been studied independently, this section investigates the interdependency of the power-to-heat option and a European supergrid. The interaction between German transmission grid extensions and energy sector coupling already revealed that the transmission grid changes role with increasing VRE share. This finding is reconfirmed on the European level by the results presented in this section.

Model setup and scenario definition

The URBS-EU model is employed to analyze European transmission grid extensions and the coupling of the power to the heat sector simultaneously. The optimization can chose the most viable VRE integration option. Following the parametric approach taken in Chapter 3, the European power system is optimized for every possible VRE share α and mix β. For the comparison of the two measures, the VRE share α is computed with respect to the original electricity demand excluding the increase in demand due to energy sector coupling. This enables the comparison of this analysis to the results from

Chapter 3, but differs from the approach in Figure 5.22.

For each configuration, the cost-optimal mix between transmission grid extensions and the coupling of the power to the heat sector is computed with the model. Just as in Chapter 3, two scenarios are taken into account: one, where current dispatchable power plants are assumed to be in place, and one, where a cost-optimal supplementary power plants fleet is assumed (see Table 5.7). The cost-optimal supplementary capacities are obtained from simultaneous grid and supplementary capacity optimization. They are taken from the results of the *Grid and Power Plants* scenario from Chapter 5. Thus, in both scenarios, VREs and supplementary capacities are defined by the input, while grid extensions and power-to-heat sector coupling are determined by the optimization.

Scenario	Grid extension	Power-to-heat	Dispatchable power plants
Grid and Coupling, current supplementary capacity	optimized	optimized	current power plant fleet
Grid and Coupling, cost-optimal supplementary capacity	optimized	optimized	cost-optimal power plant fleet (from Chapter 3, *Grid and Power Plants* scenario)

Table 5.7.: Scenario definition

Based on the results from the detailed analysis of energy sector coupling for Germany described above, two simplifying assumptions are taken. First, the coupling to the hydrogen sector is not included in this analysis, as the above results revealed its minor role. Second, only the electric heater is available as coupling technology. The results from the German model showed that, with current gas prices, the electric heater is more attractive than the heatpump, due to its low investment costs.

Furthermore, the heat sector is not modeled explicitly. Instead, the export of electricity to the heat sector is simulated via a generation process with negative variable costs: once the infrastructure, i.e., the electric heater, is installed, the generated heat can be "sold" to the heat sector for the price of the replaced fuel, the natural gas price. Taking into account the price of carbon emission allowances, the price of replaced fuel amounts to 31 €/MWh. The capacity of the electric heaters is limited to the minimal regional heat demand. The amount of electricity that can be exported to the heat sector is thus limited by a constant value across the year. Due to low availability of data on the hourly profiles of heat demand per region in Europe, the minimal regional heat demand has been chosen as upper bound in order to provide a conservative estimate of the effects of the power-to-heat option.

The minimal heat demand per model region is deduced in two steps. First, the total regional heat demand is estimated based on the heating degree days per country [45], as well as the regional electricity demand serving as indicator for energy demand in general. Second, the ratio between average and minimal computed hourly heat demand in Germany (0.33) is used to determine the minimal heat demand in other European countries.

All other data and assumptions are as defined in Chapter 3.

Results

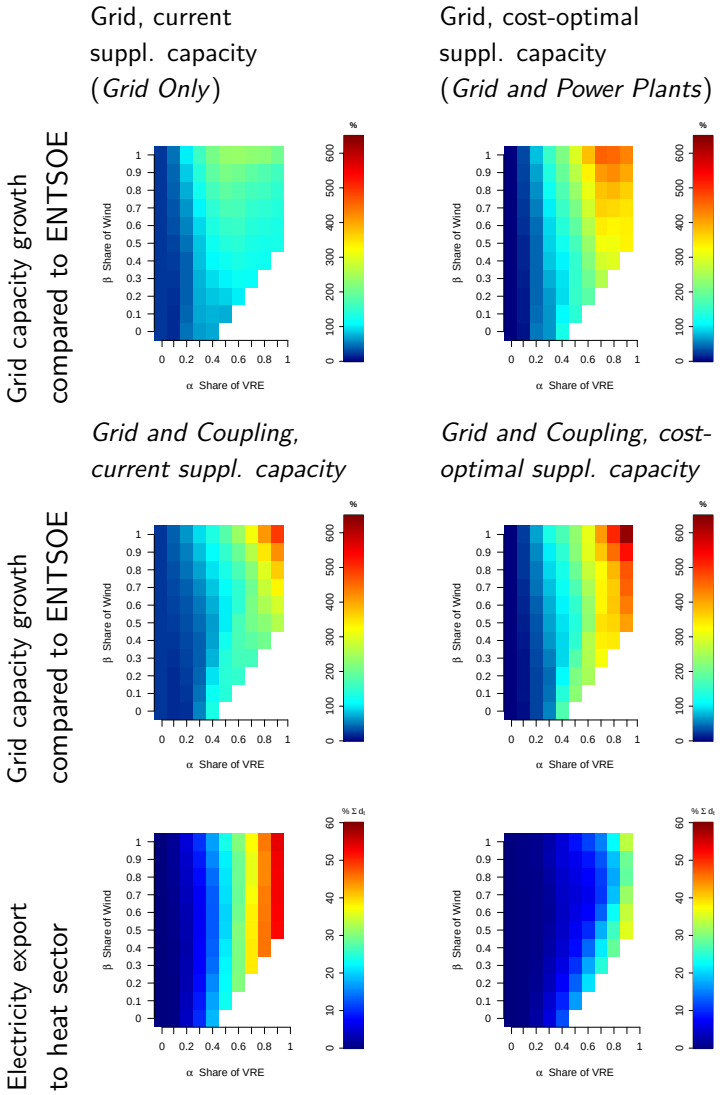

Figure 5.23.: Grid extensions and electricity export to the heat sector. The two columns show the two scenario sets: with current and with optimized supplementary capacities. The first row shows the results from Chapter 3 for grid extensions for comparison. The second and third row show the results of the scenarios where the power-to-heat option competes with European grid extensions. Grid extensions are the increase in grid capacity and length (GWkm) with respect to the current ENTSO-E grid.

The results of the interaction of the two VRE system integration measures are shown in Figure 5.23. It shows the grid extensions and electricity export to the heat sector for each VRE share α and mix β. In the first row, the results from Chapter 3 are shown for comparison.

For both scenarios, with current and with optimized supplementary capacities, the coupling to the heat sector reduces the European transmission grid capacity growth for small to intermediate VRE shares. For high VRE shares, however, the cost-optimal grid growth with coupling to the heat sector largely exceeds the grid extensions resulting for the non-coupled cases. These results confirm the finding from the German scenarios: with increasing VRE share, the transmission grid changes role. With low to intermediate VRE shares, the coupling of the power to the heat sector mitigates transmission grid extensions. It is cost-optimal to rather use the local sink for excess electricity than to export the excess to other regions via increased transmission grid extensions. This is the case until about 50% VRE share in both scenarios. The increase in grid due to the coupling is more pronounced with high solar shares ($\beta \leq$30%). With higher wind shares ($\beta \geq$50%), additional grid for coupling only results from VRE shares of 70-80% on. Generally, with increasing VRE contribution, the local sinks become insufficient and transmission grid extensions are built in the model to foster the coupling of the power to the heat sector. The power-to-heat option thus drives additional grid extensions. This effect differs depending the assumption on supplementary capacities. With current supplementary capacities, the additional grid capacity increases from 200% to 450% on top of current ENTSOE grid capacity due to the coupling; with cost optimal supplementary capacities it increases from 450% to 650%. As shown in Chapter 3, the grid growth saturates for very high VRE shares with current capacities. Existing capacity is used for the power supply in hours of low VRE availability. Through the inclusion of power-to-heat option, the benefits from grid extensions are increased as they can help to export more electricity to the heat sector. This is not the case with cost-optimal supplementary capacity, where the grid extensions for the uncoupled case do not saturate.

The last row of the figure shows the electricity export to the heat sector. It increases with VRE share. In the scenario with current supplementary, the power to heat coupling is stronger than in the scenario with cost-optimal supplementary capacity. This is due to the fact that existing power plants with low fuel costs, such as coal or nuclear power plants, export their power to the heat sector. The FLH reduction of baseload power plants due to increasing VRE contribution is compensated via the power to heat coupling. This possibility is exhausted to its maximum: the upper bound of power export to the heat sector of 60% of total electricity demand is reached. In the scenario with cost-optimal supplementary capacity, the coupling is less strong. The cost-optimal power plant fleet mainly consists of gas power plants for high VRE shares (see Figure 3.13). Therefore, the replacement of natural gas in the heat sector via power from these plants is uneconomic. The power-to-heat coupling is solely driven by the excess electricity from VRE, as can be seen if the results in this section are compared to the overproduction shown in Figure 3.3: for a wind contribution β of around 80%, for example, the overproduction remains lower for high VRE shares. The power to heat coupling is lower for this VRE mix as well.

5.5. Discussion and conclusion

In this chapter, energy sector coupling as large-scale VRE integration measures has been analyzed. The results show that the heat sector provides a large sink for the temporary electricity oversupply caused by VREs. Moreover, the export of electricity to the heat sector is economically more attractive than the export to the hydrogen sector due to its relative costs structure. While costs savings for replacing conventional fuel in the heat or hydrogen sector are comparable – in both cases natural gas is replaced, the investment costs for coupling the power to the hydrogen sector are higher. Given the large thermal demand and the relative economics of hydrogen versus heat, the model shows that the cost-optimal system would not employ long-term electricity storage via hydrogen generation both in the 2020 and the 2050 *Base* scenarios. Instead, the power sector is strongly coupled to the heat sector.

Thanks to the regionally resolved and technology specific modeling, the optimal conversion paths from power to heat can be resolved for different locations and cost assumptions. The results show that the deployed heating technologies are complementary to the regional VRE power supply: highly flexible electric heaters are used in northern Germany close to variable excess electricity from wind energy. Heat generation from CHP is centered in the south, because its seasonal supply pattern is anti-correlated to the large supply from solar PV in these regions. With increasing gas prices, electric heatpumps become more attractive, because of their high efficiency and the resulting natural gas savings.

Denying the model the option for coupling power to heat, other measures to manage VRE oversupply are deployed in the simulations. Especially for the high VRE shares in the 2050 scenarios long term electricity storage via hydrogen becomes cost-efficient. However, the power-to-gas option, i.e., using the natural gas grid as a high-capacity energy transport infrastructure, is used only in a very specific scenario setup where, in addition to the exclusive coupling of the power to the hydrogen sector, grid extensions are prohibited and a tripling of the gas price is assumed. With current gas prices and available coupling options, the power-to-gas option is not part of the cost-optimal mix.

The model excludes alternative electricity storage options, such as compressed air storage, extension of the pumped hydro storage reservoirs or batteries. Due to their restricted potential as well as their high costs compared to hydrogen, their role for the integration of large VRE shares is potentially rather limited. Energy storage in the heat sector, does not play a major role for VRE integration in the present analysis. Even assuming larger heat storage of 6 and 12h, the heat generated from electricity is consumed directly rather than being stored before. This is due to the large heat demand.

The results furthermore demonstrate that energy sector coupling helps to efficiently reduce green house gas emissions of the complete system. The mitigation costs are reduced substantially, by 15% and 65% compared to the uncoupled case in 2020 and 2050, respectively, as the energy sector coupling introduces a low cost option for emission mitigation through the replacement of natural gas in the heat sector. In the power sector, the emissions rise slightly compared to electric storage options since VRE undersupply

situations cannot be covered with stored carbon free energy but have to be closed with fossil fuel. The emission savings in the other sectors, heat and hydrogen, overcompensate this increase. This can be explained by the low efficiency of long-term electricity storage which makes direct use of temporary VRE surpluses even for "low" quality energies like heat beneficial. In the light of ambitious green house gas reduction pledges in Germany and Europe, the important cost-reduction potentials should not remain unused.

In analogy to Chapter 4, the VRE system integration measure also reduces the impacts of VREs to the electricity market. The market value of VREs is raised through energy sector coupling. A lower bound for the electricity prices is introduced as soon as the excess electricity is exported to other sectors and the electricity price stagnates at the price of the replaced fuel. VRE technologies benefit most from this change in prices. The market value of onshore wind is increased by 30% and the one of solar PV by 16%, thanks to the coupling. But also for dispatchable generators advantages arise, mainly for baseload power plants such as nuclear in the 2020 scenarios. In comparison to the benefits for market integration of VREs from European transmission grid extensions, the energy sector coupling affects VREs in a more direct manner. The reduction of zero price events is mainly to the benefit of VREs. The benefits for conventional generators are lower, i.e., the increase in market value and revenues less pronounced. European transmission grid extensions smoothen the prices instead of introducing a lower bound. Accordingly, all generation technologies see an increase in market values.

Comparing energy sector coupling to the measures of building a European supergrid analyzed in the foregoing chapters, it is found, that the achieved VRE system integration is similar. Through the energy sector coupling, additional electricity demand in hours of high VRE supply is created and the residual load becomes smoother. Excess electricity and the mismatch $|\Delta|$ between supply and demand are reduced. The comparison of the results to the those in Chapter 3 shows that the energy sector coupling achieves similar misfit and overproduction reduction as a powerful European overlay grid in the 2020 scenario. All excess electricity production due to VRE is absorbed by the heat and the hydrogen sector. In the respective European scenarios ($\alpha = 38\%$) the smoothing effect of the supergrid eliminates all overproduction as well. In the 2050 scenario, the coupling alone reduces the overproduction from 30% to 7% but can only reach the same level of 1% as the corresponding European scenario ($\alpha = 64\%$), if German transmission grid extensions are realised in the mean time.

Another observation is that the role of the transmission grid changes with increasing VRE share. In the 2020 scenarios, the absorption of regional excess electricity through the heat sector makes transmission grid extensions initially less attractive. With increasing VRE shares in the German 2050 scenarios the regional heat demand is insufficient to absorb all the oversupply, especially in regions with large VRE capacities. In this case, the model decides to realize transmission grid extensions to strengthen the energy sector coupling. Electric oversupply from northern Germany is then exported to the heat sectors of other regions.

Including the power-to-heat option in the URBS-EU model, its interaction with European transmission grid extensions is analyzed. In the results of this parametric study the change of the role of grid extensions becomes even more evident. While at lower VRE shares, the power-to-heat option helps to mitigate transmission grid extensions, from VRE shares of 50% on additional transmission grid extensions results from the model, as the regional sinks for excess electricity become insufficient.

This behavior is very advantageous for future system design as the two VRE system integration measures do not contradict each other. Temporary oversupply from VREs can be managed by energy sector coupling locally until transmission grid extensions are realized to accommodate larger VRE shares.

Having drawn these conclusions it should be noted that the results should be interpreted with caution. The analysis is centered around the challenge to integrate the VREs into the power sector and thus does not include all technical details of the hydrogen and the heat sector. Specifically, the scenarios do not consider direct renewable supply for the heat and hydrogen sector, or likely efficiency measures to reduce demand. In this case, the amount of electric energy that can be exported to these sectors would be reduced. Moreover, the transport sector is not considered, where electric or gas driven cars could provide large new sinks for electric surpluses. Given the high value of energy in the transport sector, this option could change the picture significantly, potentially in favor of the power-to-gas path with its large implicit storage potential. Despite these restrictions, the results concerning the usage of electric heaters to absorb electrical oversupply from VREs are rather robust, as this mature, low-cost technology can still fit well into other heat supply structures. In contrast, usage of electric energy in the transport sector depends significantly on new technologies that are not market competitive today.

Similarly, the analysis of the power-to-heat on a European scale has to be understood as a first order estimate, as the temporal variations in heat demand are not included. However, the methodology is sufficiently detailed to reveal the principal dynamics of the interaction between the two measures.

6. Synthesis and outlook

In this thesis, the effects of large shares of VREs on the European power system have been analysed and the system benefits of transmission grid extensions and energy sector coupling quantified. The results suggest that, under the chosen scenario assumptions, both measures are cost-effective. European transmission grid extensions smoothen the VRE supply considerably and therewith simplify their integration. The analysis of energy sector coupling reveals that the heat sector provides an attractive sink for excess electricity from VREs. In addition to the system benefits, positive effects of these measures for the market integration of VREs have been identified. A benchmarked, spatially and temporally highly resolved energy system model has been used for the analysis.

This chapter provides a synopsis of the results, after discussing the employed methodology. Finally an outlook for further research is given.

6.1. Discussion of the applied methodology

The design of future power systems with large VRE shares is optimized with the URBS model generator. The methodology allows for high spatial and temporal resolution as well as the inclusion of the technical details of the power system and its dispatch. It is therewith well suited for the analysis of VRE integration in the power system. With its position between system planning and dispatch simulation, URBS contributes to the field of hybrid energy system models.

However, several details, such as start-up times, load-dependent efficiencies, forecast uncertainties etc. are not modelled explicitly. As a consequence, the flexibility of the system is potentially overestimated and the computed VRE system challenges, such as overproduction and necessary dispatchable capacities have to be understood as lower bounds. The benefits of the analyzed integration measures, in turn, are possibly underestimated. Furthermore, the simulation of power flow is carried out with a transport model. By taking the conservative assumption of using transmission lines only at their natural power, the likely underestimation of necessary grid extensions can be addressed, as was shown in a comparison of the model results to a load flow simulation. Finally, three measures have been taken to overcome the imprecision introduced by including only a few weeks in the optimization. The careful selection of representative periods, the coupling of the time series analysis to the optimization model and the deployment of several years of meteorological data all lead to considerable increase of robustness of the results.

The benchmark of the model results to historic data demonstrates that, despite the simplifications, the model captures the large and complex system in a sufficiently realistic

way.

In this thesis, the long term development of the power system is not endogenous to the model. Instead, a parametric approach is chosen to analyze different VRE scenarios, precisely every possible VRE share and mix. This provides insights on the systematic effects of different resource mixes and may serve as a new approach to the analysis of future power system development.

With its features and the carefully selected simplifications, the model allows to analyze a large area in high temporal and geographical resolution. The inclusion of a comparatively high level of technical detail, high spatial and temporal resolution, and the coverage of a wide area and large number of possible future scenarios, makes the approach uniquely positioned to provide insights on the VRE integration challenges and measures in Europe and Germany.

6.2. Synthesis of the results

6.2.1. VRE system integration

Large shares of VREs lead to important challenges for the power system. The results of the parametric study in Chapter 3 quantify these challenges.

First, if no VRE integration measures are taken, large excess electricity generation result. Overproduction rises steeply with VRE share[a], from less than 10% of total load at a VRE shares of 30% up to 60% at a shares of 60%. This is due to the low geographic and temporal correlation of VRE supply and load as well as the high temporal variability of VRE supply. Thanks to the sampling of a large parameter space, the necessary VRE capacity to achieve any given VRE share can be quantified. It increases with overproduction and reaches up to 6 times the peak load for a VRE share of 80%. However, as the VRE capacity is limited by the technical potential for wind and solar generation, such high shares cannot be achieved, but only about 60%.

In terms of system adquacy, a challenging property of VREs is their low capacity credit, also caused by low geographic and temporal correlation of VRE supply and load. The results show that, in the absence of a supergrid, the capacity credit remains below 5% for most of the scenarios. As a consequence, large supplementary capacity is necessary.

A powerful European overlay transmission grid smoothens the VRE supply, and this entails two major benefits for VRE integration, as the results show.

First, overproduction is reduced. At 80% VRE share, the computed overproduction is reduced to 20%, down from over 100% without grid extensions. With it, the necessary wind and solar capacity decreases. Consequently, the possible achievable VRE share is increased, assuming the same technical potential. According to the results, a European supergrid would allow to increase the possible VRE share from 60% to more than 85%. Second, the average European capacity credit of wind energy is increased from less than 5% to more than 10% for VRE shares with important contributions from wind energy.

[a] VRE share refers to directly usable VRE energy, excluding oversupply.

The requirements of holding dispatchable capacity available for system reliability can thus be reduced considerably with a supergrid, from 100% of peak load less than 60%. The smoothing effect of the supergrid mainly occurs for wind energy, as the diurnal pattern of solar energy is very similar across Europe.

Both benefits lead to lower costs of electricity generation, as less VRE and supplementary capacity are necessary. For a VRE share of 60%, the analysis shows that a supergrid reduces the costs of electricity by about 10 € per MWh load (€/MWh), while the costs for the transmission grid extensions amount to 3 €/MWh only. In the entire parameter space, the costs of the supergrid do not exceed 3.5 €/MWh and are always cost-effective, according to the results. Compared to the VRE investment costs, the computed grid costs remain below 25% for all conceivable VRE scenarios.

In addition to the comprehensive cost-benefit analysis of the supergrid, the parametric approach allows to identify important features of power system design with high VRE shares.

First, ideal VRE configurations can be identified. Minimizing the mismatch between VRE supply and the load, the ideal VRE share and mix with and without European supergrid were determined. With a supergrid, a VRE share of 80%, of which 85% is wind energy and 15% solar PV, is desirable according to the results. Without transmission grid extensions, the optimal configuration is 60% VRE, 75% wind and 25% solar share. The large share of wind energy in both cases results from the shape of solar PV generation: the steep mid-day peak leads to large overproduction and thus increasing mismatch between load and supply. Wind energy in turn is also available at night. Furthermore, with a supergrid, wind energy can provide a fairly "smooth" power supply. In low-connection cases and thus with higher variability of the wind supply, the ideal share of solar energy is higher, as it has the advantage of higher temporal and also geographical correlation with the load.

Second, major transmission corridors can be identified from the findings in Chapter 3. In the so-called "must-have" grid connections, beneficial for a large range of possible future VRE shares and mixes, are identified. These are strong north-south connections from North-Western Europe to the load centers further south, an offshore grid in the North Sea and the connection of the Iberian peninsula to France. With increasing VRE share, north-south connections in central Europe as well as connections to South-Eastern Europe gain importance, as wind generation in the North Sea increases. Given the uncertainty of future development of wind and solar installations in Europe, the identified corridors, which are no-regret options, can provide valuable guidance to grid infrastructure planning.

Finally, conclusions on the supplementary electricity generation can be drawn. The model results indicate that the dispatchable power plant fleet should become more flexible with increasing VRE contribution. In the scenarios with a supergrid, the share of baseload power plants is drastically reduced in the cost-optimal mix from a VRE share of 40% on. They are displaced by more flexible, less capital intensive power plant types such as natural gas CCGTs or GTs. In proximity to VRE hotspots, this displacement

happens at lower VRE shares already and is, of course, more pronounced without major transmission grid extensions.

In contrast to the pan-European measure of building a supergrid, the more local VRE integration measure of energy sector coupling has been evaluated for the example of Germany in Chapter 5. Especially, if no grid extensions are realized, high excess electricity occurs. This local electricity surplus can be used to replace other means of generation in the coupled sectors, the heat and hydrogen sector. The findings demonstrate that this measure is also very effective in terms of VRE system integration.

According to the results, energy sector coupling reduces the excess electricity production in Germany considerably. For a VRE share of about 40%, it is reduced from 5% in the uncoupled case to zero and for a VRE share of about 65% from 30% to 7%. For the lower VRE share, the achieved elimination of excess is identical to the effects of a supergrid. For the higher VRE share, the effect of the supergrid is more pronounced: it reduces overproduction to 1%. Only with German transmission grid extensions, the same reduction of misfit can be achieved with energy sector coupling.

The second benefit of energy sector coupling is its potential contribution to the decarbonization of other sectors. A fully decarbonized power sector could thus serve as driver to mitigate CO_2 emissions in the heat and the hydrogen sector, which is a very cost-effective measure for emission reduction, as the findings show. Through the coupling, the mitigation costs are reduced by up to 50% compared to the uncoupled case.

Through the inclusion of several plausible conversion and storage technologies in the optimization, most economic technology choices in energy sector coupling can be identified. The interrelations between the different conversion technologies, storage options and the transmission grid are taken into account and therefore detailed recommendations for future system design can be extracted from the results.

The results in Chapter 5 reveal a dominant role of the heat sector providing a large sink for the temporary electricity oversupply caused by VREs. Moreover, the export of electricity to the heat sector is economically more attractive than the export to the hydrogen sector due to its relative costs structure. As a consequence, long term storage and methanation are displaced by the power-to-heat option. All excess electricity is exported to the heat sector for VRE shares of 40% and 66% in the *Base* scenario, where energy sector coupling and national transmission grid extensions are included.

Thanks to technological and geographical detail included in the model, optimal conversion paths from power to heat could be identified for different locations. The deployed heating technologies are complementary to the regional VRE power supply: highly flexible electric heaters are used in northern Germany close to highly variable excess electricity from wind energy. Heat generation from CHP is centered in the south because its seasonal supply pattern is anti-correlated to the large supply from solar PV in these regions.

The third important finding concerning the system design is the interaction of transmission grid extensions and energy sector coupling. The results from the study of Ger-

many and the estimate of the interaction between energy sector coupling and European transmission grid extensions both show that the role of the transmission changes with increasing VRE share. At lower VRE shares, the absorption of regional excess electricity through the heat sector makes transmission grid extensions initially less attractive. With increasing VRE shares, the local sink, the heat demand, is insufficient to absorb all the excess electricity, and transmission grid extensions are realized to strengthen the energy sector coupling. The parametric study of the interaction of both measures on European level reveals, that this switch occurs at a VRE share of 50%.

This behavior is very advantageous for future system design: the two VRE system integration measures do not contradict each other. Energy sector coupling can be used to manage temporary oversupply from VREs locally until transmission grid extensions are realized to accommodate larger VRE shares.

6.2.2. VRE market integration

The VRE system integration challenge is also reflected in the electricity market. The inclusion of highly fluctuating resources, where regional excess occurs and, additionally, zero marginal costs reign, leads to significant impacts on the electricity price in energy-only markets.

The results presented in Chapter 4 quantify this effect. For a VRE scenario reflecting European targets for 2020, the merit order effect reduces the average electricity price by 5 €/MWh or 8%, assuming nodal prices. In regions with high VRE supply, the effect is more pronounced. For example in North-Western Germany the average price is reduced by 9 €/MWh or 17%. Furthermore, the price dynamic changes from demand to supply driven leading to an increased price uncertainty.

As a consequence of the merit order effect, the market value of VREs is reduced: whenever high VRE supply is available in a market region, the prices in this region are lowered by the VRE supply itself. However, according to the findings, the lower wholesale prices also affect other market participants. The market value and revenues of conventional generators are reduced as well, especially for base load technologies in proximity to high VRE supply, such as nuclear power plants in North Germany for example. The reduced average electricity prices lead to an increased gap between total average costs of power supply and average electricity price. These results show that the possibility to recover the total system costs on an energy-only electricity market is reduced substantially due to high VRE shares.

The analyzed VRE integration measures make the power system more flexible. The findings show, that this increased flexibility facilitates the market integration of VREs.

A European supergrid smoothens VRE supply. Through increased interconnection the burden of integrating VRE supply is shared between market regions. VRE supply peaks can be exported to other regions and conventional power generation is run more continuously in regions with high VRE capacity. Chapter 4 quantifies the consequences for the electricity markets: the geographic price variability is reduced and the average price level is raised. In the importing region more expensive generation will be displaced,

but in the exporting region zero price events can be avoided. Thanks to the non-linear shape of the merit order curve, in total, this leads to an increase in average price level, as the results show. The effect on European average is a 2 €/MWh price increase. For regions with high VRE supply this effect is more pronounced. In North-Western Germany for example, the price is raised by 5 €/MWh. Opposite to the raised price level, the total costs of electricity supply are reduced by about 1 €/MWh (including the costs for grid extensions). The gap between costs of electricity and the electricity price can thus be reduced by the supergrid.

The higher prices but also the more continuous dispatch of conventional power plants thanks to grid extensions bears important benefits for all generators: the average market value and revenue is increased for all technologies. VREs and baseload power plants benefit most: their market values and revenues is found to increase sharply, by 31% and 14% for onshore wind and nuclear repectively. This effect is especially pronounced in regions with large VRE capacities such as Germany, Spain and Great Britain or with large nuclear capacities, such as France. For the majority of mid and peak load technologies, the results show an increase in market value as well, but in regions importing VREs, an economic disadvantage can result, i.e., lower market values. This is for example the case for Gas CCGTs in Italy, where the import of electricity from France and Germany impacts on this generation technology.

In summary, the findings show that transmission grid extensions help to reduce the effects of VREs to the market. The increased exchange through larger interconnector capacity is to the advantage of most, but not all countries and technologies.

With energy sector coupling, local electricity surplus is used to replace natural gas in the coupled sectors, the heat and the hydrogen sector. Excess electricity regains a value. As the results in Chapter 5 indicate, this effect leads to a reduction of the impacts of VREs to the electricity market.

Energy sector coupling introduces a lower bound for the electricity prices. The level of the lower bound is defined by the value of the replaced fuel. On average, this leads to an increase of electricity prices of 4 €/MWh to 7 €/MWh for the 2020 and 2050 scenario respectively. As the energy sector coupling mainly occurs during hours of high VRE supply, its effects are most pronounced for wind and solar generators. According to the model results, the market value of wind onshore and solar PV increases by 30% and 16% respectively for the 2020 scenario. The market effects of the European supergrid for wind energy are comparable, but for solar PV, the supergrid leads to an increase in market value of only 3%. This reaffirms the above findings, that solar PV benefits less from transmission grid extensions in Europe, but also shows that, the energy sector coupling acts more directly on VRE generators than the European supergrid. The increase in market value for conventional generators due to the coupling amounts to only 1-3%, an order of magnitude below the effect of the supergrid of up to 13% market value increase. In absolute terms, the market values achieved in Germany with coupling remain below the level achieved in the scenario with a European supergrid, as the replaced fuel price in the heat sector is lower than the electricity price, to which the system restores with

grid extensions.

Other than European transmission grid extensions, energy sector coupling only slighlty alleviates the market impact of VREs to dispatchable power plants, yet it provides an attractive business case for excess electricity from VREs.

The combined analysis of VRE system integration measures and their implications for the electricity markets reveals that the analyzed measures entail important benefits for VRE market integration. The more flexible or VRE-adapted the system, the higher is the values of VREs to the system and consequently, their market value increases. Additionally, some dispatchable generators can benefit from a more flexible power system.

6.3. Outlook

The findings provided insights on VRE integration with transmission grid extensions and energy sector coupling, based on a hybrid energy system model. Further improvements of the methodology but also the application of the URBS model generator to other VRE integration questions are recommended. Selected aspects are provided below.

With its position between detailed simulation and long term planning models, possible improvements of the URBS model generator can, on the one hand, be directed towards more technical detail. More realistic power flow simulation should be included, the lower voltage level grid and also more detailed modeling of power plant dispatch. The latter may furthermore allow for a more realistic simulation of the wholesale market. On the other hand, the inter-temporal characteristics of infrastructure investment decisions could be included in the model via a coupling of the model to an inter-temporal optimization or the extension of the optimization horizon to several years or decades.

Having studied two VRE system integration measures with URBS, the analysis of other VRE integration measures in terms of system and market integration effects is desirable. The parameter space defined in Chapter 3 and the identified system parameters proved to be very helpful and could serve as metric for future studies of the long term development of power systems. The analysis of the interaction of local and large scale integration measures in Chapter 5 only provides first insights and is recommended to be pursued further. Last but not least, further quantitative analysis of the relevance of the technical system properties for VRE market integration is suggested.

A. Related author publications

The individual chapters are based on the following peer-reviewed publications.

- Katrin Schaber, Florian Steinke Pascal Mühlich and Thomas Hamacher: Parametric study of variable renewable energy integration in Europe: Advantages and costs of transmission grid extensions. *Energy Policy*, 42:498-508, 2012. (Chapter 3)
- Katrin Schaber, Florian Steinke and Thomas Hamacher: Transmission Grid Extensions for the Integration of Variable Renewable Energies: Who Benefits Where?. *Energy Policy*, 43:123-135, 2012. (Chapter 4)
- Katrin Schaber, Florian Steinke and Thomas Hamacher: Managing Temporary Oversupply from Renewables Efficiently: Electricity Storage Versus Energy Sector Coupling in Germany, *Conference Paper at the International Energy Workshop, Paris*, 2013. (Chapter 5)

Related work was published in the following selected peer-reviewed papers and conference contributions.

Papers:

- Tobias Aigner, Katrin Schaber, Thomas Hamacher and Terjie Gjengedal: Integrating wind - influence of transmission grid extension on European electricity market prices. *IEEE PES Innovative Smart Grid Technologies Europe (ISGT)*, 978-1-4673-2597-4/12:1-8 ,2012.
- Tino Aboumahboub, Katrin Schaber, Peter Tzscheutschler and Thomas Hamacher: Optimization of the Utilization of Renewable Energy Sources in the Electricity Sector. *WSEAS Transactions on Power Systems*, 5(2):120-129 ,2010.

Conference contributions:

- Andreas Dotzler, Thomas Hamacher, Christoph Hellings, Matthias Huber, Katrin Schaber, Wolgang Utschick: Decomposition Methods for Large-Scale Optimization of Power System Infrastructure. *Colloquium of the Munich School of Engeneering, Munich*, 2013
- Florian Steinke, Katrin Schaber, Philipp Ahlhaus and Thomas Hamacher: Die netzabhängige Dynamik zukünftiger Elektrizitätsmärkte. *Internationaler ETG-Kongress, Würzburg*, 2011

- Katrin Schaber, Florian Steinke and Thomas Hamacher: The challenge of integrating Variable Renewable Energies to the power system: Baseload power plants and grid extensions. *International Working Party on Nuclear Energy Economics Workshop on "The System Effects of Nuclear Power", Paris*, 2011
- Katrin Schaber, Pascal Mühlich, Florian Steinke and Thomas Hamacher: Integration of variable energy resources in a global energy system model. *Energy Technology System Analysis Program (ETSAP) Workshop, Stockholm*, 2011
- Katrin Schaber, Thomas Hamacher, Bernhard Grotz: A high renewable case for Europe: On the Integration of Renewable Energies in the European Electricity System, *Wind Energy Symposium of the European Physical Society*, 2009
- Katrin Schaber, Thomas Hamacher, Nina Heitmann, Bernhard Grotz: The Integration of Renewable Energies in the European Electricity grid, *International Energy Workshop, Venice*, 2009

B. Linear programming

The mathematical, standard formulation of a linear optimization problem is

$$\min c^T x \tag{B.1}$$

$$\text{with} \quad Ax = b \tag{B.2}$$

$$x \geq 0 \tag{B.3}$$

x are the variables to be determined by the optimization, c, b and A are exogeneous parameters. The boundary conditions $Ax = b$ and $x \geq 0$ define the feasible solution space. Many energy system models can be written in this form.

Numerous algorithms to efficiently solve the above defined linear program, i.e., to find the minimum of the objective function in the allowed solution space, have been developed in the field of mathematical optimization. In this thesis, the CPLEX solver is applied. It is based on the simplex algorithm. This algorithm takes advantage of the fact, that the optimal solution of a linear problem is always located at a vertex of the feasible region. The simplex algorithm therefore evaluates the value and the gradient of objective function at a starting vertex. Based on the gradient, the next vertex is chosen and the procedure is repeated until the optimal solution is found . With this iterative method, the algorithm approaches the global optimum [118].

Optimization theory shows in the "duality principle", that every optimization problem has a dual problem. It states that, if the primal or dual problem has an optimal solution, the corresponding problem has an optimal solution as well. Furthermore, the solutions of the dual and the primal problem are identical. For the above defined primal problems, the dual problem is

$$\max b^T w \tag{B.4}$$

$$\text{with} \quad A^T w \leq c \tag{B.5}$$

It can be shown that the dual solution w corresponds to the derivative of the primal objective function with respect to the corresponding boundary condition [118].

The economic interpretation of the dual solution is of importance: if the objective function is a cost function, the dual variables are the marginal costs. They quantify by how much the total costs would change if the respective boundary condition was relaxed by one unit. The dual variable to the condition guaranteeing that demand is met (in URBS the Energy Balance Equation (equation 2.34)), gives the increase in costs if unit unit more was to be produced. These marginal costs of energy, can be interpreted as wholesale price of the commodity [16].

C. Annuity of investment costs

Investments in power system infrastructure are taken over several years, while in the model one typical year is optimized. The total investment costs $\mathcal{K}_i^I$ given in Table 2.10 are therefore taken into account in the optimization with their annuities. An annuity is the annual capital expenditure occurring for an investment. It is computed based on a Weighted Average Cost of Capital (WACC), also known as discount rate, r of 7% and a technology-specific depreciation period T_i.

$$\kappa_i^I = \mathcal{K}_i^I \cdot \frac{(1+r)^{T_i} \cdot r}{(1+r)^{T_i} - 1} \tag{C.1}$$

The depreciation periods T_i per technology are given listed in the table below.

Technology	T (years)
Bioenergy	25
Coal	30
Gas GT	25
Gas CCGT	25
Geothermal	25
Lignite	30
Oil GT	25
Oil CCGT	25
Nuclear	40
Hydro run of river	40
Wind Onshore	20
Wind Offshore	20
Solar PV	25
Hydro storage	70
HV lines	40
HV cable	40

Table C.1.: Depreciation periods per technology assumed for the computation of the annuity of investment costs (the depreciation period can differ from the technical lifetime given in Table E.1).

D. List of symbols for URBS

Symbol		Explanation
Sets	Size	
$co, co^{in}, co^{out} \in Co$		Commodities
$Co^{vre} \subset Co$		Variable renewable commodities
$Co^{de} \subset Co$		Demand commodities
$Co^{sec} \subset Co$		Secondary commodities
$g \in G$		grid type
$i \in I$	$\lvert X \times P \times Co \times Co \rvert$	Generation unit
$I^{vre} \subset I$	$\lvert X \times P \times Co \times Co^{vre} \rvert$	Generation unit with variable renewable input
$j \in J$	$\lvert X \times St \times Co \rvert$	storage unit
$k \in K$	$\lvert X \times \mathcal{N}(x) \times G \times Co \rvert$	grid line
$p \in P$		Generation process type
$t^r \in TR$		Real time steps
$t \in T, T \subset TR$		Modeled time steps
$t0, tN$		First and last modeled time step
$tf \in TF, TF \subset T$		First time steps in modeled periods
$tl \in TL, TL \subset T$		Last time steps in modeled periods
$te \in TE, TE := TF \cup TL$		Edge time steps of modeled periods
tf_t, tl_t		First and last time steps for period of step t
$st \in St$		storage type
$x \in X$		Model regions

Table D.1.: List of symbols for sets

Symbol		Explanation
Parameters	Domain	
af_i	I	availability factor for generation units
$c_i^{0,min,max}$	I	Installed, minimal and maximal generation capacity
$cf_i(t)$	$I^{vre} \times T$	Capacity factor for VREs
$cStin_j^{0,min,max}$	J	Installed, minimal and maximal storage input capacity
$cStout_j^{0,min,max}$	J	Installed, minimal and maximal storage output capacity
$cSt_j^{0,min,max}$	J	Installed, min. and max. storage size
$cTr_k^{0,min,max}$	K	Installed, minimal and maximal grid capacity
$d(co, x, t)$	$X \times T \times Co^{de}$	Demand for a commodity
η_i	I	transformation efficiency
$\eta_j^{in,out}$	J	Storage in- and output efficiency
$f^{prod}(p, co^{in}, co^{out}, x)$	$X \times P \times Co \times Co$	Share of one generation unit in total commodity production per region
$f^{cons}(p, co^{in}, co^{out}, x)$	$X \times P \times Co \times Co$	Share of one generation unit in total commodity consumption per region
κ_i^{inv}	I	Annuity of inv. costs for generation units
κ_i^{fix}	I	Fix O&M costs for generation units
κ_i^{var}	I	Variable costs for generation units
$\kappa_i^{fuel}, \kappa_i^{co2}, \kappa_i^{O\&Mvar}$	I	fuel, CO_2 and variable O&M costs for generation
$\kappa_j^{inv}, \kappa_j^{fix}$	J	Annuity of inv. and fix costs for storage
$\kappa_j^{inv,in/out}, \kappa_j^{fix,in/out}$	J	Annuity of inv. and fix costs for storage in- and output
κ_j^{var}	J	Variable storage in- and output costs
$\kappa_k^{var}, \kappa_k^{fix}, \kappa_k^{inv}$	K	Annuity of inv., fix and variable costs for transport
λ_k	K	Losses along line k
$lg(p, co^{in}, co^{out}, x)$	$P \times Co \times Co^{de} \times X$	Flag indicating local generation
τ_i	I	power change factor for generation unit
v_j^0	J	Storage filling level energy at $t0$
$w(t)$	T	Weight of modeled time step

Table D.2.: List of symbols for parameters

Symbol		Explanation
Variables	Domain	Note: all variables are positive
C_i	I	Generation unit capacity
CSt_j	J	Storage size
$CStin_j$, $CStout_j$	J	Storage in- and output capacity
$Cons(x, co, t)$	$X \times T \times Co$	Total commodity consumption and export
$E_i^{in}(t)$	$T \times I$	Energy consumption (input)
$E_i^{out}(t)$	$T \times I$	Energy production (output)
$ESt_j^{in}(t), ESt_j^{out}(t)$	$J \times T$	Storage in- and output
$\epsilon(p, co^{in}, co^{out}, x)$	$P \times Co \times Co^{de} \times X$	Total local generation per unit
$F_k^{imp}(t)$	$K \times T$	Import along grid line k
$F_k^{exp}(t)$	$K \times T$	Export along grid line k
$K^{inv}, K^{fix}, K^{var}$		Cost components
$Prod(x, co, t)$	$X \times T \times Co$	Total commodity production and import
$V_j(t)$	$J \times T$	Stored energy
$V_j^{seas}(te)$	$J \times TE$	Counter for seasonal storage
z		Total system costs

Table D.3.: List of symbols for variables

E. Data

E.1. Input data for URBS-EU

Process	Lifetime (yrs)
Bioenergy	35
Coal	45
Gas CCGT, GT	30
Geothermal	30
Lignite	45
Oil CGGT, GT	30
Solar PV	30
Wind	30
Nuclear	50
Hydro run of river	75

Table E.1.: Average lifetime per technology [75, 115]

Region	Coal	Gas GT	Gas CCGT	Lignite	Oil	Nuclear
A	47	1 167	1 767	-	6	-
B	17	2 445	2 997	-	15	4 207
BG	130	741	118	2 550	-	4 000
BH-Co	550	160	103	3 055	100	-
Ch	-	150	381	-	1	1 220
CZ	193	1 188	845	2 473	22	3 902
D-EnBW	2 666	1 387	508	-	2	1 310
D-EON-M	136	342	20	-	-	1 360
D-EON-N	5 070	1 200	442	-	2	2 739
D-EON-S	448	1 698	947	-	8	2 698
D-RWE	9 263	3 285	2 520	3 438	42	-
D-VET	2 501	1 872	3 725	6 294	340	-
DK-O	582	209	661	-	112	-
DK-W	857	264	679	-	95	-
ES-NW	800	969	12 631	50	1 038	1 960
ES-O	711	6 728	14 861	80	908	5 300
ES-S	-	900	4 023	-	32	-
F-NO	13	1 663	4 542	375	785	25 386
F-NW	-	492	564	-	7	21 294
F-SO	-	353	1 865	-	232	10 406
F-SW	-	159	29	-	2	6 530
FIN-N	-	0	-	-	-	-
FIN-S	560	1 289	173	-	159	6 700
GB-N	1 860	1 042	518	-	17	1 364
GB-S	1 630	11 630	27 521	-	144	8 340
GR	-	1 473	3 799	2 007	842	-
H	330	2 389	2 325	440	174	3 000
I-N	7 124	18 355	5 853	-	61	-
I-S	-	3 280	895	-	240	-
I-Sar	650	-	555	-	80	-
I-Siz	-	1 656	115	-	-	-
IRL	-	1 022	3 500	-	202	-
IRL-NI	-	560	587	-	87	-
Kro	710	421	803	-	-	-
Lux	-	16	445	-	0	-
N-M	-	325	-	-	-	-
N-N	-	215	0	-	-	-
N-S	-	260	432	-	-	-
NL	4 790	3 807	9 442	-	20	1 000
P-M	616	41	830	-	41	-
P-N	-	5	1 005	-	63	-
P-S	800	592	3 689	-	193	-
PL	12 028	1 129	3 372	4 557	-	3 000
Ro	800	739	1 074	786	53	2 880
S-M	114	0	0	-	2	3 240
S-N	-	-	-	-	-	-
S-S	-	434	0	-	13	3 506
SK	46	437	1 761	341	13	3 874
SLO	-	318	112	600	-	727
SRB	-	-	560	1 093	-	-
Total	56 041	78 808	123 598	28 138	6 154	129 943

Table E.2.: Remaining conventional power plant capacity in 2020 in Europe (MW_{el}). Input for scenarios in Chapter 4.

Region	Hydro	Geothermal	Bioenergy	Solar PV	Wind Onshore	Wind Offshore
A	9 887	1	952	322	2 578	-
B	111	-	815	1 340	1 959	2 361
BG	1 851	-	344	303	855	401
BH-Co	4 220	-	220	17	400	200
Ch	11 270	-	272	922	300	-
CZ	975	-	508	1 695	743	-
D-EnBW	970	-	456	10 713	475	-
D-EON-M	254	-	357	3 881	2 584	-
D-EON-N	20	-	706	3 985	6 190	17 692
D-EON-S	878	-	668	11 903	332	-
D-RWE	350	-	2 083	11 334	6 275	-
D-VET	1 357	8	1 781	9 937	10 579	1 624
DK-O	3	-	290	4	520	1 073
DK-W	1	-	140	2	1 941	426
ES-NW	4 940	-	624	2 178	14 717	-
ES-O	8 151	-	3 597	7 825	13 953	-
ES-S	893	-	507	3 442	4 366	-
F-NO	4 155	4	852	957	5 039	-
F-NW	720	4	116	708	12 598	-
F-SO	11 551	4	145	2 470	1 637	-
F-SW	3 332	4	100	1 265	4 535	-
FIN-N	1 772	-	156	1	294	1 176
FIN-S	1 282	-	1 849	9	441	588
GB-N	1 365	-	273	65	9 158	9 581
GB-S	162	-	8 366	2 615	2 290	6 851
GR	2 451	-	600	2 450	6 964	536
H	51	-	1 040	63	750	-
I-N	11 952	843	9 081	2 812	476	1 585
I-S	949	-	1 823	4 962	4 850	1 585
I-Sar	106	-	-	826	1 617	-
I-Siz	95	-	574	-	2 568	-
IRL	162	-	970	9	3 655	-
IRL-NI	76	-	303	7	618	377
Kro	1 788	-	190	8	1 400	660
Lux	44	-	18	113	131	-
N-M	5 696	-	30	-	1 740	-
N-N	3 783	-	10	-	1 410	-
N-S	18 319	-	56	4	510	480
NL	39	-	1 642	722	5 629	
P-M	767	10	24	291	2 294	504
P-N	2 334	10	41	190	1 464	504
P-S	1 257	10	292	1 019	1 102	1 007
PL	808	-	310	3	4 988	1 663
Ro	6 655	-	417	260	2 720	1 280
S-M	4 478	-	425	5	350	350
S-N	11 640	-	219	1	839	909
S-S	251	-	716	2	700	1 399
SK	1 559	-	86	300	350	-
SLO	932	-	11	139	106	-
SRB	2 153	-	1	17	80	-
Total	148 817	899	45 057	92 096	152 070	54 812

Table E.3.: Renewable energy technology capacities in 2020 in Europe (MW_{el}). Input for scenarios in Chapter 4

E.2. Input data for URBS-D

Region	Coal	Gas GT	Gas CCGT	Lignite	Oil	Nuclear	Gas heating	Gas reformation
DE21	306	31	21	-	116	-	8 179	175
DE22	1 313	2 728	114	586	33	-	11 455	137
DE23	2 738	1 531	43	785	2	-	13 174	137
DE24	-	217	326	74	5	-	15 272	172
DE25	1 050	2 078	256	92	21	-	16 878	177
DE26	730	1 455	3 479	-	268	1 410	14 656	153
DE41	2 876	149	1 454	-	43	1 310	8 068	118
DE42	786	1 061	135	-	217	-	23 383	207
DE71	711	3 339	510	-	3	1 329	7 259	98
DE72	8 121	1 925	2 833	3 273	52	-	17 677	272
DE73	1 456	1 791	1 616	40	82	-	18 869	208
DE74	157	1 262	1 832	4 681	81	-	14 734	153
DE75	2 218	1 049	2 285	685	36	-	17 141	210
DE76	-	336	28	-	22	-	6 000	74
DE81	742	2 911	2 515	440	292	-	21 470	164
DE82	409	62	271	-	80	-	5 864	77
DE83	639	404	1 770	2 292	28	-	12 257	116
DE84	-	330	-	-	18	-	13 159	92
Total	24 251	22 660	19 489	12 949	1 400	4 049	245 495	2 740

Table E.4.: Assumed installed conventional (MW) capacities in Germany 2020.

Region	Hydro	Geothermal	Bio CHP	Solar PV	Wind
DE21	-	-	1 163	3 126	5 118
DE22	27	-	1 219	2 261	5 178
DE23	51	-	1 319	1 649	4 237
DE24	91	-	402	2 409	1 171
DE25	487	-	1 129	7 198	819
DE26	1 549	4	1 285	8 952	81
DE41	148	4	759	2 819	213
DE42	697	-	1 436	6 709	533
DE71	-	-	619	1 738	1 335
DE72	40	-	1 277	2 623	1 316
DE73	58	-	821	2 330	1 808
DE74	143	-	445	1 771	1 533
DE75	215	-	745	3 106	1 660
DE76	657	-	665	4 615	94
DE81	1 033	0	2 275	2 664	8 885
DE82	0	-	245	186	328
DE83	34	-	1 066	2 651	3 409
DE84	119	-	1 131	3 192	3 881
DE80	-	-	-	-	4 534
DE20	-	-	-	-	11 266
Total	5 350	8	18 000	60 000	57 400

Table E.5.: Assumed installed renewable energy capacities (MW) in Germany 2020.

Region	Hydro	Geothermal	Bio CHP	Solar PV	Wind	Gas reformation
DE21	-	-	209	4 647	6 965	110
DE22	20	-	326	6 590	8 194	86
DE23	37	-	455	8 562	6 715	86
DE24	66	-	478	7 509	3 840	107
DE25	356	-	743	11 914	1 340	111
DE26	1 131	4	846	10 075	980	95
DE41	108	4	311	5 071	600	73
DE42	508	-	828	10 239	3 675	130
DE71	-	-	201	3 070	2 455	61
DE72	29	-	923	7 455	2 255	170
DE73	42	-	336	6 623	4 480	130
DE74	105	-	446	6 646	2 170	96
DE75	157	-	798	9 274	3 655	131
DE76	480	-	297	4 170	1 410	46
DE81	754	0	1 429	10 829	14 285	102
DE82	0	-	341	1 549	200	48
DE83	25	-	954	8 095	4 865	73
DE84	87	-	642	7 124	6 840	58
DE80	-	-	-	-	6 710	-
DE20	-	-	-	-	36 454	-
Total	3 904	8	10 563	129 441	118 088	1 712

Table E.6.: Assumed installed capacities (MW) in Germany 2050.

	2020 Electricity		2050 Electricity		2020/50 Heat
Model region	In/Output power C (MW)	Reservoir size CSt (MWh)	In/Output power C (MW)	Reservoir size CSt (MWh)	C, CSt (MW,MWh)
DE21	-	-	-	-	4638
DE22	120	600	456	1242	5952
DE23	220	940	230	1093	6810
DE24	-	-	940	4336	8431
DE25	328	1850	464	2980	9194
DE26	515	5330	598	6468	7838
DE41	-	-	-	-	4464
DE42	5164	32316	4816	37390	12420
DE71	-	-	-	-	3863
DE72	153	590	154	605	9770
DE73	150	747	168	859	10177
DE74	500	6500	750	6500	8076
DE75	-	-	-	-	9264
DE76	-	-	-	-	3105
DE81	126	987	94	987	10579
DE82	-	-	-	-	3105
DE83	1603	12638	1603	13231	6574
DE84	1170	4609	1260	4609	6617

Table E.7.: Heat and electricity storage size in the *Base* scenarios in Chapter 5

Region	Household	sITS	Industry[a]
DE21	21.39	9.66	10.82
DE22	29.05	11.98	13.42
DE23	35.73	11.99	13.43
DE24	39.54	15.02	16.84
DE25	44.74	15.52	17.39
DE26	36.51	13.34	14.94
DE41	18.51	10.28	11.52
DE42	65.37	18.12	20.30
DE71	17.21	8.53	9.56
DE72	39.05	23.76	26.63
DE73	50.75	18.17	20.37
DE74	43.09	13.36	14.97
DE75	42.08	18.39	20.60
DE76	12.50	6.50	7.28
DE81	67.41	13.53	15.17
DE82	13.53	6.73	7.54
DE83	34.83	10.15	11.37
DE84	40.93	8.06	9.03
Total	652.22	233.08	261.18

Table E.8.: German heat demand per sector and region (TWh), 2010

[a] excludes high temperature process heat.

F. Revenues with national prices

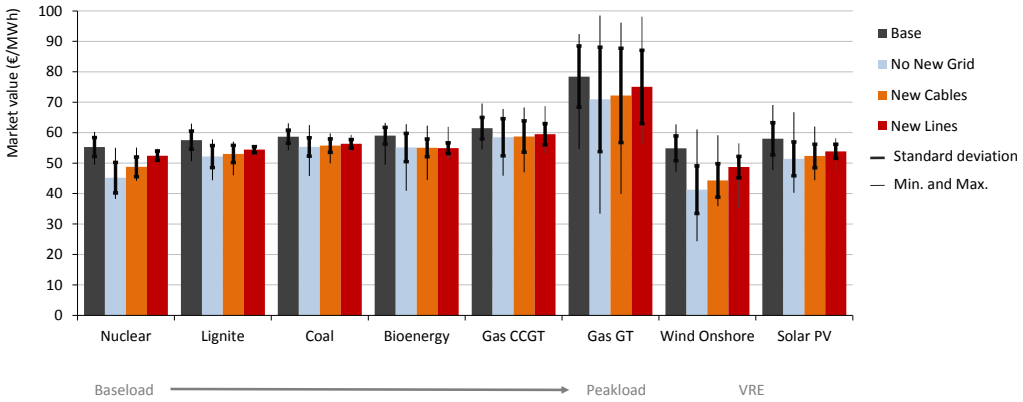

Figure F.1.: Market value per generation technology for the four scenarios with current market areas. Standard deviation and minimal and maximal values across the model regions are indicated with the black lines.

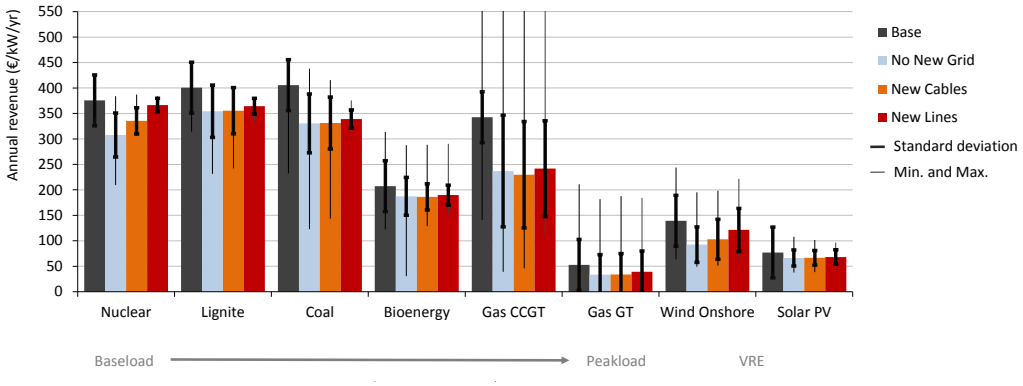

Figure F.2.: Revenues per generation technology for the four scenarios with current market areas. Standard deviation and minimal and maximal values across the model regions are indicated with the black lines.

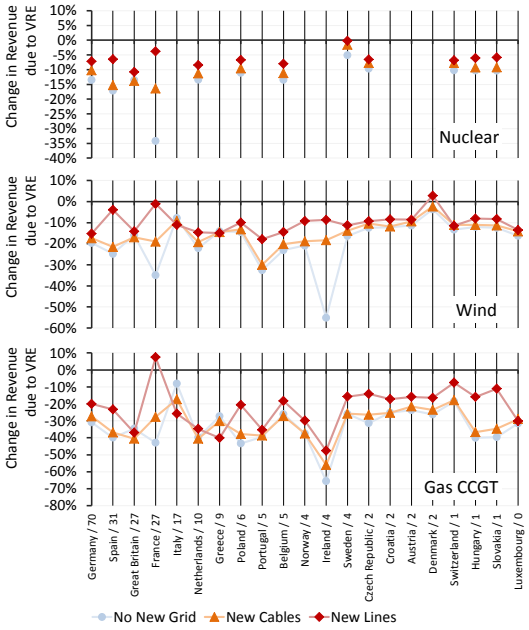

Figure F.3.: Relative change in revenue with VRE additions compared to *Base*. The countries are plotted in decreasing order of VRE capacity additions. After the country names VRE additions until 2020 are indicated in GW. Current market areas are assumed.

List of Figures

List of Tables

Bibliography

[1] T. Aboumahboub. *Development and Application of a Global Electricity System Optimization Model with a Particular Focus on Fluctuating Renewable Energy Sources*. PhD thesis, Lehrstuhl für Energiewirtschaft und Anwendungstechnik, Technical University Munich, Prof. U. Wagner, 2011.

[2] T. Aboumahboub, K. Schaber, P. Tzscheutschler, and T. Hamacher. Optimization of the utilization of renewable energy sources in the electricity sector. *WSEAS Transactions on Power Systems*, 5:120–129, 2010. ISSN 1790-5060.

[3] ABS Energy Research. *Global Transmission and Distribution Report*. ABS Energy Research, London, United Kingdom, 2010.

[4] AG Energiebilanzen e.V. *Anwendungsbilanzen für die Endenergiesektoren in Deutschland in den Jahren 2009 und 2010*. Bundesministerium für Wirtschaft und Technologie, Projektnummer 23/11, November 2011.

[5] P. Ahlhaus and P. Stursberg. Transmission Capacity Expansion: An Improved Transport Model. *Innovative Smart Grid Technologies (ISGT Europe), 4th IEEE PES International Conference and Exhibition*, (in preparation):1–6, 2013.

[6] T. Aigner, K. Schaber, T. Hamacher, and T. Gjengedal. Integrating wind - influence of transmission grid extension on European electricity market prices. *IEEE PES Innovative Smart Grid Technologies Europe (ISGT)*, 978-1-4673-2597-4/12: 1–8, 2012.

[7] G. Anderson. *Modeling and Analysis of Electric Power System, Lecture 227-0526-00*. ETH Zürich, EEH Power Systems Laboratory, Zürich, Switzerland, 2008. URL `http://www.eeh.ee.ethz.ch/uploads/tx_ethstudies/modelling_hs08_script_02.pdf`.

[8] Arbeitsgemeinschaft für Sparsamen und Umweltfreundlichen Energieverbrauch e.V. (ASUE). *BHKW-Kenndaten 2011. Module, Anbieter, Kosten*. Energiereferat der Stadt Frankfurt am Main, Frankfurt am Main, Germany, 2011. URL `http://asue.de/cms/upload/broschueren/2011/bhkw-kenndaten/asue-bhkw-kenndaten-0311.pdf`.

[9] M.P. Bahrman and B.K. Johnson. The ABCs of HVDC transmission technologies. *IEEE Power and Energy Magazine*, 5(2):32 –44, March-April 2007. ISSN 1540-7977. doi: 10.1109/MPAE.2007.329194.

[10] M. Beller, A. Doernberg, A. Hermelee, and K. C. Hoffman. Impacts of new energy technologies as measured against reference energy systems. *Energy*, 4(5):891 – 909, 1979. ISSN 0360-5442. doi: 10.1016/0360-5442(79)90020-3. Proceedings of a Conference on Non-Fossil Fuel and Non-Nuclear Fuel Energy Strategies.

[11] FL.W.M. Beurskens and M. Hekkenberg. *Renewable Energy Projections as Published in the National Renewable Energy Action Plans of the European Member States Covering all 27 EU Member States*. European Environment Agency, 2011. URL `http://www.ecn.nl/units/ps/themes/renewable-energy/projects/nreap/`.

[12] M. Biberacher. *Modeling and optimization of future energy system using spacial and temporal methods*. PhD thesis, Institute of Physics, University of Augsburg, 2004.

[13] S. Birkhaeuser. *Technisches Potenzial der erneuerbaren Stromerzeugung in der Europäischen Union*. Bachelorthesis, Lehrstuhl für Energiewirtschaft und Anwendungstechnik, Technische Universität München, 2012.

[14] J.K.B. Bishop, T. Potylitsina, and W.B. Rossow. Documentation and Description of Surface Solar Irradiance Data Sets Produced for SeaWifs. *Department of Applied Physics of Columbia University, EO Lawrence Berkeley Laboratory, NASA/Goddard Institute for Space Studies*, 2000.

[15] S. Bofinger, L. von Bremen, K. Knorr, K. Lesch, K. Rohrig, Y. Saint-Drenan, and M. Speckmann. *Raum-zeitliche Erzeugungsmuster von Wind- und Solarenergie in der UCTE-Region und deren Einfluss auf elektrische Transportnetze: Abschlussbericht für Siemens Zentraler Forschungsbereich*. Institut für Solare Energieversorgungstechnik, ISET e.V., Kassel, Germany, 2008.

[16] J. Borchert, R. Schemm, and S. Korth. *Stromhandel: Institutionen, Marktmodelle, Pricing und Risikomanagement*. Schäffer-Poeschel, Stuttgart, Germany, 2006. ISBN 3-791-02542-2. URL `http://www.gbv.de/dms/bsz/toc/bsz25421794xinh.pdf`.

[17] V. Bosetti, C. Carraro, M. Galeotti, E. Massetti, and M. Tavoni. WITCH: A World Induced Technical Change Hybrid Model. *The Energy Journal*, 2006. Special Issue. Hybrid Modeling of Energy-Environment Policies: Reconciling Bottom-up and Top-down.

[18] J. Bower. A review of european electricity statistics. *Journal of Energy Literature*, 2003:1–15, 2003. URL `http://www.oxfordenergy.org/pdfs/jelsample.pdf`.

[19] H. Brakelmann. *Netzverstärkungs-Trassen zur Übertragung von Windenergie: Freileitung oder Kabel?* Universität Duisburg-Essen, Essen, Germany, October

2004. URL www.ets.uni-duisburg-essen.de/~bra/Freileitung_Kabel.pdf.

[20] O. Brückl. *Globales Potenzial der Stromerzeugung aus Windenergie: Endbericht der Studie für die BMW AG*. Lehstuhl für Energiewirtschaft und Anwendungstechnik, Technische Universität München, München, Germany, 2005.

[21] R. Buckminster Fuller. *The World Game: Integrative Resource Utilization Planning Tool*. World Resources Inventory, Southern Illinois University, Carbondale, Illinois 62901, USA, 1971. URL www.bfi-internal.org/pdfs/world_game_series_document1.pdf.

[22] Bundesministerium für Wirtschaft und Technologie (BMWi), Bundesministerium für Umwelt, Naturschutz und Reaktorsicherheit (BMU). *Energiekonzept für eine umweltschonende, zuverlässige und bezahlbare Energieversorgung*. BMWi, BMU, Berlin, Germany, 2010. URL http://www.bundesregierung.de/Webs/Breg/DE/Themen/Energiekonzept/_node.html.

[23] Bundesverband der deutschen Gas- und Wasserwirtschaft. *Anwendung von Standardlastprofilen zur Belieferung nicht-leistungsgemessener Kunden. Praxisinformation P2006/8 Gastransport/Betriebswirtschaft*. Wirtschafts- und Verlagsgesellschaft Gas und Wasser mbH, 2006.

[24] Bundesverband Kraft-Wärme-Kopplung e.V. *Kraft-Wärme-Kopplung in der Industrie. effizient produzieren - nachhaltig wirtschaften*. B.KWK Bundesverband, Berlin, Germany, 2011. URL www.bkwk.de/industrie/Broschuere_KWK_in_der_Industrie.pdf.

[25] J. A. Casazza and W. S. Ku. The coordinated use of A-C and D-C network analyzers. *Proc. Amer. Power Conf. Illinois Institute of Technology*, 16:447 – 453, 1954. Chicago, IL.

[26] G. Czisch. *Szenarien zur zukünftigen Stromversorgung , Kostenoptimierte Variationen zur Versorgung Europas und seiner Nachbarn mit Strom aus erneuerbaren Energien*. PhD thesis, Elektrotechnik / Informatik der Universität Kassel, 2005.

[27] M. A. Delucchi and M. Z. Jacobson. Providing all global energy with wind, water, and solar power, Part II: Reliability, system and transmission costs, and policies. *Energy Policy*, 39(3):1170 – 1190, 2011. ISSN 0301-4215. doi: 10.1016/j.enpol.2010.11.045.

[28] Deutsche Energie-Agentur GmbH. *dena-Netzstudie I: Energiewirtschaftliche Planung für die Netzintegration von Windenergie in Deutschland an Land und Offshore bis zum Jahr 2020, Endbericht*. Deutsche Energie-Agentur GmbH, Berlin, Germany, 2005. URL http://www.dena.de/de/themen/thema-esd/publikationen/publikation/netzstudie/. Study conducted by DEWI, E.ON Netz, EWI, RWE Transportnetz Strom and VE Transmission.

[29] Deutsche Energie-Agentur GmbH. *Kurzanalyse der Kraftwerks-und Netzplanung in Deutschland bis 2020 (mit Ausblick auf 2030).* Deutsche Energie-Agentur GmbH, Berlin, Germany, 2008. URL http://www.dena.de/themen/thema-esd/projekte/projekt/kraftwerks-und-netzplanung/.

[30] Deutsche Energie-Agentur GmbH. *dena-Netzstudie II: Integration enerneuerbarer Energien in die deutsche Stromversorgung im Zeitraum 2015-2020 mit Ausblick 2025.* Deutsche Energie-Agentur GmbH, Berlin, Germany, 2010. URL www.dena.de/fileadmin/user_upload/Publikationen/Erneuerbare/Dokumente/Endbericht_dena-Netzstudie_II.PDF. Study conducted by Amprion GmbH, BARD Engineering GmbH, BMU, BMWi, BDEW, EnBW Transportnetze AG, E.ON Netz GmbH, EWE Netz GmbH, Siemens AG, Stiftung Offshore Windenergie Offshore Forum Windenergie GbR, TenneT TSO GmbH, FNN, BWE, VDMA, VGB PowerTech e.V., ZVEI and 50Hertz Transmission GmbH .

[31] Deutsche Energie-Agentur GmbH. *dena -Verteilnetzstudie. Ausbau - und und Innovationsbedarf der Stromverteilnetze in Deutschland bis 2030. Endbericht*. Deutsche Energie-Agentur GmbH, Berlin, Germany, 2012. URL http://www.dena.de/presse-medien/studien/dena-verteilnetzstudie.html. Bearbeiter:Annegret Cl. Agricola, Bernd Höflich, Philipp Richard, Jakob Völker, Christian Rehtanz, Marco Greve, Björn Gwisdorf, Jan Kays, Theresa Noll, Johannes Schwippe, André S, Jan Teuwsen, Gert Brunekreeft, Roland Meyer, Vanessa Liebert.

[32] Deutsches Zentrum für Luft- und Raumfahrt (DLR). *Trans-Mediterranean Interconnection for Concentrating Solar Power (TRANS-CSP), Final Report*. German Aerospace Center (DLR), Institute of Technical Thermodynamics, Section Systems Analysis and Technology Assessment and Federal Ministry for the Environment, Nature Conservation and Nuclear Safety (BMU), Germany, 2006. URL www.dlr.de/tt/desktopdefault.aspx/tabid-2885/4422_read-6588/.

[33] Deutsches Zentrum für Luft- und Raumfahrt (DLR), Fraunhofer ISE, RWTH Aachen and FGH. *Perpektiven von Elektro-/Hybridfahrzeigen in einem Versorgungssystem mit hohem Anteil dezentraler und erneuerbarer Energiequellen*. Bundesministerium für Wirtschaft und Technologie (BmWi), BmWi - FKZ - 0328005 A-C, 2012.

[34] O. Edenhofer, B. Knopf, T. Barker, L. Baumstark, E. Bellevrat, B. Chateau, P. Criqui, M. Isaac, A. Kitous, S. Kypreos, M. Leimbach, K. Lessmann, B. Magné, S. Scrieciu, H. Turton, and D. van Vuuren. The Economics of Low Stabilization: Model Comparison of Mitigation Strategies and Costs. *The Energy Journal*, 31, 2010.

[35] Energy Exchange Austria (EXAA). Market data, 2010. URL www.exaa.at.

[36] European Commission. Directive 96/92/EC of the European Parliament and of the Council of 19 December 1996 concerning common rules for the internal market in electricity. *Official Journal of the European Union*, L 27/20, 1996.

[37] European Commission. Directive 2003/54/EC of the European Parliament and of the council of 26 June 2003 concerning common rules for the internal market in electricity and repealing Directive 96/92/EC. *Official Journal of the European Union*, L 176/37, 2003.

[38] European Commission. Commission of the European Communities: Renewable Energy Road Map: Renewable Energies in the 21st century: building a more sustainable future. *Communication from the Commission to the Council and the European Parliament*, 848, 2006.

[39] European Commission. Directive 2009/72/EC of the European Parliament and of the council of 13 July 2009 concerning common rules for the internal market in electricity and repealing Directive 2003/54/EC. *Official Journal of the European Union*, L 211/55, 2009.

[40] European Commission. A Roadmap for moving to a competitive low carbon economy in 2050. *Communication from the European Commission*, 112, 2011. URL `http://ec.europa.eu/clima/documentation/roadmap/docs/com_2011_112_en.pdf`.

[41] European Commission. Renewable Energy: Progressing towards the 2020 target. *Communication from the European Commission*, 31, 2011. URL `http://eur-lex.europa.eu/LexUriServ/LexUriServ.do?uri=COM:2011:0031:FIN:EN:PDF`.

[42] European Commission. Energy Markets in the European Union in 2011. *Communication from the Commission to the European Parliament, the Council, the European Economic and Social Committee and the Comittee of Regions*, SWD 368 final, 2012. URL `http://ec.europa.eu/energy/gas_electricity/doc/20121121_iem_swd_0368_part1_en.pdf`.

[43] European Commission, DG Energy. *Quarterly Report on European Electricity Markets*, volume 5. European Commission, 2012.

[44] European Energy Exchange. German Day-Ahead Electricity Market, 2009. URL `www.eex.com`.

[45] European Environment Agency (EEA). Heating degree days (CLIM 047), 2013. URL `http://www.eea.europa.eu/data-and-maps/indicators/heating-degree-days-1`.

[46] European Network of Transmission System Operators for Electricity (ENTSO-E). Statistical Data, 2010. URL `https://www.entsoe.eu/`.

[47] European Network of Transmission System Operators for Electricity (ENTSO-E). Some definitions of Fundamental Electricity Data. *ENTSO-E Working Paper*, 2010. URL https://www.entsoe.net/res/10111520ENTSO-Edraftdefintionsforentsoe.net.pdf.

[48] European Network of Transmission System Operators for Electricity (ENTSO-E). Net Transfer Capacities, 2011. URL https://www.entsoe.eu/.

[49] European Network of Transmission System Operators for Electricity (ENTSO-E). *Overview of transmission tariffs in Europe: Synthesis 2011*. ENTSO-E, 2011. URL https://www.entsoe.eu/market/transmission-tariffs/.

[50] European Network of Transmission System Operators for Electricity (ENTSO-E). *Ten-Year Network Development Plan 2010-2020*. ENTSO-E, 2012. URL https://www.entsoe.eu/fileadmin/user_upload/_library/SDC/TYNDP/2012/TYNDP_2012_report.pdf.

[51] European Photovoltaic Industry Association (EPIA). *Global Market Outlook for Photovoltaics until 2017*. EPIA, 2013.

[52] European Wind Energy Association (EWEA). *European Wind Energy Association: Pure Power - Wind Energy Scenarios up to 2030*. EWEA, 2008. URL http://www.ewea.org/fileadmin/ewea_documents/documents/publications/reports/purepower.pdf.

[53] European Wind Energy Association (EWEA). *Oceans of Opportunity: Harnessing Europe's largest domestic energy resource*. EWEA, 2009. URL www.ewea.org/fileadmin/ewea_documents/documents/publications/reports/Offshore_Report_2009.pdf.

[54] European Wind Energy Association (EWEA). *Powering Europe: wind energy and the electricity grid*. EWEA, 2010. URL www.ewea.org/fileadmin/ewea_documents/documents/publications/reports/Grids_Report_2010.pdf.

[55] G. Giebel. *On the Benefits of Distributed Generation of Wind Energy in Europe*. PhD thesis, Fachbereich Physik der Universität Oldenburg, 2000.

[56] Global Wind Energy Council (GWEC). *Global Wind Report; Annual Market Update 2010*. GWEC, 2011.

[57] Global Wind Energy Council (GWEC). *Global Wind Report; Annual Market Update 2012*. GWEC, 2013.

[58] R. Green and N. Vasilakos. Market behaviour with large amounts of intermittent generation. *Energy Policy*, 38(7):3211 – 3220, 2010.

[59] Greenpeace and 3E. *A North Sea electricity grid [r]evolution: electricity output of interconnected offshore wind power: a vision of offshore wind power integration*. Greenpeace, 2008. URL `http://www.greenpeace.org/raw/content/eu-unit/press-centre/reports/A-North-Sea-electricity-grid-(r)evolution.pdf`.

[60] B. Grotz. *Untersuchung der Korrelation zwischen Wind- und Solarangebot mit spezeiller Berücksichtigung von Extremwetterlagen*. Diplothesis, Universität Augsburg, 2009.

[61] T. Haase. *Anforderungen an eine durch Erneuerbare Energien geprägte Energieversorgung – Untersuchung des Regelverhaltens von Kraftwerken und Verbundnetzen*. PhD thesis, Fakultät für Informatik und Eletroktechnik der Universität Rostock, 2006.

[62] W. C. Hahn. Load studies on the D-C calculating table. *General Electric Review*, 34:444 – 445, 1931. Schenectady, NY.

[63] M. Haller. *CO_2 Mitigation and Power System Integration of Fluctuating Renewable Energy Sources: A Multi-Scale Modeling Approach*. PhD thesis, Technische Universität Berlin, Potsdam Institut für Klimafolgenforschung, 2012.

[64] D. Heide, L. von Bremen, M. Greiner, C. Hoffmann, M. Speckmann, and S. Bofinger. Seasonal optimal mix of wind and solar power in a future, highly renewable Europe. *Renewable Energy*, 35(11):2483 – 2489, 2010.

[65] N. Heitmann. *Solution of energy problems with the help of linear programming*. Diplomathesis, Naturwissenschaftliche Fakultät der Universität Augsburg, 2005.

[66] N. Heitmann and T. Hamacher. Stochastic Model of the German Electricity System. *Energy Systems: Optimization in the Energy Industry*, 3:365–385, 2009.

[67] J. Herrmann. *Optimierung der städtischen Energieversorgung am Beispiel der Stadt Augsburg unter besonderer Berücksichtigung von Wärmetransportmechanismen*. PhD thesis, Mathematisch-Naturwissenschaftlichen Fakultät der Universität Augsburg, Max-Planck-Institut für Plasmaphysik, Garching, 2012.

[68] L. Hirth. The Market Value of Variable Renewables. *USAEE Working Paper*, 2110237, 2012. URL `http://ssrn.com/abstract=2110237`.

[69] L. Hirth and F. Ueckerdt. Redistribution Effects of Energy and Climate Policy: The Electricity Market. *Nota di Lavoro, Fondazione Eni Enrico Mattei*, 82, 2012.

[70] R. Hofer. *Analyse der Potenziale industrieller Kraft-Wärme-Kopplung*. IfE Schriftenreihe, Heft 28, Lehrstuhl für Energiewirtschaft und Andwendungstechnik, 1994.

[71] M. Huber, J. Dorfner, and T. Hamacher. *Final Report: Electricity system optimization in the EUMENA region*. Lehrstuhl für Energiewirtschaft und Anwendungstechnik, Technische Universität München, 2012. Project report for the Desertec Industry Initiative (dii) GmbH, Munich.

[72] M. Huber, T. Hamacher, C. Ziems, and H. Weber. Combining LP and MIP approaches to model the impacts of renewable energy generation on individual thermal power plant operation. *IEEE PES General Meeting, Vancouver (accepted)*, pages 1–5, 2013.

[73] Intergovernmental Panel on Climate Change (IPCC). *Climate Change 2007: Synthesis Report. Contribution of Working Groups I, II and III to the Fourth Assessment Report of the IPCC*. IPCC, Geneva, Switzerland, 2007. URL `www.ipcc.ch/pdf/assessment-report/ar4/syr/ar4_syr.pdf`. Core Writing Team, Pachauri, R.K and Reisinger, A. (eds.).

[74] Intergovernmental Panel on Climate Change (IPCC). *IPCC Special Report on Renewable Energy Sources and Climate Change Mitigation*. IPCC, 2011. leading authors: O. Edenhofer, R. Pichs-Madruga. Y. Sokona, K. Seyboth, P. Matschoss, S. Kadner, T. Zwickel, P. Eickemeier, G. Hansen, S. Schlomer and C. Stechow.

[75] International Energy Agency (IEA). Interactive renewable energy calculator - recalculator - renewable energy cost and benefit to society, 2009. URL `http://recabs.iea-retd.org/energy_calculator`.

[76] International Energy Agency (IEA). *Electricity Information 2011 (IEA Statistics)*. OECD, Paris, France, 2011. ISBN 978-92-64-10200-2.

[77] International Energy Agency (IEA). *World Energy Outlook 2011*. OECD, Paris, France, 2011. ISBN 978-92-64-12413-4.

[78] International Energy Agency (IEA). *Medium-Term Renewable Energy Market Report 2012 – Market Trends and Projections to 2017*. OECD, Paris, France, 2012. ISBN 978-92-64-17799-4.

[79] International Energy Agency (IEA). *World Energy Outlook 2012*. OECD, Paris, France, 2012. ISBN 978-92-64-18084-0.

[80] H. K. Jacobsen and E. Zvingilaite. Reducing the market impact of large shares of intermittent energy in Denmark. *Energy Policy*, 38(7):3403–3413, 2010. doi: 10.1016/j.enpol.2010.02.014. Special issue: Large-scale wind power in electricity markets with Regular Papers.

[81] K. Karlsson and P. Meibom. Optimal investment paths for future renewable based energy systems-using the optimisation model Balmorel. *Int. J. Hydrogen Energy*, 33:1777–1787, 2008.

[82] W. Kerner. *TEN-ENERGY Policy; Trans-European Energy Networks: DG TREN/C2*. European Commission, presentation, 2007. URL http://www.trade-wind.eu/fileadmin/documents/Seminar_UCTE/presentations/7_Kerner_EC.pdf.

[83] J. C. Ketterer. The Impact of Wind Power Generation on the Electricity Price in Germany. *Ifo Working Paper*, 143, 2012.

[84] J. Kindersberger. *Elektrische Energietechnik: Vorlesungsskript*. Lehrstuhl für Hochspannungs-und Anlagentechnik, Technische Universität München, München, 2001.

[85] J. Kindersberger. *Grundlagen der Hochspannungs- und Energieübertragungstechnik: Vorlesungsskript*. Lehrstuhl für Hochspannungs-und Anlagentechnik, Technische Universität München, München, 2009.

[86] Kombikraftwerk 2. Das regenerative Kombikraftwerk. *Projektbericht (in Vorbereitung)*, 2012. URL http://www.kombikraftwerk.de.

[87] P. Kuhn. *Iteratives Modell zur Optimierung von Speicherausbau und -betrieb in einem Stromsystem mit zunehmend fluktuierender Erzeugung*. PhD thesis, Technische Universität München, Lehrstuhl für Energiewirtschaft und Anwendungstechnik, 2012.

[88] P. Kuhn and M. Kühne. Optimierung des Kraftwerks- und Speicherausbaus mit einem iterativen und hybriden Modell. *VDI-Bericht*, 2157:305–317, 2011.

[89] A. L'Abbate and G. Migliavacca. *Review of costs of transmission infrastructures, including cross-border connections*. Presentation during a general meeting of Realise Grid in Paris, 2010. URL http://realisegrid.erse-web.it.

[90] M. Leimbach, N. Bauer, L. Baumstark, M. Lüken, and O. Edenhofer. International trade and technological change, Insights from REMIND. *The Energy Journal*, 31, 2009.

[91] U. Leprich, H. Guss, K. Weiler, M. Ritzau, U. Macharey, M. Igel, and J. Diegler. *Ausbau elektrischer Netze mit Kabel oder Freileitung unter besonderer Berücksichtigung der Einspeisung erneuerbarer Energien*. IZES GmbH, BET GmbH and PowerEngS, June 2011. URL www.erneuerbare-energien.de/files/pdfs/allgemein/application/pdf/studie_netzausbau_bf.pdf.

[92] F. Leuthold, T. Jeske, H. Weigt, and C. von Hirschhausen. When the Wind Blows Over Europe. A Simulation Analysis and the Impact of Grid Extensions. *Electricity Markets Working Papers*, WP-EM-31, 2009. URL http://www.tu-dresden.de/wwbwleeg/publications/wp_em_31_Leuthold_etal_EU_wind.pdf.

[93] F. U. Leuthold, H. Weigt, and C. von Hirschhausen. ELMOD - A Model of the European Electricity Market. *Electricity Markets Working Paper*, WP-EM-00, 2008. URL http://ssrn.com/abstract=1169082orhttp://dx.doi.org/10.2139/ssrn.1169082.

[94] S. Lorenzik. DIANA - Dispatch and Network Analysis. *EWI Homepage – Model description*, 2012. URL www.ewi.uni-koeln.de/forschung/modelle/diana.

[95] H. Lund. Large-scale integration of wind power into different energy systems. *Energy*, 30:2402–2412, 2005.

[96] H. Lund and B.V. Mathiesen. Energy system analysis of 100% renewable energy systems-the case of denmark in 2030 and 2050. *Energy*, 34:524–531, 2009.

[97] J. MacCormack, A. Hollis, H. Zareipour, and W. Rosehart. The large-scale integration of wind generation: Impacts on price, reliability and dispatchable conventional suppliers. *Energy Policy*, 38(7):3837 – 3846, 2010. doi: 10.1016/j.enpol.2010.03.004. Special issue: Large-scale wind power in electricity markets with Regular Papers.

[98] B. V. Mathiesen and H. Lund. Comparative analysis of seven technologies to facilitate the integration of fluctuating renewable energy sources. *IET Renewable Power Generation*, 2:190–204, 2009.

[99] N. May. *Eco-balance of a Solar Electricity Transmission from North Africa to Europe*. Master's thesis, Faculty for Physics and Geological Sciences, Technical University of Braunschweig, 2005.

[100] C. Mayhew and R. Simmon. *Earth at Night*. NASA/GSFC, NOAA/NGDC, DMSP Digital Archive, 2012. URL http://earthobservatory.nasa.gov/Features/NightLights/.

[101] McKinsey, KEMA, The Energy Futures Lab at Imperial College London, Oxford Economics, and European Climate Foundation. *RoadMap 2050: A practical guide to a prosperous, low-carbon Europe: Technical Analysis: Volume I*. European Climate Foundation, 2010. URL http://www.roadmap2050.eu/.

[102] P. Meibom, J. Kiviluoma, R. Barth, H. Brand, C. Weber, and H.V. Larsen. Value of electric heat boilers and heat pumps for wind power integration. *Wind Energy*, 10:321–337, 2007.

[103] Mercado de Electricidad, OMEL. Market data, 2010. URL www.omel.es.

[104] P. Muehlich and T. Hamacher. Global transportation scenarios in the multi-regional EFDA-TIMES energy model. *Fusion Engineering and Design*, 84(7-11): 1361–1366, 2009.

[105] National Centers for Environmental Prediction (NCEP) and National Center for Atmospheric Research (NCAR). Reanalysis Project, 2008. URL http://dss.ucar.edu/pub/reanalysis/rean_proj_des.html.

[106] Nemeth, I. et al. *Stadtlabor Nürnberger Weststadt Endbericht*. Zentrum für energieeffizientes und nachhaltiges Planen und Bauen, 2012.

[107] Niedersächsische Staatskanzlei Hannover. Netzausbau Niedersachsen, 2010. URL www.netzausbau-niedersachsen.de.

[108] W.D Nordhaus. An Optimal Transition Path for Controlling Greenhouse Gases. *Science*, 258:1315 – 1319, 1992.

[109] W.D Nordhaus and Z. Yang. A regional dynamic general-equilibrium model of alternative climate-change strategies. *American Economic Review*, 86:741 – 765, 1996.

[110] Nordic Power Exchange, NordPool. Market data, 2010. URL www.nasdaqomxcommodities.com.

[111] Nuclear Energy Agency (NEA). *Nuclear Energy and Renewables: System Effects in Low-carbon Electricity Systems*. OECD, Paris, France, 2012. ISBN 978-92-64-18851-8.

[112] A. Ockenfels, V. Grimm, and G. Zoettl. *Strommarktdesign: Preisbildung im Auktionsverfahren für Stromkundenkontrakte an der EEX; Gutachten im Auftrag der European Energy Exchange AG zur Vorlage an die Sächsiche Börsenaufsicht*. Laboratorium für Wirtschaftsforschung, Universität zu Köln, Köln, 2008. URL http://www.eex.com/de/document/38614/gutachten_eex_ockenfels.pdf.

[113] G. Oettinger. *The completion of the EU internal energy market "Getting to 2014"*. DG Energy Internal Market Conference, Speech/11/614, 2011. URL http://europa.eu/rapid/press-release_SPEECH-11-614_en.htm.

[114] Offshore Grid. Offshore Wind Project: Inventory list of possible wind farm locations with installed capacities for the 2020 and 2030 scenarios, 2010. URL http://www.offshoregrid.eu/index.php/results.

[115] Öko-Institut e.V. Globales Emissions-Modell Integrierter Systeme (GEMIS) Version 4.5, 2008. URL www.gemis.de.

[116] B. R. Oswald. *Vergleichende Studie zu Stromübertragungstechniken im Höchstspannungsnetz – Technische, betriebswirtschafliche und umweltfachliche Beurteilung von Freileitungen, VPE-Kabel und GIL am Beispiel der 380-kV-Trasse Ganderkesee - St. Hülfe*. ForWind - Zentrum für Windenergieforschung der Universitäten Oldenburg und Hannover, September 2005. URL www.forwind.de/forwind/files/forwind-oswald-studie-langfassung_05-09-23_1.pdf.

[117] B. R. Oswald and L. Hofmann. *Wirtschaftlichkeitsvergleich unterschiedlicher Übertragungstechniken im Höchstspannungsnetz anhand der 380-kV-Leitung Wahle-Mecklar*. Leibniz Universität Hannover, March 2010. URL `www.tennettso.de/site/binaries/content/assets/netzausbau/projekte/wahle-meckar/wirtschaftlichkeitsvergleich-wahle-mecklar.pdf`.

[118] C.H. Papadimitriou and K. Steiglitz. *Combinatorial optimization: Algorithms and complexity*. Prentice-Hall, Englewood Cliffs, NJ, USA, 1982 1982. ISBN 0 13 152462 3.

[119] A. Pina, S. Carlos, and P. Ferrao. High-resolution modeling framework for planning electricity system with high penetration of renewables. *International Energy Workshop 2012*, 2012.

[120] Platts, UDI Products Group. *Data Base Description and Research Methodology: UDI Wold Electric Power Plant Data Base (WEPP)*. Platts, a Division of The McGraw-Hill Companies, Washington DC, 2009. URL `http://www.platts.com/Products/worldelectricpowerplantsdatabase`.

[121] M. Pollitt. *Electricity Liberalization in the European Union*. Presentation at FEEM, Electricity Policy Research Group University of Cambridge, 2009. URL `www.feem.it/userfiles/attach/2010126184084Pollitt_MCR.pdf`.

[122] PricewaterhouseCoopers (PWC), Potsdam Institute for Climate Impact Research (PIK), International Institute for Applied System Analysis (IIASA), and European Climate Forum (ECF). *100% Renewable Energy: A Roadmap to 2050 for Europe and North Africa*. PricewaterhouseCoopers LLP, 2010.

[123] J. Richter. DIMENSION - A Dispatch and Investment Model for European Electricity Markets. *EWI Working Papers*, 2011-3, 2011. URL `http://EconPapers.repec.org/RePEc:ris:ewikln:2011_003`.

[124] S. Richter. *Entwicklung einer Methode zur integralen Beschreibung und Optimierung urbaner Energiesysteme. Erste Anwendung am Beispiel Augsburg.* PhD thesis, Lehrstuhl für Experimentelle Plasmaphysik, Wissenschaftszentrum Umwelt, Universität Augsburg , Max-Planck-Institut für Plasmaphysik, Garching, 2004.

[125] M. M. Rienecker, M. J. Suarez, R. Gelaro, R. Todling, J. Bacmeister, E. Liu, M.G. Bosilovich, S. D. Schubert, L. Takacs, G.-K. Kim, S. Bloom, J. Chen, D. Collins, A. Conaty, and A. da Silva et al. MERRA - NASA's Modern-Era Retrospective Analysis for Research and Applications. *J. Climate*, pages 3624–3648, 2011. doi: 10.1175/JCLI-D-11-00015.1.

[126] S. von Rohn and M. Huck. Merit Order des Kraftwerksparks. *Forschungsstelle für Energiewirtschaft e.V.*, 0:1–6, 2010. URL `http://www.ffe.de/download/wissen/20100607_Merit_Order.pdf`.

[127] R. Rudervall, J. P. Charpentier, and R. Sharma. High Voltage Direct Current (HVDC) Transmission Systems. *Energy Week, Washington D.C., USA*, 78, March 2000. URL www2.internetcad.com/pub/energy/technology_abb.pdf.

[128] P. Russ and P. Criqui. Post-Kyoto CO2 emission reduction: The soft landing scenario analysed with POLES and other world models. *Energy Policy*, 35, 2007. URL http://www.sciencedirect.com/science/article/pii/S0301421506001145.

[129] G. Sáenz de Miera, P. del Rio Gonzalez, and I. Vizcaíno. Analysing the impact of renewable electricity support schemes on power prices: The case of wind electricity in Spain. *Energy Policy*, 36(9):3345 – 3359, 2008.

[130] Sander & Partner GmbH. World Wind Atlas: high resolution wind speed data from 1970-2010, based on reanalysis data, 2010. URL http://sander-partner.ch.

[131] K. Schaber, F. Steinke, and T. Hamacher. Transmission Grid Extensions for the Integration of Variable Renewable Energies: Who Benefits Where? *Energy Policy*, 43:123–135, 2012.

[132] K. Schaber, F. Steinke, P. Mühlich, and T. Hamacher. Parametric study of variable renewable energy integration in Europe: Advantages and costs of transmission grid extensions. *Energy Policy*, 42:498–508, 2012.

[133] K. Schaber, F. Steinke, and T. Hamacher. Managing Temporary Oversupply from Renewables Efficiently: Electricity Storage Versus Energy Sector Coupling in Germany. *Conference Paper at the International Energy Workshop, Paris*, 2013.

[134] Y. Scholz. *Renewable Energy based electricity supply at low costs - Development of the REMix model and application for Europe*. PhD thesis, Universität Stuttgart and German Aerospace Center (DLR), Institute of Technical Thermodynamics, 2012.

[135] F. Sensfuss, M. Ragwitz, and M. Genoese. The merit-order effect: A detailed analysis of the price effect of renewable electricity generation on spot market prices in Germany. *Energy Policy*, 36(8):3086 – 3094, 2008.

[136] K. Siala. *Technical, Economic and Ecological Analysis of Conventional and Innovative Power Transmission Technologies*. Bachelor thesis, Lehrstuhl für Energiewirtschaft und Anwendungstechnik, Technische Universität München, 2012.

[137] C. Siebels. *Perspektiven für HGÜ on- und offshore aus der Sicht eines Übertragungsnetzbetreibers*. Presentation during the general meeting of the Federal Network Agency (Bundesnetzagentur), Bonn, Germany, July 2010. URL www.bundesnetzagentur.de/SharedDocs/Downloads/DE/BNetzA/Sachgebiete/Energie/VortraegeVeranstaltungen/WorkshopTechnoOptionenJuli2010/VortragSiebelsPerspektivenHGUE_pdf.pdf?__blob=publicationFile.

[138] Sintef Energieforskning AS, Riso DTU, 3E, Kema Nederland BV, Technical Research Centre of Finland, Garrad Hassan and Partner Ltd, Tracabel Engineering, and Deutsche Energie-Agentur GmbH (dena). *Integrating Wind - TradeWind: Developing Europe's power market for the large-scale integration of wind power*. European Wind Energy Association (EWEA), 2009. URL `http://www.ewea.org/fileadmin/ewea_documents/documents/publications/reports/TradeWind_Report_01.pdf`.

[139] M. Staudacher. *Analyse der Herstellungs- und Anwendungsverfahren für Wasserstoff und Synthesegas*. Bachelorthesis, Lehrstuhl für Energiewirtschaft und Anwendungstechnik, Technische Universität München, 2011.

[140] F. Steinke, P. Wolfrum, and C. Hoffmann. Grid vs storage in a 100% renewable Europe. *Renewable Energy*, 50:826–832, 2013.

[141] M. Sterner. *Bioenergy and renewable power methane in integrated 100% renewable energy systems*. PhD thesis, Universität Kassel, Frauenhofer IWES, Institut für Rationelle Energiewandlung, 2009.

[142] P. Twomey and K. Neuhoff. Wind power and market power in competitive markets. *Energy Policy*, 38(7):3198–3210, 2010.

[143] P. Tzscheutschler. *Globales technisches Potenzial solarthermischer Stromerzeugung*. PhD thesis, Lehrstuhl für Energiewirtschaft und Anwendungstechnik, Technische Universität München, 2005.

[144] Übertragungsnetzbetreiber Deutschland. *EEG-Anlagenstammdaten Gesamtdeutschland*. 50 Hz Transmission, Amprion, Tennet TSO, TransetBW, 2011. URL `www.eeg-kwk.net`.

[145] Umweltbundesamt (UBA). Datenbank: Kraftwerke in Deutschland: Liste der sich in Betrieb befindlichen Kraftwerke bzw. Kraftwerksblöcke ab einer elektrischen Bruttoleistung von 100 Megawatt, 2012. URL `http://www.umweltbundesamt.de/energie/archiv/kraftwerke_in_deutschland_datenbank.xls`.

[146] United Nations Climate Change Secretariat (UNFCC). Summary of GHG Emissions for Germany, 2011. URL `http://unfccc.int/files/ghg_emissions_data/application/pdf/deu_ghg_profile.pdf`.

[147] US Department of Commerce. *Handbook for Forecasters in the Mediterranean*. Naval Environmental prediction research facility, AD-A024 271, 1975.

[148] K. Vaillancourt and G. Tosato. Implementing agreement for a programme of energy technology systems analysis joint studies for new and mitigated energy systems final report of annex xi (2008-2010). *International Energy Agency*, 1, 2011. URL `www.iea-etsap.org/web/FinReport/ETSAP-Annex-XI-final-report-final%20version-June-2012-v03.pdf`.

[149] Verband der Elektrotechnik Elektronik Informationstechnik e.V. (VDE). *Demand Side Integration - Lastverschiebungspotenziale in Deutschland*. VDE, Frankfurt am Main, Germany, 2012. URL `https://www.vde.com/de/InfoCenter/Seiten/Details.aspx?eslShopItemID=db6adb35-482e-4ae6-be64-07964dc8f2c7`.

[150] Verband der Elektrotechnik Elektronik Informationstechnik e.V. (VDE). Übersichtsplan "Deutsches Hochspannungsnetz", 2012. URL `http://www.vde.com/de/fnn/dokumente/seiten/uebersichtsplan.aspx`.

[151] Verband der Elektrotechnik Elektronik Informationstechnik e.V. (VDE): Energietechnische Gesellschaft (ETG), Task Force Flexibilisierung des Kraftwerksparks. *Erneuerbare Energie braucht flexible Kraftwerke - Szenarien bis 2020*. VDE, ETG, Frankfurt am Main, Germany, 2012. URL `www.vde.com/de/fg/ETG/Arbeitsgebiete/V1/Aktuelles/Oeffentlich/Seiten/StudieFlexibilisierung.aspx`.

[152] D. Wheeler and K. Ummel. Calculating CARMA: Global Estimation of CO2 Emissions from the Power Sector. *Center for Global Development: Working Paper*, 145:1–36, 2008.

[153] P. Wimmer. *Electromobility in Bavaria*. Diplomathesis, Lehrstuhl für Energiewirtschaft und Anwendungstechnik, Technische Universität München, 2012.

[154] C.K. Woo, I. Horowitz, J. Moore, and A. Pacheco. The impact of wind generation on the electricity spot-market price level and variance: The Texas experience. *Energy Policy*, 39(7):3939 – 3944, 2011. ISSN 0301-4215. doi: 10.1016/j.enpol.2011.03.084. Special Section: Renewable energy policy and development.

Vielen Dank!

This thesis would not have been possible without the support, guidance and encouragement of a number of people. I want to express my gratitude to all of them.

The scientific guidance and inspiring ideas of my supervisor, Prof. Thomas Hamacher, provided invaluable contribution to this thesis. I would like to thank him very much for offering me the possibility to work on this topic and for his continuous support over the last years.

I am also very thankful to Prof. Reinhard Haas for acting as a second reviewer.

I would like to express my warm thanks to all colleagues from the *Max Planck Institute for Plasmaphysics* and the *Lehrstuhl für Energiewirtschaft und Anwendungstechnik* for numerous thought-provoking discussions, their help and support and the great time I shared with all colleagues. Special thanks go to Dr. Philipp Kuhn, who provided very valuable comments, from the conceptual phase to proofreading, and to Matthias Huber for his equally helpful critical review of this thesis and his important contributions to the improvement of URBS. I would like to extend my thanks to Peter Böhme for sharing the PhD experience from the first days. Furthermore, I am very thankful to Nina Heitmann for initially introducing me to URBS and to Johannes Dorfner for facilitating the handling of the model considerably.

Thanks to the cooperation with Dr. Florian Steinke many of the presented results gained substantially in quality and precision. I am very grateful for his suggestions throughout the course of this work. I would also like to thank Simon Müller for his constructive comments.

The first 18 months of this work were financed by a PhD scholarship from the Munich Re, for which I am very thankful.

Finally, I would like to thank my friends and my parents for their encouragement and support, especially during the last months of writing this thesis.